MICROCOPY RESOLUTION TEST CHART
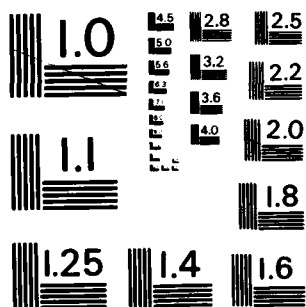
NATIONAL BUREAU OF STANDARDS-1963-A

NAVAL POSTGRADUATE SCHOOL
Monterey, California

THESIS

OPERATIONAL PERFORMANCE CHARACTERISTICS OF
A MULTIPLY-SHROUDED, ANGLED-DIFFUSER STACK
GAS EDUCTOR IN TURUBLENT CROSS-FLOW

by

Ralph Eugene Staples, Jr.

September 1983

Thesis Advisor: P. F. Pucci

DTIC
ELECTE
APR 1 0 1984
E

84 04 09 199

SECURITY CLASSIFICATION OF THIS PAGE *(When Data Entered)*

REPORT DOCUMENTATION PAGE		READ INSTRUCTIONS BEFORE COMPLETING FORM
1. REPORT NUMBER	2. GOVT ACCESSION NO. AD-$H139$ 953	3. RECIPIENT'S CATALOG NUMBER
4. TITLE *(and Subtitle)* Operational Performance Characteristics of a Multiply-Shrouded, Angled-Diffuser Stack Gas Eductor in Turbulent Cross-Flow		5. TYPE OF REPORT & PERIOD COVERED Master's Thesis; September 1983
		6. PERFORMING ORG. REPORT NUMBER
7. AUTHOR(s) Ralph Eugene Staples, Jr.		8. CONTRACT OR GRANT NUMBER(s)
9. PERFORMING ORGANIZATION NAME AND ADDRESS Naval Postgraduate School Monterey, California 93943		10. PROGRAM ELEMENT, PROJECT, TASK AREA & WORK UNIT NUMBERS
11. CONTROLLING OFFICE NAME AND ADDRESS Naval Postgraduate School Monterey, California 93943		12. REPORT DATE September 1983
		13. NUMBER OF PAGES 218
14. MONITORING AGENCY NAME & ADDRESS(*If different from Controlling Office*)		15. SECURITY CLASS. *(of this report)* Unclassified
		15a. DECLASSIFICATION/ DOWNGRADING SCHEDULE

16. DISTRIBUTION STATEMENT *(of this Report)*

Approved for public release; distribution unlimited.

17. DISTRIBUTION STATEMENT *(of the abstract entered in Block 20, If different from Report)*

18. SUPPLEMENTARY NOTES

19. KEY WORDS *(Continue on reverse side if necessary and identify by block number)*

Gas Eductor	Diffuser Rings	Cooling
Multiple Nozzle	Hot Flow	Secondary Flow
Mixing Stack	Hot Primary Flow	Tertiary Flow
Shroud	Exhaust	Turbulent Cross-Flow

20. ABSTRACT *(Continue on reverse side if necessary and identify by block number)*

abstract
    Performance characteristics of two multiple-ring diffuser eductors were determined from collected data. The performance characteristics of a five ring diffuser model were compared with a geometrically similar model tested in cold flow. Model similarity for comparison was maintained through the mach number.

DD $_{1 JAN 73}^{FORM}$ 1473   EDITION OF 1 NOV 65 IS OBSOLETE   1   Unclassified
S/N 0102-LF-014-6601

Both models were tested in a turbulent cross-flow simulating a 29.5 knot relative wind. Minor improvement in the pumping coefficient was seen to occur when cross-flow was introduced.

External surface temperature measurements along the model assembly were recorded by two methods for comparative analysis. The effect of cross-flow is seen in a significant surface temperature reduction in the shroud assembly while apparent degradation of film cooling effectiveness at the diffuser rings resulted in minimal temperature change.

Accession For	
NTIS GRA&I	☒
DTIC TAB	☐
Unannounced	☐
Justification	
By	
Distribution/	
Availability Codes	
	Avail and/or
Dist	Special
A-1	

DTIC
COPY
INSPECTED
1

Operational Performance Characteristics of a
Multiply-Shrouded, Angled-Diffuser Stack Gas
Eductor in Turbulent Cross-Flow

by

Ralph E. Staples, Jr.
Lieutenant Commander, United States Navy
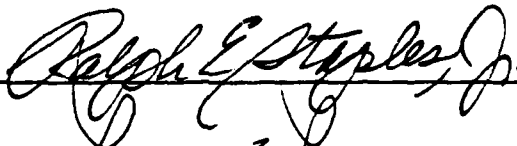B.S. Mar.Eng., Maine Maritime Academy, 1971

Submitted in partial fulfillment of the
requirements for the degree of

MASTER OF SCIENCE IN MECHANICAL ENGINEERING

from the

NAVAL POSTGRADUATE SCHOOL
September 1983

Author _____

Approved by: _____
                                          Thesis Advisor

_____
Chairman, Department of Mechanical Engineering

_____
Dean of Science and Engineering

3

ABSTRACT

Performance characteristics of two multiple-ring diffuser
eductors were determined from collected data. The performance
characteristics of a five ring diffuser model were compared
with a geometrically similar model tested in cold flow. Model
similarity for comparison was maintained through the Mach
number.

Both models were tested in a turbulent cross-flow simula-
ting a 29.5 knot relative wind. Minor improvement in the
pumping coefficient was seen to occur when cross-flow was
introduced.

External surface temperature measurements along the model
assembly were recorded by two methods for comparative analysis.
The effect of cross-flow is seen in a significant surface
temperature reduction in the shroud assembly while apparent
degradation of film cooling effectiveness at the diffuser
rings resulted in minimal temperature change.

TABLE OF CONTENTS

LIST OF TABLES

LIST OF FIGURES

TABLE OF SYMBOLS

ENGLISH LETTER SYMBOLS

A   - Area, in^2, ft^2

B   - Atmospheric pressure, in Hg

c   - Sonic velocity, ft/sec

C   - Coefficient of discharge

D   - Diameter, in (as a reference quantity, refers to
           the inside diameter of the mixing stack)

DELPN   - Pressure drop across the entrance reducing
           section, in H_2O

DELPU   - Pressure drop across the burner U-tube, in H_2O

f   - Friction factor

F_{fr} - Wall skin-friction force, lbf

g   - Proportionality factor in Newton's Second Law
           $g = 32.174$ lbm-ft/lbf-sec^2

h   - Enthalpy, Btu/lbm

1   - Arbitrary length, in

L   - Length of the mixing stack assembly, in

P   - Pressure, in H_2O

PMS   - Static pressure in the mixing stack, referenced
           to atmospheric, in H_2O

PNH   - Inlet air pressure upstream of the reducing
           section, in Hg

PPLN   - Pressure differential across the measurement plenum
           secondary flow nozzles, in H_2O

PUPT	– Pressure in the uptake, in H_2O
r	– Radial distance from the axis of the mixing stack, in
R	– Gas Constant, for air ≈ 53.34 ft-lbf/lbm-°R
ROTA	– Fuel mass flow rotameter reading
Rms	– Interior radius of the mixing stack, in
s	– Entropy, Btu/lbm-R
S	– Standoff, distance between the discharge plane of the primary nozzles and the entrance plane of the mixing stack, in
T	– Temperature, °F, °R
TAMB	– Ambient temperature, °F
TAMBR	– Ambient temperature, °R
TBURN	– Burner temperature, °F
TEP	– Exit plane temperature, °F
TMS	– Mixing stack wall temperature, °F
TNH	– Inlet air temperature, °F
TNHR	– Inlet air temperature, °R
TSURF	– Surface temperature of shroud and diffusers, °F
TUPT	– Uptake temperature, °F
TUPTR	– Uptake temperature, °R
u	– Internal Energy (Btu/lbm)
U	– Velocity, ft/sec
UM	– Average velocity in the mixing stack, ft/sec
UP	– Primary flow velocity at nozzle exit, ft/sec
UU	– Primary flow velocity in uptake, ft/sec
v	– Specific volume (ft^3/lbm)

W   — Mass flow rate, lbm/sec

WF   — Mass flow rate of fuel, lbm/sec

WP   — Primary mass flow rate, lbm/sec

WS   — Secondary mass flow rate, lbm/sec

WPA   — Mass flow rate of primary air, lbm/sec

X   — Axial distance from mixing stack entrance, in

DIMENSIONLESS GROUPINGS

A^* — Secondary flow area to primary flow area ratio

$A\ ^*$ — Tertiary flow area to primary flow area ratio

K_e — Kinetic energy correction factor

K_m — Momentum correction factor at mixing stack exit

K_p — Momentum correction factor at primary nozzle exit

M,UMACH — Mach number

P^* — Pressure Coefficient for secondary flow

$P\ ^*$ — Pressure coefficient for tertiary flow

PMS* — Pressure coefficient for mixing stack pressures

Re   — Reynolds number

T^* — Secondary flow absolute temperature to primary
           flow absolute temperature ratio

T_t^* — Tertiary flow absolute temperature to primary
           flow absolute temperature ratio

W^* — Secondary mass flow rate to primary mass flow
           rate ratio

W_t^* — Tertiary mass flow rate to primary mass flow
           rate ratio

ρ *   - Secondary flow density to primary flow
           density ratio

ρ *   - Tertiary flow density to primary flow
           density ratio

GREEK LETTER SYMBOLS

β - $K + (f/2)*(A/A)$

β - Ratio of ASME long radius metering nozzle
           throat diameter to inlet diameter

γ - Ratio of specific heats for air

μ - Absolute viscosity, $lbf-sec/ft^2$

ρ - density, lbm/ft^3

ϕ - "Function of"

SUBSCRIPTS

0   - Section within the measurement plenum

1   - Section at primary nozzle exit

2   - Section at mixing stack exit

a   - Atmospheric

b   - Burner

m   - Mixed flow

ms   - Mixing stack

or   - orifice

P   - Primary

s   - Secondary

t   - Tertiary

u   - Uptake

w   - Mixing stack wall

ACKNOWLEDGEMENTS

Completion of the research contained in this thesis is
owed in a large part to the advice, assistance and support
of a number of other people. In particular, I would like to
express my sincere appreciation to the following:

Professor Paul F. Pucci, of the Mechanical Engineering

Department, my thesis advisor, whose support and

guidance made this such a worthwhile experience.

Mr. John Moulton, modelmaker and craftsman, whose

detailed work provided the foundation of this research.

Mr. Ron Longueira, laboratory technician, whose hard

work and good humor provided much support in the

accomplishment of this work.

Lieutenant Steve Daughety, USN, a friend and classmate,

who, in spite of his own duties, was always ready to

lend a hand.

And, most importantly, my wife, Danna, whose support,

patience, and incredible flexibility have meant so much

to me during my career.

19

I. INTRODUCTION

The increased introduction of marine gas turbines into naval ship propulsion plants has presented several problems associated with the attendant high mass flow rates and escalating operating temperatures presented by these units. Exhaust gas temperatures above 900 degrees Fahrenheit develop an exhaust plume with an intense infrared signature providing a target source for heat seeking offensive weapons. Additionally, these high temperatures can significantly degrade the performance of mast mounted electronic equipments, and provide an undesirable environment for helicopter operations.

Investigations conducted at the Naval Postgraduate School have shown considerable promise in alleviation of these problems by reducing the exhaust gas temperatures through the use of multiply-shrouded eductor systems which induce both secondary and tertiary air into the primary flow stream under turbulent conditions. Significant temperature reductions have been realized with this relatively simple apparatus with latest developments resulting in both size and weight reductions. It is important to note that these temperature reductions have been achieved without an unacceptable degradation of engine performance.

The gas eductor system has proven more feasible than the alternatives of water injection or energy recovery systems (when specifically utilized with the main propulsion engines). It should be noted however that significant promise exists for an energy recovery system such as RACER (Rankine Cycle Energy Recovery) which is currently receiving some interest for installation in the follow-on ships of the DDG-51 class.

The mixing process under the turbulent conditions encountered in the gas eductor is complex and not well understood although significant research efforts are being directed at a better understanding of the phenomenon. Dividing operation of gas eductors into three regimes on the basis of Mach number, the first regime ($M \geq 1.0$) becomes of interest in applications such as thrust augmentation for aircraft and rocket engines, the second regime ($0.4 \leq M \geq 0.6$) is especially relevant to thrust enhancement in Vertical Takeoff or Landing (VTOL) aircraft, and the last regime ($M \leq 0.2$) is the range of interest in dilution cooling of engine exhaust glows. This latter regime is of direct interest to this research and that of ongoing research at the Naval Postgraduate School.

II. BACKGROUND

Naval combatant vessels having marine gas turbine propulsion units currently utilize simple gas eductor systems. The design of gas eductors for destroyers of the DD-963 class was guided by Charwat [Ref. 1] at the University of California at Los Angeles and uses a solid wall mixing stack which re'' es on the length of the mixing stack to provide complete mixing. Initial investigations at the Naval Postgraduate School, which began in 1976, involved determination of the effects of various parameters on the pumping and mixing performance of gas eductors. The ultimate objectives of both past and present research is to effect reductions in the size and weight of the fabricated eductor structure while optimizing eductor performance specifically in terms of plume temperature and stack surface temperature.

A. THE TEST FACILITIES

To carry out the aforementioned research objectives, two test facilities have been constructed. The first facility, the "cold flow" facility, readily permits rapid evaluation of a wide variety of eductor configurations. Its primary benefit is the expediency of data collection resulting from easily fabricated models which to not undergo high temperatures in the testing cycle. Additionally, inexpensive

22

materials afford evaluation of numerous models at minimal

cost. The second test facility, the "hot flow" facility,

is designed to test models at actual operating temperatures.

In addition to confirming the pumping characteristics of

geometrically similar models tested in cold flow, it provides

the needed data on exhaust temperatures and stack surface

temperatures.

B. INITIAL INVESTIGATIONS AT NPS

The initial investigation of gas eductor performance at

the Naval Postgraduate School was undertaken by Ellin [Ref.

2]. This work was based on a simple one dimensional gas

eductor model developed by Pucci [Ref. 3]. Testing three

basic eductor geometries, Ellin attempted to determine the

effects of varying the area of the primary jet with respect

to the area of the mixing stack. Ellin verified a correla-

tion between dimensionless parameters representing the

pressure depression in and the induced flow from a secondary

environment by the eductor. These parameters were suggested

by a one dimensional analytic model. Ellin's work was

followed by Moss [Ref. 4], and Harrell [Ref. 5].

The work of Ellin, Moss, and Harrell was conducted ex-

clusively in the cold flow facility, and it was considered

essential that actual operating conditions be investigated

to verify these results. Ross [Ref. 6] undertook the actual

construction, calibration, and test verification of the hot

flow test facilty. Under the recommendations of the previous
researchers, Welch [Ref. 7] conducted the initial hot flow
testing using a four nozzle, solid walled mixing stack
eductor.

C. IMPROVEMENTS IN MIXING STACK CONFIGURATION

Reports of significant pressure depression throughout
the length of the original straight, solid walled mixing
stacks suggested that additional, or tertiary flow could be
induced into the mixing stack along its length. Additionally,
it was considered that this flow could be used to reduce ex-
ternally detectable surface temperatures by means of film
cooling. Staehli and Lemke [Ref. 8] investigated the use
of cooling ports in the mixing stack at the cold flow facility
to determine its potential.

Hill [Ref. 9] followed Welch in hot flow testing and con-
sidered the performance of a slotted mixing stack under actual
operating parameters. Eick [Ref. 10] and Kavalis [Ref. 11]
conducted follow-on research in the hot flow test facility
using the slotted mixing stack with multiply-shrouded eductors
and observed excellent results confirming the cold flow
analysis.

D. CURRENT OBJECTIVES

The objectives of this investigation were to verify the
high temperature performance of an eductor configuration

tested by Pritchard [Ref. 12] in the cold flow facility, conduct calibration of the entrance nozzle for more accurate determination of air mass flow rates, and determine the effects of turbulent cross-flow on eductor performance.

III.   THEORY AND MODELING

Eductors are relatively simple devices in which a jet of fluid (primary jet) is directed into a co-axial mixing chamber in such a manner that a volume of secondary fluid becomes entrained in the flow and a pumping action occurs. The fluids may be in liquid or gaseous form, or a combination.

The eductor described in this research is used to pump gases at relatively low velocities. Of specific consideration is the ability of a relatively hot primary gas jet to entrain and mix with a cooler ambient fluid (air) to produce a uniform flow at some desirable intermediate temperature. Mach number similarity has been chosen as the link in dynamic similarity between the primary gas flow rates of the models and the prototype. Dimensionless parameters controlling the flow are used throughout the analysis. These parameters were derived from a one-dimensional analysis of a simple eductor.

A.   MODELING TECHNIQUE

Based on the average flow properties of the eductor prototype, the air flow in the mixing stack eductor system is turbulent ($Re > 10^5$). As a consequence of this turbulence, momentum exchange is predominant over shear interaction, and the kinetic and internal energy terms are more influential on the flow than are viscous forces. It can be shown that

26

the Mach number is a more significant parameter than Reynolds number in describing this turbulent flow; therefore, as stated previously, it is the Mach number which has been maintained to more accurately represent the primary flow relationship between prototype and model.

B. ONE-DIMENSIONAL ANALYSIS OF A SIMPLE EDUCTOR

The theoretical analysis of an eductor may be approached in two ways. One method attempts to analyze the details of the mixing process of the primary and secondary air streams as it takes place inside the mixing stack. This requires an interpretation of the mixing phenomenon which, when applied to a multiple nozzle system, becomes extremely complex. The other method, which was chosen here, analyzes the overall performance of the eductor system and is not concerned with the actual mixing process. To avoid repetition of previous reports only the main parameters and assumptions will be presented here. A complete derivation of the analysis used can be found in [Ref. 2] and [Ref. 3]. The one-dimensional flow analysis of the simple eductor system (Fig. 1) described depends on the simultaneous solution of the continuity, momentum, and energy equations coupled with the equation of state, all compatible with specific boundary conditions.

The idealizations made for simplifying the analysis are as follows:

1) The flow is steady state and incompressible.

27

2) Adiabatic flow exits throughout the eductor with
isentropic flow of the secondary stream from the plenum
(at section 0) to the throat of entrance of the mixing
stack (at section 1) and irreversible adiabatic mixing
of the primary and secondary streams occurs in the mixing
stack (between sections 1 and 2).

3) Isentropic flow of the tertiary flow exists from the
tertiary plenum to the minimum area at Section 2, with irre-
versible adiabatic mixing of the flows between Sections 2
and 3.

4) The static pressure across the flow at the entrance
and exit planes of the mixing-tube (at sections 1 and 2) is
uniform.

5) At the mixing stack entrance (section 1) the primary
flow velocity U_p and temperature T_p are uniform across the
primary stream, and the secondary flow velocity U_s and temper-
ature T_s are uniform across the secondary stream, but U_p does
not equal U_s, and T_p does not equal T_s.

6) At Section 2, the mixing of primary and secondary
air has an average velocity, U_x, and an average temperature,
T_x.

7) Incomplete mixing of the primary, secondary, and
tertiary streams in the mixing stack is accounted for by
the use of a non-dimensional momentum correction factor K_m
which relates the actual momentum rate to the pseudo-rate
based on the bulk-average velocity and density and by the

use of a non-dimensional kinetic energy correction factor K_e which relates the actual kinetic energy rate to the pseudo-rate based on the bulk-average velocity and density.

8) Both gas flows behave as perfect gases.

9) Changes in gravitational potential energy are negligible.

10) Pressure changes P_{os} to P_1, P_{ot} to P_2, P_1 to P_2 and P_2 to P_3 ($=P_a$) are small relative to the static pressure, so that the gas density is essentially dependent upon temperature and atmospheric pressure.

11) Wall friction in the mixing stack is accounted for with the conventional pipe friction factor term based on the bulk-average flow velocity U_m and the mixing stack wall area A_w.

The following parameters, defined here for clarity, will be used in the following development.

$\dfrac{A_P}{A_M}$ ratio of primary flow area to mixing stack cross section area

$\dfrac{A_W}{A_M}$ ratio of wall friction area to mixing stack cross sectional area

K_P momentum correction factor for primary mixing

K_M momentum correction factor mixed flow

f wall friction factor

29

Based on the continuity equation, the conservation of
mass principle for steady flow yields

$$W_M = W_P + W_S + W_T \qquad \text{(eqn 3.1)}$$

where

$$W_P = \rho_P U_P A_P$$

$$W_S = \rho_S U_S A_S$$

$$W_T = \rho_T U_T A_T$$

$$W_M = \rho_M U_M A_M \qquad \text{(eqn 3.2)}$$

All of the above velocity and density terms, with the
exception of ρ_M and U_M, are defined without ambiguity by
virtue of idealizations (4) and (5) above. Combining equa-
tions (3.1) and (3.2) above, the bulk average velocity at
the exit plane of the mixing stack becomes

$$U_M = \frac{W_s + W_t + W_p}{\rho_M A_M} \qquad \text{(eqn 3.3)}$$

where A_M is fixed by the geometric configuration and

$$\rho_M = \frac{P_a}{R T_M} \qquad \text{(eqn 3.4)}$$

where T_M is calculated as the bulk average temperature from
the energy equation (3.11) below. The momentum equation

stems from Newton's second and third laws of motion and is
the conventional force and momentum-rate balance in fluid
mechanics.

$$K_p \left(\frac{W_p U_p}{g_c} \right) + \left(\frac{W_s U_s}{g_c} \right) + \left(\frac{W_t U_t}{g_c} \right) + P_1 A_1 = K_M \left(\frac{W_m U_m}{g_c} \right) + P_2 A_2 + F_{fr}$$

(eqn 3.5)

Note the introduction of idealizations (4) and (7). To
account for a possible non-uniform velocity profile across
the primary nozzle exit, the momentum correction factor K_p
is introduced here. It is defined in a manner similar to
that of K_M and by idealization (5), supported by work conducted
by Moss, it is set equal to unity. K_p is carried through
this analysis only to illustrate its effect on the final
result. The momentum correction factor for the mixing stack
is defined by the relation

$$K_M = \frac{1}{W_m U_m} \int_o^{A_m} U_3^2 \, \rho_3 dA$$

(eqn 3.6)

where U is evaluated as the bulk-average velocity from equa-
tion (3.3). The wall skin friction force F can be related
to the flow stream velocity by

$$F_{fr} = f A_w \left(\frac{U_m^2 \rho_m}{2 g_c} \right)$$

(eqn 3.7)

31

using idealization (11). As a reasonably good approximation
for turbulent flow, the friction factor may be calculated
from the Reynolds number

$$F = 0.046 \ (Re_m)^{-0.2} \qquad \text{(eqn 3.8)}$$

Applying the conservation of energy principle to the steady
flow system in the mixing stack between the entrance and
exit plane,

$$W_p(h_p + \frac{U_p^2}{2g_c}) + W_s(h_s + \frac{U_s^2}{2g_c}) + W_t(h_t + \frac{U_t^2}{2g_c})$$

$$= W_m(h_m + Ke \ \frac{U_m^2}{2g_c}) \qquad \text{(eqn 3.9)}$$

neglecting potential energy of position changes (idealization
9). Note the introduction of the kinetic energy correction
factor K_e, which is defined by the relation

$$Ke = \frac{1}{W_m U_m^2} \ \int_o^{A_m} U_3^2 \ \rho_3 dA \qquad \text{(eqn 3.10)}$$

It may be demonstrated that for the purpose of evaluating
the mixed mean flow temperature T_m, the kinetic energy terms
may be neglected to yield

$$h_m = \frac{W_p}{W_m} \ h_p + \frac{W_s}{W_m} \ h_s + \frac{W_t}{W_m} \ h_t \qquad \text{(eqn 3.11)}$$

where $T_m = \emptyset(h_m)$ only, with the idealization (8).

The energy equation for the isentropic flow of the
secondary air flow from the plenum to the entrance of the
mixing stack may be shown to reduce to

$$\frac{P_{os} - P_s}{\rho_s} = \frac{U_s^2}{2g_c} \qquad \text{(eqn 3.12)}$$

similarly, the energy equation for the tertiary air flow
reduces to

$$\frac{P_o - P_t}{\rho_t} = \frac{U_t^2}{2g_c} \qquad \text{(eqn 3.13)}$$

The previous equations may be combined to yield the vacuum
produced by the eductor action in either secondary or tertiary
air plenums. Letting $P_3 = P_m = P_a$ and assuming that
$A_3 = A_m \approx A_2 \approx A_1$ and assuming the friction between sections
2 and 3 is negligible, the vacuum produced for the secondary
air plenum is

$$P_a - P_{os} = \frac{1}{g_c A_m} [K_p \frac{W_p^2}{A_p \rho_p} + \frac{W_s^2}{A_s \rho_s}(1-1/2 \frac{A_m}{A_s}) + \frac{W_t^2}{A_t \rho_t} -$$

$$\frac{W_m}{A_m \rho_m} (K_m + \frac{f}{2} \frac{A_m}{A_m})] \qquad \text{(eqn 3.14)}$$

where it is understood that A_p and ρ_p apply to the primary
flow at the entrance to the mixing stack, A_s and ρ_s apply to
the secondary flow at this same section, and A_m and ρ_m apply

to mixed flow at the exit of the mixing stack system. P_a is atmospheric pressure, and is equal to the pressure at the exit of the mixing stack. A_w is the area of the inside wall of the mixing stack.

For the tertiary air plenum, the vacuum produced is

$$P_a - P_{ot} = \frac{1}{g_c A_m} \left[K_2 \left(\frac{W_p + W_s}{\rho_2 A_m} \right)^2 + \frac{W_t^2}{\rho_t A_m} \left(1 - 1/2 \frac{A_m}{A_t} \right) - K_m \frac{W_m^2}{\rho_m A_m} \right] \qquad \text{(eqn 3.15)}$$

where the primary flow now consists of both the primary and secondary air flows, and where K_2 is the momentum correction factor at section 2.

C. NON-DIMENSIONAL FORM OF THE SIMPLE EDUCTOR EQUATION

In order to satisfy the criteria of geometrically similar flows, the non-dimensional parameters which govern the flow must be determined. The means chosen for determining these parameters was to normalize equations (3.14) and (3.15) with the following dimensionless groupings.

$$P* = \frac{\frac{P_a - P_{os}}{\rho_s}}{\frac{U_p^2}{2g_c}}$$

a pressure coefficient which compares the pumped head $(P_a - P_{os})$ for the secondary flow to the driving head $(U_p^2/2g_c)$ of the primary flow

$$PT* = \frac{\frac{P_a - P_{ot}}{\rho_t}}{\frac{U_p^2}{2g_c}}$$

a pressure coefficient which compares the pumped head $(P_a - P_{ot})$ for the tertiary flow to the driving head $(U^2/2g_c)$ of the primary flow

34

$W^* = \dfrac{W_s}{W_p}$ a flow rate ratio, secondary to primary mass flow rate

$WT^* = \dfrac{W_t}{W_p}$ a flow rate ratio, tertiary to primary mass flow rate, W_t^*

$T^* = \dfrac{T_s}{T_p}$ an absolute temperature ratio, secondary to primary

$TT^* = \dfrac{T_t}{-}$ an absolute temperature ratio, tertiary to primary, T_t^*

$\rho_s^* = \dfrac{\rho_s}{\rho_p}$ a flow density ratio of the secondary to primary flow. Note that since the fluids are considered perfect gases,

$\rho_s^* = \dfrac{T_p}{T_s} = \dfrac{1}{T_s^*}$; $P_s \approx P_p$ and $P_t \approx P_p$

$\rho_t^* = \dfrac{\rho_t}{\rho_p}$ a flow density ratio of the tertiary or film cooling flow to primary flows. (Note that since the fluids are considered perfect gases

$\rho_t^* = \dfrac{T_p}{T_t} = \dfrac{1}{T^*}$)

$A_s^* = \dfrac{A_s}{A_p}$ a ratio of secondary flow area to primary flow area

$A_t^* = \dfrac{A_t}{A_p}$ a ratio of tertiary flow area to primary flow area

With these non-dimensional groupings, equations (3.14) and (3.15) can be rewritten in dimensionless form.

$$\frac{P*}{T*} = 2\frac{A_p}{A_m} \{ (K_p - \frac{A_p}{A_m}\beta) - W*(1+T*)\frac{A_p}{A_m}\beta + \frac{W_t * T_t *}{A_t *}$$

$$+ W*^2 T* (\frac{1}{A*}(1 - \frac{A_m}{2A*A_p}) - \frac{A_p}{A_m}\beta)\} \qquad \text{(eqn 3.16)}$$

where

$$\beta = K_m + f_2 \frac{A_w}{A_m} \qquad \text{(eqn 3.17)}$$

This may be rewritten as

$$\frac{P*}{T*} = C_1 + C_2 W*(T*+1) + C_3 W* T + C_4 W_t *^2 T_t * \qquad \text{(eqn 3.18)}$$

where

$$C_1 = 2\frac{A_p}{A_m}(K_p - \frac{A_p}{A_m}\beta), \qquad \text{(eqn 3.19)}$$

$$C_2 = -2(\frac{A_p}{A_m})^2 \beta, \qquad \text{(eqn 3.20)}$$

$$C_3 = 2\frac{A_p}{A_m} \{\frac{1}{A*}(1 - \frac{A_m}{2A*A_p})\beta - \frac{A_p}{A_m}\beta\}, \qquad \text{(eqn 3.21)}$$

$$\text{and} \quad C_4 = \frac{1}{A_t *} \qquad \text{(eqn 3.22)}$$

The additional dimensionless quantities listed below have been used in past research to correlate the static pressure distribution down the length of the mixing stack.

36

$$PMS = \frac{\frac{PMS}{\rho_s}}{\frac{U_p^2}{2g_c}}$$

a pressure coefficient which compares the pumping head (PMS/ρ_s) for the secondary flow to the driving head ($U_p^2/2g_c$) of the primary flow, where PMS = static pressure along the mixing stack length

$\frac{X}{D}$ ratio of the axial distance from the mixing stack entrance to the diameter of the mixing stack

D. EXPERIMENTAL CORRELATION

For the geometries and flow rates investigated, it was confirmed by Ellin [Ref. 2] and Moss [Ref. 4] that a satisfactory correlation of the variable P*, T* and W* takes the from

$$\frac{P*}{T*} = \emptyset \ (W*T*^n) \qquad\qquad \text{(eqn 3.23)}$$

where the exponent "n" was determined to be equal to 0.44. The details of the determination of n = 0.44 as the correlating exponent for the geometric parameters of the gas eductor model being tested is given by Ellin. To obtain a gas eductor model's pumping characteristic curve, the experimental data is correlated and analyzed by using equation (3.23), that is, P*/T* is plotted as a function of $W*T*^{0.44}$. This correlation is used to predict the open to the environment operating point for the gas eductor model. Variations in the model's geometry will change the pumping ability,

37

which can be evaluated from the plot of equation (3.23).
The value of parameter $W*T*^{0.44}$ when $P*/T* = 0$ is referred
to as the pumping coefficient. Since the tertiary flow is
much less than the secondary flow, it has been demonstrated
by Lemke and Staehli [Ref. 8], and Drucker [Ref. 13] that
the pumping characteristic is relatively insensitive to
tertiary flow.

E. PUMPING COEFFICIENT

The pumping coefficient derived from non-dimensional
parameters provides a basis for analyzing the eductor's
pumping capability. Changes in stack geometries such as
L/D ratio, slotting, shrouding, diffuser rings, and spacing
between stack and shroud, and between shroud and diffuser
rings will alter the eductor's pumping performance and the
pumping coefficient. The pumping coefficients for the model
should correspond to the coefficients for the shipboard
eductor system. At the shipboard operating point, the
eductor is exposed to no restrictions in the secondary or
tertiary air flows. In the model, this is simulated by com-
pletely opening the air plenums which provides an open-to-
the-environment simulation. Unfortunately, at this condition
and secondary and/or tertiary air flow rates cannot be measured.
The eductor model's characteristics are first established over
the measurable flow range and then extrapolated to the desired
operation point.

38

The data for this extrapolation is established by varying the associated induced air flow rate, either secondary or tertiary, from zero to its maximum measurable rate. These rates are determined by sequentially opening the ASME flow nozzles mounted to the plenum and recording the pressure drop across the nozzles. Values for nozzle cross sectional areas, pressure drops, induced flow are temperatures, and barometric pressure are then used to calculate the dimension- less parameters $P*/T*$, and $W*T*^{0.44}$. The dimensionless para- meters are then plotted as illustrated in Figure 42. Data point (1) is the maximum vacuum which is produced by the eductor with no secondary flow, obtained by closing all ASME flow nozzles. Data points in region (2) correspond to opening most of the ASME flow nozzles and the final point corresponds to opening all flow nozzles. Although the data points in region 2 appear to be zero or nearly so, they do have a small finite value. The uncertainty associated with these points is relatively high with the data collected in this research considered qualitively accurate to within ± 0.05 of the re- ported value which was obtained via linear regression. The data points in region (3) provide the most consistent and accurate data. Extrapolation of the pumping characteristic curve to intersect with the abscissa at $P*/T*=0$ locates the appropriate operating point for the eductor model configuration.

IV. EXPERIMENTAL APPARATUS

The test facility apparatus currently in use was designed, fabricated, and installed by Ross [Ref. 6] and used by all follow-on researchers for hot primary flow analysis. A Boeing 502 gas turbine engine combustor section and turbine nozzle were used to construct the gas generator. Various components of the engine's fuel system were modified by Ross to support a simplified combustor layout. Air for combustion is supplied by a Carrier centrifugal air compressor (three stage) which is located in building 230 of the Naval Postgraduate School Annex. The actual model testing and gas generator operation is controlled from the hot test facility, building 249. Appendix A provides detailed instructions for safe and proper operation of the gas generator.

A. COMBUSTOR AIR PATH

Combustion air and cooling air supplied by the centrifugal air compressor pass from the compressor discharge via underground pipe between buildings 230 and 249. Air enters the test facility through a vertical standpipe containing an eight inch butterfly valve in parallel with a remote-manual bypass globe valve (Figure 16). This butterfly valve is normally closed with flow through the bypass valve being of sufficient volume to operate the gas generator. Figure 7 is the layout of the gas generator. At the top of the standpipe is a "T"

40

connection. In one direction flow passes through an eight

inch butterfly valve and enters a short section of piping

which is used by the Aeronautical Engineering Department to

supply various experiments. The second arm of the "T"

supplies the combustion gas generator through an eight inch

to four inch reducing section (entrance nozzle). The flow

characteristics of this entrance nozzle were determined from

calibration data collected by this researcher and are pre-

sented in Appendix B. The pressure drop across this section

is used to determine the mass flow rate of air through the

gas generator assembly. A linear curve was fit to the data

of Table XXIX for use in data reduction programs. The corre-

lation is presented in Figure 41. Air flow next passes

through a manual isolation valve and enters a splitter section.

In the splitter section, a portion of the air flow is

directed through the motor operated burner air control valve

and the U-tube to the combustor section. The flow character-

istics of this section as determined by Ross are presented

in [Ref. 6]. The remaining air passes through the motor

operated cooling air bypass valve and enters the mixing

section. The mixing section was fabricated by Ross from

the nozzle box of the Boeing engine. A device was installed

in the nozzle box to introduce a swirl into the cooling air

which is counter to that produced by the nozzles. Hot gases

from the combustion section enter the mixing section through

the nozzles and the effect of the counter-rotating flow is to produce rapid and thorough mixing. Downstream of the mixing section is a flow straightener which is followed by an uptake section which delivers the gas flow to the primary nozzles.

B. FUEL SYSTEM

1. System Arrangement

Service fuel is stored in a 55 gallon drum mounted on an elevated stand adjacent to the building. Fuel flows from the storage tank through a tank isolation valve to a bulkhead isolation valve located inside building 249. A tank stripping and drain connection is located in the supply line outside the building. Adjacent to the interior bulk-head valve is a thermocouple connection for measuring fuel temperature. Fuel then passes through the flow measuring rotameter to a fuel filter. Taking suction on the filter is a 24V DC motor driven fuel supply pump. This positive displacement pump contains an internal bypass and pressure regulating feature. Normal pump discharge pressure is 14-16 PSIG.

The supply pump provides positive suction head for the high pressure pump. This pump has no internal bypass and must be provided with an external recirculation loop when in operation. Valves placed in the recirculation are used to control the pump discharge pressure and thus, the

42

flow of fuel to the burner nozzle. Downstream of the recir-
culation connection is a system drain valve and a manually
operated discharge valve, Figure 25. From the discharge
valve, fuel is piped to an electrically operated solenoid
valve located at the entrance to the combustor.

2. Fuel System Flow Rate Measurement and Control

A Fischer Porter Model 10A3565A rotameter is installed
to monitor fuel flow rate. Calibration was performed in place
by Eick using the fuel supply pump to discharge fuel into a
container for a fixed period of time. The quantity of fuel
discharged was weighed on a gram scale and the mass determined.
Flow rate was controlled using a needle valve at the pump out-
let. Rotameter calibration data is given in Table I. Figure
40 plots fuel mass flow against rotameter reading. A linear
curve fit to the data results in the expression

$$WF = -3.076 + 0.4048 * ROTA \qquad (eqn \ 4.1)$$

Hill [Ref. 9] had recommended that the system's fuel
control valve be replaced with a needle valve to improve sen-
sitivity and control. The existing arrangement used a ball
valve mounted on the pump table as a fuel control valve. A
long mechanical linkage extended across the building to the
control station. Not only did this linkage seriously impede
access around the gas generator, but this arrangement made
accurate adjustment of the fuel flow difficult; therefore,

43

a 3/8 inch stainless steel tubing was used to extend the high
pressure pump recirculation line to the control station. The
ball valve was retained as the control valve and mounted on
the bench at the control station. This valve permits the
operator to rapidly select any desired operating pressure in
a single motion.

To increase the sensitivity of the fuel control valve,
a needle valve was installed in parallel with it close to the
high pressure pump, Figure 25. This valve, which is always
partially open, permits flow through the recirculation line
even when the fuel control valve is fully closed. Thus flow
through the pump is assured even when both the fuel control
and the pump discharge valves are closed.

This needle valve ("trimmer" valve) is used to estab-
lish the range of control for the fuel control valve. When
properly adjusted this system provides smooth operation over
a range of high pressure pump discharge pressures from 80 to
350 psig. Since the high pressure pump's maximum output
pressure is specified to be 375 psig, control is obtained
over most of the pump's useful range. Fuel pressure is
easily adjusted to within 5 psig of a desired setpoint and
with some care can accurately be varied in increments as
small as 2 psig.

C. THE MEASUREMENT PLENUM

1. The Rear Seal

A flexible seal is installed at the rear wall. This diaphragm seal is formed from a rubberized fabric. The fabric is bedded in a layer of silicone sealant and clamped to the uptake with a band clamp. A similar layer of sealant is applied to the plenum rear wall and the seal attached with a split clamping ring. Figure 18 is a view of the plenum interior showing the finished uptake and the diaphragm seal. The rear seal provides uniformity in uptake gas temperature, with temperatures between the uptake mid-section and the primary nozzle now varying less than two degrees F.

2. The Forward Seal

The forward seal bulkhead is within the plenum and seal plates are provided to clamp to the entrance section of the mixing stack. A double O-ring assembly is utilized on the outer circumference of the inlet to the mixing stack to provide proper sealing.

3. Model Installation and Alignment

An adjustable support stand was designed and constructed to support the mixing stack assembly independently of the seal plates. This stand facilitates model installation and alignment. Alignment is accomplished by mounting the model on the stand, installing centering plates in each end of the mixing stack and in the open of the uptake pipe, and adjusting the stand until the alignment bar passes

freely through holes in the centering plates. The alignment apparatus can be seen in Figure 27. Standoff distance is then set by installing the straight primary nozzles on the uptake and measuring the required distance from the nozzle exit plane to the mixing stack entrance plane (the termination of the entrance radius -- 0.5 inch) using a combination square. This adjustment normally requires no more than 0.125 inch movement of the model when a 0.5 standoff distance is desired.

Due to the longitudinal expansion observed by Eick, the installed standoff distance was modified from 3.5610 inches to 3.6875 inches to compensate accordingly.

D. INSTRUMENTATION

1. Temperature Measurement

Two types of thermocouple displays are installed with each having the capability to accept eighteen (18) channels. A type K display provides data on combustion temperatures, uptake temperatures and mixing stack wall temperatures. Table II gives the current channel assignments. The type T display is used to measure inlet air, ambient air, fuel, and shroud and diffuser temperatures. Table III gives the current channel assignments. The display installation is shown in Figure 12.

2. Pressure Measurement

Five manometers, shown in Figure 14, are installed for gas generator operation and data collection. They include a 20 inch water manometer for measurement of differential pressure across the inlet reducing section (DELPN), an oil manometer (range 0-17 inches water) for measuring uptake pressure (PUPT), a 20 inch mercury manometer for measuring inlet air pressure (PNH), a 2 inch inclined water manometer used to measure the differential pressure across the burner U-tube (DELPU), and a 6 inch inclined water manometer connected to a distribution manifold. Five individual manifolds located in the main control panel (Figure 13) are interconnected to permit measurement of plenum and mixing stack pressures with respect to atmospheric pressure. Mixing stack pressures both above and below atmospheric can be displayed.

E. THE MODELS

Two eductor models were tested. Both models were tested with and without a cross-flow. Each model consisted of a primary nozzle plate mounted on the end of the uptake piping and a mixing stack, shroud and diffuser assembly. Characteristic eductor dimensions are given in Figure 6. In both models tested the mixing stack interior diameter "D", was 7.122 inches. This dimension is the same as used in previous hot primary flow testing and is 0.6087 scale of the cold flow models. Both models tested employed a standoff ratio, "S/D", of 0.5. Table IV provides a comparison of the key model characteristics.

1. Model A

Model A is shown in the test installation apparatus
in Figure 31. This configuration includes a primary nozzle
plate with four (15/20) tilted and angled nozzles. The
configuration of the nozzles refers to the characteristic
angles. The tilt of the nozzle is 15 degrees from the
vertical with the nozzle being rotated or "angled in" 20
degrees from the tangential direction. Figure 35 details
these angles for clarification. The ratio of the mixing
stack area to primary nozzle area is 2.5.

The mixing stack is enclosed in a low carbon, cold
rolled sheet steel shroud extending from X/D = 0.15 to X/D =
1.125. Five sheet steel diffuser rings 0.375 diameters long
are installed to bring the overall length of the assembly to
1.5 diameters. Film cooling clearance between the stack and
the shroud varies along the length of the model while the
film cooling clearance between the diffuser rings is 0.188
inches. The dimensions of this model are shown in Figure 4.
One row of thermocouples was installed along the length of
the shroud and diffusers oriented ninety degrees from a hori-
zontal plane passing through the model's centerline axis.
These twelve (12) type T thermocouple readouts were used as
a comparison to external readings obtained from an Omega
Engineering 871 digital thermocouple with fully remote prob-
ing capability.

2. Model A Modified

The second model tested was a modified version of the first in that an extra diffuser ring was located outside the fifth ring of Model A. This ring was of the same thickness, material and length, and was geometrically concentric to diffuser ring number five of model A. The annular clearance between diffuser rings five and six was 0.188 inches. The dimensions of the modified model are shown in Figure 5.

F. THE CROSS-FLOW CENTRIFUGAL FAN

1. Installation and Configuration

The fan used to model the relative wind (cross-flow) was of the centrifugal type. It was manufactured by the Joy Manufacturing Company, General Products Division, New Philadelphia, Ohio.

The centrifugal fan was installed at the experimental site to be as mobile and portable as practicable considering its weight. To afford mobility for proper standoff positioning in relation to the model and facilitate certain data collection, the fan was mounted on a platform having heavy duty ball bearing casters. The lower section of the platform facilitated installation of a "step-up" transformer and provided adequate stowage of the power cable when the fan was not in service.

A converging nozzle was attached to the fan exit volute to provide directional stability to the air discharge,

and additionally to provide a datum for theoretical deter-
mination of discharge velocity. The fan nozzle exit area
was chosen arbitrarily to provide a nozzle discharge area
to model discharge area ratio of 3:1.

The fan is driven by a Reliance Duty Master AC motor.
The motor is a 440V, 3 phase, 4.8 amp, 60 Hz unit designed
for continuous duty at 1755 RPM when connected to the high
speed windings as was the case for this research.

Since the test facility, Bldg 249, does not have
440V power available, it was necessary to utilize 220V power
provided to a step-up transformer to provide the necessary
voltage. Once proper electrical connection and grounding
was made, starting the stopping of the fan was facilitated
safely by utilizing a five amp circuit breaker specifically
installed for the fan 220V supply circuit. A picture of the
cross-flow fan is shown in Figure 32.

2. Performance Capabilities

The cross-flow fan utilized has a nominal air flow
rate of 3000 CFM at a total pressure of 3.0 inches of water.
Maximum air flow rate is established at 4200 CFM at or below
1.0 inches of water total pressure. Since the total pressure
developed by the installed convergent nozzle was not known,
it was necessary to determine the fan's discharge velocity
profile experimentally, and thereby determine a quasi-optimum
nozzle to model standoff distance to provide a relatively

50

uniform flow field. Based upon theoretical calculations, discounting any losses, the maximum velocity achievable from the fan was estimated at thirty-five (35) knots.

To determine the actual velocity distribution at the exit plane of the fan nozzle and to determine a suitable standoff distance (nozzle to model), a flow measurement experiment using a pitot tube to measure total pressure was devised. The basic equation for estimation of the velocity in the flow stream is given by equation (7-53) of [Ref. 14].

$$P_0 - P_\infty = 1/2 \rho U_\infty^2 \qquad \text{(eqn 4.1)}$$

Four sets of data were collected. One data set was collected for each of the following pitot traverses: horizontal traverse at the nozzle exit plane, horizontal traverse at a standoff distance of twenty-four inches, vertical traverse at a twenty-four inch standoff, and a 4.5 inch vertical traverse at the bottom of the model (diffuser ring 5 on the model centerline) to a horizontal plane coincident with the model support and alignment base. This data is presented in Tables XXIII through XXVI.

Based upon the collected data the standoff distance of twenty-four inches (nozzle exit plane to model centerline) was determined suitable in representing an average flow field velocity of 29.5 knots.

V.   EXPERIMENTAL RESULTS

A.   MODEL A RESULTS

1.   Pumping Performance

The pumping performance of Model A is shown in Figures 43 through 48 with supporting data presented in Tables V through X.   Using the correlation previously developed in section (d) of Chapter III, a linear regression technique was utilized to determine the pumping coefficient for the specific uptake test temperature and cross-flow condition. Given the inherent uncertainty of the linear fit, specific- ally considering the uncertainty and data scatter present in the lower plenum pressure differential regime, the data presented for pumping coefficients is considered qualitively accurate to within ± 0.05. The pumping coefficient comparison to a geometrically similar model tested by Pritchard [Ref. 12] at the cold flow facility is considered valid.

A table of comparative results is presented in Table XXVII.

2.   Mixing Stack Temperatures

Figures 53 through 57 graphically present the data obtained from this model. Tabular results of the collected data are contained in Table XVII.

This model is equipped with twelve (12) type "K" thermocouples imbedded in the stack walls at various locations

to measure the film cooling effectiveness of the mixing stack slotted ports. The mixing stack thermocouple numbering system is referenced to a specific type "K" channel in Table II. Determination of film cooling effectiveness is achieved by referencing the appropriate temperature of thermocouples imbedded both upstream and downstream of the two selected cooling ports. An noted by Kavalis, [Ref. 11], it is suspected that due to the tilted angle of the nozzles, the flow is not uniform across the mixing stack and the sector between consecutive nozzles exhibit lower temperatures.

The data collected appears relatively consistent throughout when corrections for variation in ambient temperature are considered. The data reported has consistently higher temperatures than those reported by Eick [Ref. 10] and Kavalis [Ref. 11] who both used the tilted and angled primary nozzles with the slotted mixing stack but whose models used straight vice angled shrouds and diffusers. Since the entrance nozzle calibration conducted preliminary to actual model testing resulted in a lower air mass flow rate correlation, it is theorized that the lower temperatures observed by Eick and Kavalis were a result of the larger cooling effect from the induced tertiary air flow of the higher mixing stack air mass flow rates under which their investigations were conducted. The maximum wall temperatures reported by Eick and Kavalis are $306^{\circ}F$ and $320^{\circ}F$ respectively. This research resulted in a maximum wall temperature for Model A of $357^{\circ}F$.

Relative to cross-flow effects, no depression in
temperature was noticeable throughout the data when correc-
tion for the effect of ambient temperature is considered.

3. Mixing Stack Pressures

The data obtained for mixing stack pressure is pre-
sented in Figures 62 through 66 and in Table XV.

As noted by Eick, due to the small size of the pres-
sure tap and extremely long run of tubing (over 20 feet) to
the manometer, a substantial period of time was required for
the manometer reading to reach its final value. No oscilla-
tions were noticeable once a final value was reached. The
data collection was found to be consistently stable and
repeatable.

Comparison of the data is remarkably consistent
throughout the range of uptake temperatures. This model
compared to the straight shroud and diffuser models tested
by Eick and Kavalis tends to show an increase in mixing
stack pressure which might account for the increased wall
temperatures noted. The effect of cross-flow appears to be
an improvement in the mixing stack pressure profile. An
average increase of 15% was noted.

4. Shroud and Diffuser Temperatures

Shroud and diffuser temperatures were obtained util-
izing two methods. A type "T" thermocouple system having a
digital output servicing twelve channels of interest was used
in conjunction with a fully remote Omega Engineering model 871

thermocouple probe. The Omega remote reading thermocouple
was a portable battery operated device with a hand-held
surface probe and was of the type "K". Comparison between
these two temperature monitoring devices in an equilibrium
condition resulted in a mean temperature differential of
+0.5°F. This differential is acceptable under steady state
conditions; however, the transient effects observed during
the experimental data collection lead this researcher to
believe that the type "T" thermocouple readings were more
accurate. During data collection, and particularly during
cross-flow data collection, significant oscillations in
temperature were noticed with the remote probe device.
When the Omega probe was used to determine shroud and
diffuser external temperatures, an equilibrium condition
did not appear achievable for recording of a discrete tem-
perature. Initially, oscillation in the sensed temperature
occurred rapidly and then damped somewhat although oscilla-
tion did continue. This necessitated that the recorded
temperature be an average value with inherent error intro-
duced as a function of the data recorder. Despite this
drawback the surface probe did provide comparative data
and it was decided to continue data collection with this
device for a qualitative comparison with the type "T" data.

Using the "A" model for comparative analysis of the
noted differential in shroud and diffuser temperature between
the type "T" thermocouples and the Omega portable thermocouple

55

external probe readings, an uptake temperature of 950 degrees F was selected. In a no cross-flow condition (qualitively normalizing the data to account for a difference in ambient temperature) relative to shroud temperatures, only a minimal differential is observed with exception of the far end of the shroud which exhibits approximately a 20 degree difference. The maximum difference noted in diffuser ring temperature occurs for rings three and five. This difference is ten (10) degrees F. When cross-flow was introduced, the difference in shroud temperatures was minimal with the exception of the shroud end closest to the diffusers which showed an approximately ten (10) degrees F difference. Diffuser ring temperature differential was more pronounced in the cross-flow relative to the two temperature sensors with a maximum deviation of 25 degrees F for diffuser ring five and a mean diffuser ring temperature differential of 15 degrees F.

The surface probe temperature measurements were taken along the model's length starting at diffuser ring five and working rearward toward the after section of the shroud. The point of each measurement was taken along the surface of the model coincident with the model's centerline and oriented 180 degrees from the cross-flow. The sequence of the temperature measurements and relative distance from the mixing stack entrance are given by the X/D parameter values as shown in Figure 36.

Figures 71 through 75 present the shroud and diffuser temperatures obtained via the type "T" thermocouples while Figures 80 through 84 present the external surface probe data.

Data collected for the shroud in the no cross-flow condition show a consistently increasing temperature with the most notable increase being at the X/D = 1.068 position. When cross-flow was introduced the slope of the temperature profile appeared to flatten somewhat but again the X/D = 1.068 position showed a sharp increase in temperature. Cross-flow did result in a significant reduction in this high temperature reducing it approximately fifty degrees.

The five diffuser rings showed good temperature reduction potential until the fourth ring was reached when the effects of film cooling appeared to be dissipating and a continued increase of diffuser ring temperature was noticeable.

The effects of cross-flow resulted in an overall increase in diffuser ring temperature and resulted in an erratic although predictable temperature profile. The ultimate effect of the cross-flow appeared to be an overall shroud and diffuser assembly temperature reduction with some distortion of film cooling effects being induced by the cross-flow.

5. **Exit Plane Temperatures**

Figures 89 through 93 display the exit plane temperature data. Table XXI is a compilation of the data points presented in these figures.

A comparison of exit plane temperatue profiles, with and without cross-flow, is presented for the maximum uptake temperature of 950 degrees F. Good symmetry is observed in those profiles displayed with no cross-flow introduced with the exception of the 850°F uptake profile. It is considered that this asymmetry was caused by an inadvertent movement of the traversing mechanism which was noted during the data collection process.

Upon introduction of cross-flow it is noted that a depression of profile temperature takes place resulting in an average temperature reduction of greater than 50 degrees F. At the same time some increase in downstream profile temperature was noted in Model A.

The peak temperatures observed in Model A at uptake temperatures of 850°F and 950°F were 531°F (with cross-flow) and 586°F (no cross-flow) respectively.

B. MODEL A MODIFIED RESULTS

1. Pumping Performance

The pumping performance characteristics for the modified model were extremely close in comparison to those of Model A. A comparative summary is provided in Table XXVII.

Pumping coefficient plots are shown in Figures 49 through 52. Supporting tabular data is contained in Table XI.

2. Mixing Stack Temperatures

As anticipated, the modification of adding an additional diffuser ring to this model had little effect to change the mixing stack temperatures.

The temperature reduction noted upon introduction of cross-flow with Model A was also consistently noted for the data collected. It should be noted that any comparative analysis in this regard should be normalized to account for ambient temperature conditions.

Data collected for this model is presented in Figures 58 through 61 and Table XVIII.

3. Mixing Stack Pressures

This data which is presented in Figures 67 through 70 and Table XVI is consistent with the findings of Model A. The only minor exception being a slight reduction noted in the average pressure increase reported with the model under cross-flow conditions.

4. Shroud and Diffuser Temperatures

A reduction in temperature of approximately $20^\circ F$ was noted for diffuser ring five (5) which directly received the effects of the film cooling resulting from the addition of an extra diffuser ring. This temperature reduction effect was present both with and without the cross-flow introduced.

Without cross-flow no appreciable modification in shroud and diffuser temperatures was noticeable when normalization for ambient temperature is considered with the exception

59

of ring five as noted above. In a cross-flow condition the added film cooling effect of the additional diffuser ring resulted in an overall reduction in diffuser ring temperatures.

5. Exit Plane Temperatures

Figures 94 through 97 present the exit plane temperature for the modified model. Table XXII is a compilation of this data.

No appreciable change in peak temperature was observed for the modified model in comparison with Model A. The temperature depression effect induced by the cross-flow noted in Model A was also evident. In contrast with Model A, however, no increase in downstream profile temperature was noted. This is shown in Figure 99.

VI. CONCLUSIONS

This investigation studied the thermal and pumping performance of two multiply-shrouded, angled-diffuser stack gas eductors with five and six diffuser rings and how cross-flow at a mean velocity of 29.5 knots affected such performance. Based on the data presented the following conclusions are drawn:

1) Pumping coefficient data obtained in this investigation correlates with that of a geometrically similar model tested in the cold facility.

2) Introduction of cross-flow results in a slight improvement in eductor pumping performance.

3) Cross-flow effects in the mean velocity range studied in this investigation (29.5 knots) result in an overall temperature reduction at the surface of the assembly but tend to result in some distortion or degradation of the desired diffuser film cooling effects.

4) Cross-flow did not appear to have any significant effect upon a modification of the peak exit plane temperature.

5) The modified model produced superior film cooling effects in comparison to Model A.

6) Improvements in overall eductor performance and reduction in exit plane temperature appear feasible by optimization of the angled diffuser design to account for maximum film cooling effectiveness.

VII. RECOMMENDATIONS

Considering the experience gained in the conduct of this research and specifically in view of the results obtained, the following research recommendations are offered for future investigations.

1) Diffuser ring number one should be extended to a length approximately twice the current length to attempt to reduce the high temperature noted at the end of the shroud.

2) The cross-flow fan should be modified for two speed operations and other nozzle designs should be tested to provide a range of cross-flow velocities for model evaluation.

3) Further investigation of the flow phenomenon at end around the model's shroud and diffuser assembly should be conducted to explain the noted intermittent degradation of film cooling effectiveness.

4) Additional research should be performed to determine the variation in induced tertiary air flow resulting from a modification in air mass flow rate.
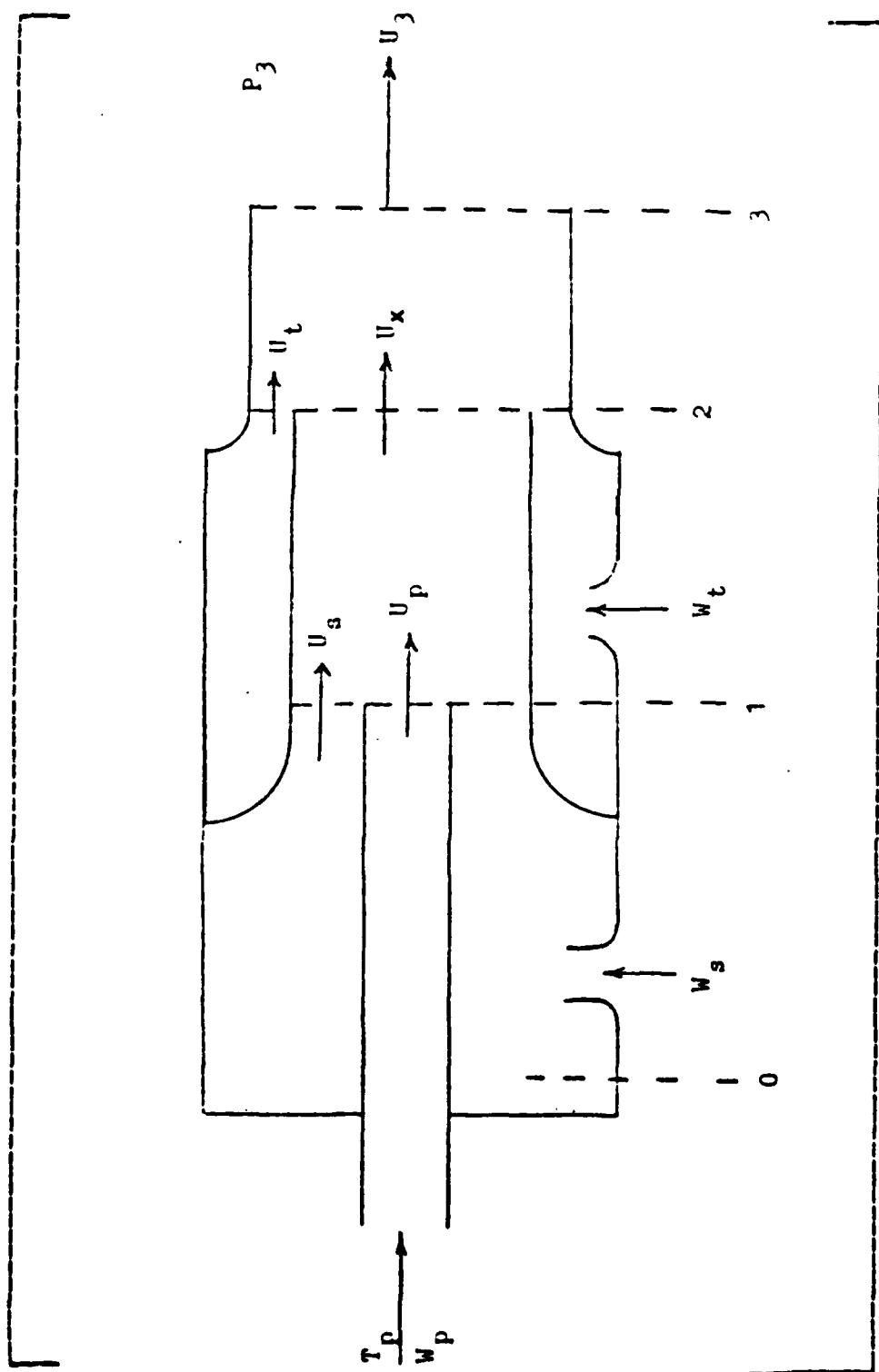
Figure 1. Simple Nozzle Eductor System.

63
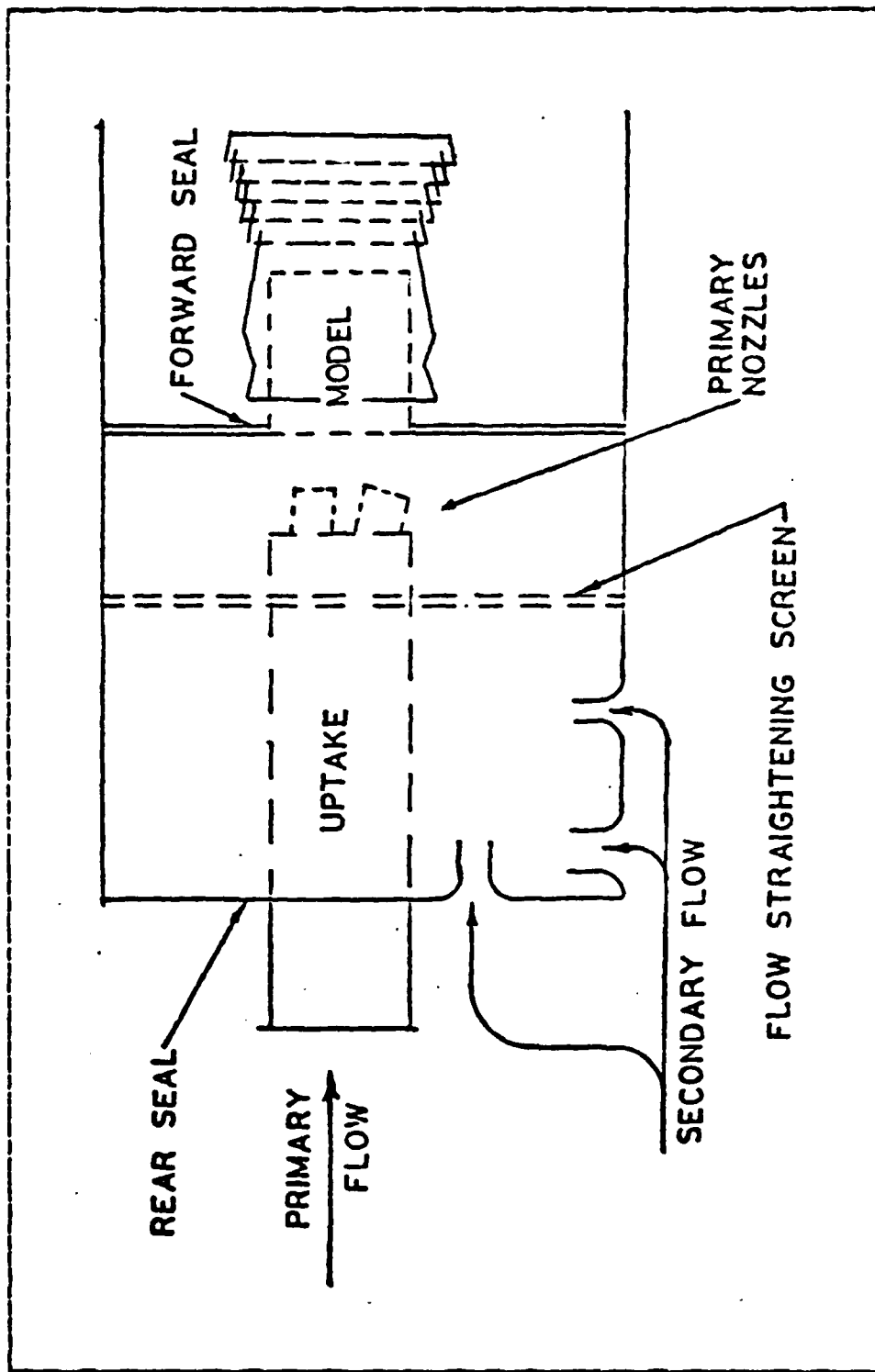
Figure 2. Plan of Uptake, Model, and Measurement Plenum.

64
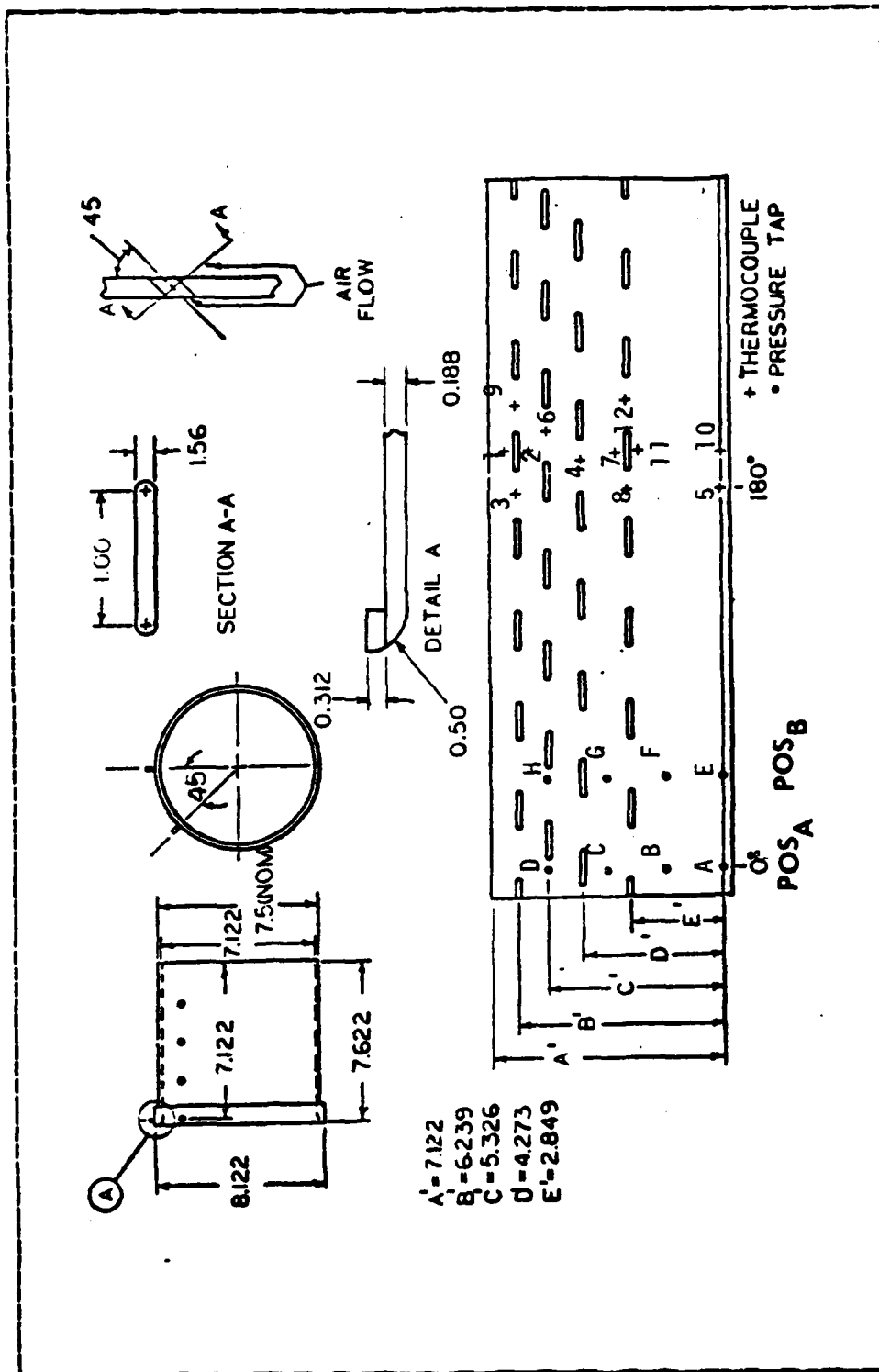
Figure 3. Dimensional Diagram of Slotted Mixing Stack.
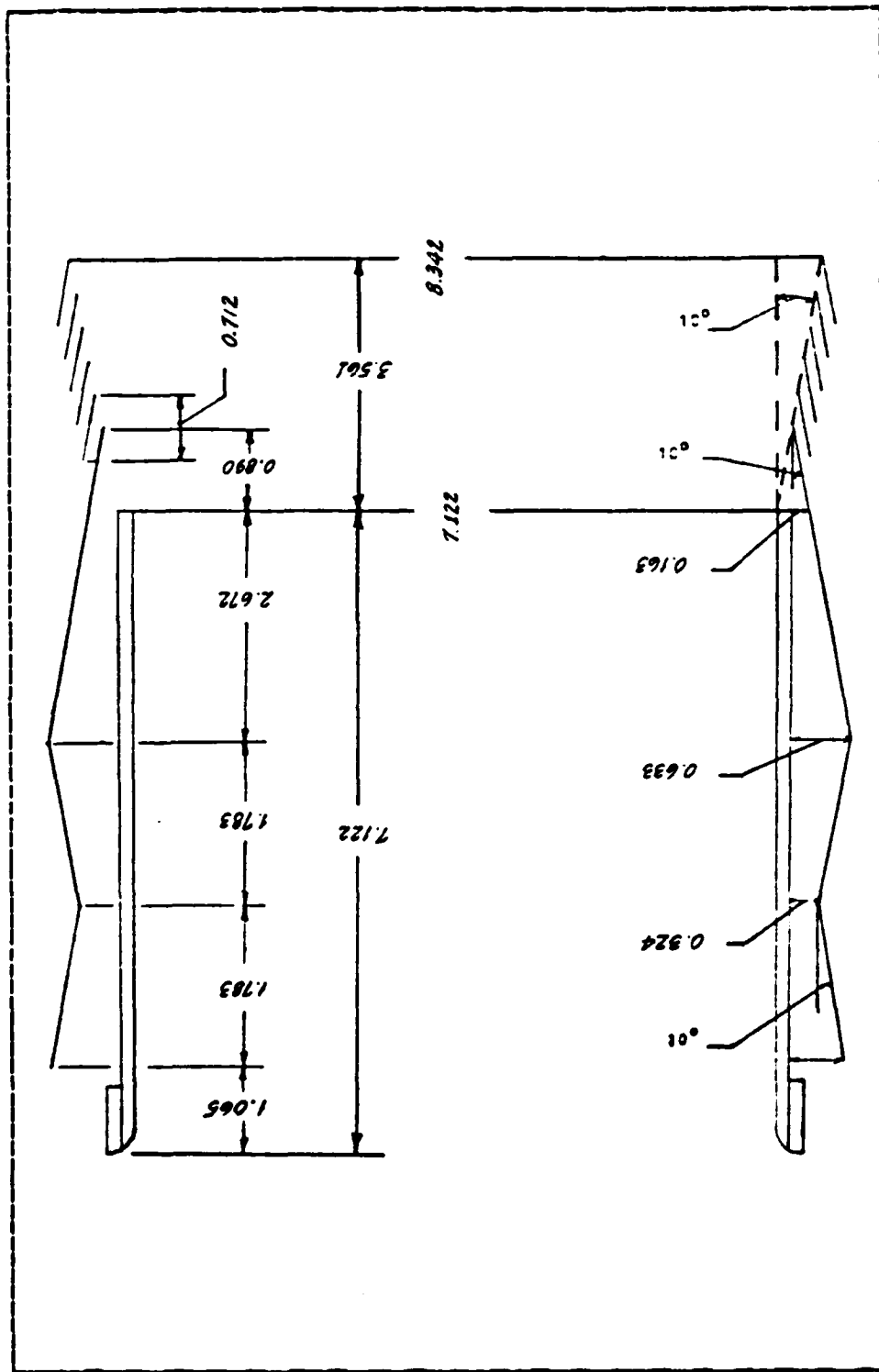
Figure 4. Schematic of Model A – Shroud and Diffuser Rings.
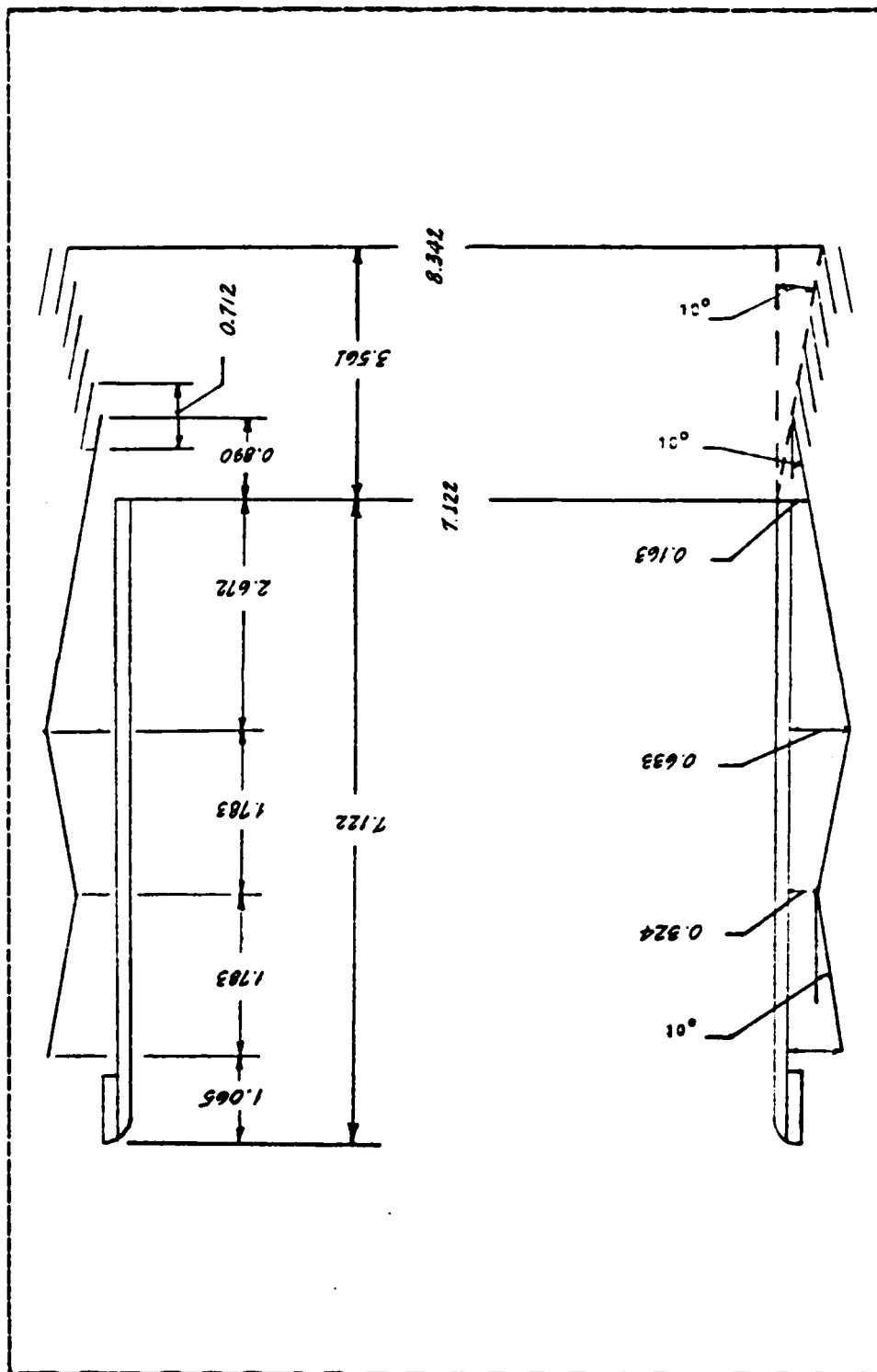
Figure 5. Schematic of Model A Modified – Shroud and Diffuser Rings.
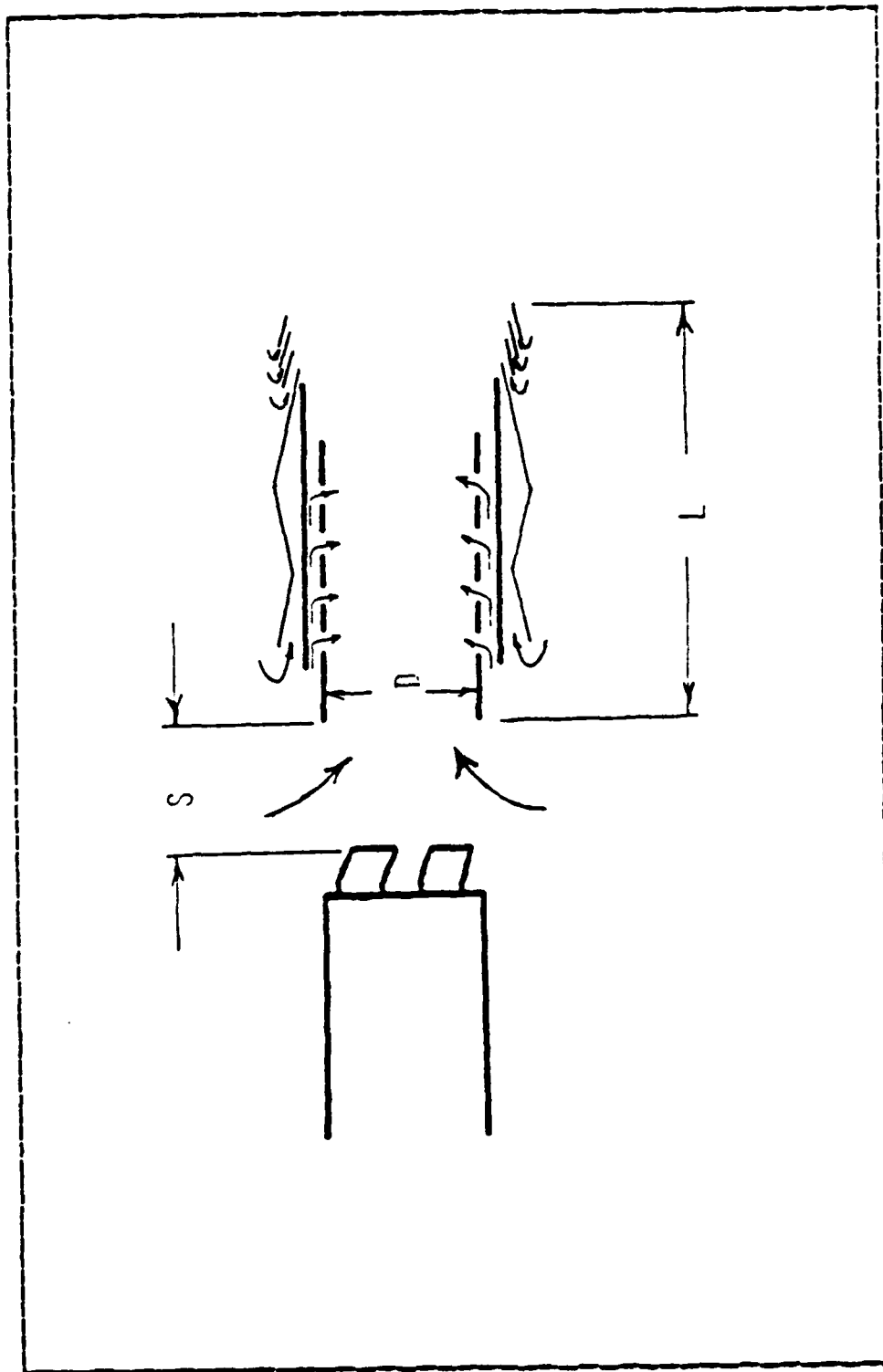
Figure 6.   Characteristic Eductor Dimensions.
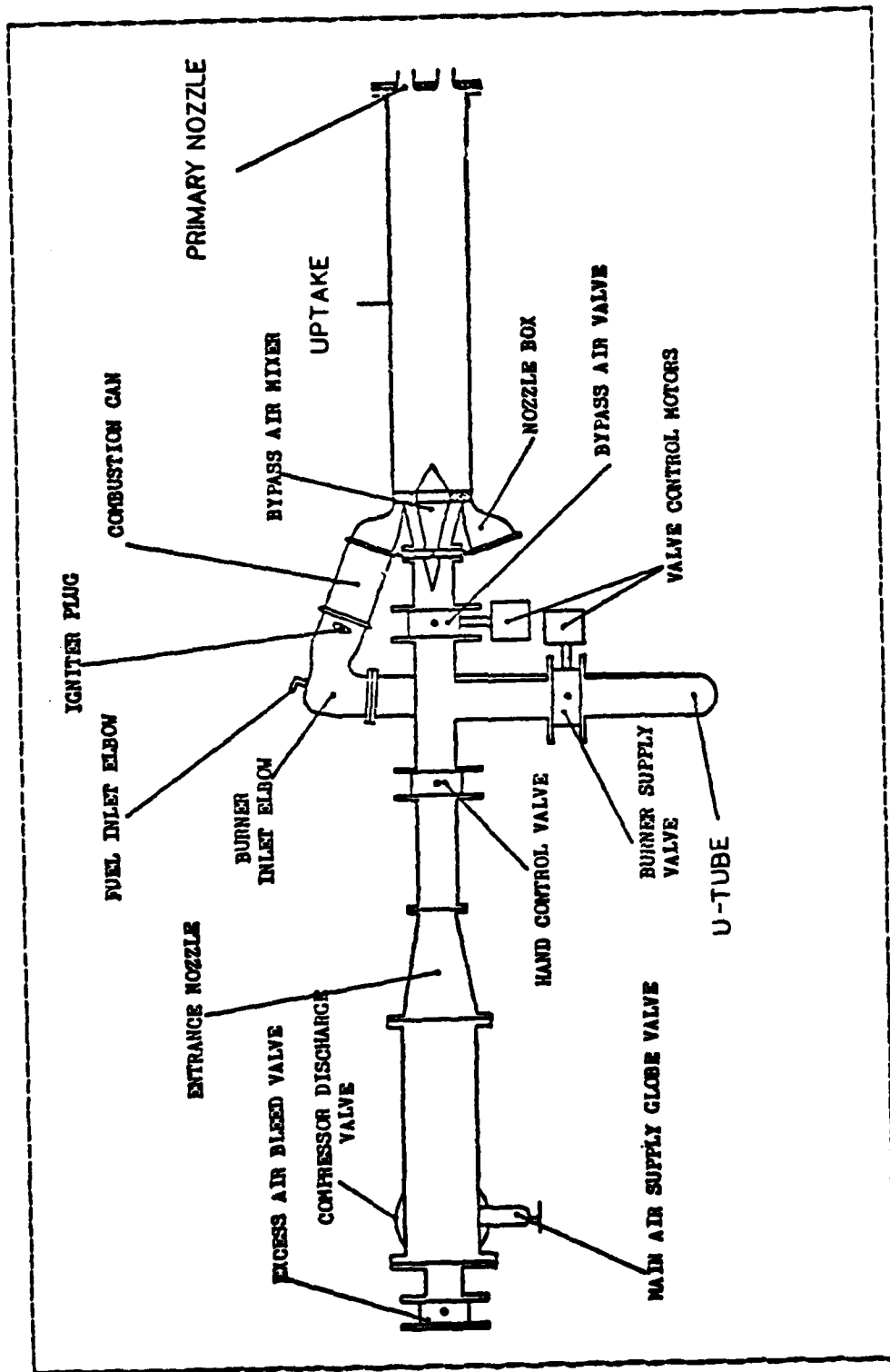
Figure 7. Gas Generator Arrangement.

PRIMARY NOZZLE

UPTAKE

COMBUSTION CAN

BYPASS AIR MIXER

NOZZLE BOX

BYPASS AIR VALVE

IGNITER PLUG

VALVE CONTROL MOTORS

FUEL INLET ELBOW

BURNER INLET ELBOW

HAND CONTROL VALVE

BURNER SUPPLY VALVE

U-TUBE

ENTRANCE NOZZLE

EXCESS AIR BLEED VALVE

COMPRESSOR DISCHARGE VALVE

MAIN AIR SUPPLY GLOBE VALVE

69
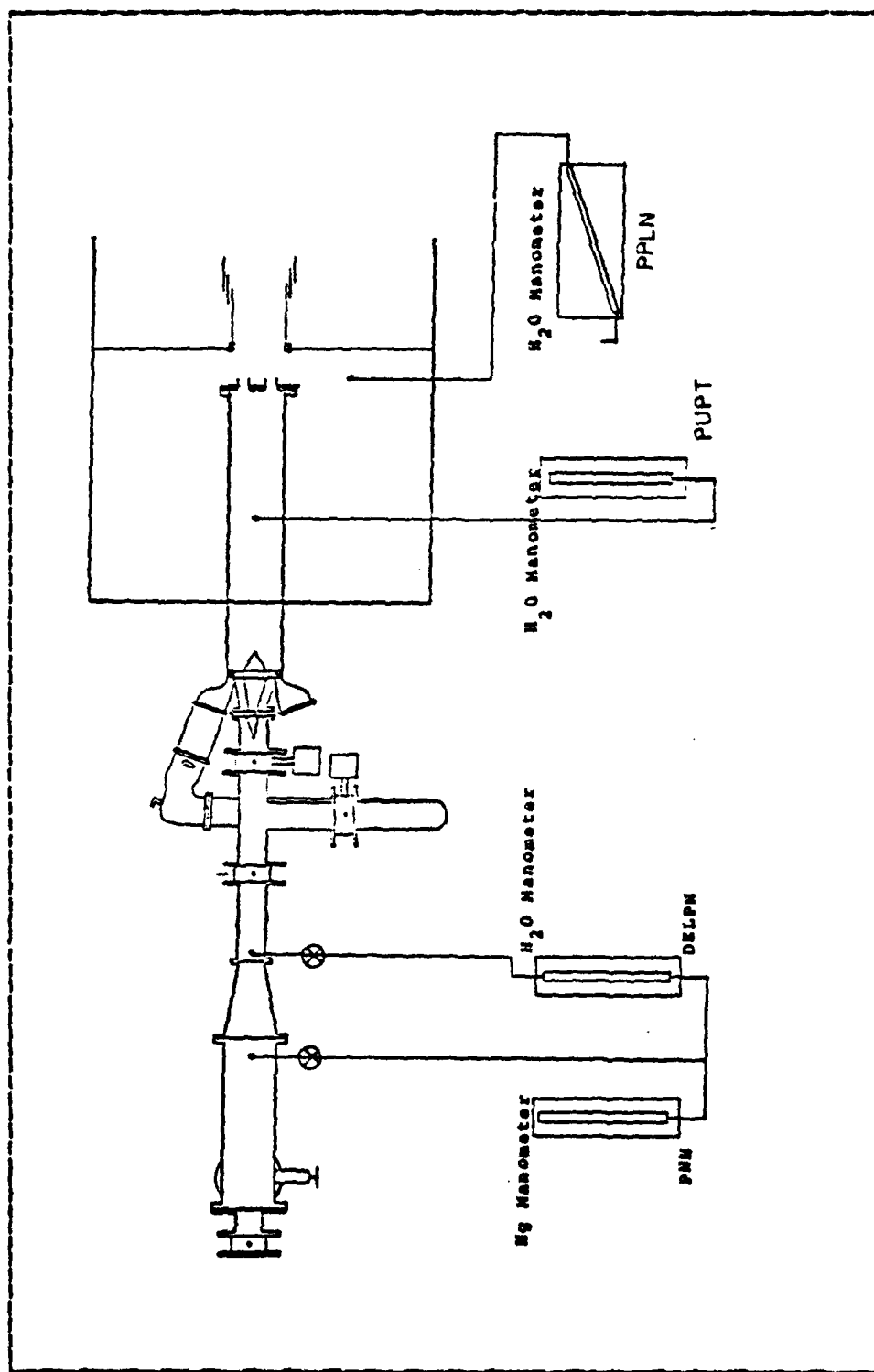
Figure 8.   Schematic Diagram of Pressure Measurement System.
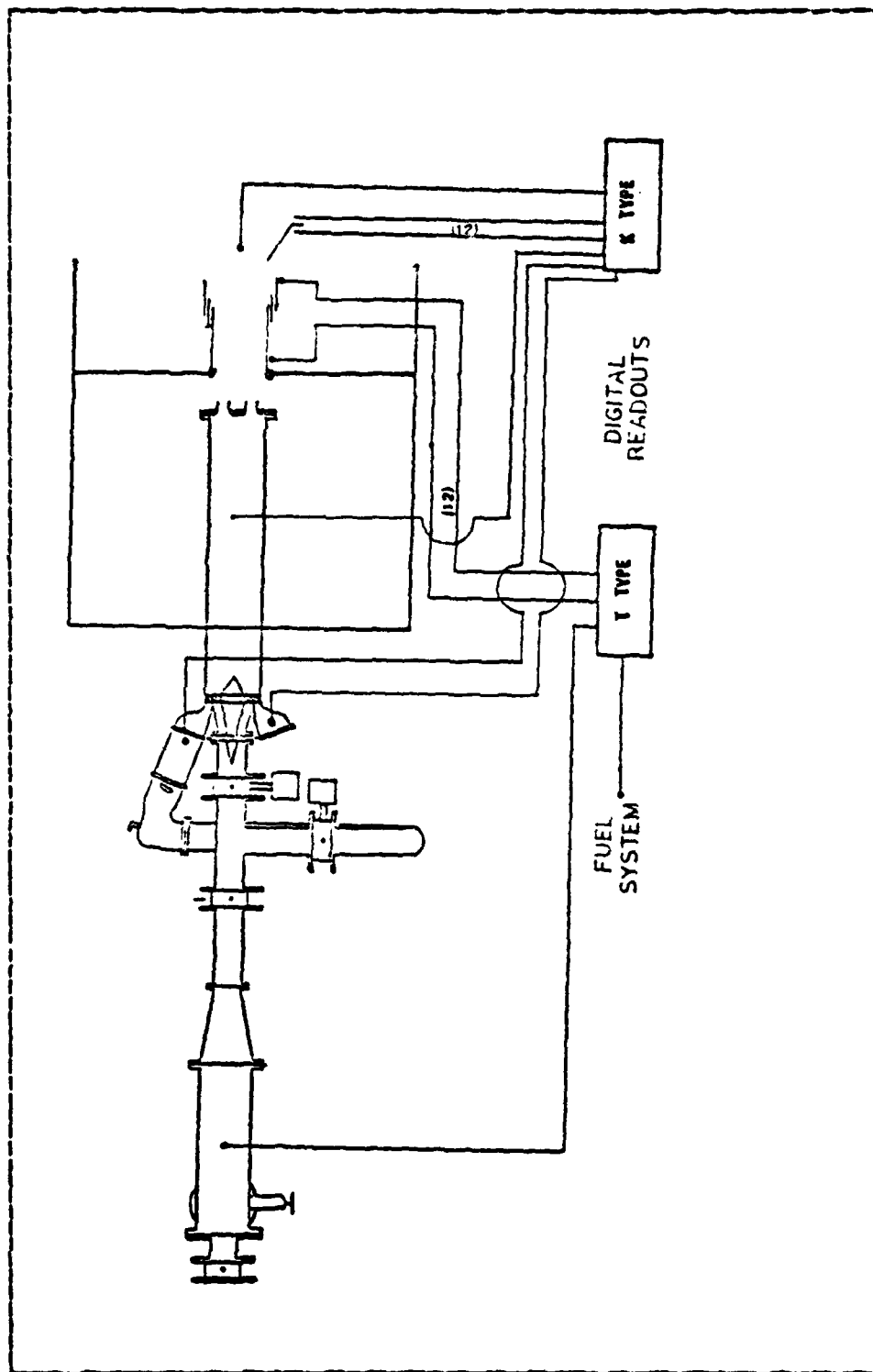
Figure 9. Schematic Diagram of Temperature Measurement System.
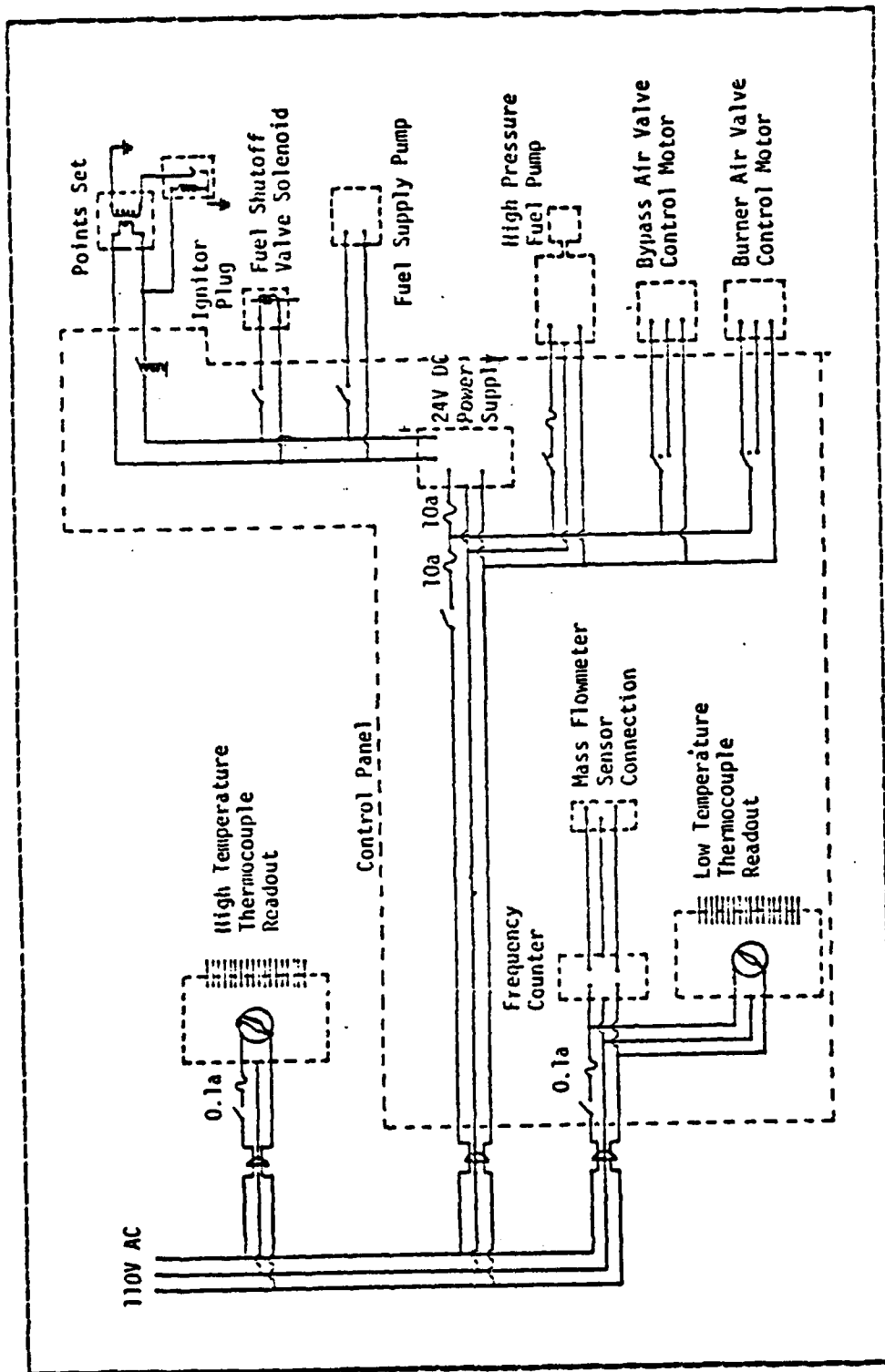
Figure 10. Gas Generator Electrical System.

72
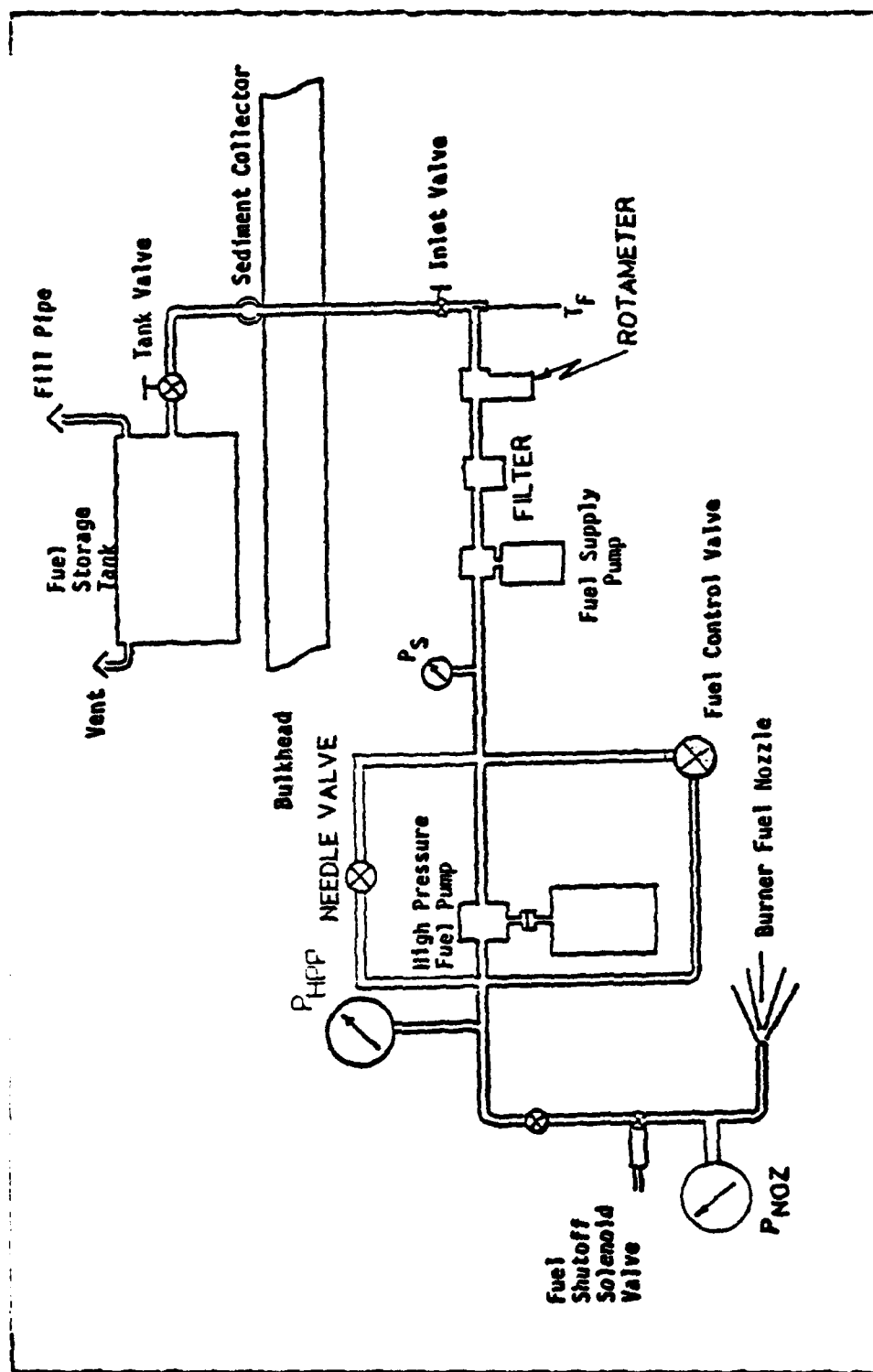
Figure 11. Gas Generator Fuel System.

CONTROL PANEL

TYPE T READOUT

FUEL CONTROL VALVE

TYPE K READOUT
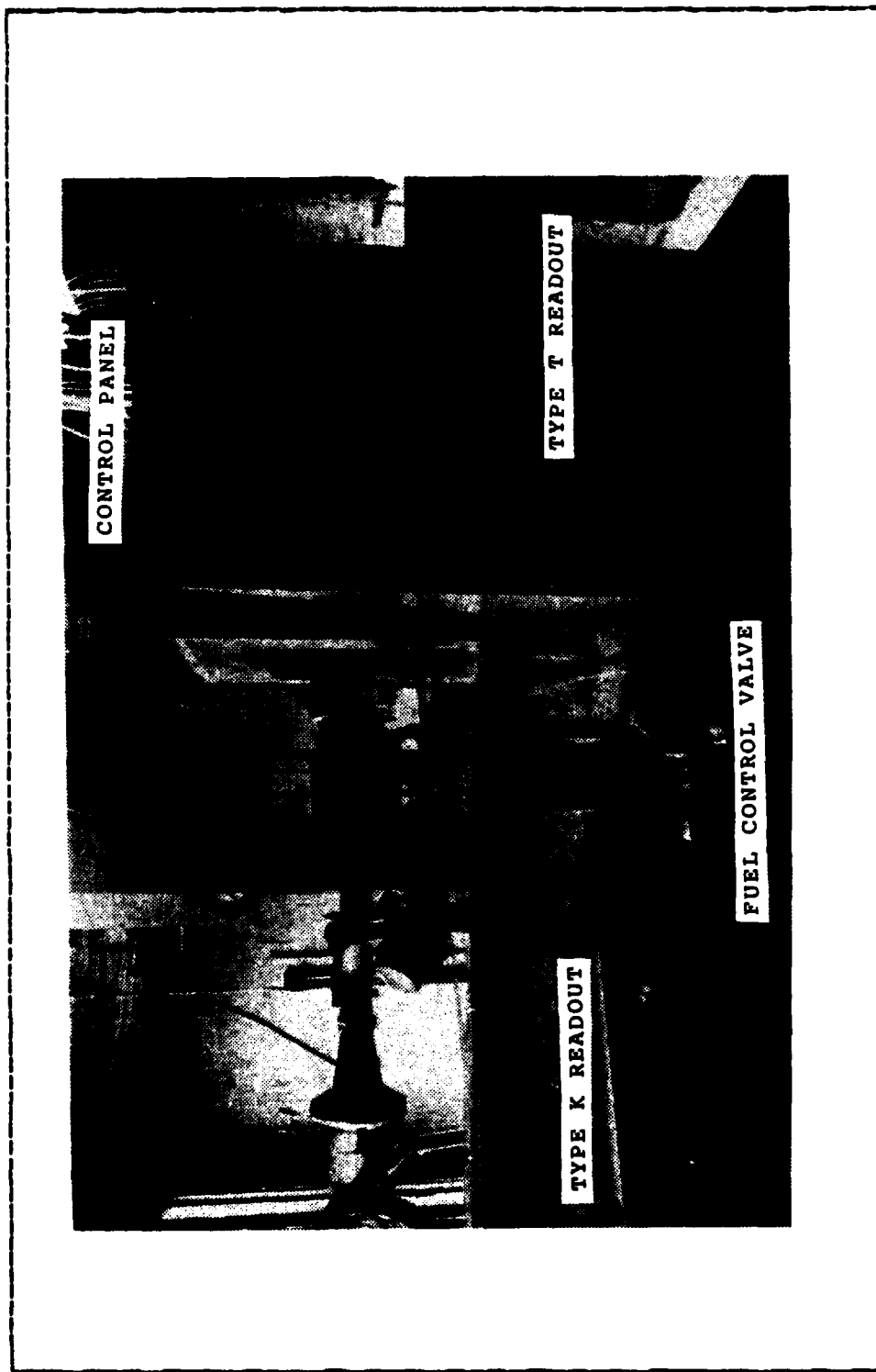
Figure 12. Gas Generator Control Station.

Figure 13.   Main Power Supply and Control Panel.
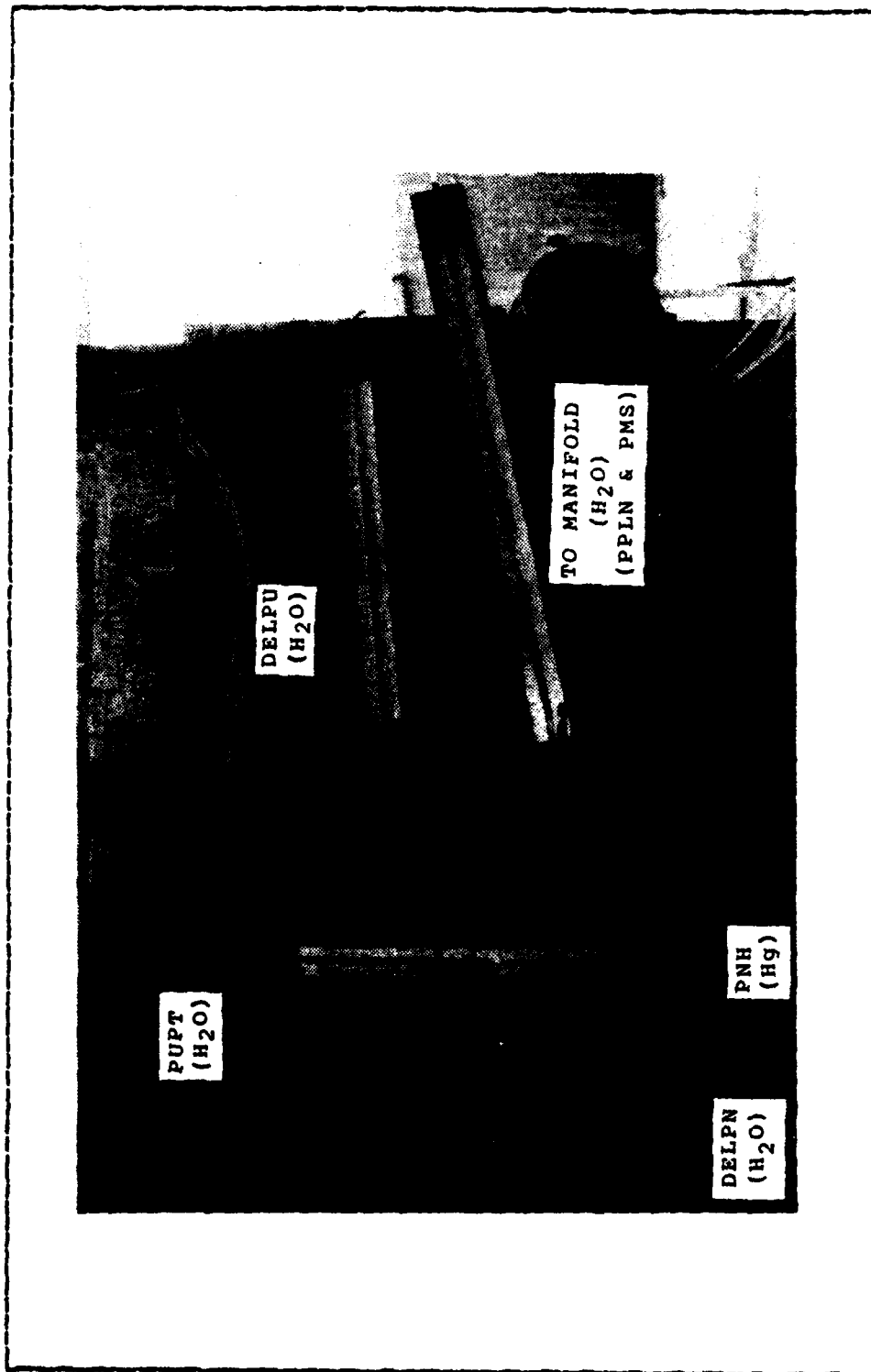
Figure 14. Manometer Installation.

Labels visible in figure:
- DELPU (H$_2$O)
- TO MANIFOLD (H$_2$O) (PPLN & PMS)
- PUPT (H$_2$O)
- PNH (Hg)
- DELPN (H$_2$O)

PLENUM

MODEL

UPTAKE

GAS GENERATOR
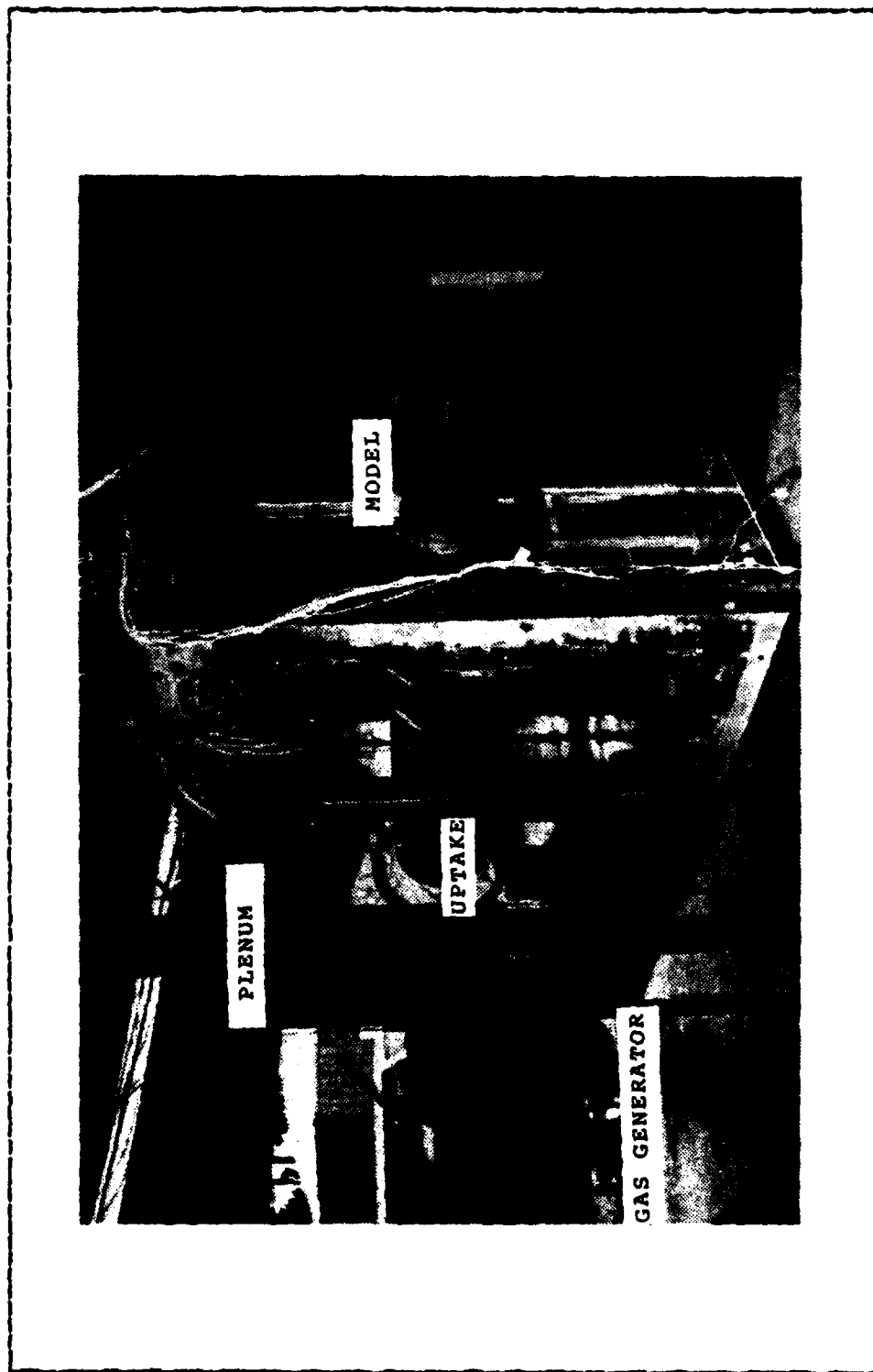
Figure 15.   Hot Flow Test Facility.
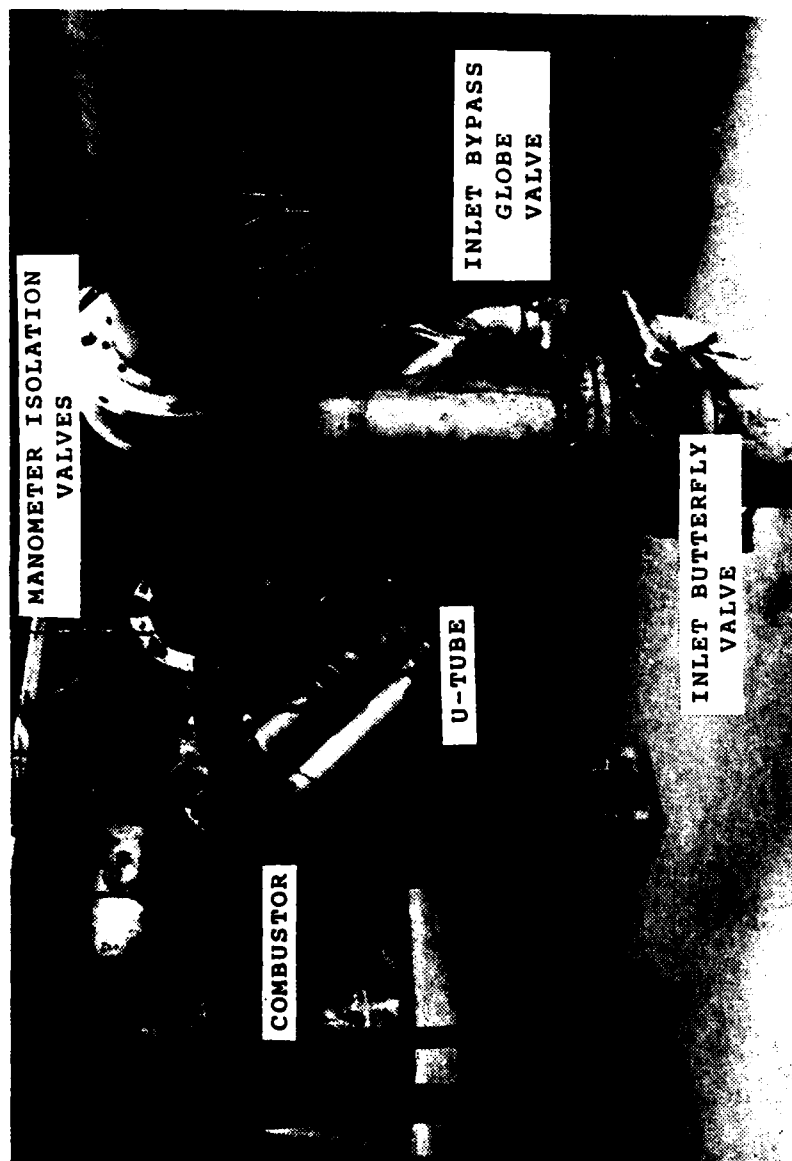
Figure 16. Air Supply Standpipe and Valving.

INLET BYPASS
GLOBE
VALVE

MANOMETER ISOLATION
VALVES

INLET BUTTERFLY
VALVE

U-TUBE
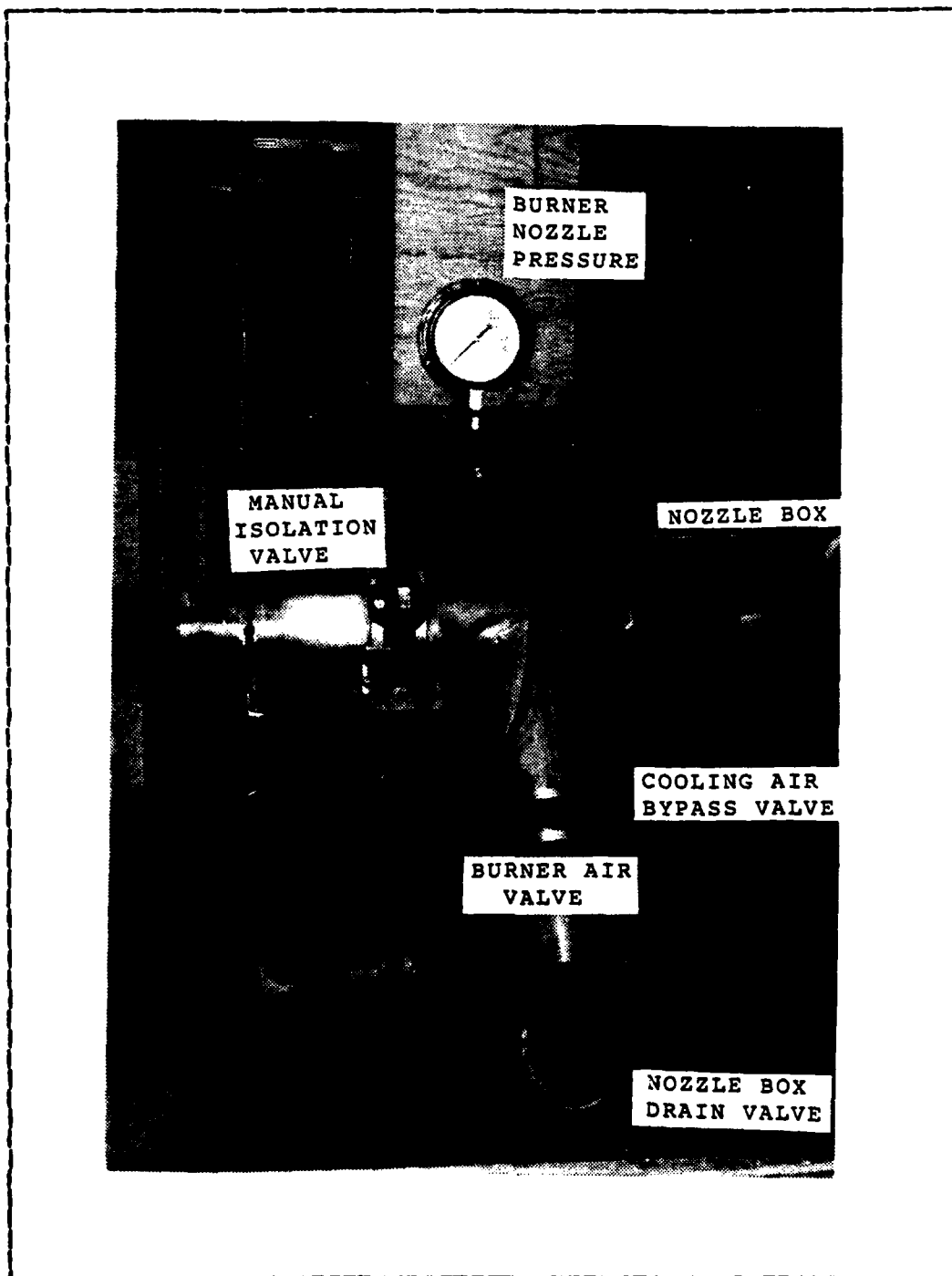
COMBUSTOR

Figure 17. Combustor Air Piping.
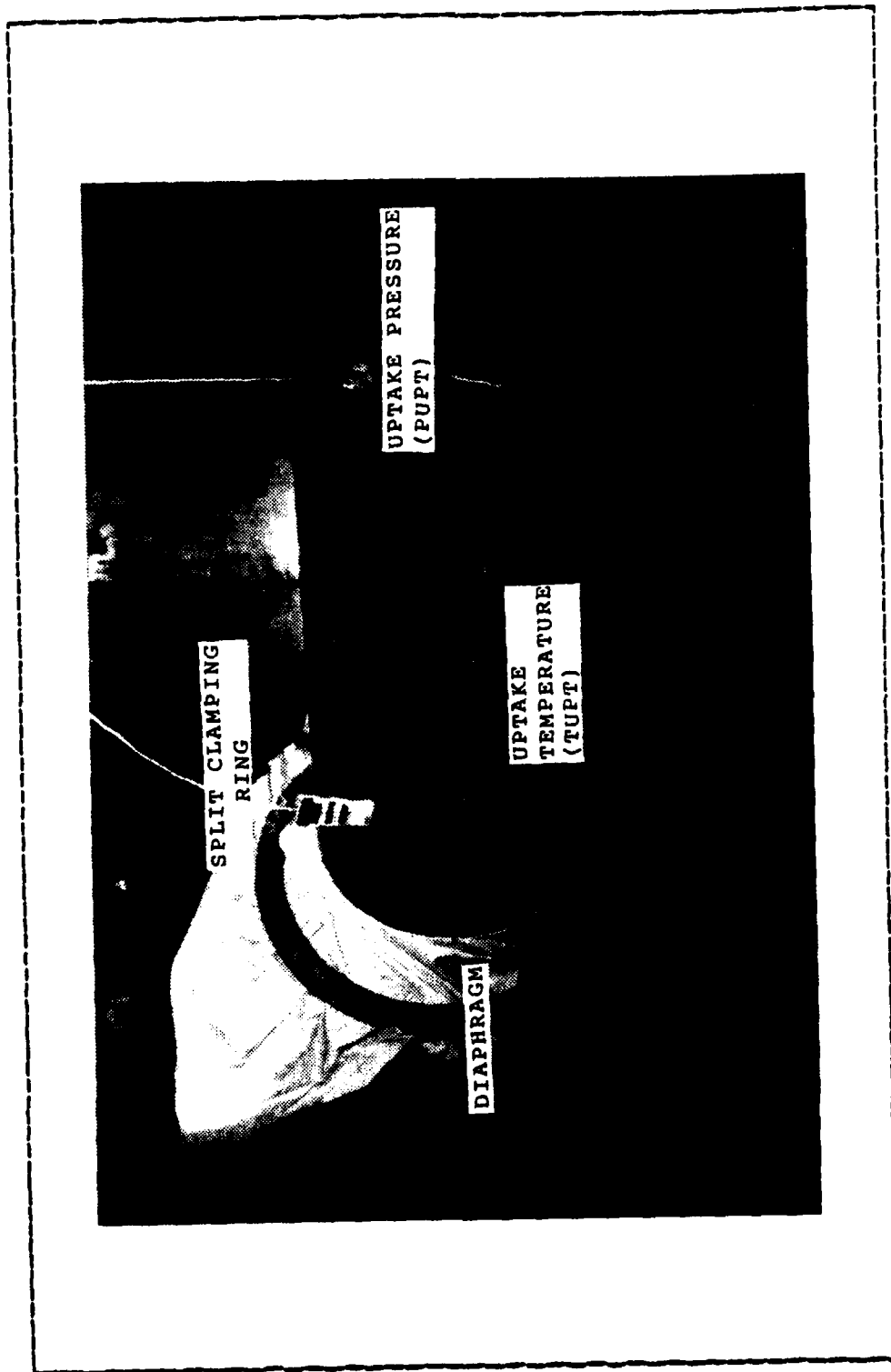
Figure 18. Uptake Section.
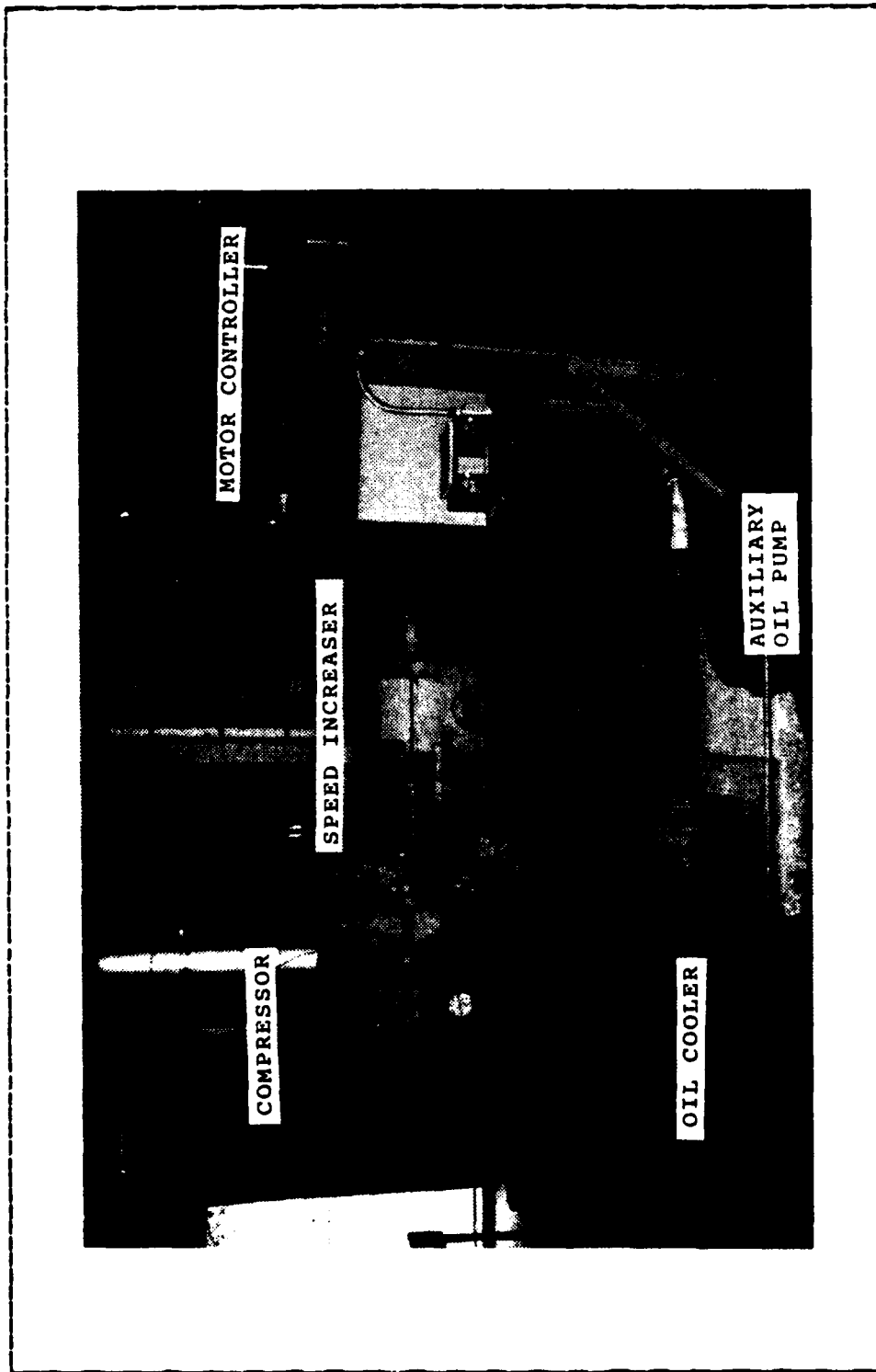
Figure 19. Carrier Air Compressor.

POSITION
INDICATOR
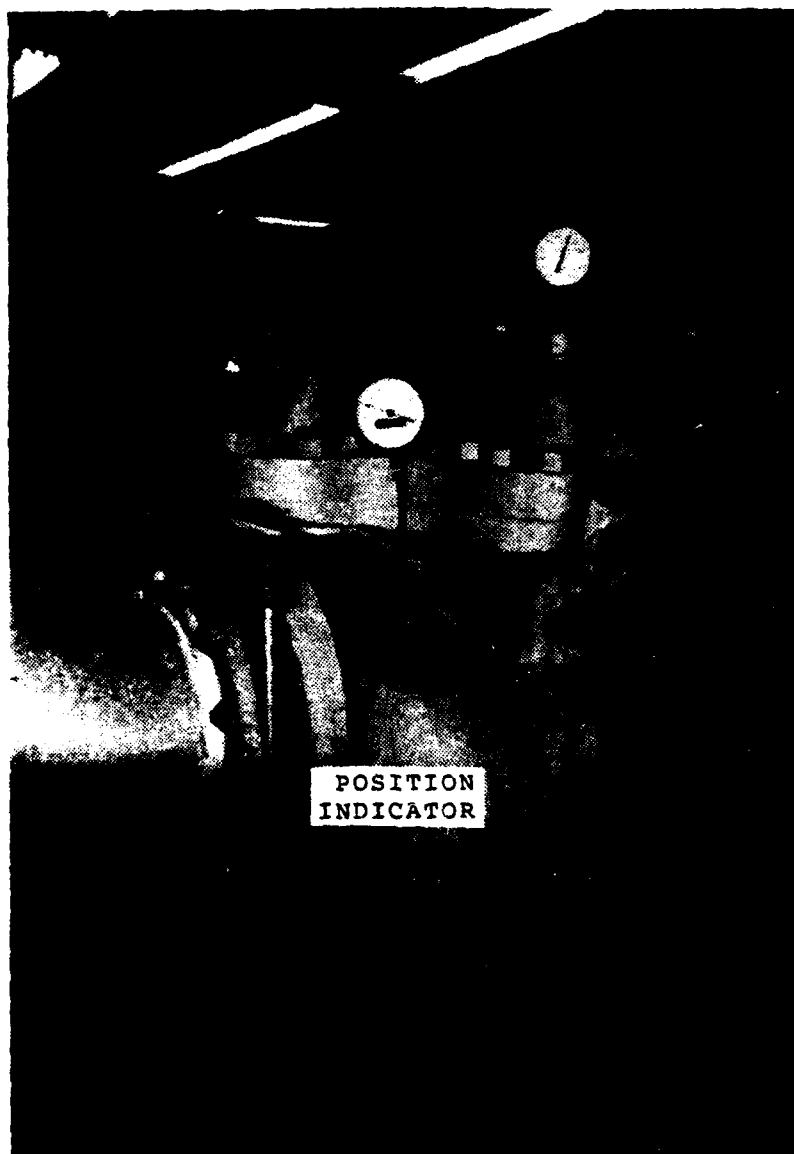
Figure 20.   Air Compressor Suction Valve.

BYPASS AIR
DISCHARGE

AIR COOLING
BANK ISOLATION
VALVE

COOLING BANK
DRAIN VALVE
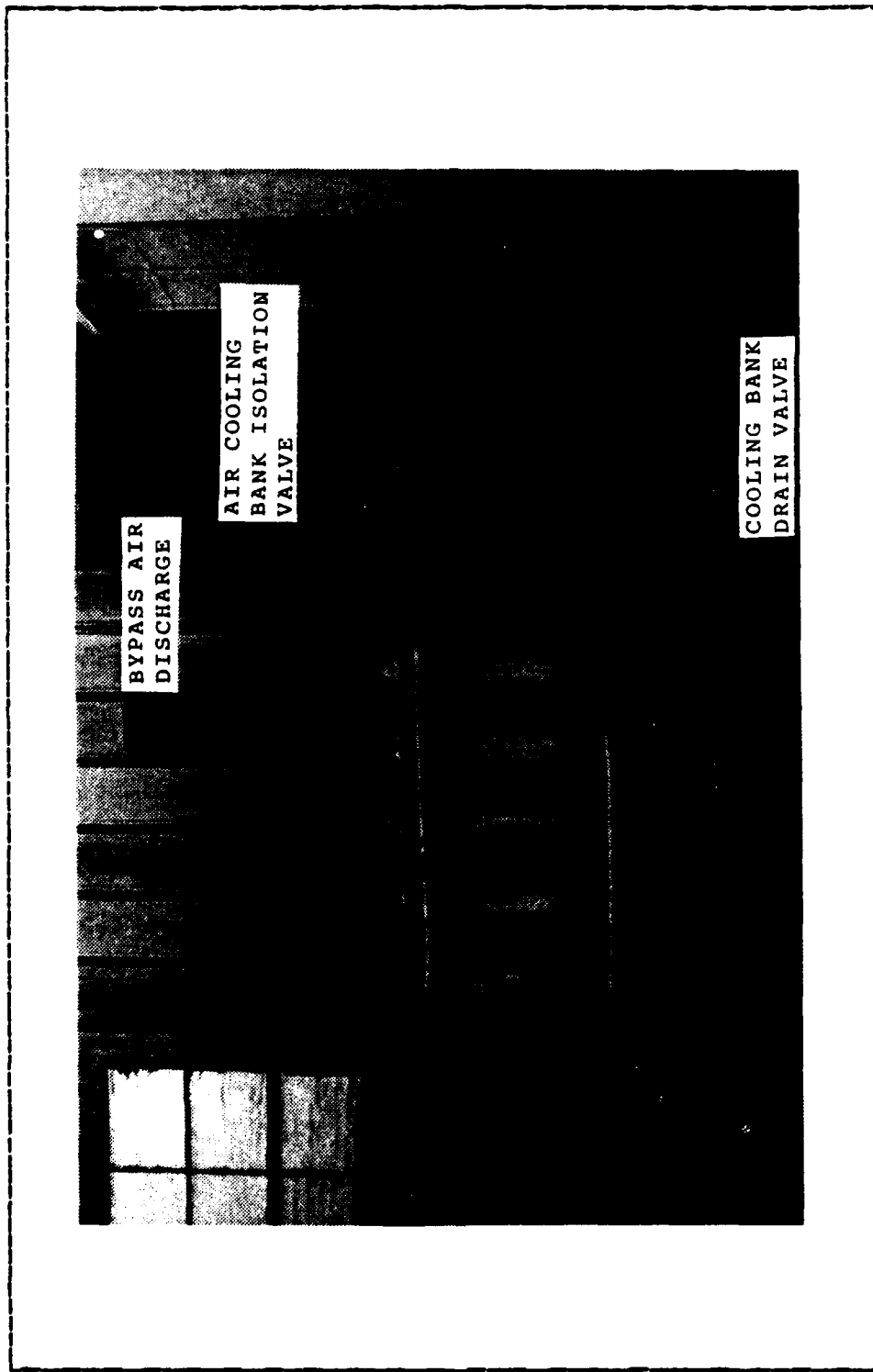
Figure 21. Air Cooling Bank and Bypass Discharge.

83

VALVE MUST
BE CLOSED
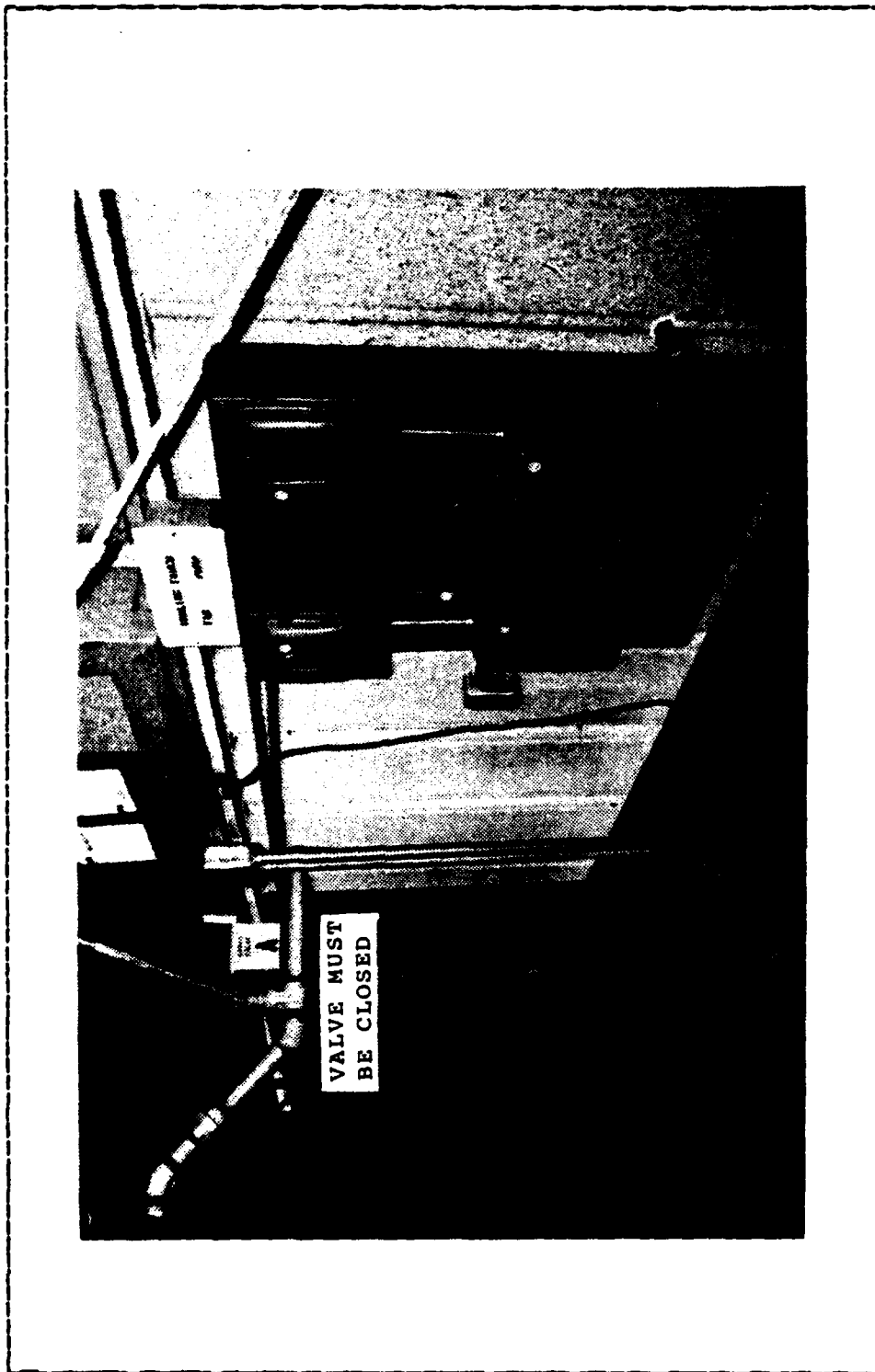
Figure 22.   Cooling Water Pump and Tower Fan Controllers.

84

AUXILIARY OIL
PUMP SWITCH

EXTERNAL OIL
SUMP
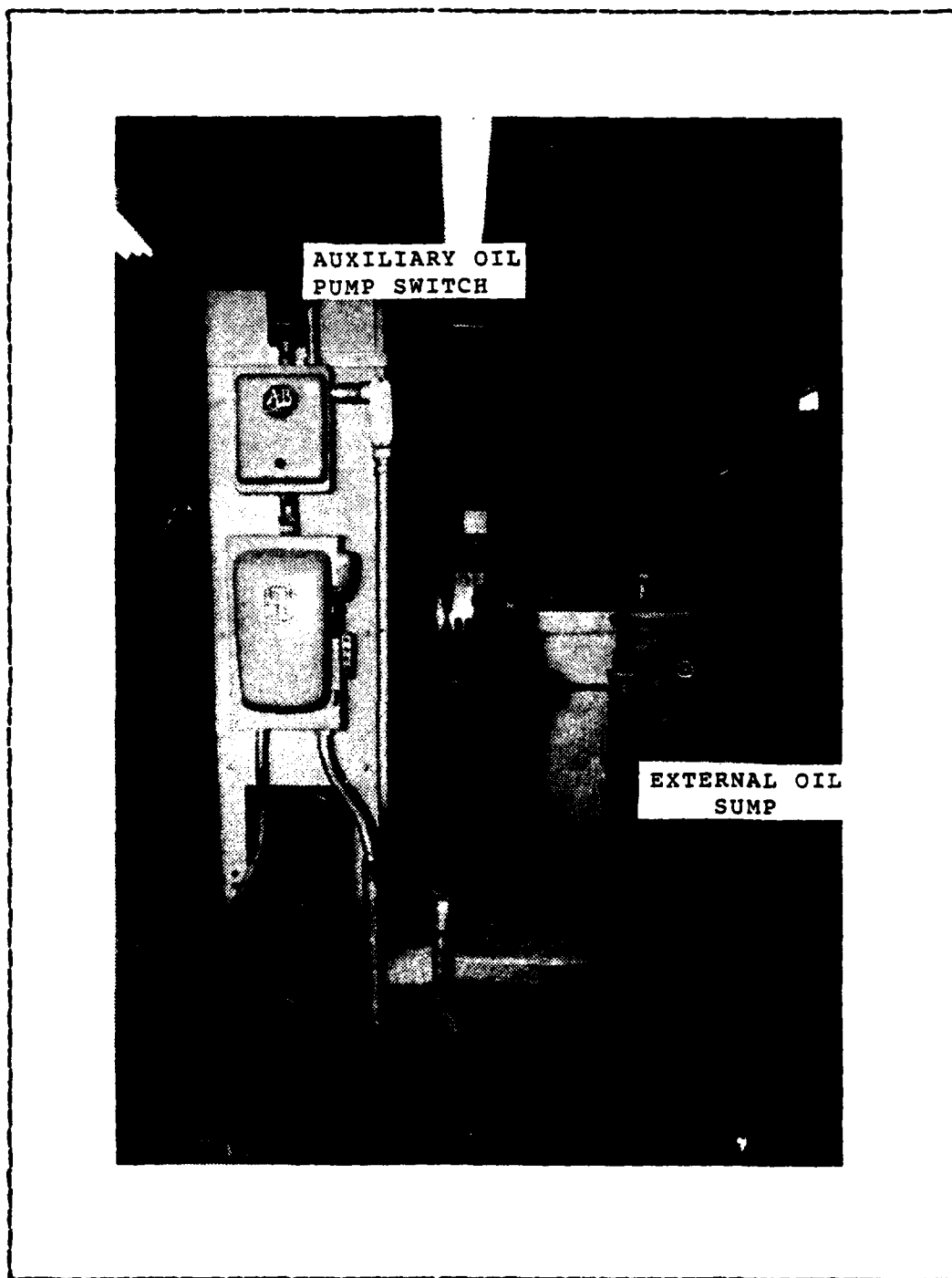
Figure 23.   Auxiliary Oil Pump Control.

85
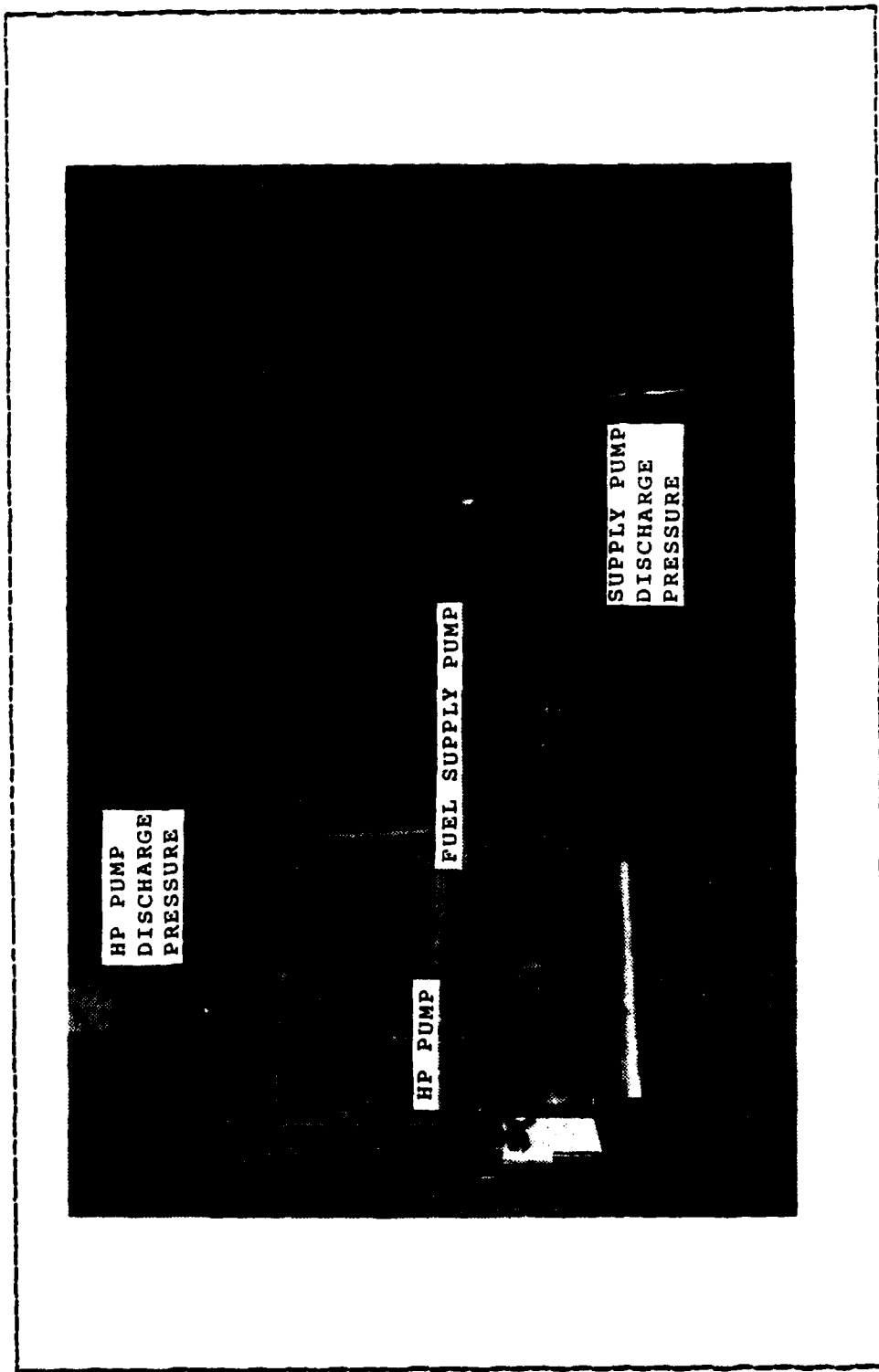
Figure 24. Fuel Pump Installation.
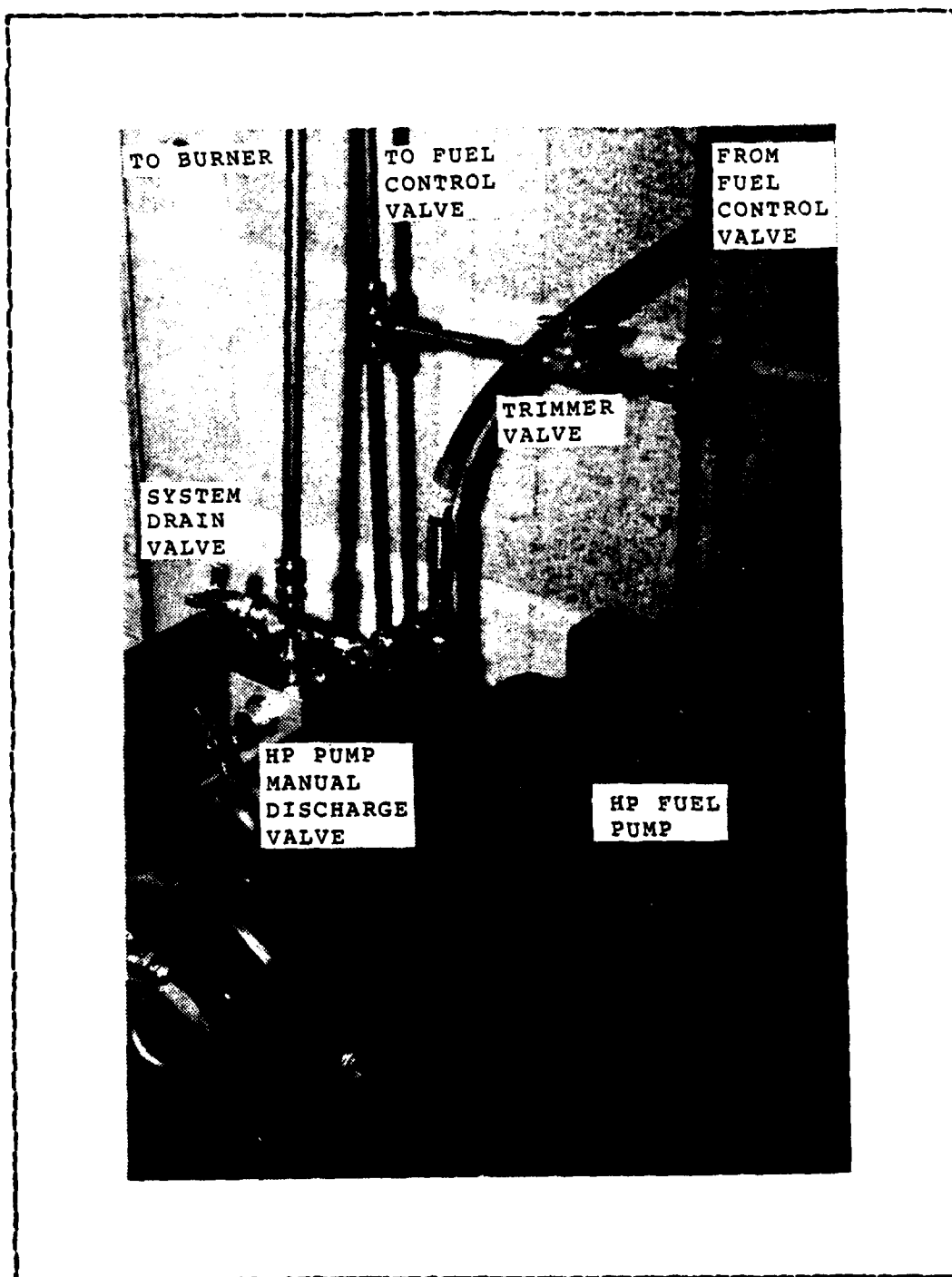
Figure 25.   H. P. Fuel Piping and Valves.
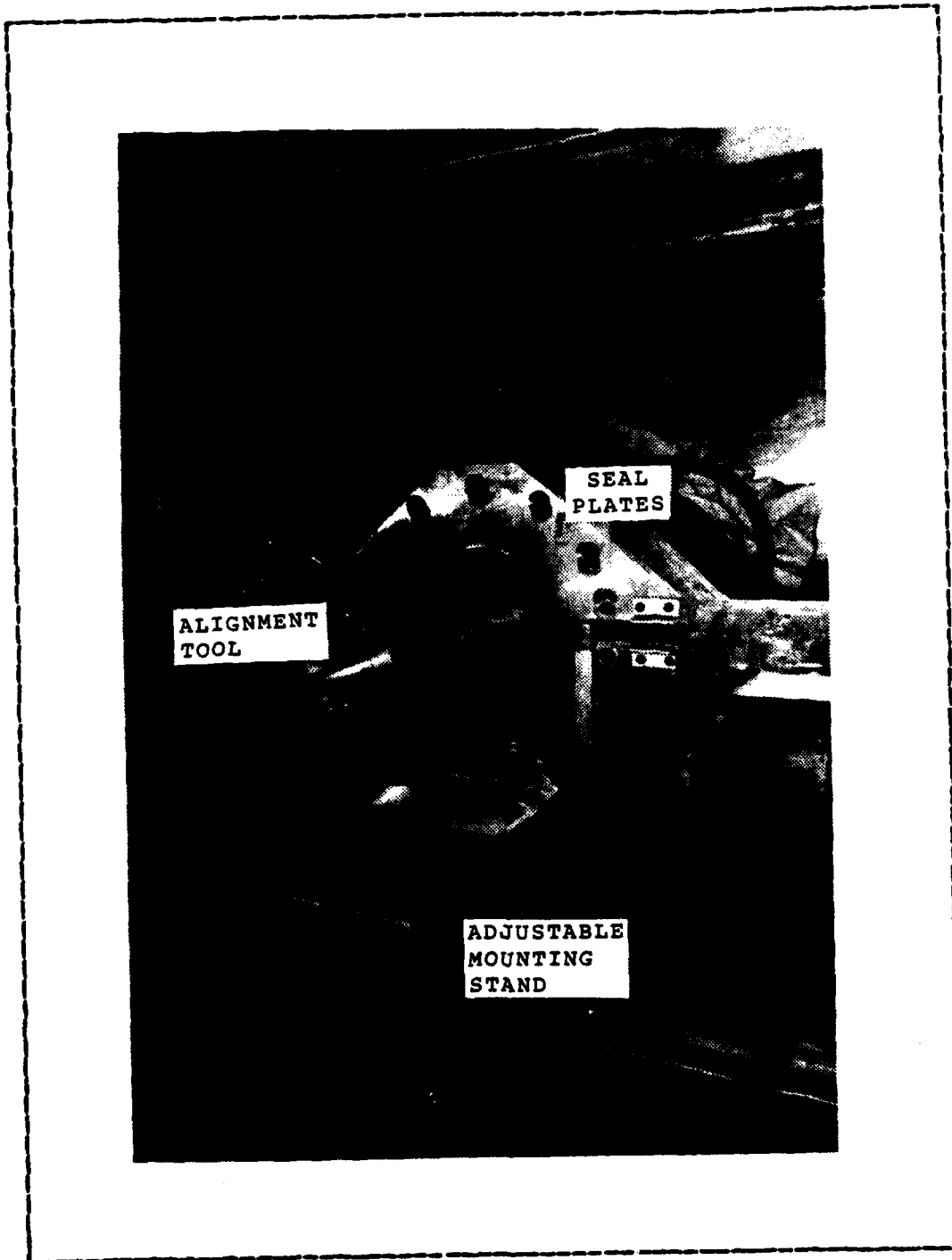
Figure 26. Model Installation.

88
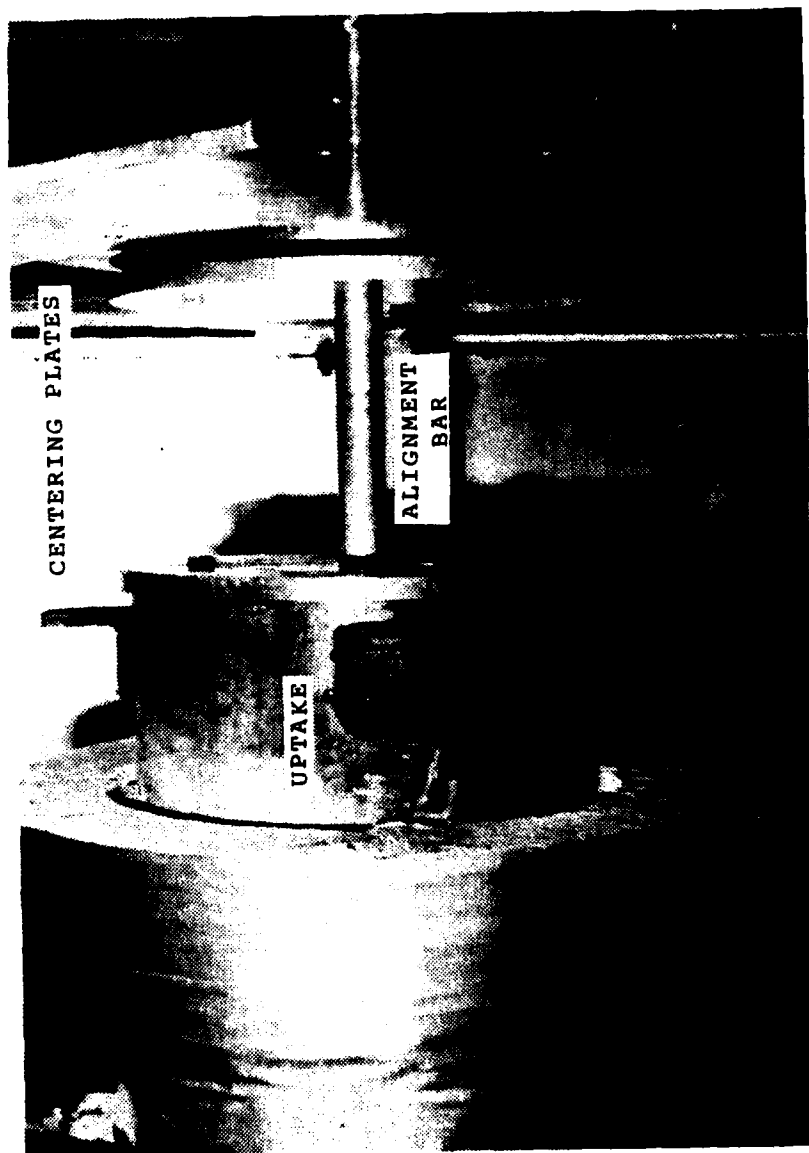
Figure 27. Model Alignment.

89
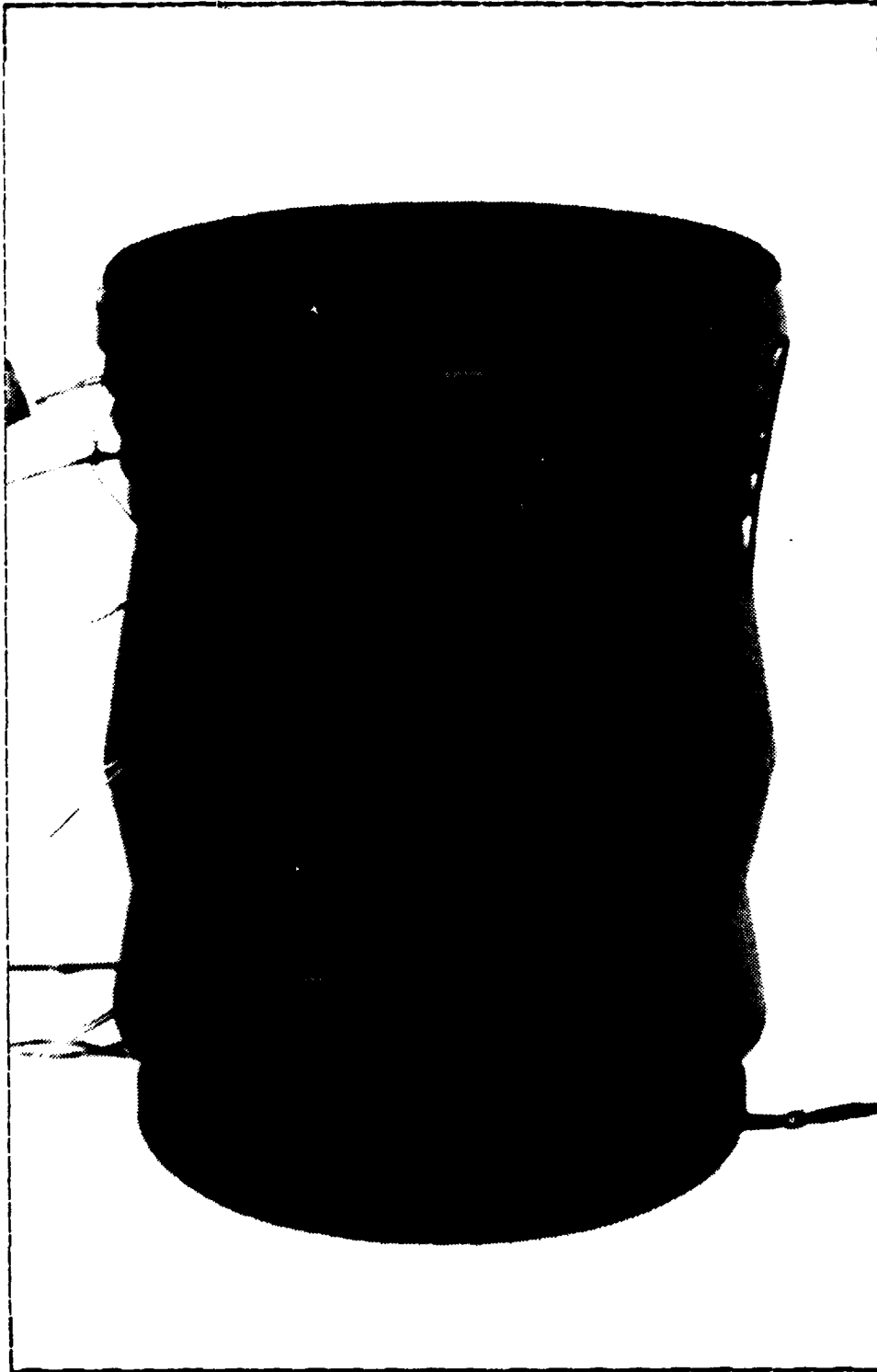
Figure 28. Model A.

Figure 29. Model A Entrance.
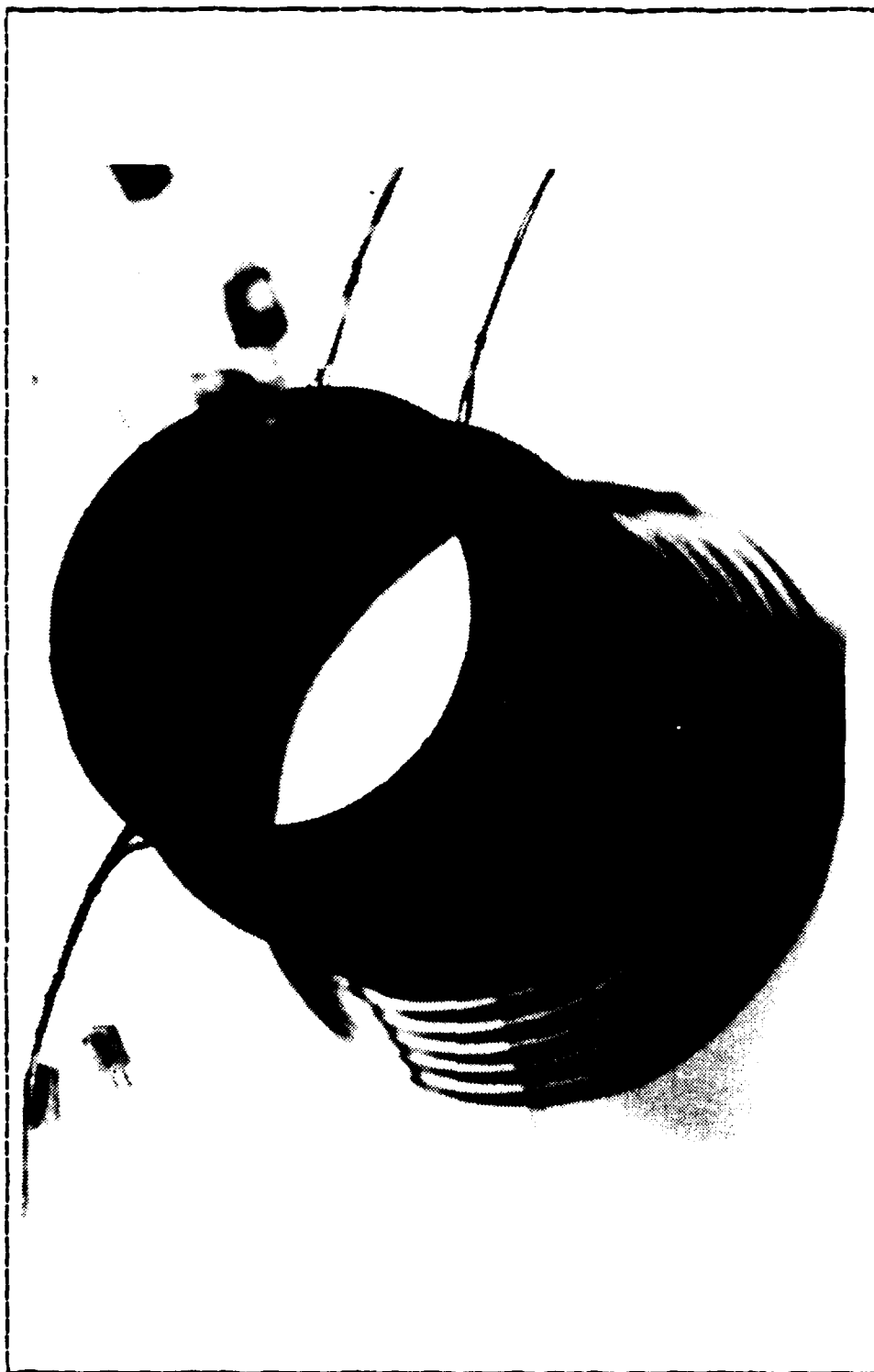
Figure 30. Model A Exit.

92

Figure 31. Model A Installed.
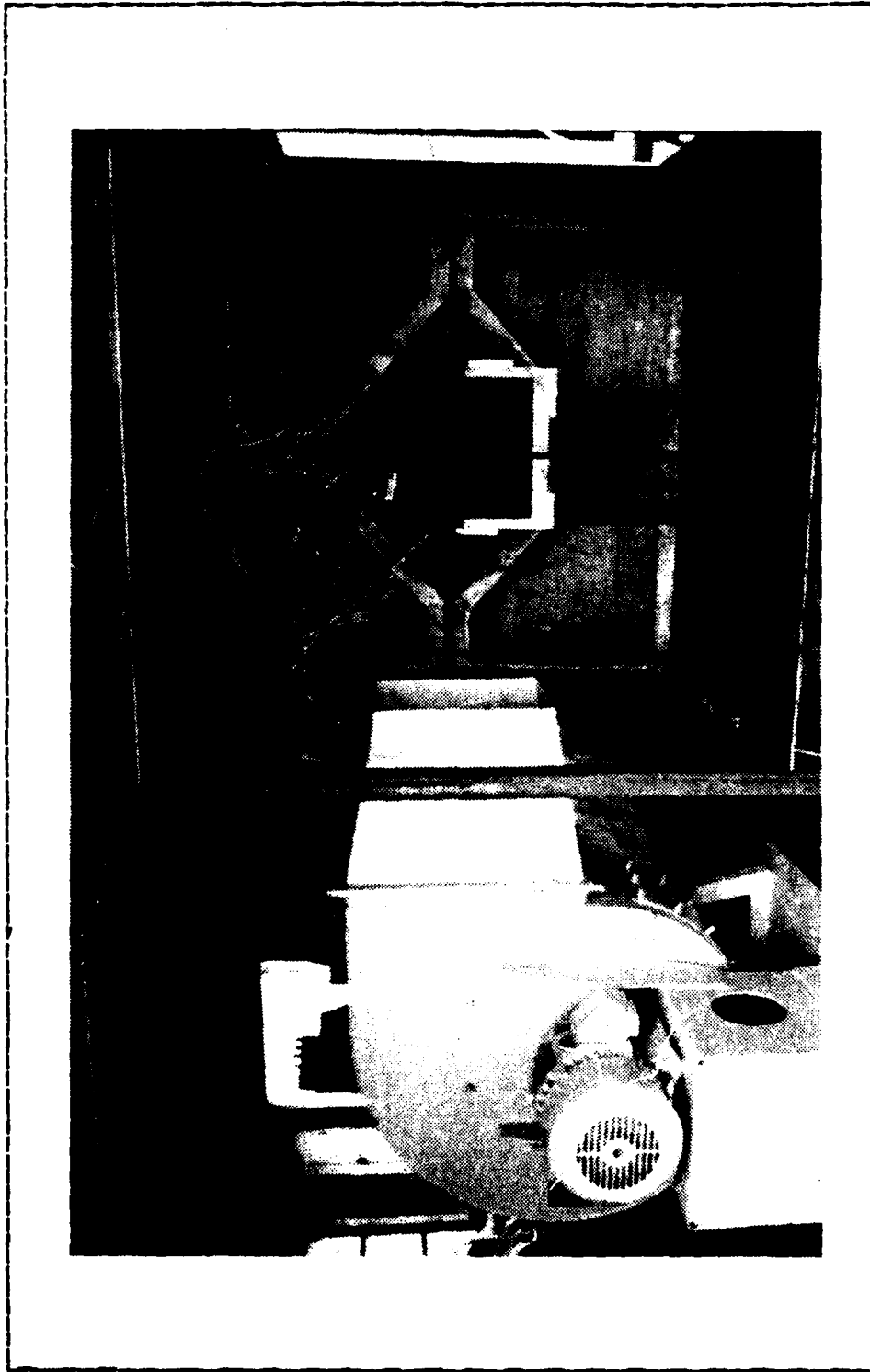
Figure 32. Crossflow Fan with Model A Installed.
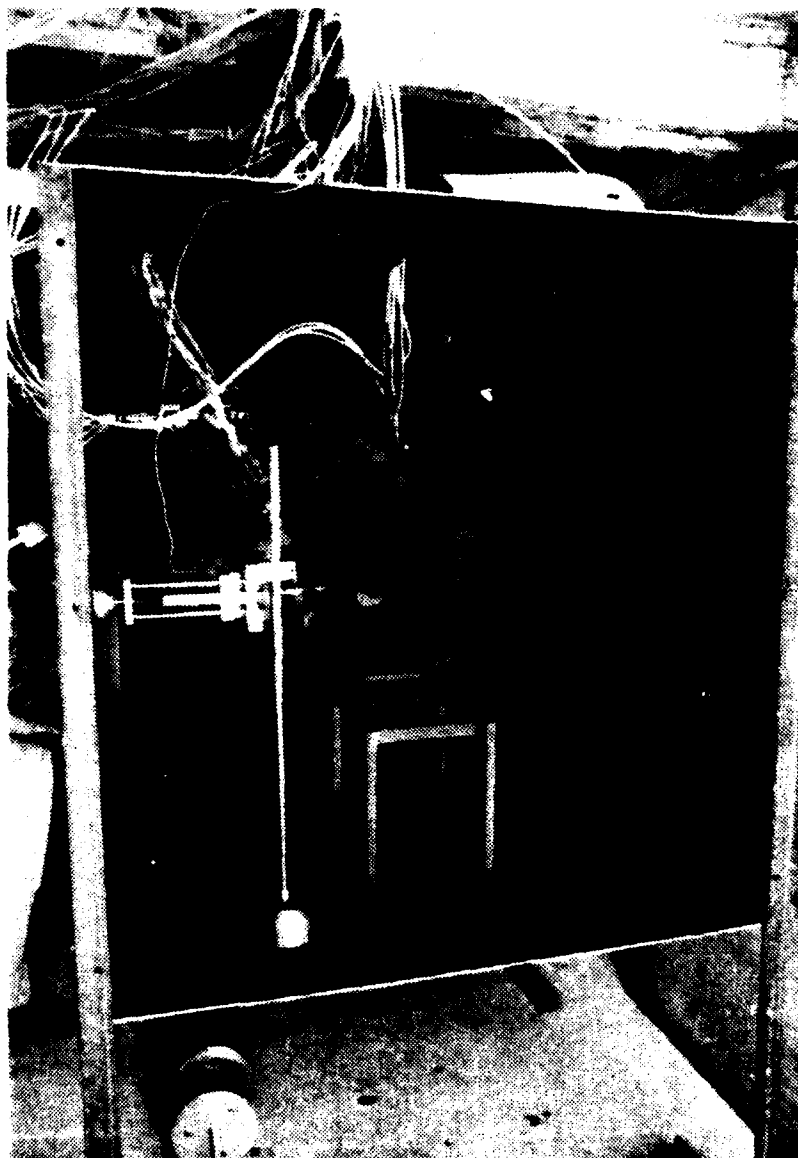
Figure 33.   Exit Plane Temperature Measurement.
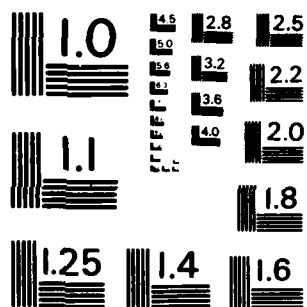
MICROCOPY RESOLUTION TEST CHART

NATIONAL BUREAU OF STANDARDS-1963-A
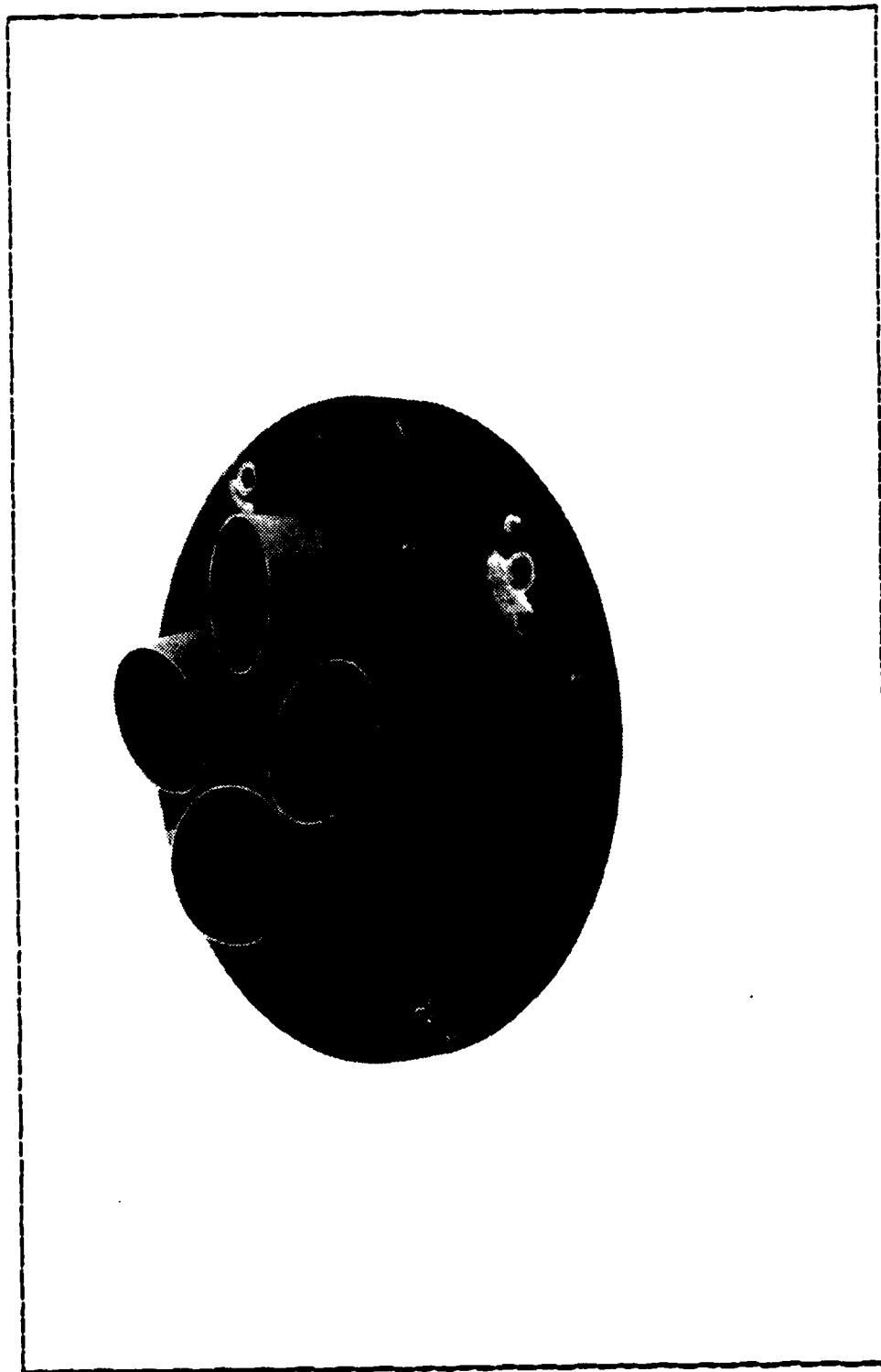
Figure 34. Tilted-Angled Nozzle Plate.
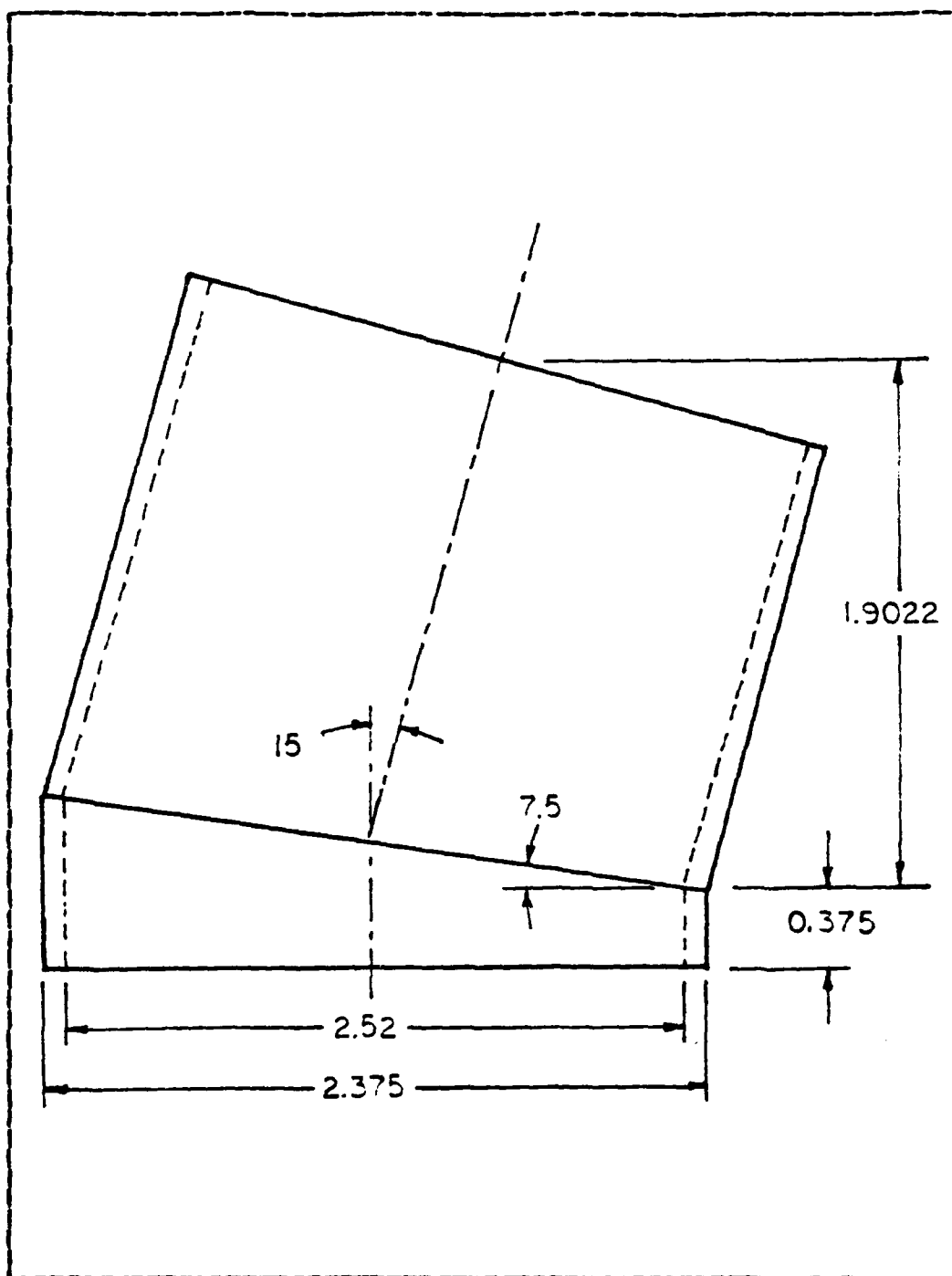
Figure 35.   Tilted Nozzle Geometry.

97
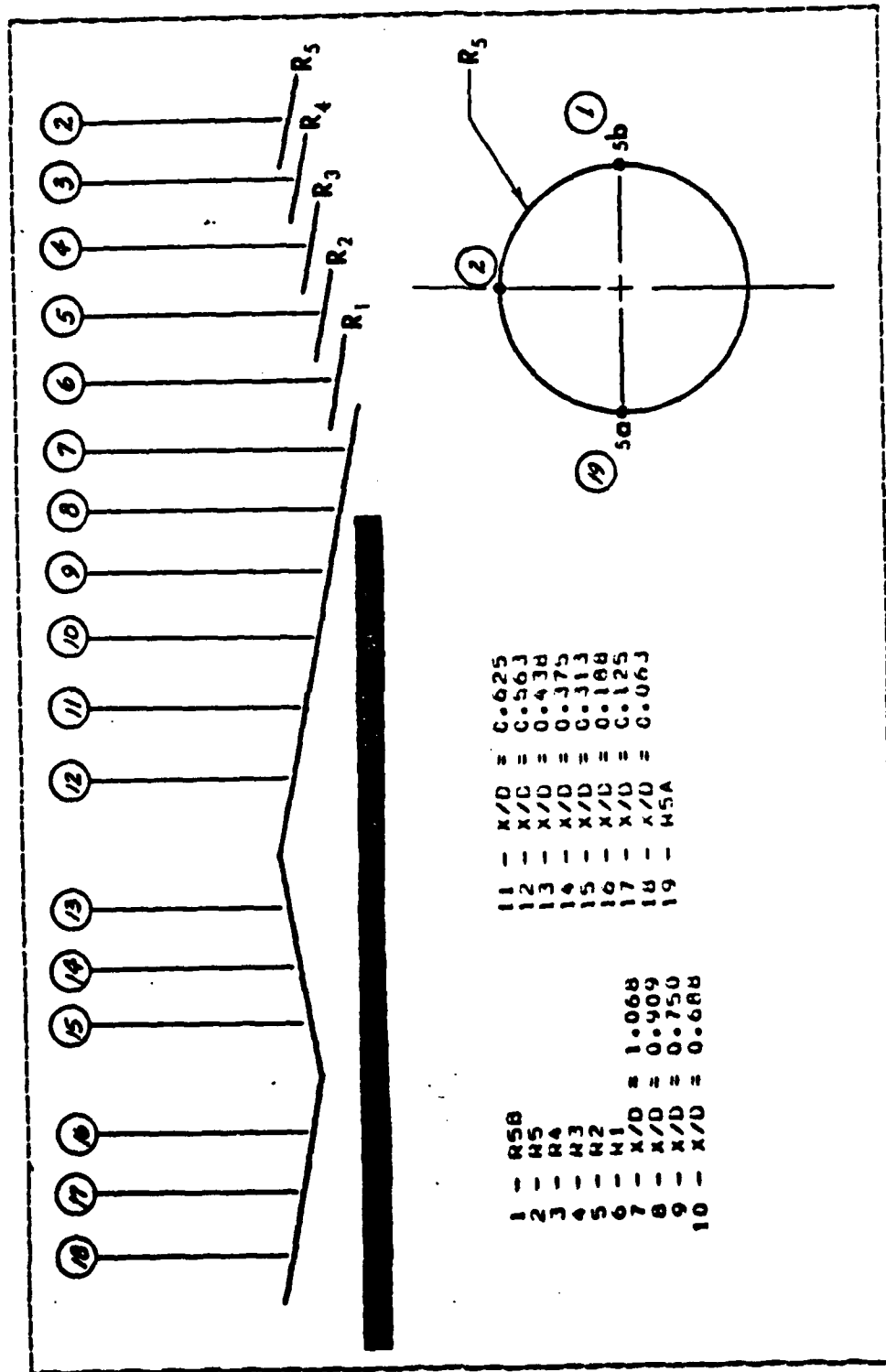
Figure 36. External Temperature Measurement Points, Model A.
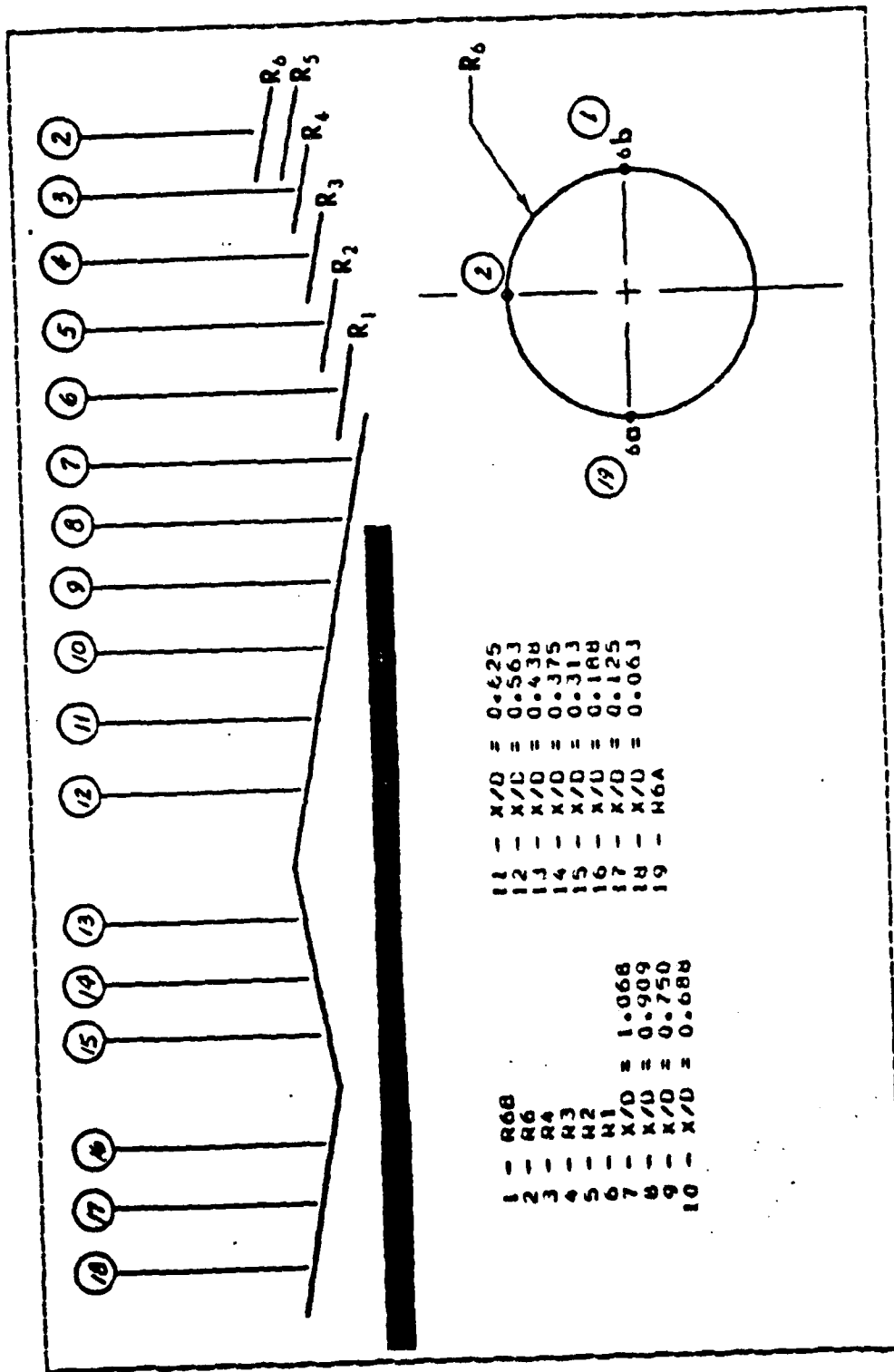
Figure 37. External Temperature Measurement Points, Model A Mod..

99
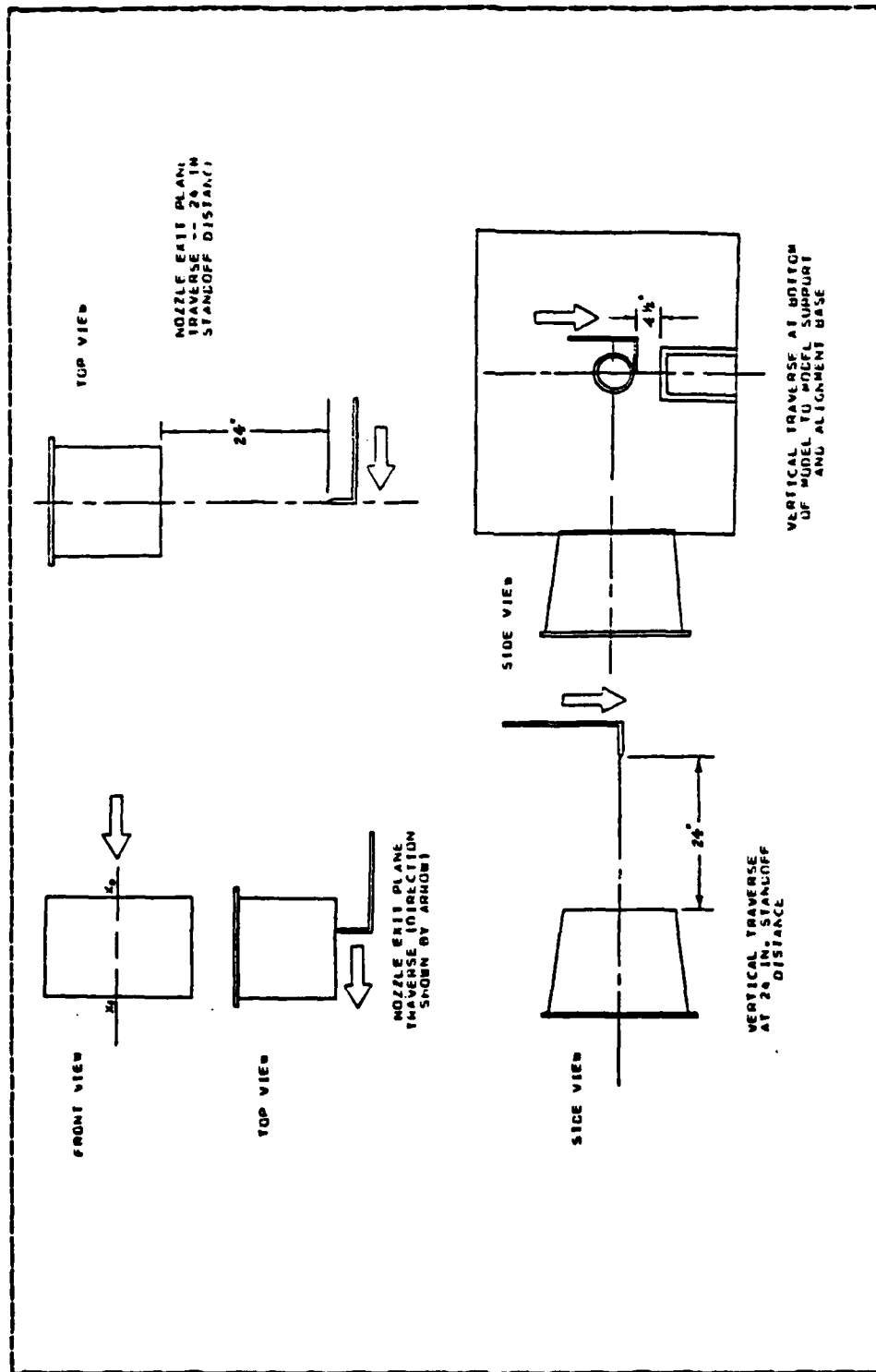
Figure 38. Schematic of Crossflow Fan Pitot Tube Traverses.
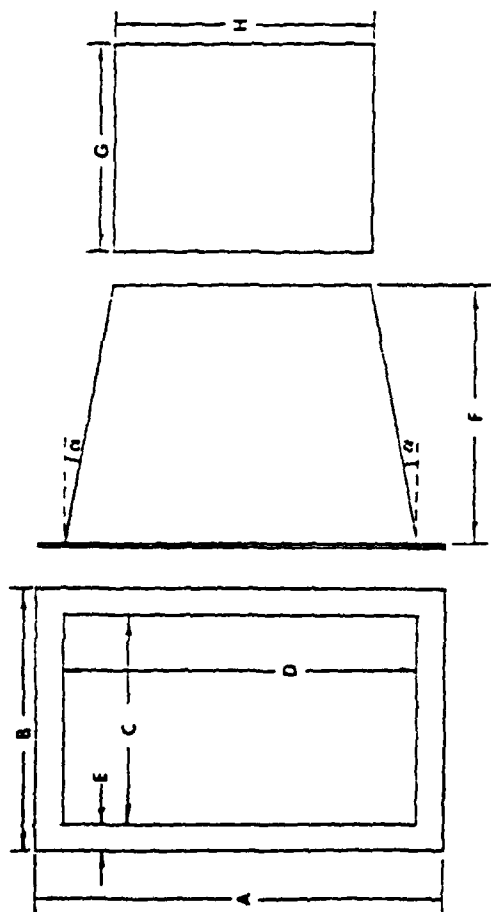
A: 22.375
B: 14.750
C: 11.750
D: 9.375
E: 4.500
F: 14.500
G: 14.250
H: 14.250
α: 10°

ALL DIMENSIONS IN INCHES

Figure 39. Crossflow Fan Nozzle Geometry.
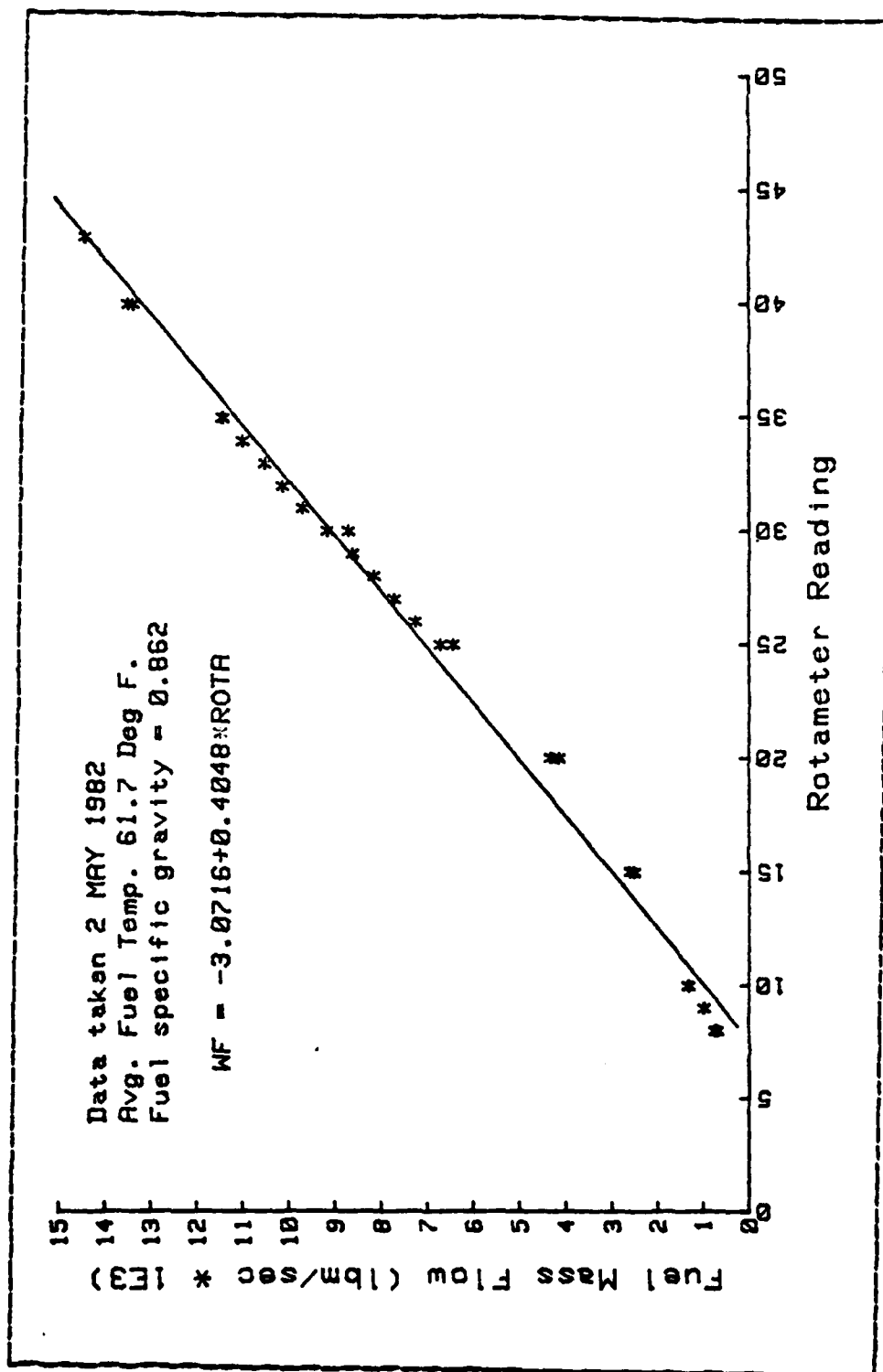
Figure 40. Rotameter Calibration Curve.
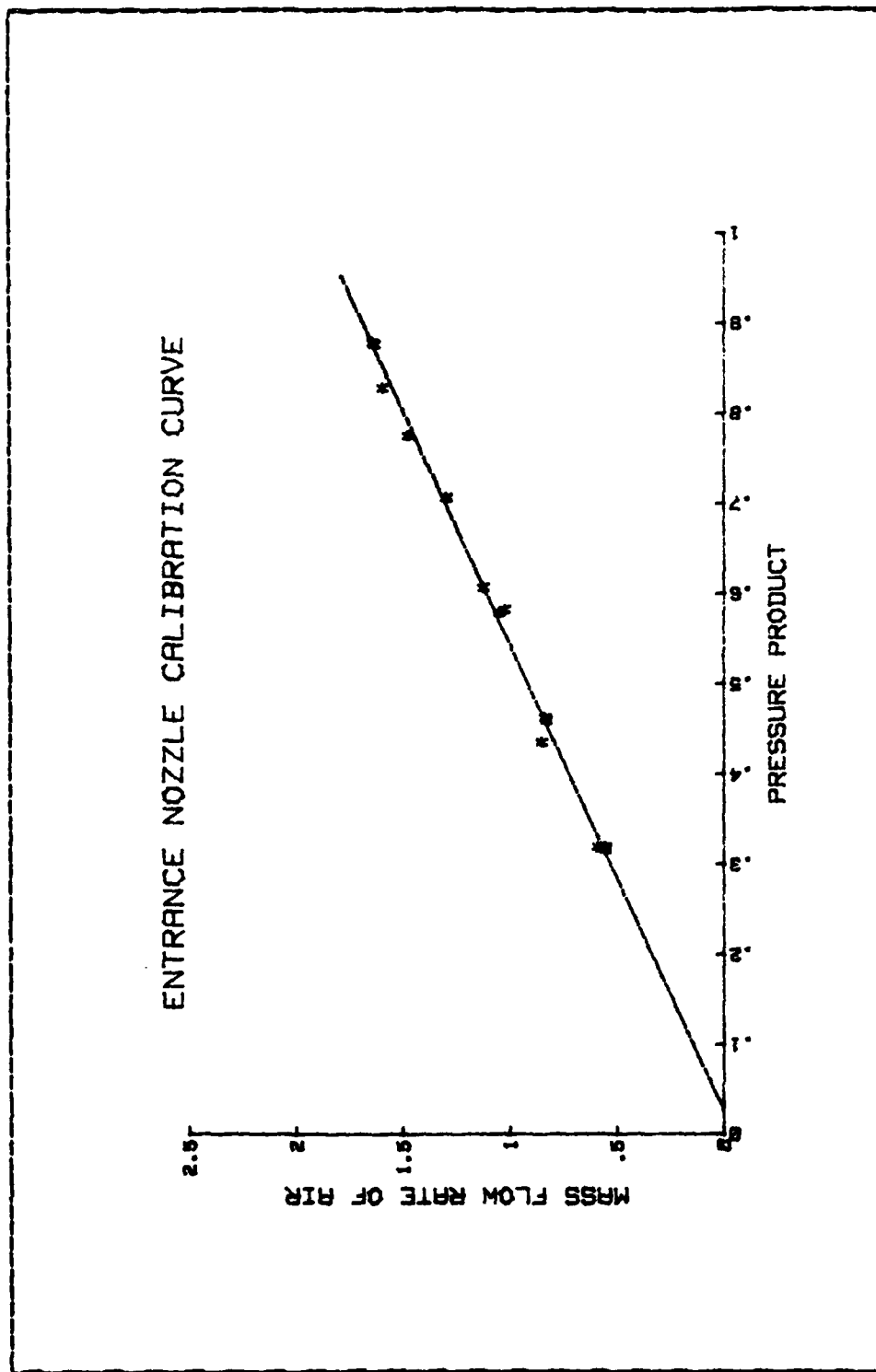
Figure 41. Air Mass Flow Rate Calibration Curve.
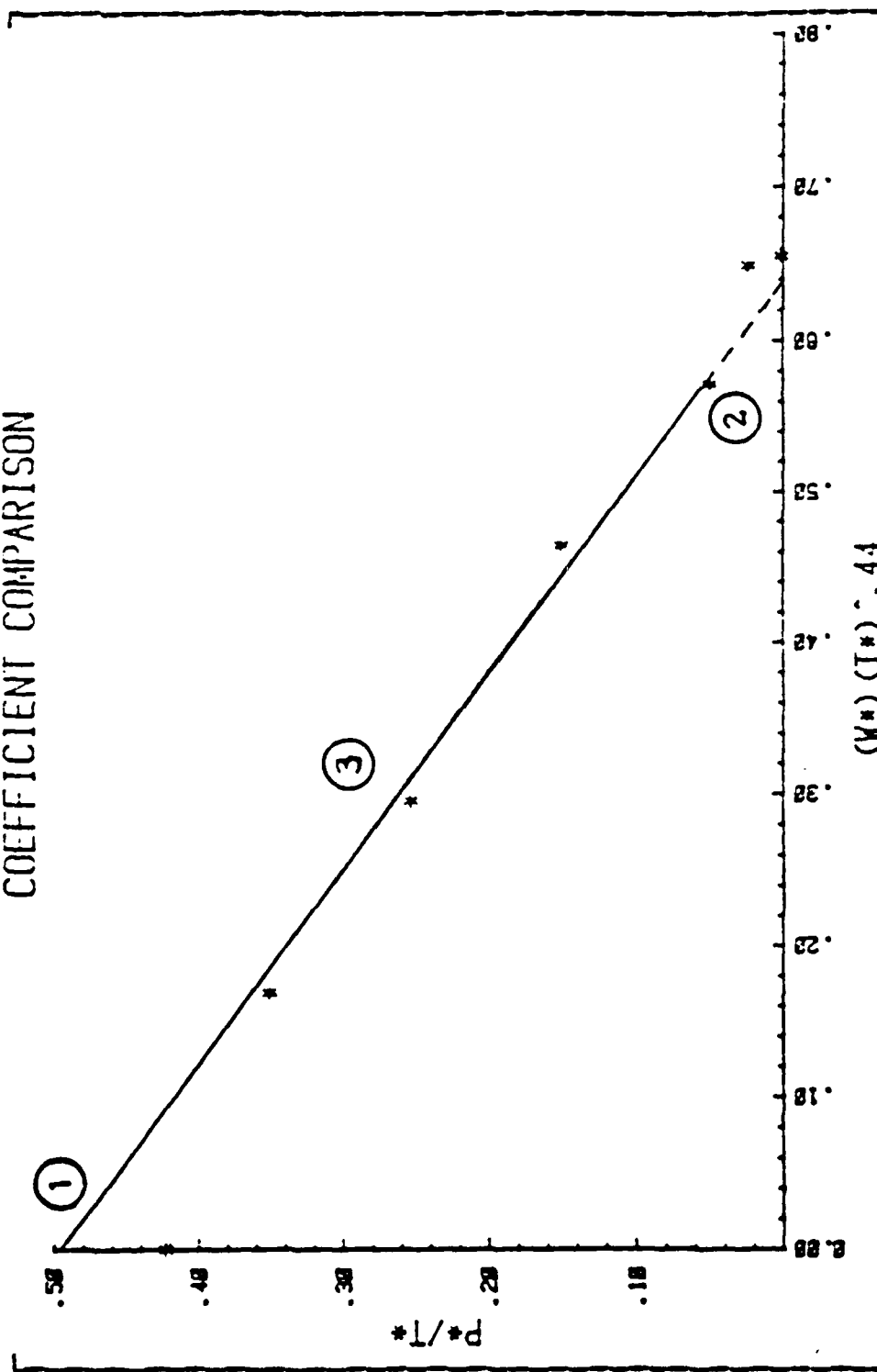
Figure #2.   Sample Pumping Coefficient Plot.
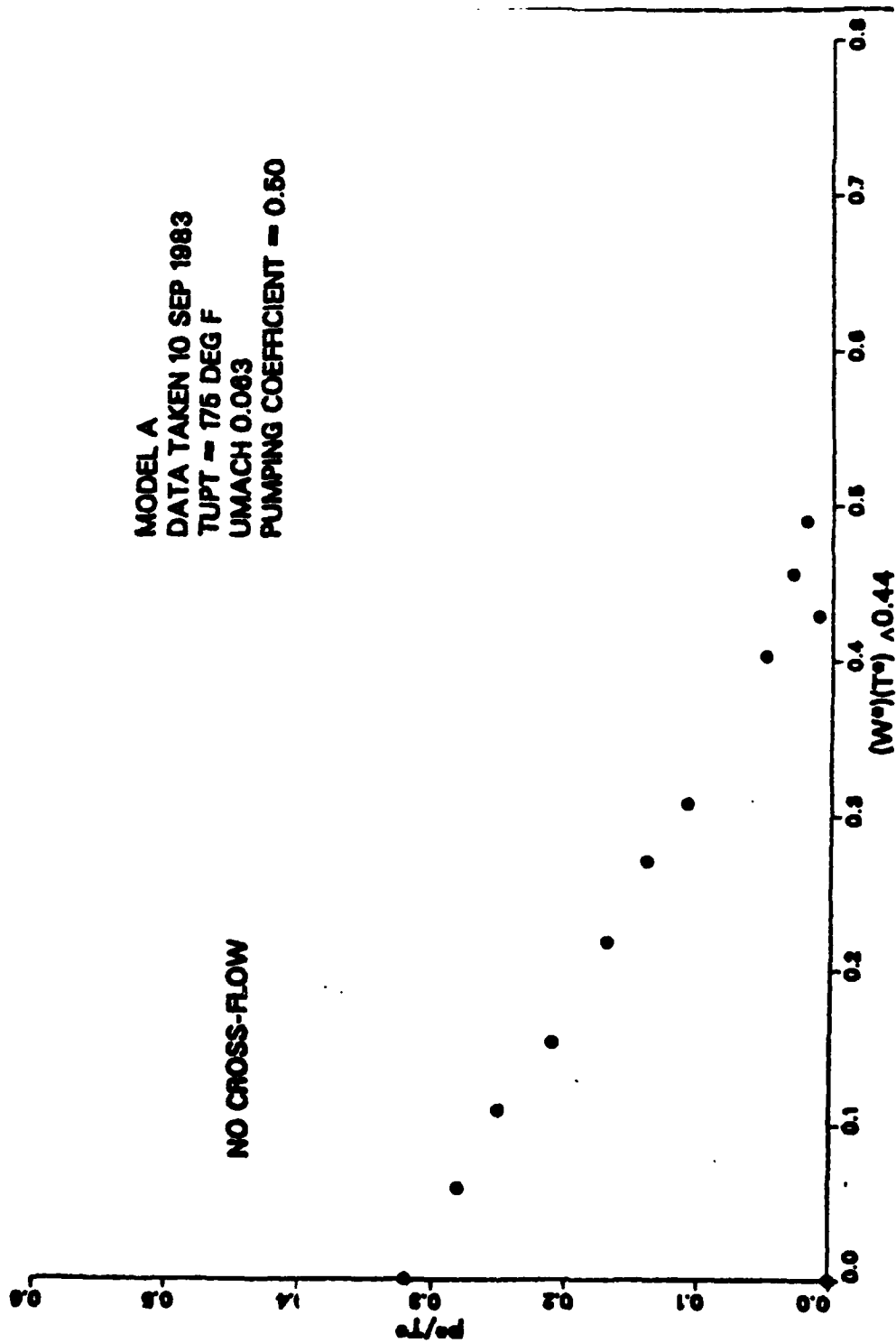
Figure 43. Pumping Coefficient, Model A (175 F) - No Crossflow.

105
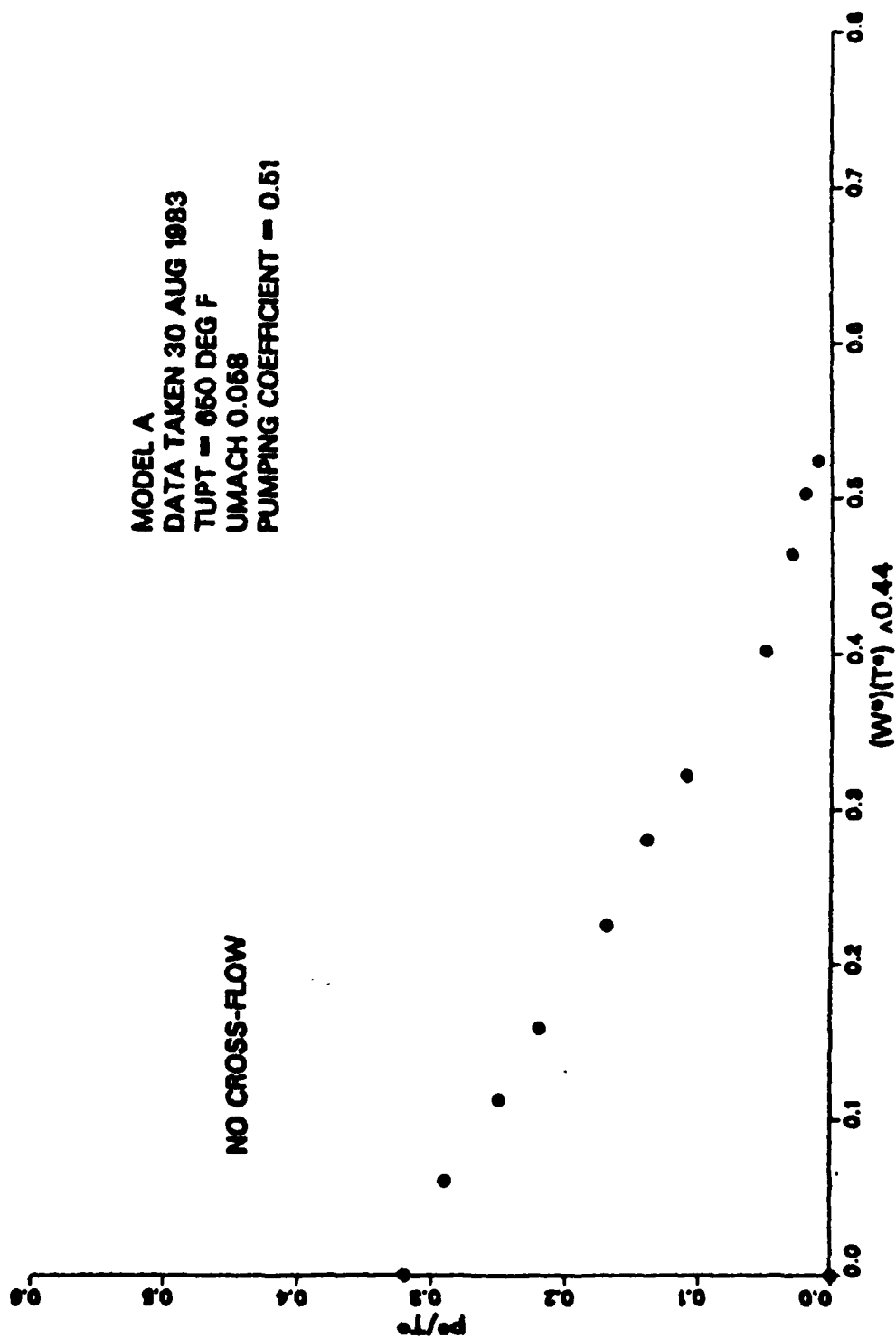
Figure 44. Pumping Coefficient, Model A (650 F) - No Crossflow.
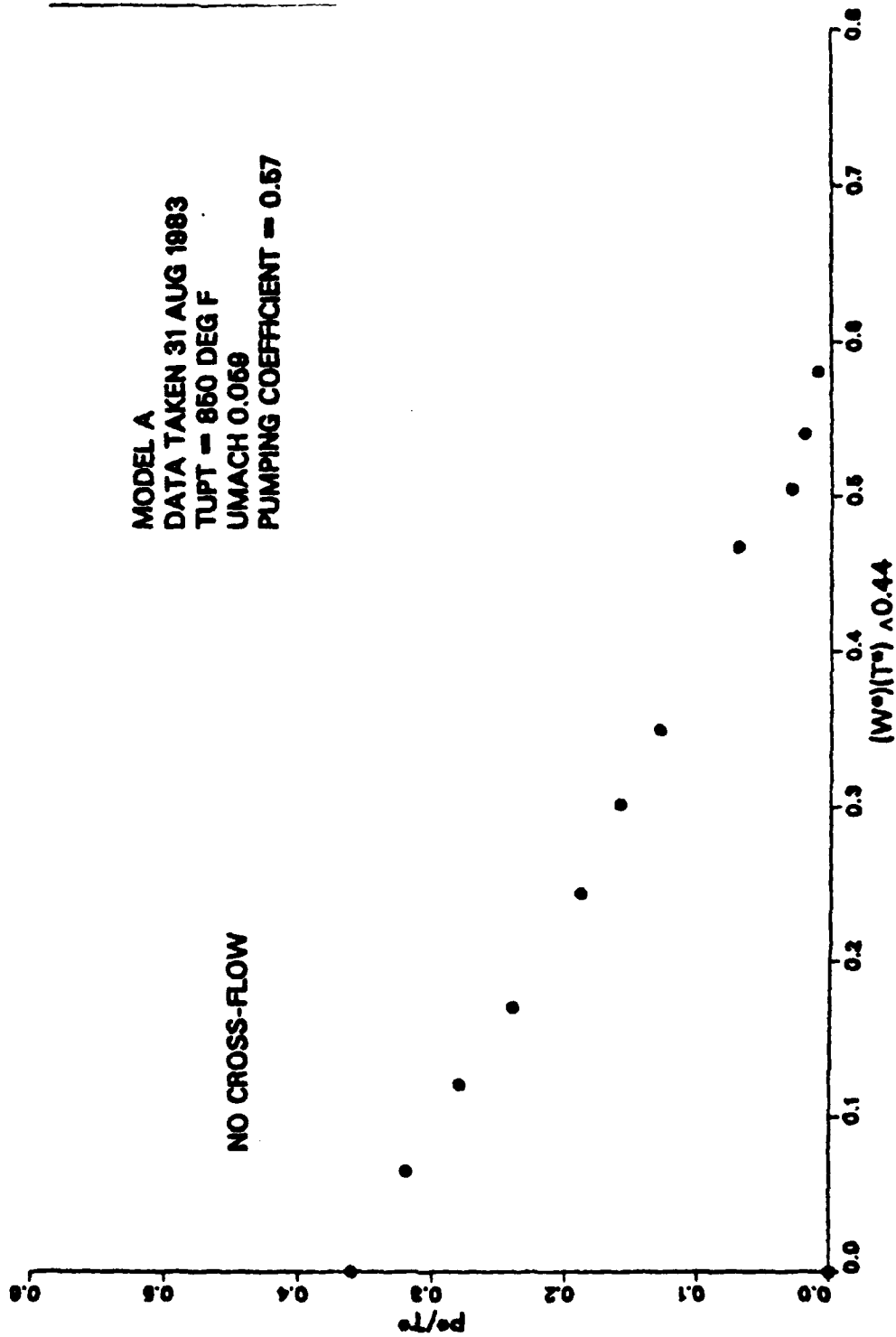
Figure 45. Pumping Coefficient, Model A (850 F) - No Crossflow.

WITH CROSS-FLOW

MODEL A
DATA TAKEN 02 SEP 1983
TUPT = 850 DEG F
UMACH 0.059
PUMPING COEFFICIENT = 0.59

$(W^\circ)(T^\circ) \wedge 0.44$

Pq/Tq
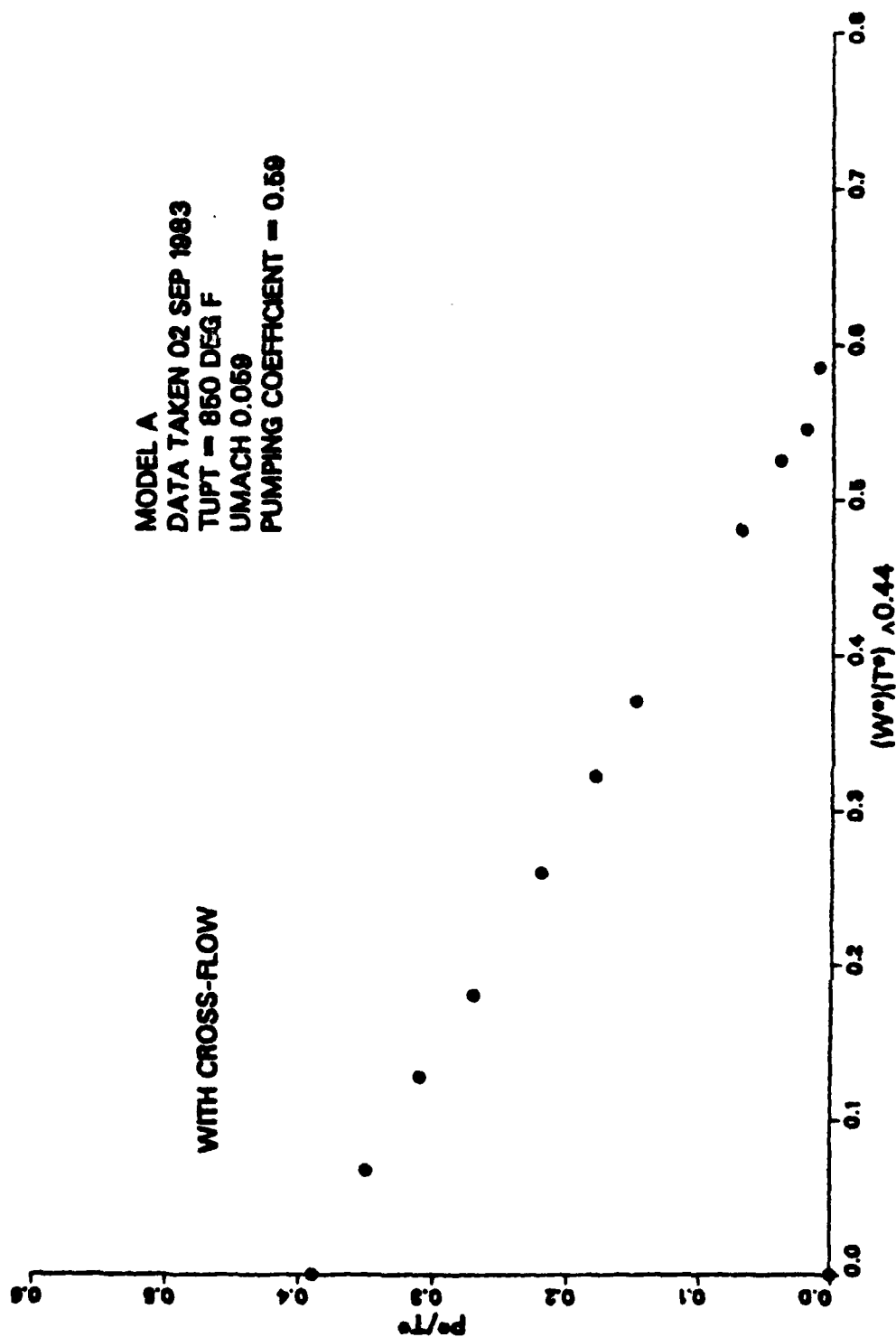
Figure 46. Pumping Coefficient, Model A (850 F) - Crossflow.

NO CROSS-FLOW

MODEL A
DATA TAKEN 02 SEP 1983
TUPT = 950 DEG F
UMACH 0.069
PUMPING COEFFICIENT = 0.55

$(We)(T^\circ)^{\wedge}0.44$

Pe/Te
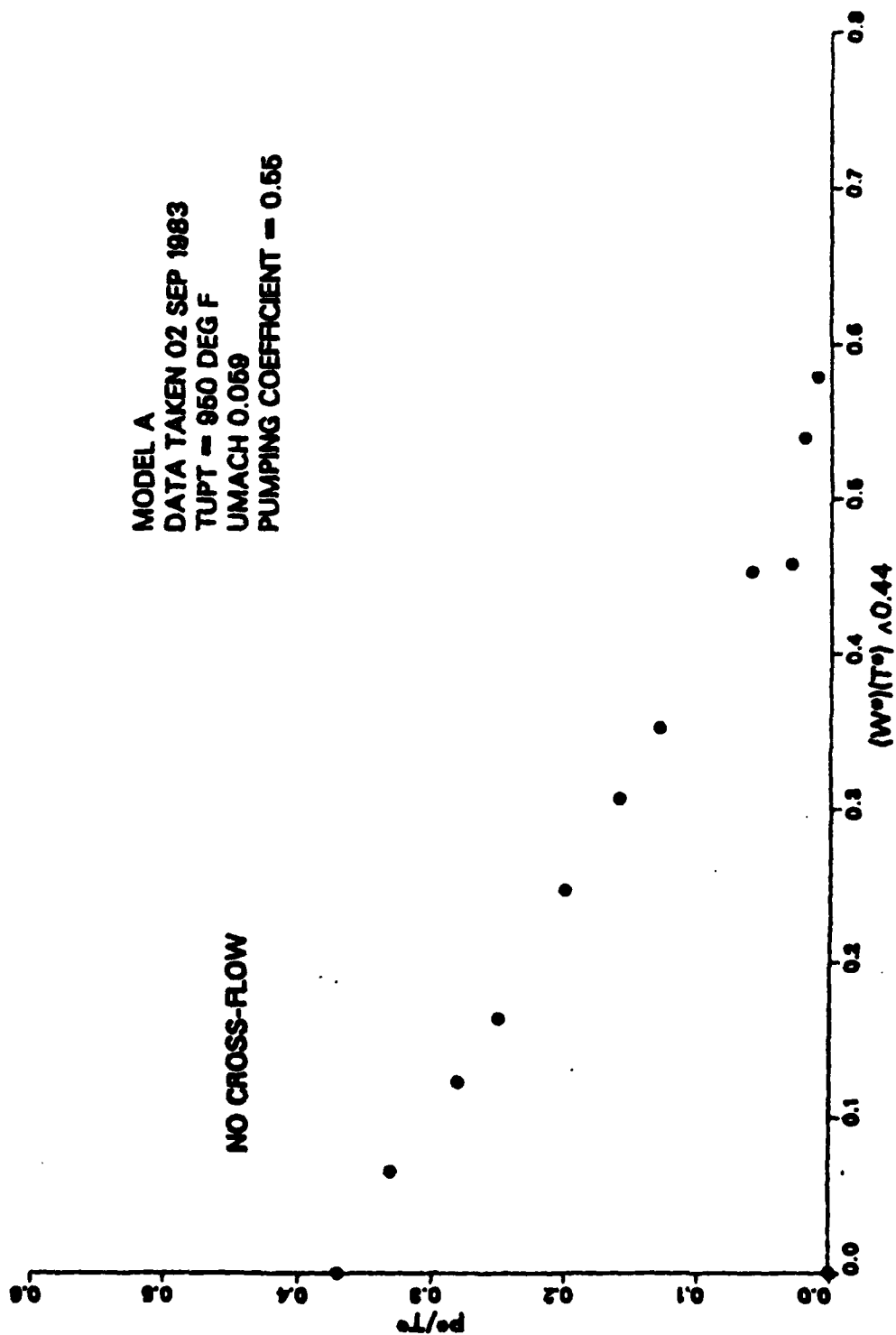
Figure 47.   Pumping Coefficient, Model A (950 F) - No Crossflow.

MODEL A
DATA TAKEN 04 SEP 1983
TUPT = 950 DEG F
UMACH 0.069
PUMPING COEFFICIENT = 0.61

WITH CROSS-FLOW

$(W^o)(T^o) ^0.44$

Pd/Ts
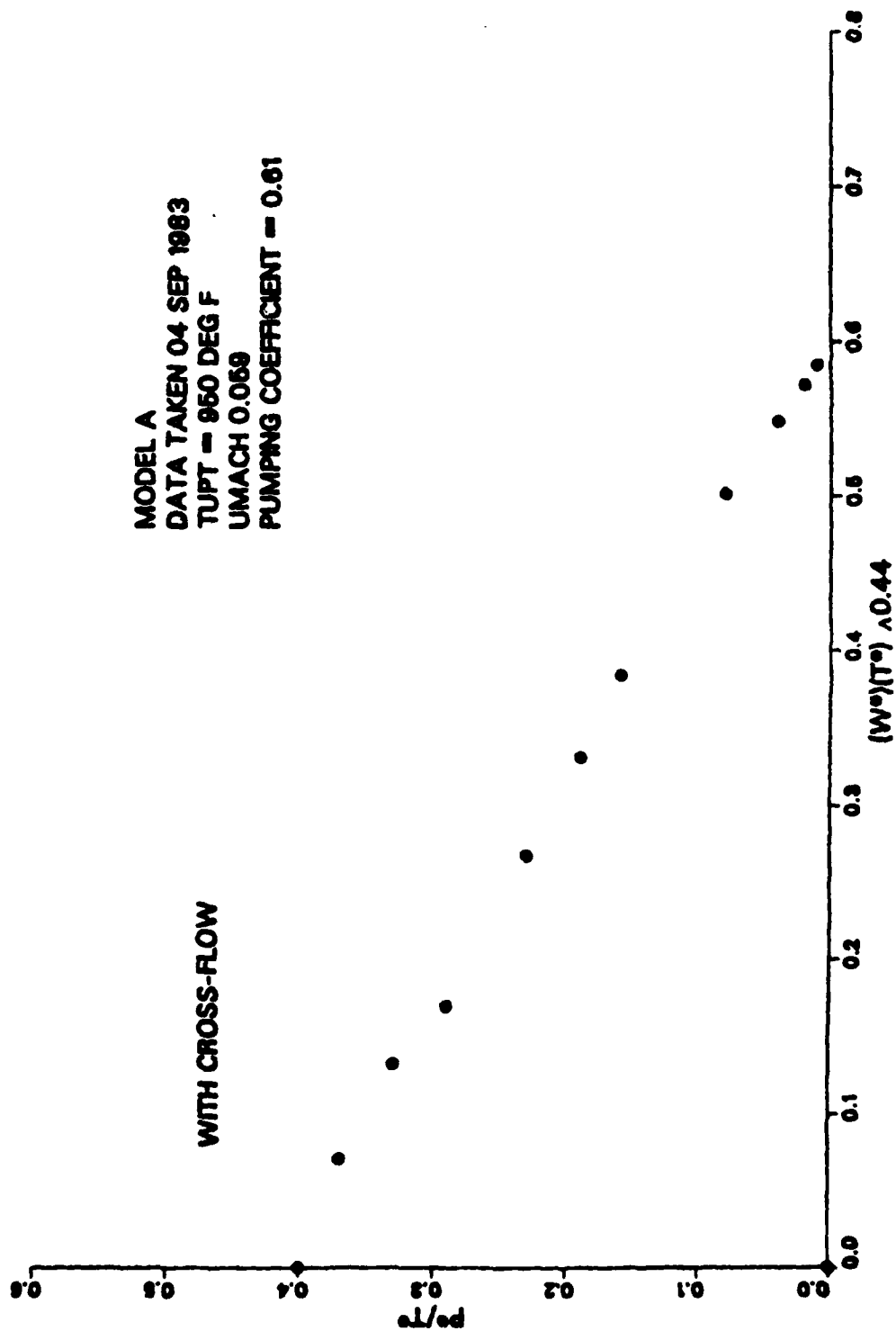
Figure 48.   Pumping Coefficient, Model A (950 F) - Crossflow.
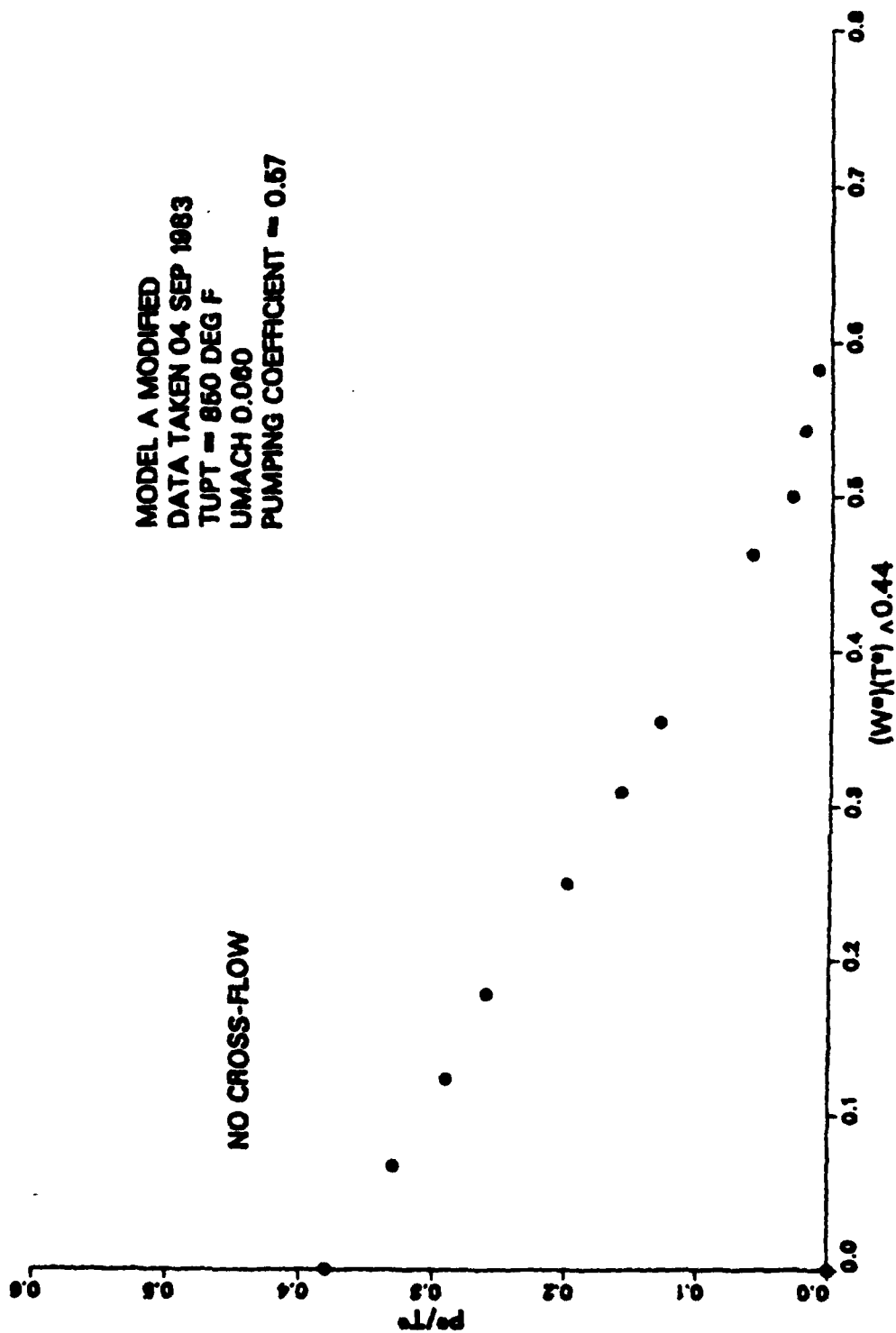
Figure 49. Pumping Coefficient, Model A Mod (850 F) - No Crossflow.

111
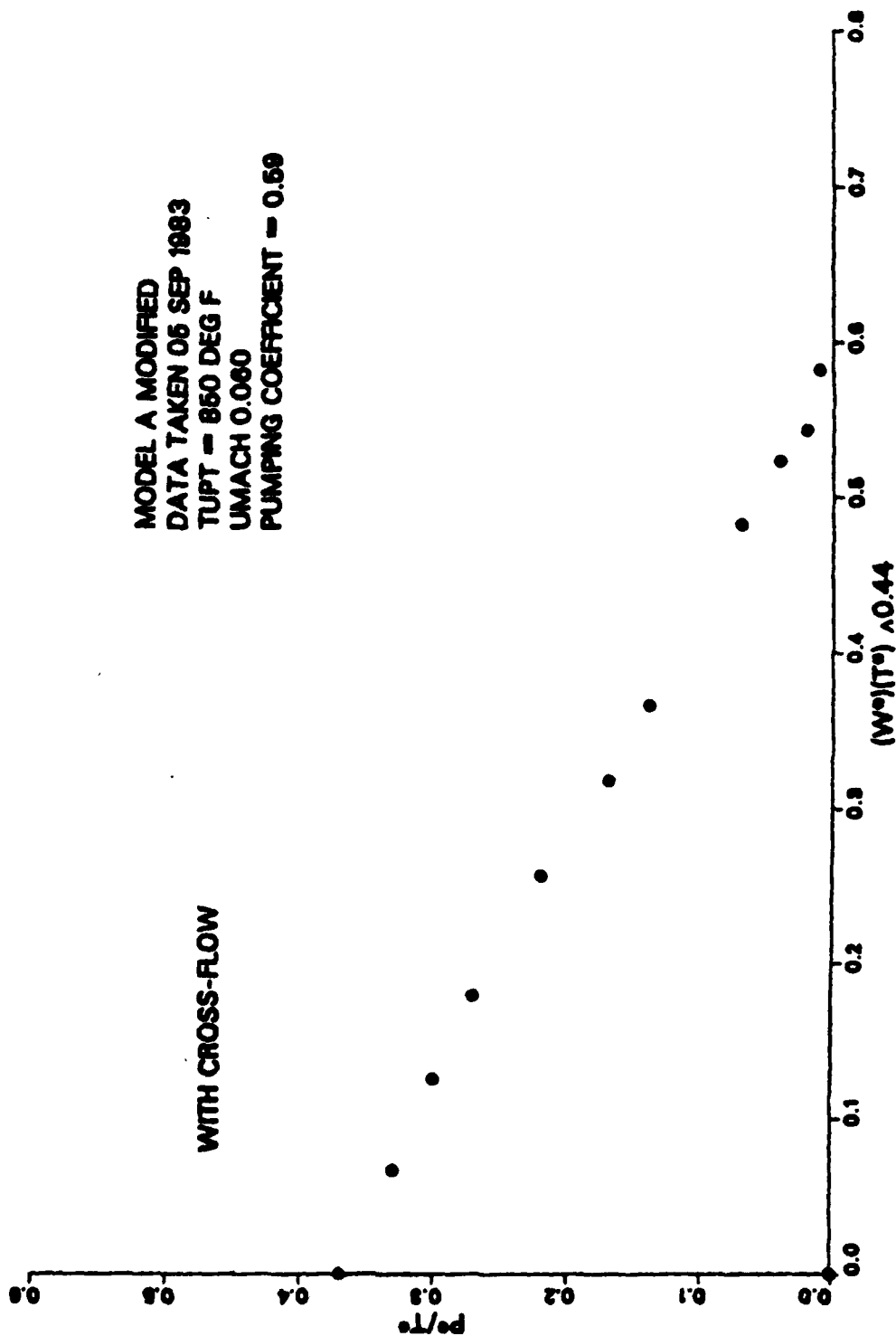
Figure 50. Pumping Coefficient, Model A Mod (850 F) - Crossflow.
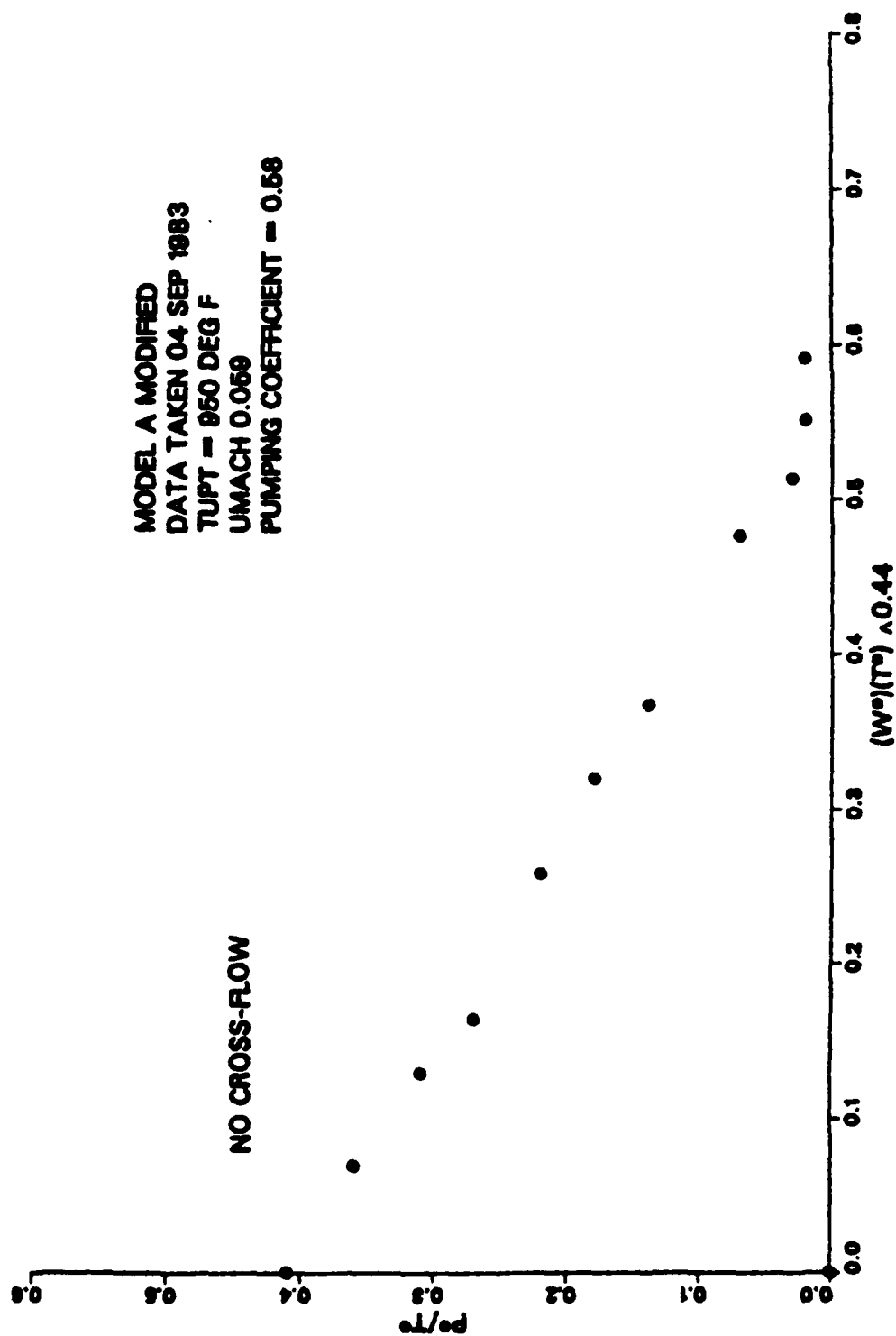
Figure 51. Pumping Coefficient, Model A Mod (950 F) - No Crossflow.

113
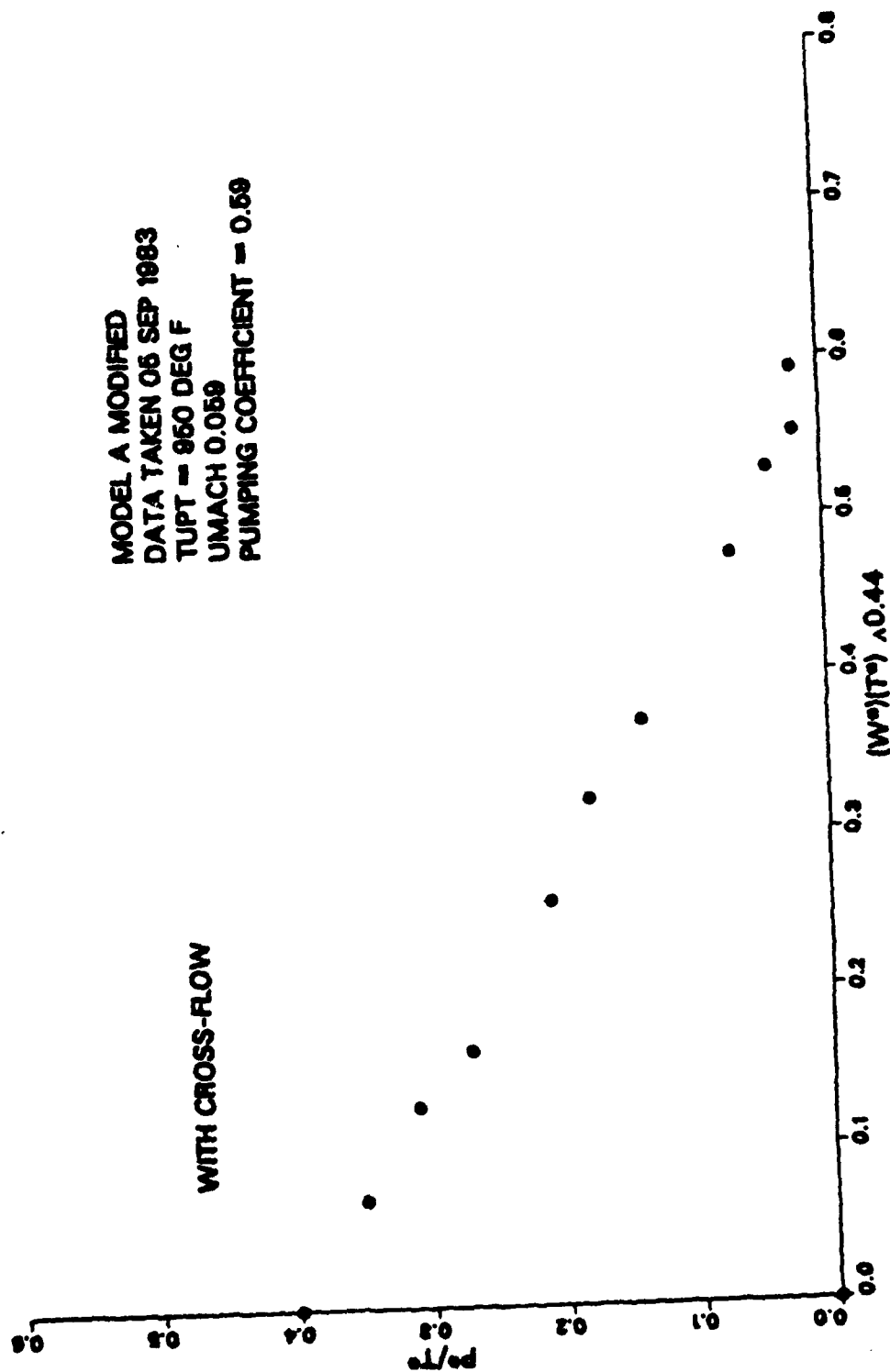
Figure 52. Pumping Coefficient, Model A Mod (950 F) - Crossflow.
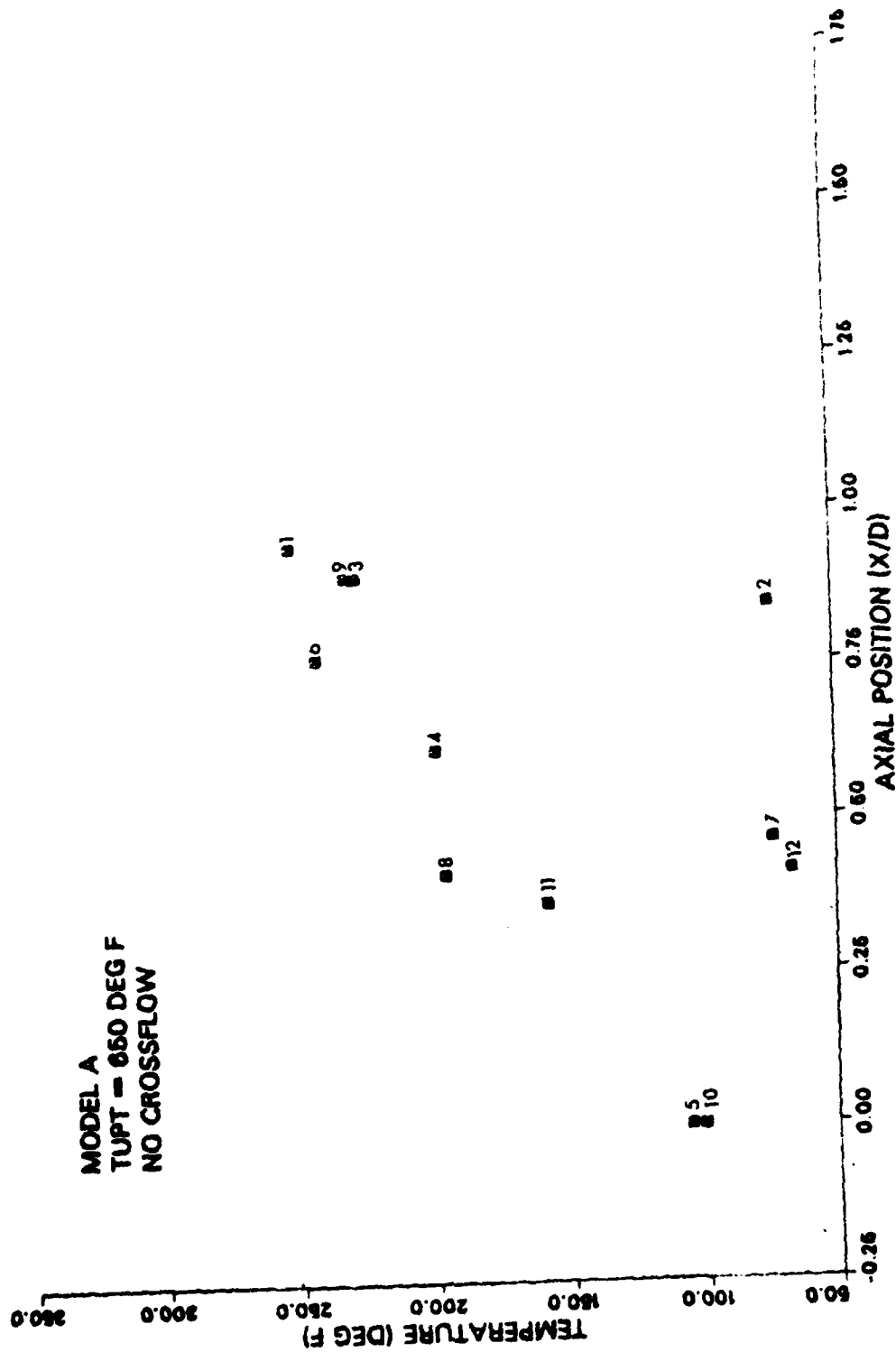
Figure 53. Mixing Stack Temp., Model A (650 F) - No Crossflow.
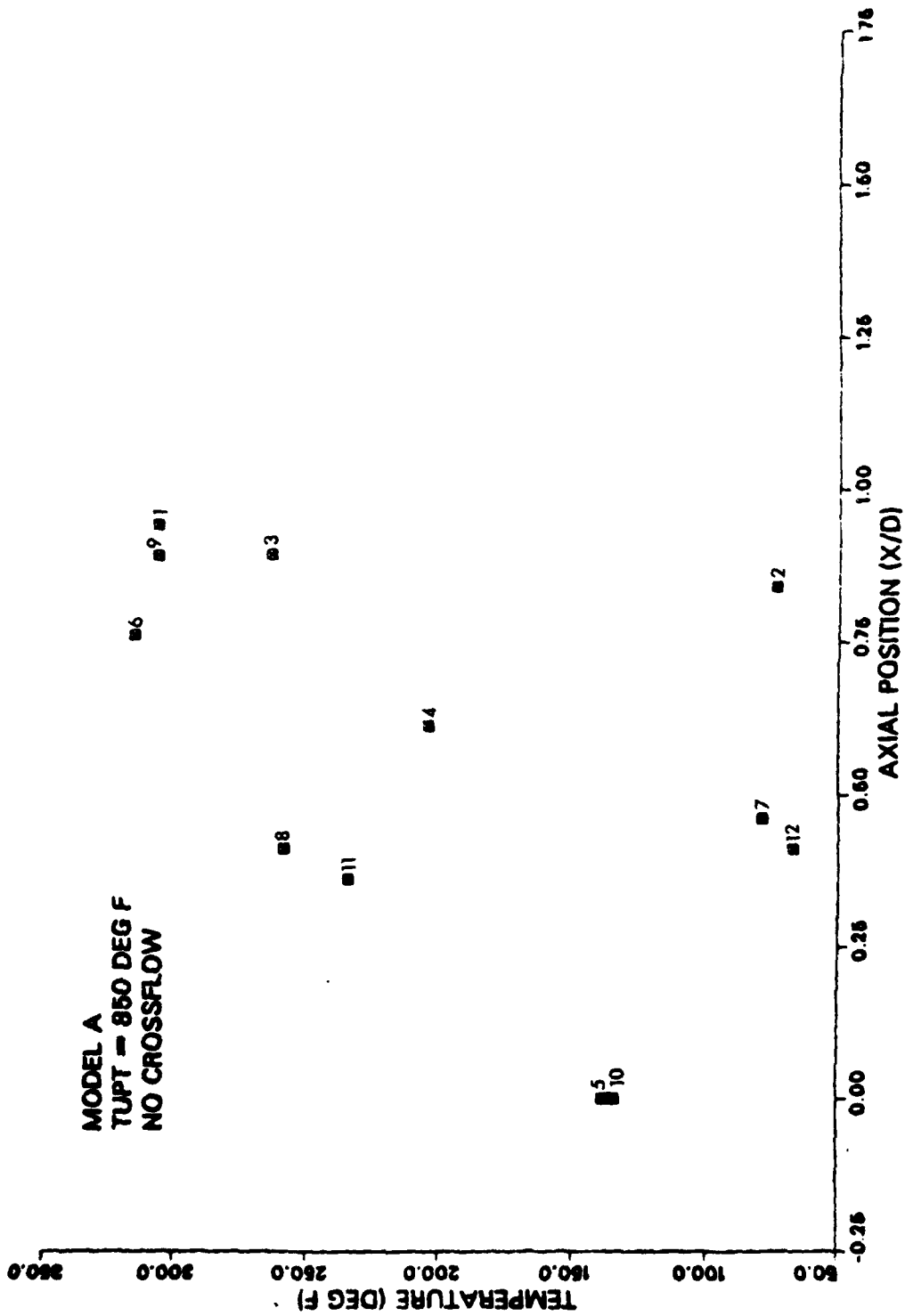
Figure 54. Mixing Stack Temp., Model A (850F) - No crossflow.

116
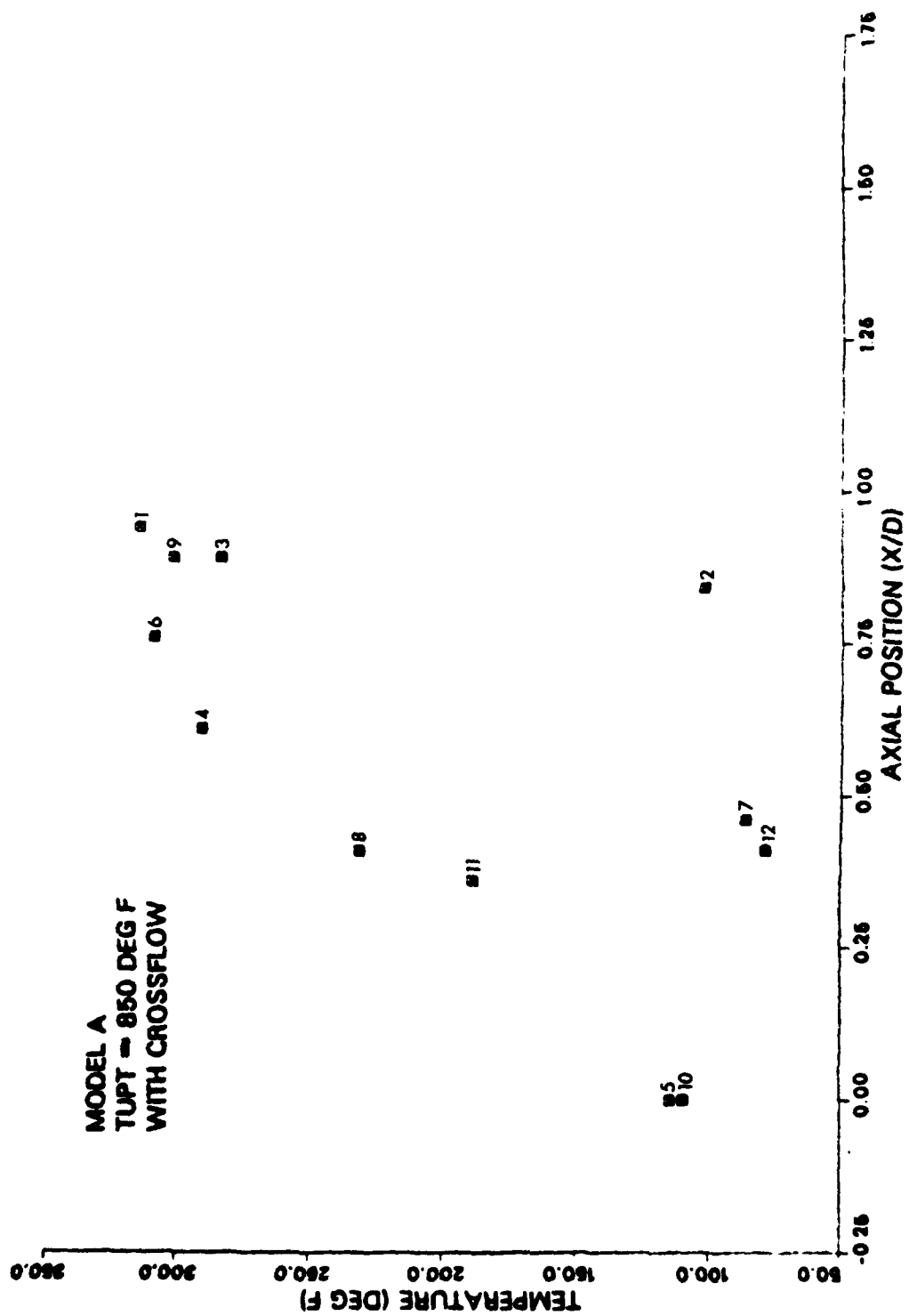
Figure 55. Mixing Stack Temp., Model A (850 F) - Crossflow.
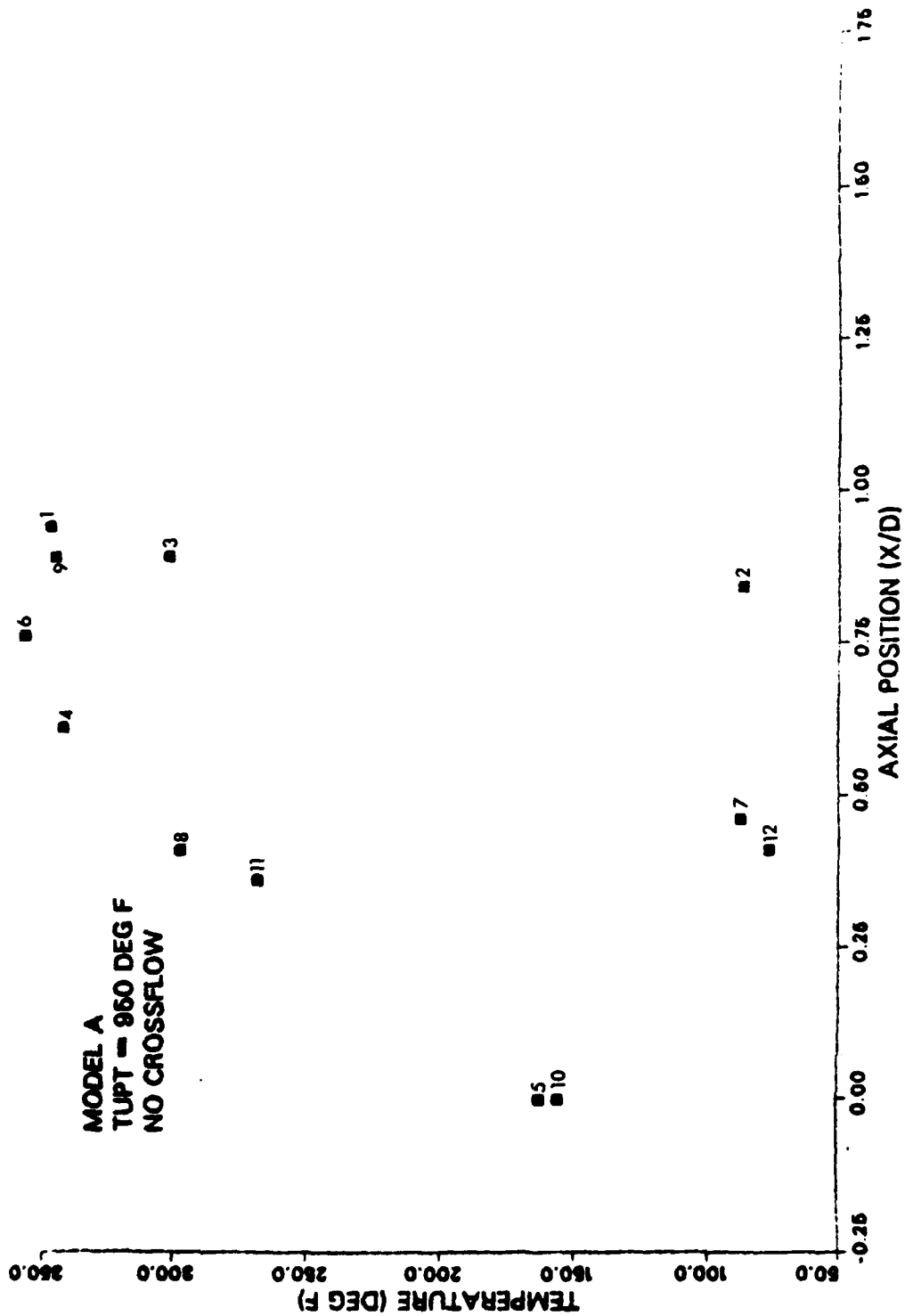
Figure 56. Mixing Stack Temp., Model A (950 F) – No Crossflow.
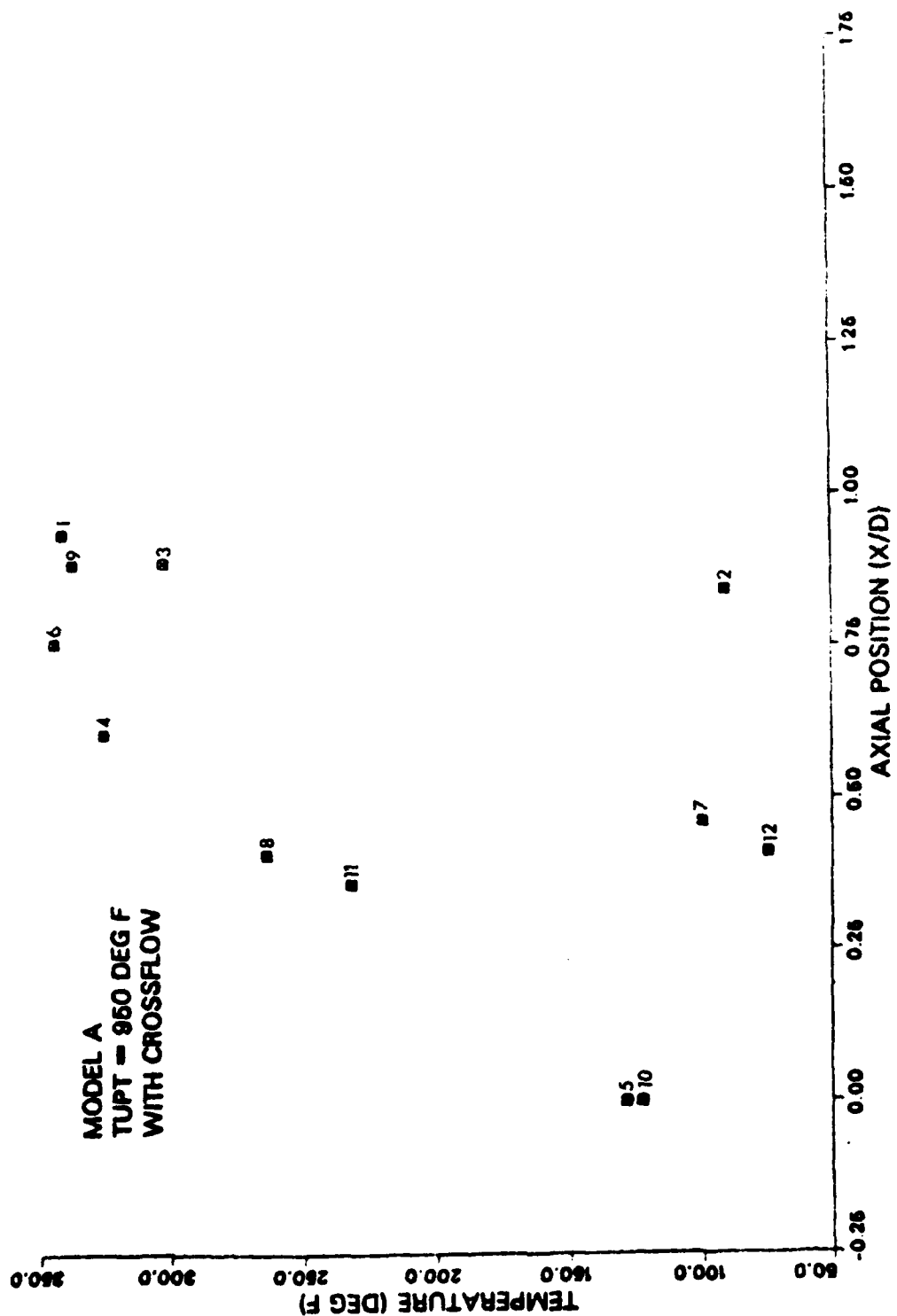
Figure 57. Mixing Stack Temp., Model A (950 F) - Crossflow.

119
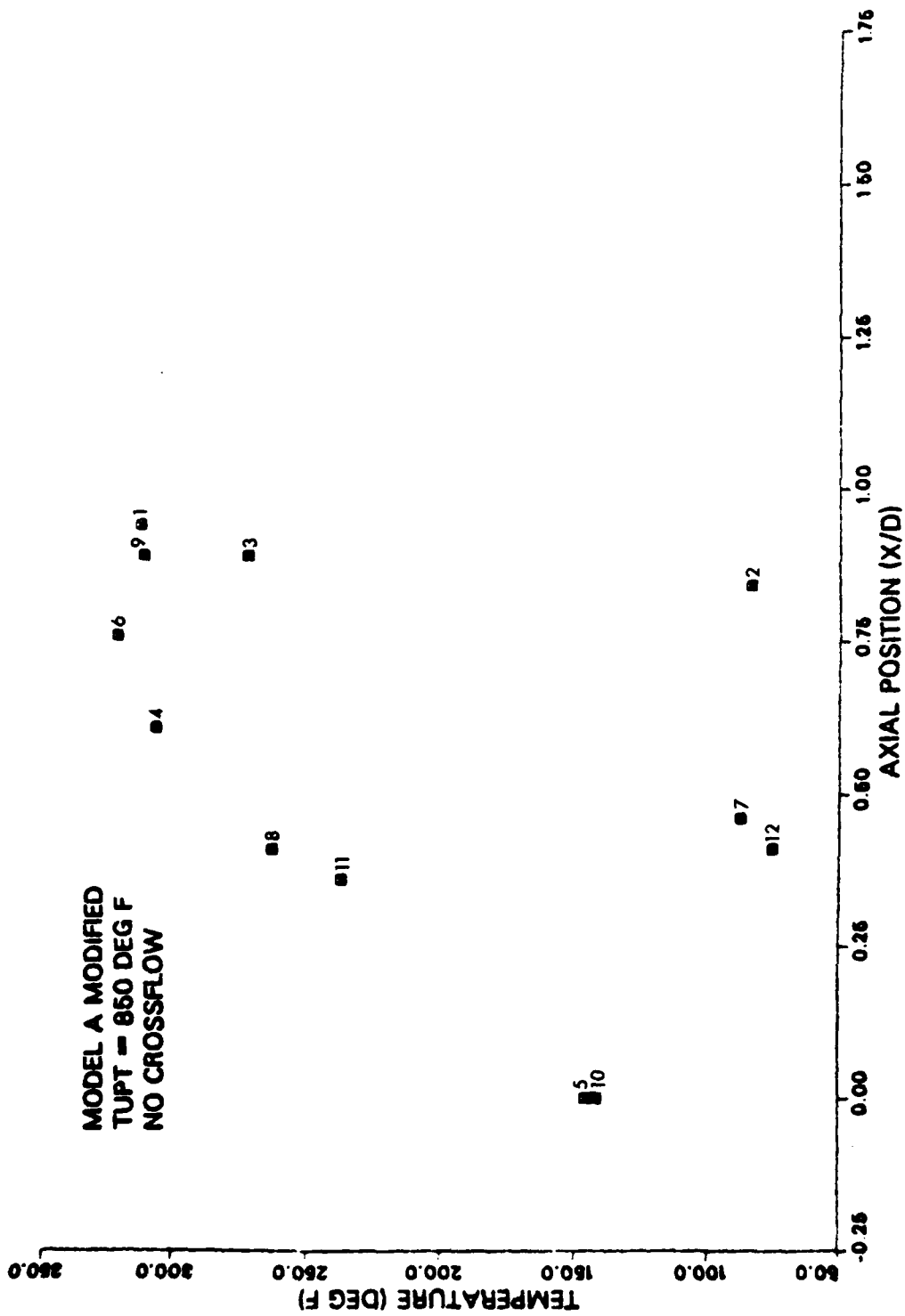
Figure 58. Mixing Stack Temp., Model A Mod (850 F) — No Crossflow.

120
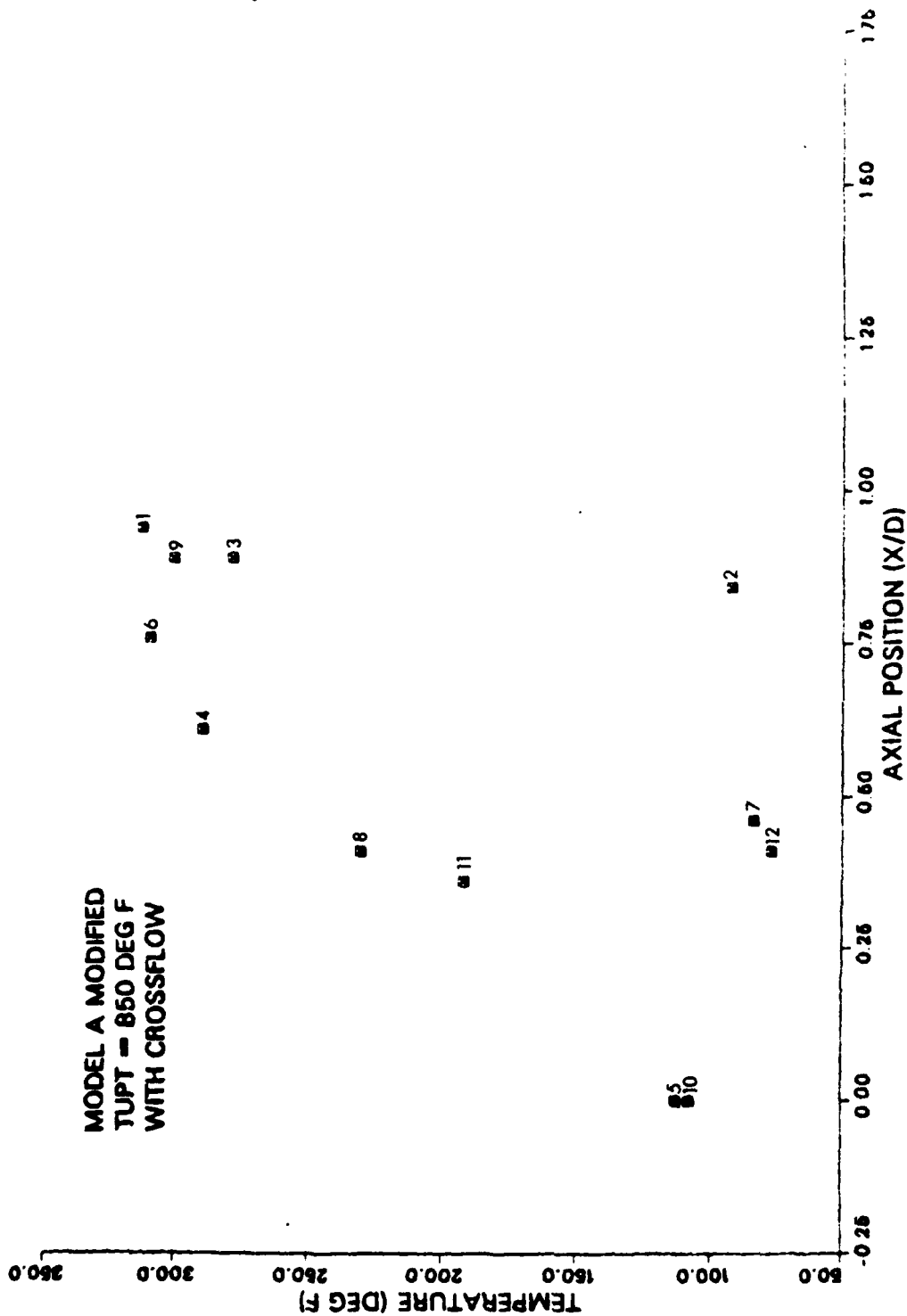
Figure 59. Mixing Stack Temp., Model A Mod (850 F) - Crossflow.

121
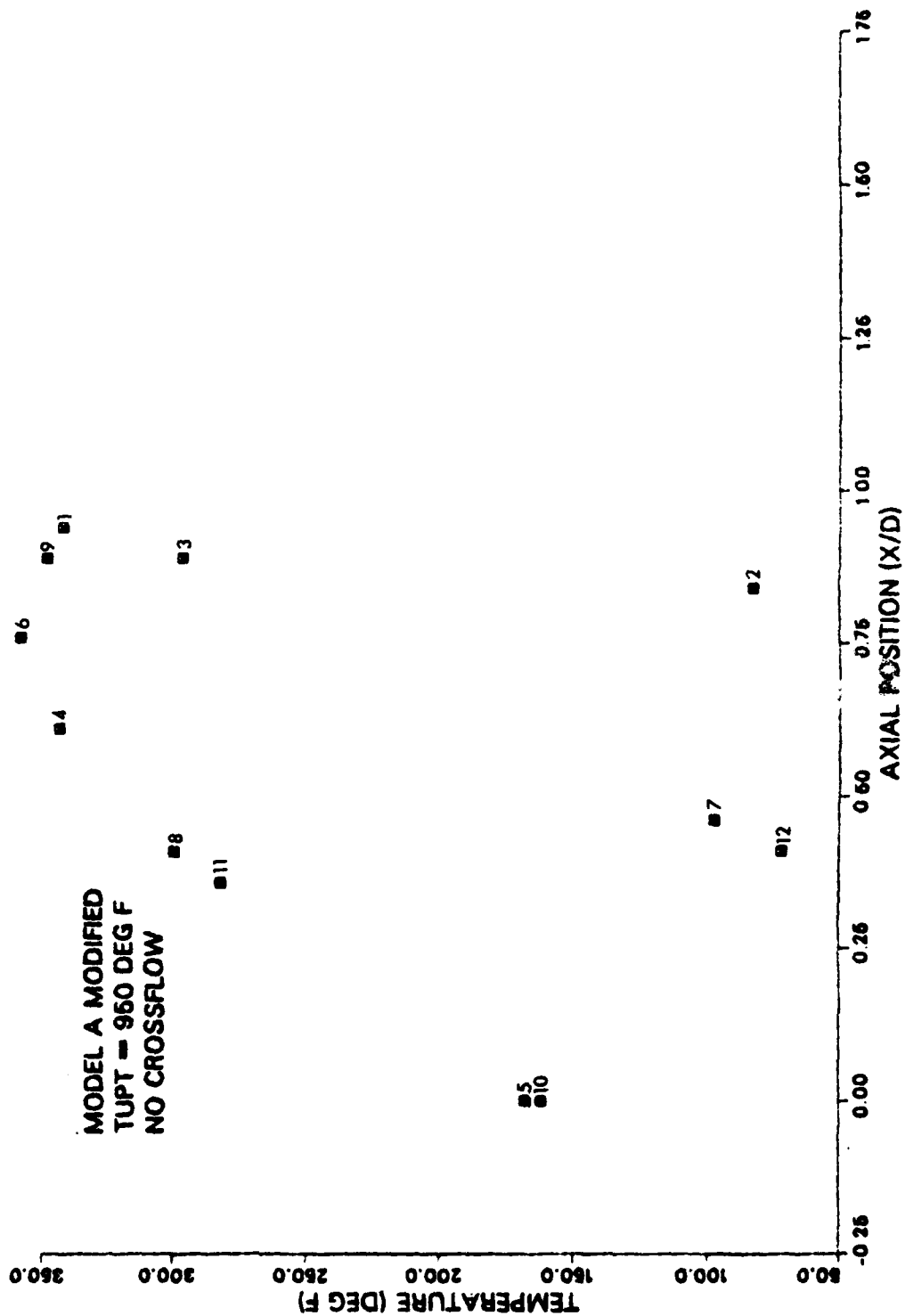
Figure 60. Mixing Stack Temp., Model A Mod (950 F) - No Crossflow.
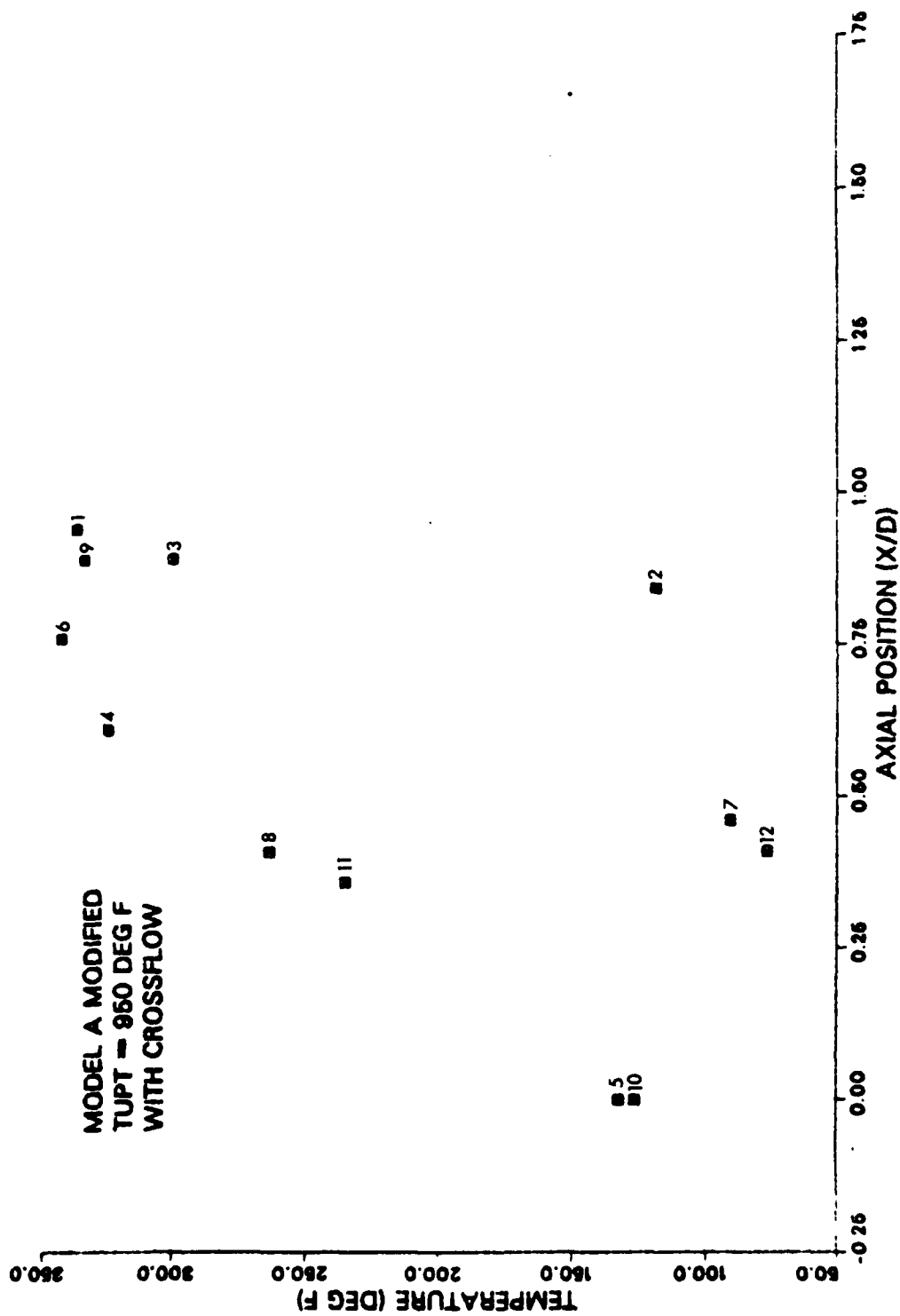
Figure 61. Mixing Stack Temp., Model A Mod (950 F) - Crossflow.
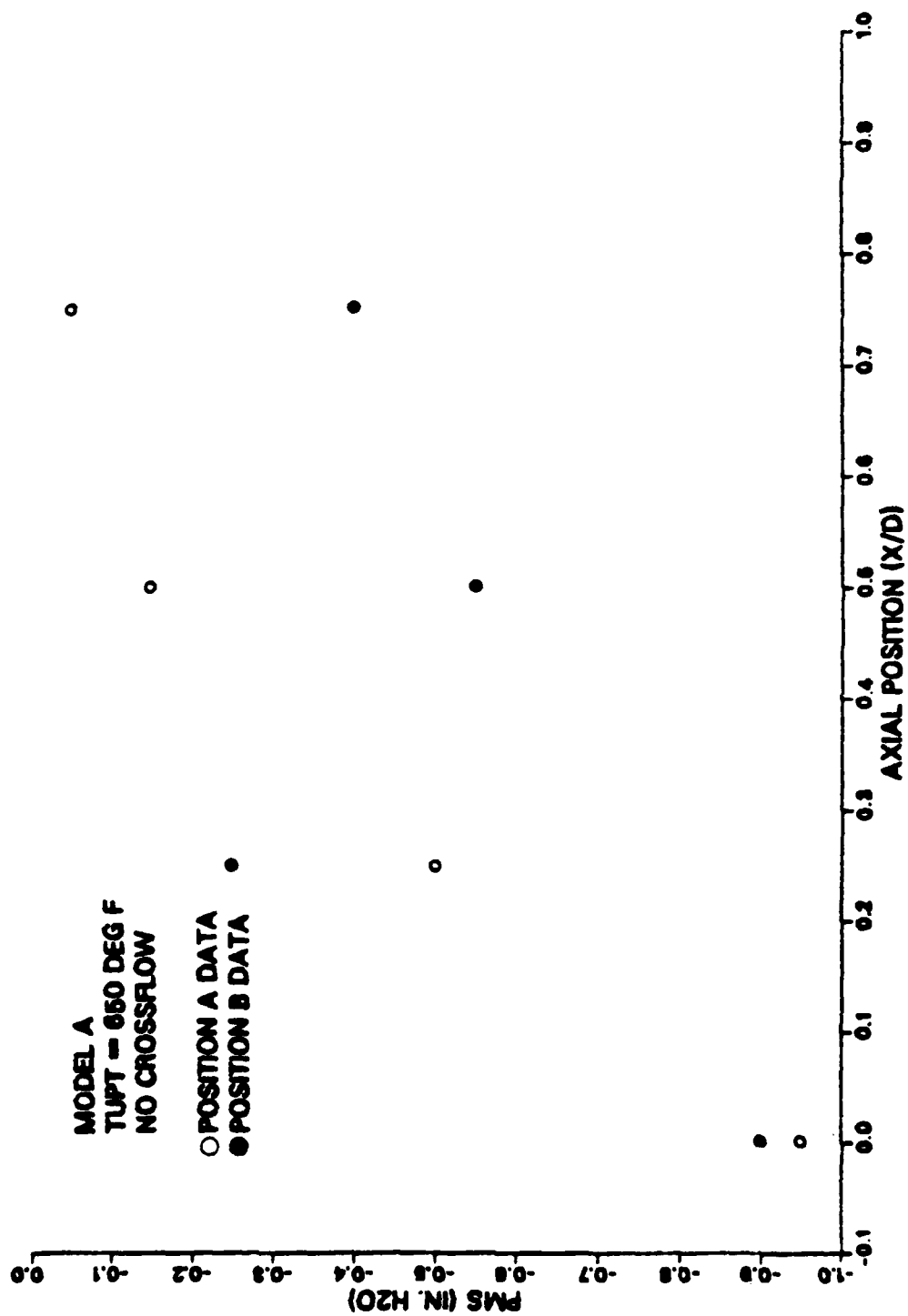
Figure 62. Mixing Stack Press., Model A (650 F) - No Crossflow.
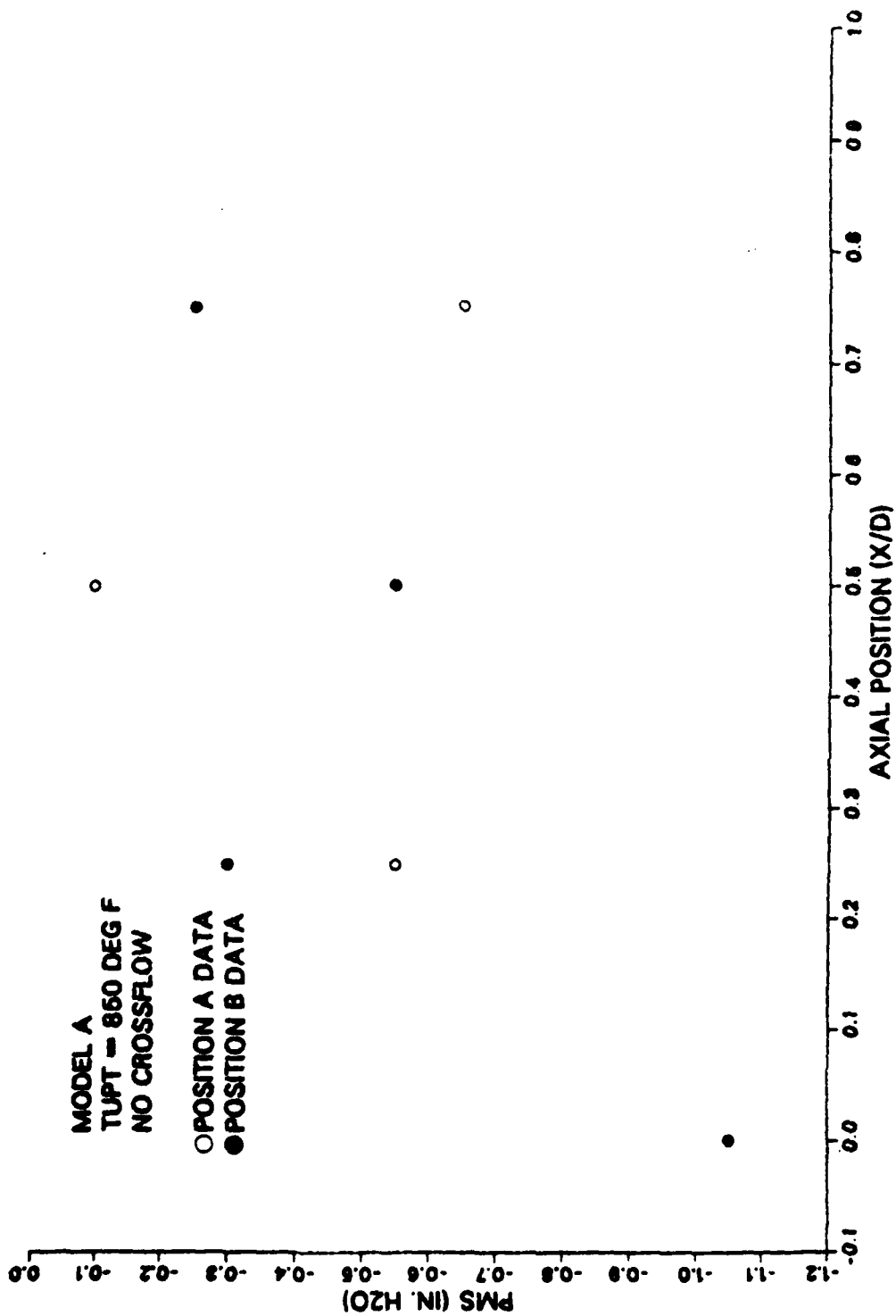
Figure 63. Mixing Stack Press., Model A (850 F) - No Crossflow.
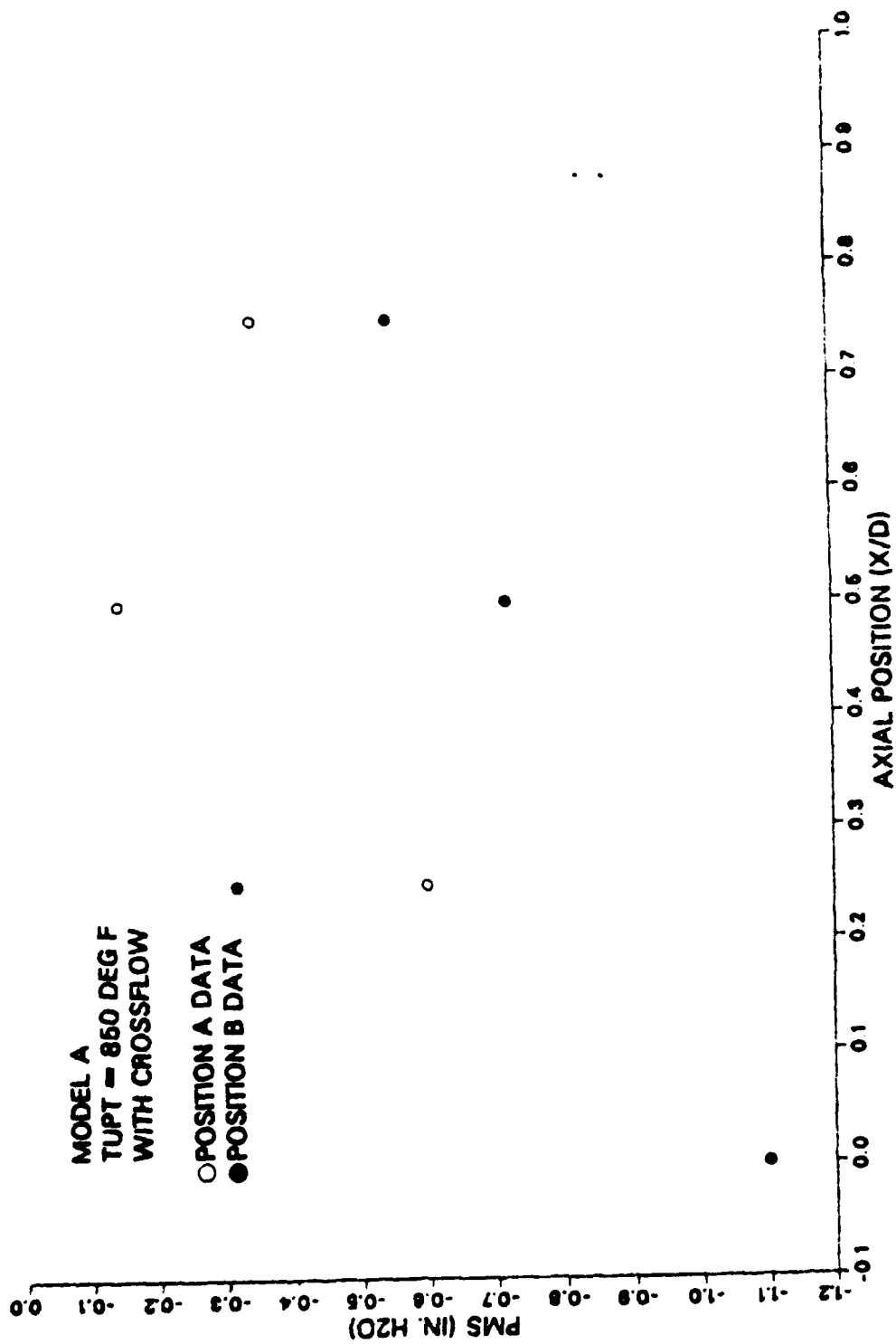
Figure 64.   Mixing Stack Press., Model A (850 F)   - Crossflow.

MODEL A
TUPT = 950 DEG F
NO CROSSFLOW

○ POSITION A DATA
● POSITION B DATA

PMS (IN. H2O)

AXIAL POSITION (X/D)
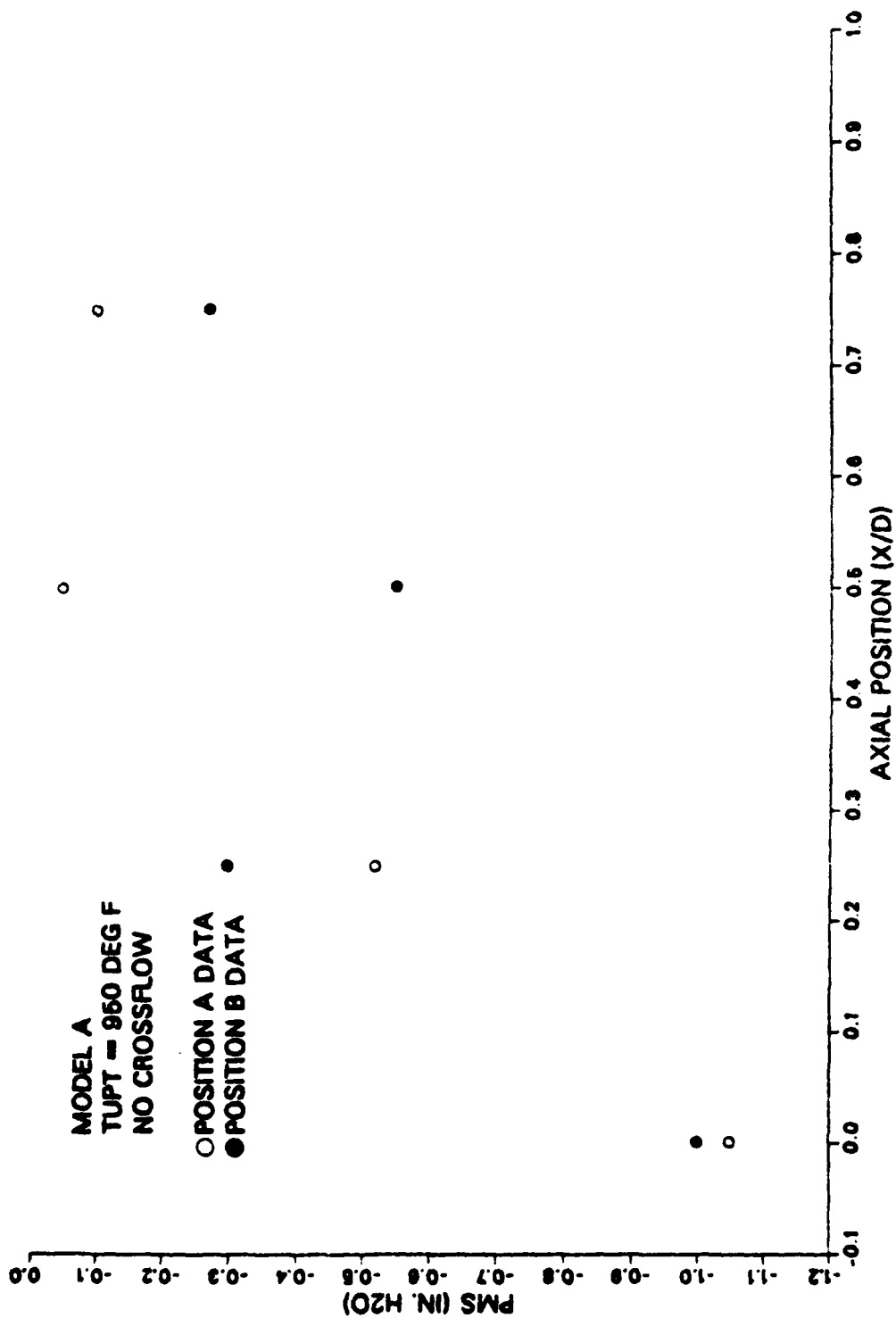
Figure 65.   Mixing Stack Press., Model A (950 F) - No Crossflow.
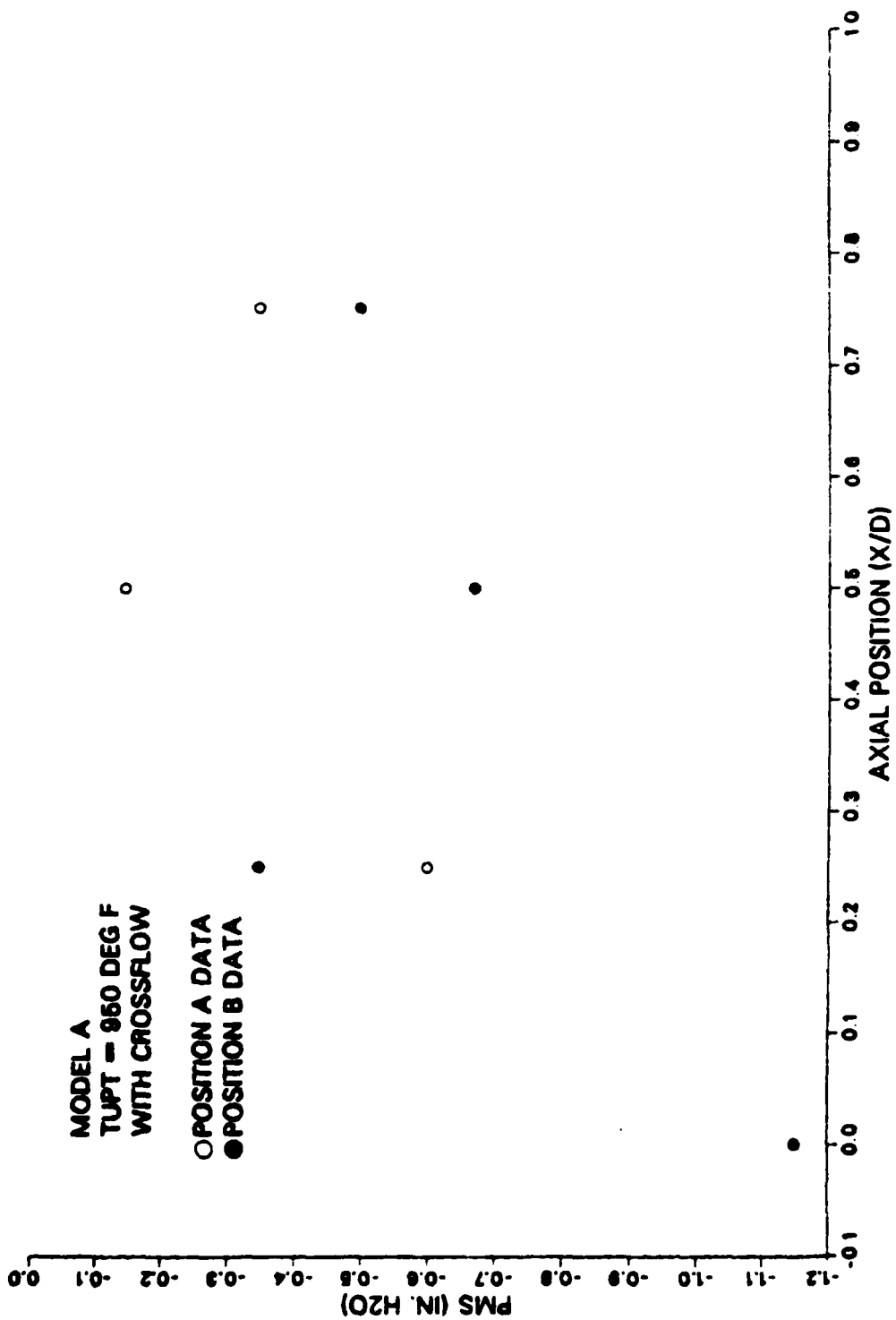
Figure 66. Mixing Stack Press., Model A (950 F) - Crossflow.

128
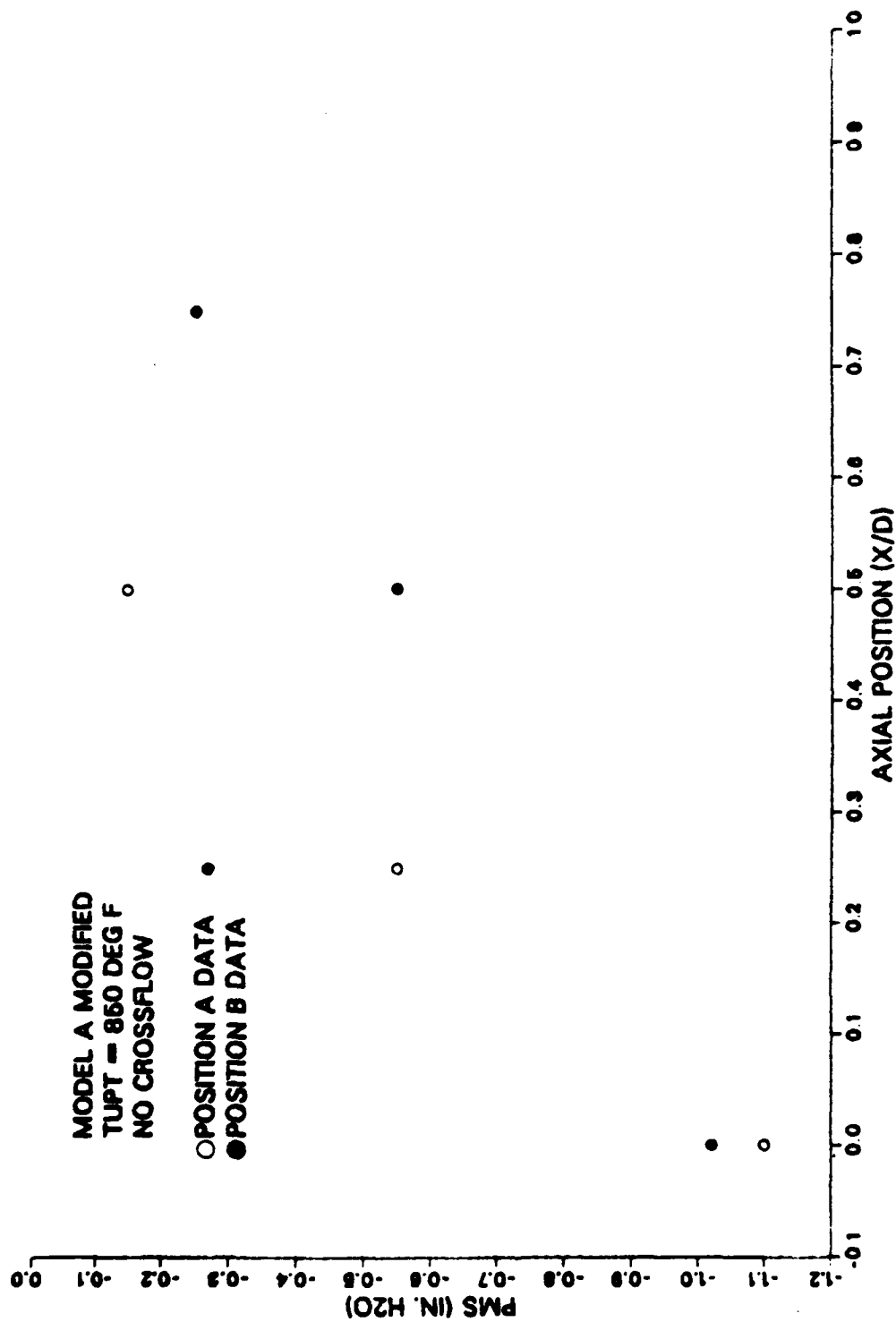
Figure 67. Mixing Stack Press., Model A Mod (850 F) - No Crossflow.
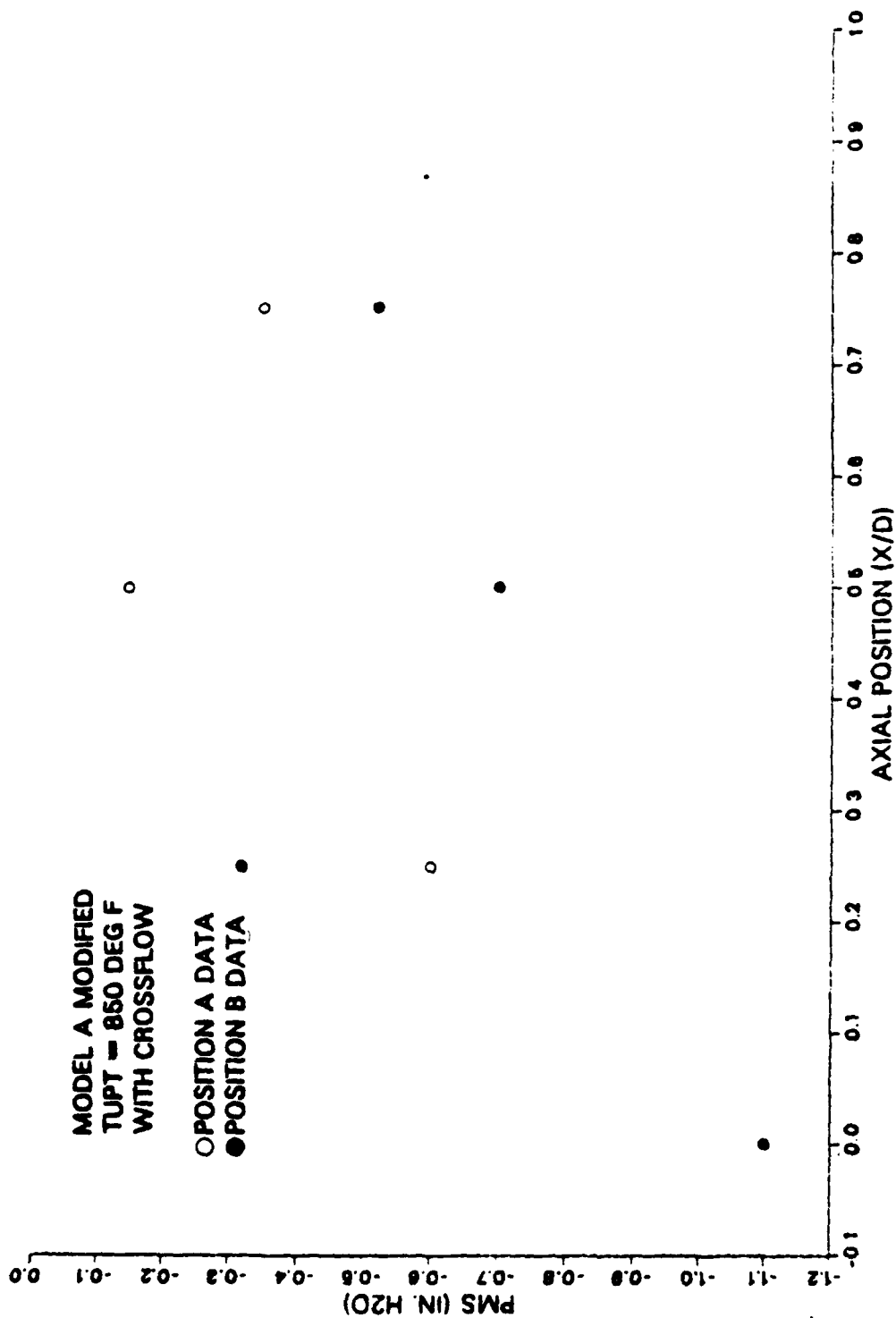
Figure 68. Mixing Stack Press., Model A Mod (850 F) - Crossflow.

MODEL A MODIFIED
TUPT = 950 DEG F
NO CROSSFLOW

O POSITION A DATA
● POSITION B DATA

● POSITION A DATA
O POSITION B DATA

PMS (IN. H2O)

AXIAL POSITION (X/D)

0.0 -0.1 -0.2 -0.3 -0.4 -0.5 -0.6 -0.7 -0.8 -0.9 -1.0 -1.1 -1.2

-0.1 0.0 0.1 0.2 0.3 0.4 0.5 0.6 0.7 0.8 0.9 1.0
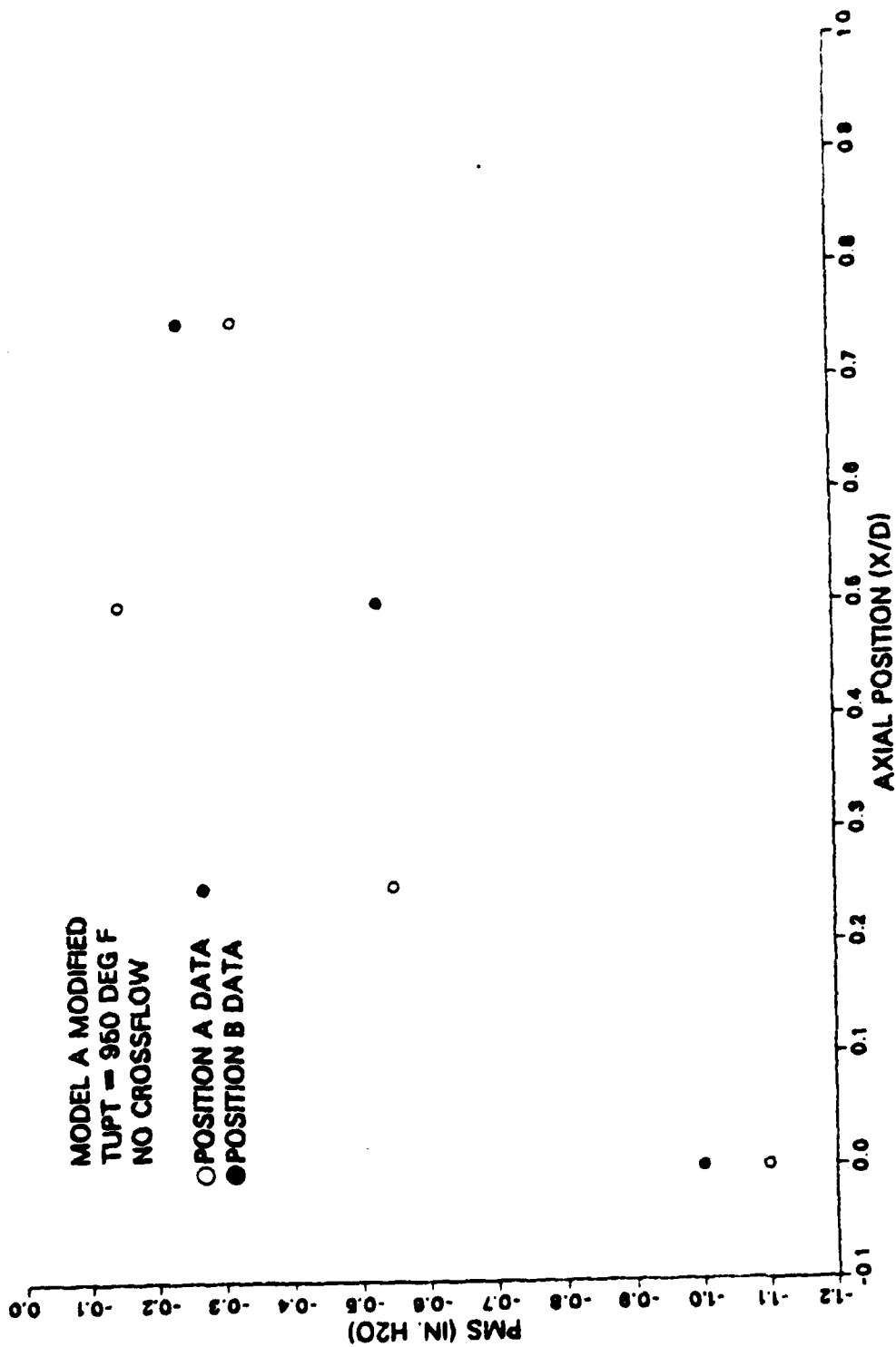
Figure 69. Mixing Stack Press., Model A Mod (950 F) - No Crossflow.
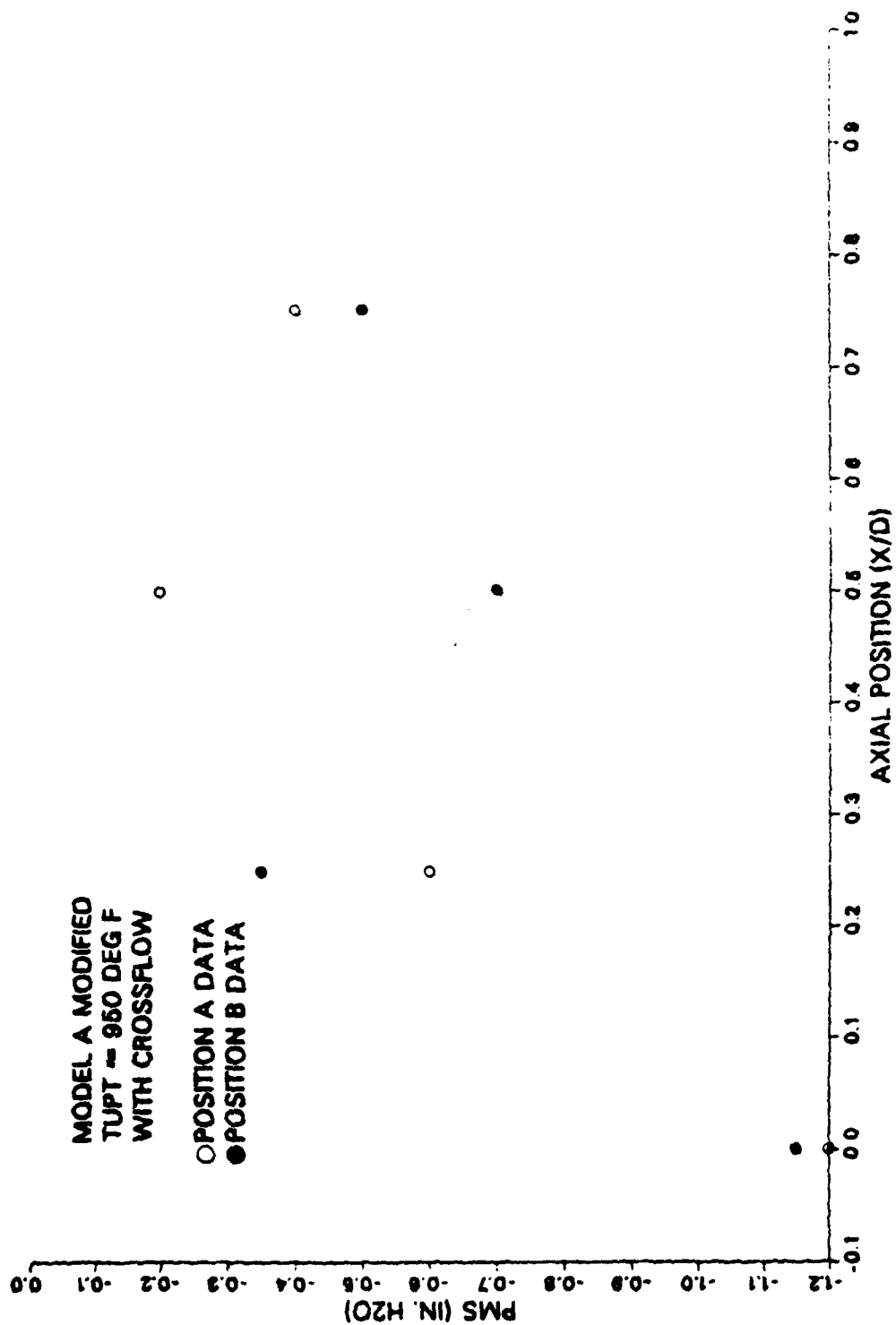
Figure 70. Mixing Stack Press., Model A Mod (950 F) - Crossflow.

132
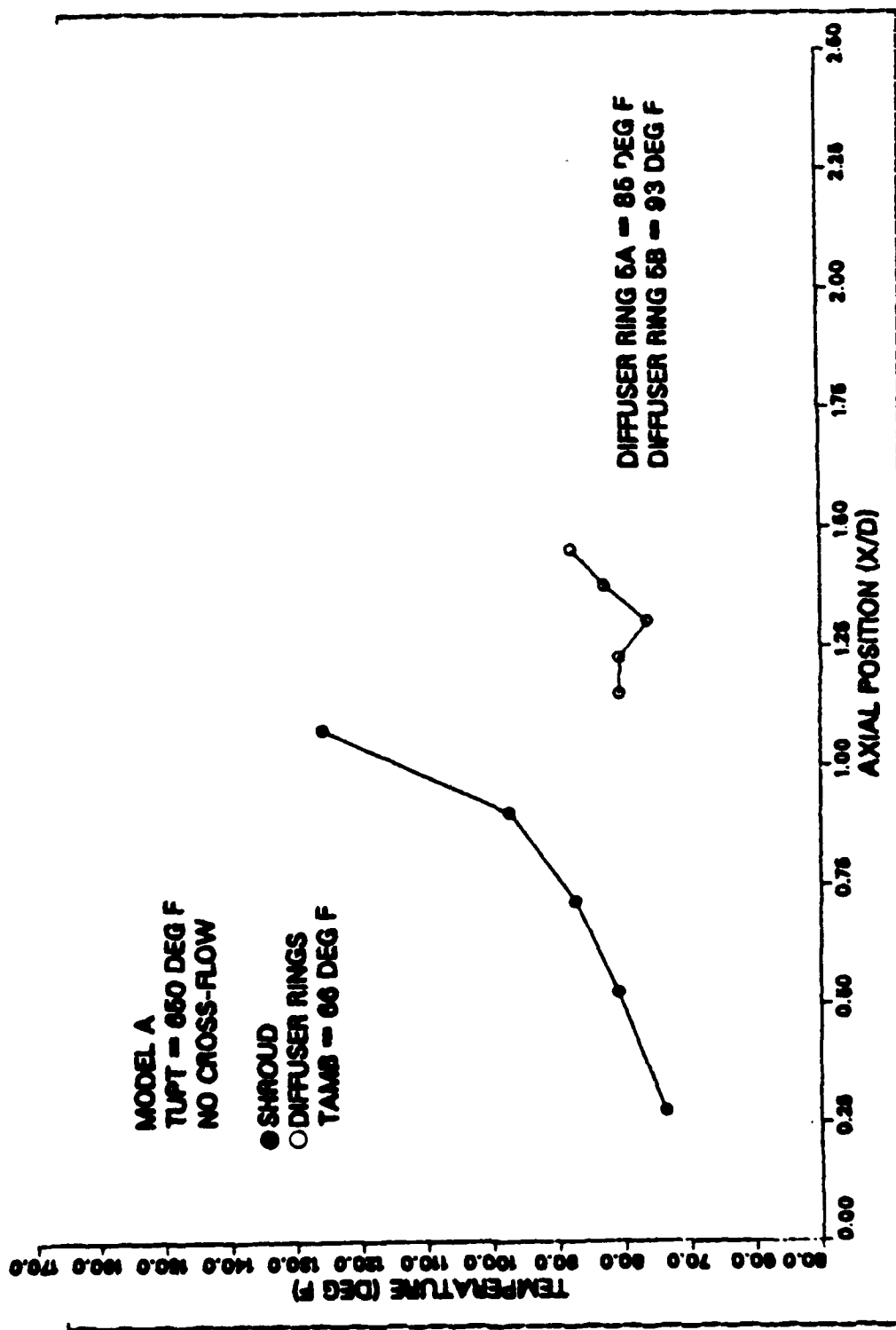
Figure 71. Type T External Temp., Model A (650 F) - No Crossflow.

133
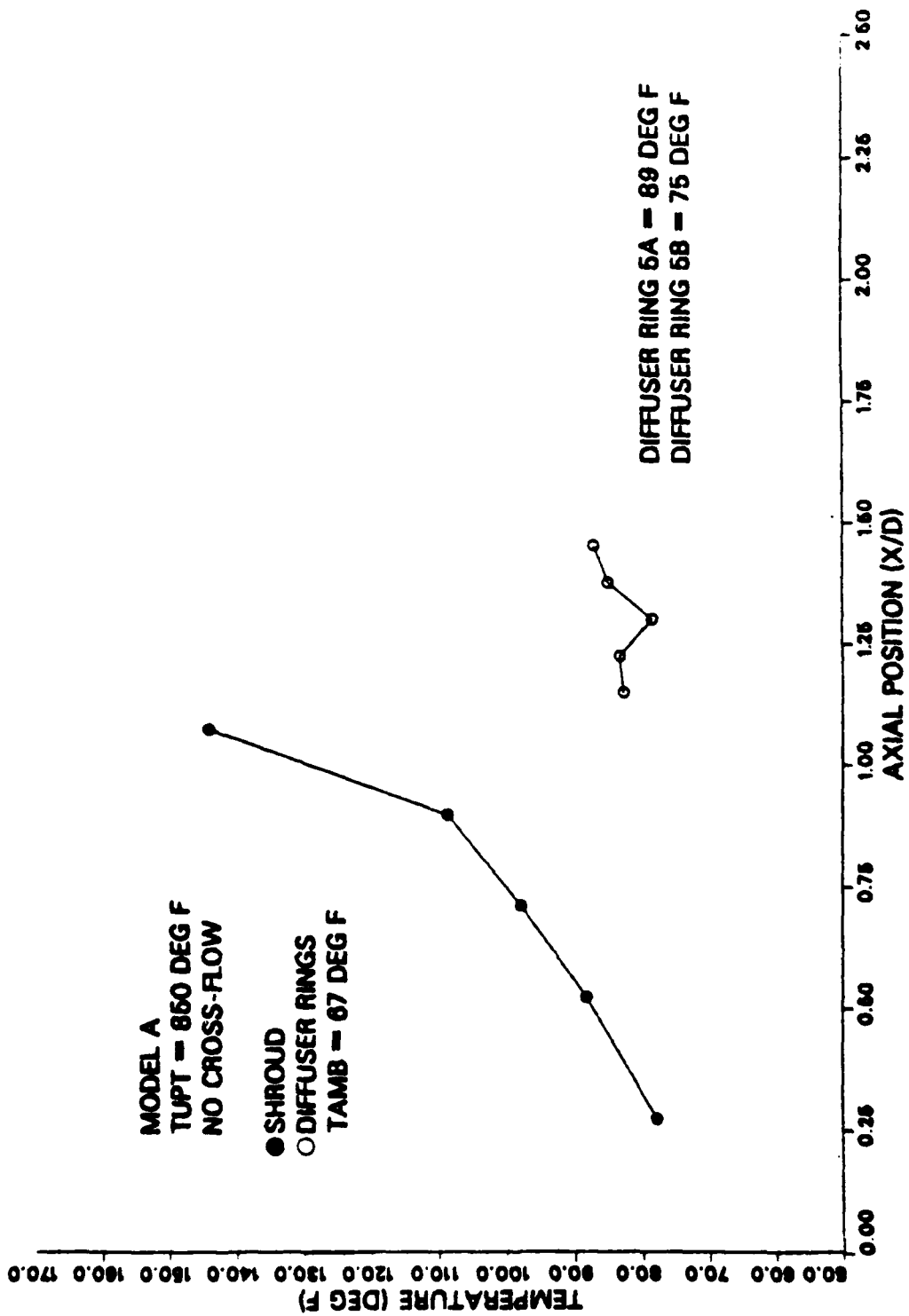
Figure 72. Type T External Temp., Model A (850 F) - No Crossflow.
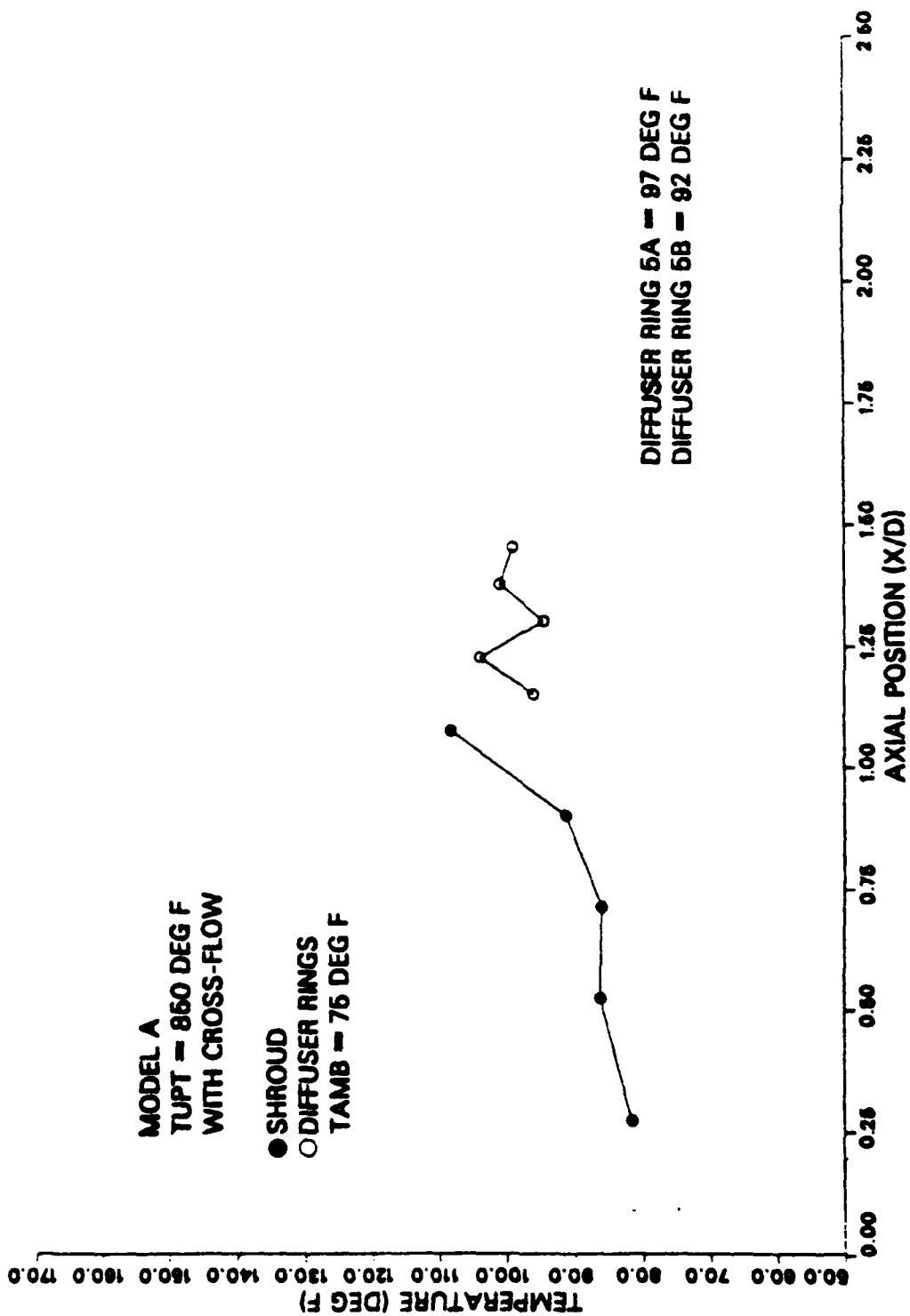
Figure 73. Type T External Temp., Model A (850 F) - Crossflow.

135
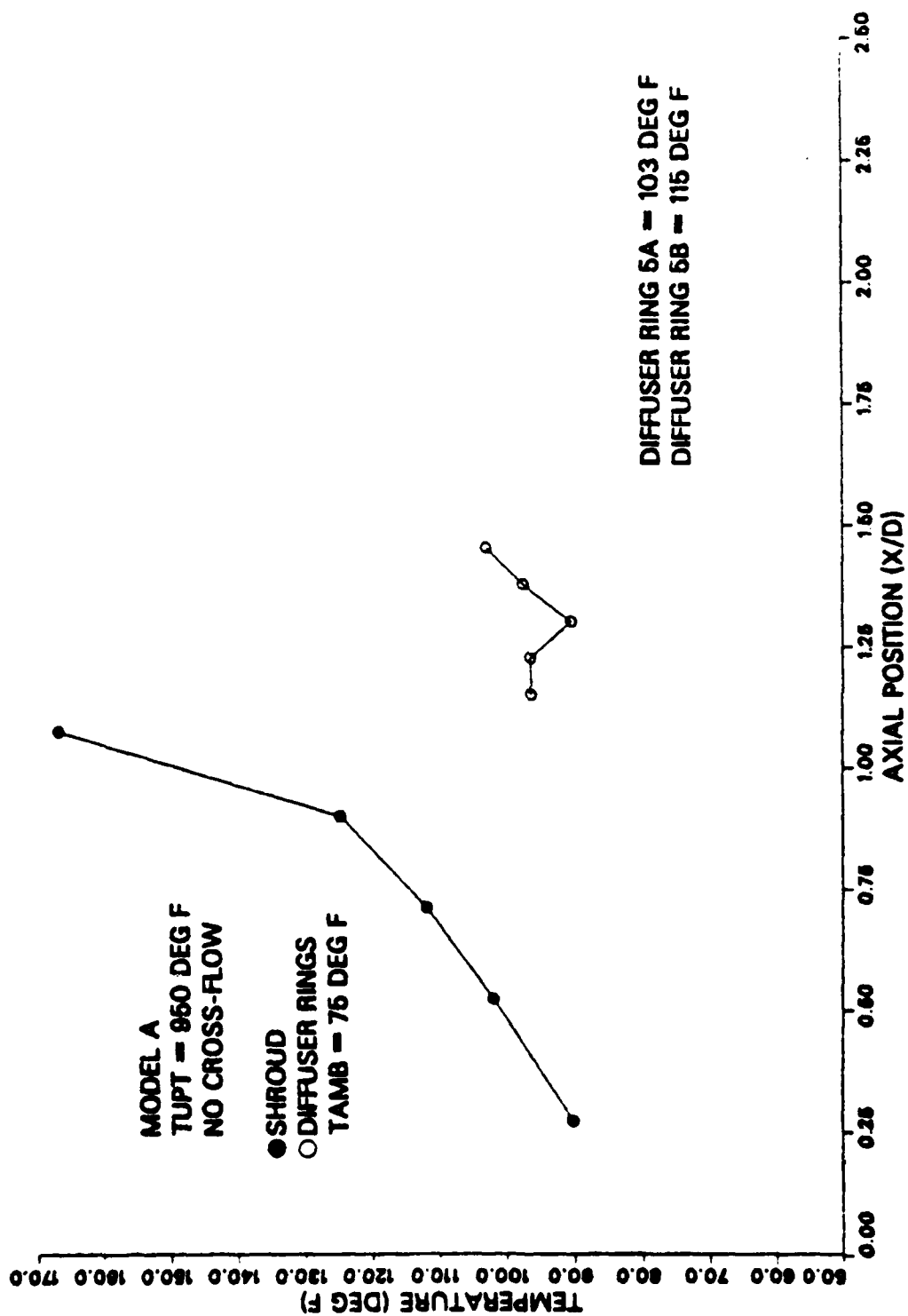
Figure 74. Type T External Temp., Model A (950 F) - No Crossflow.

136
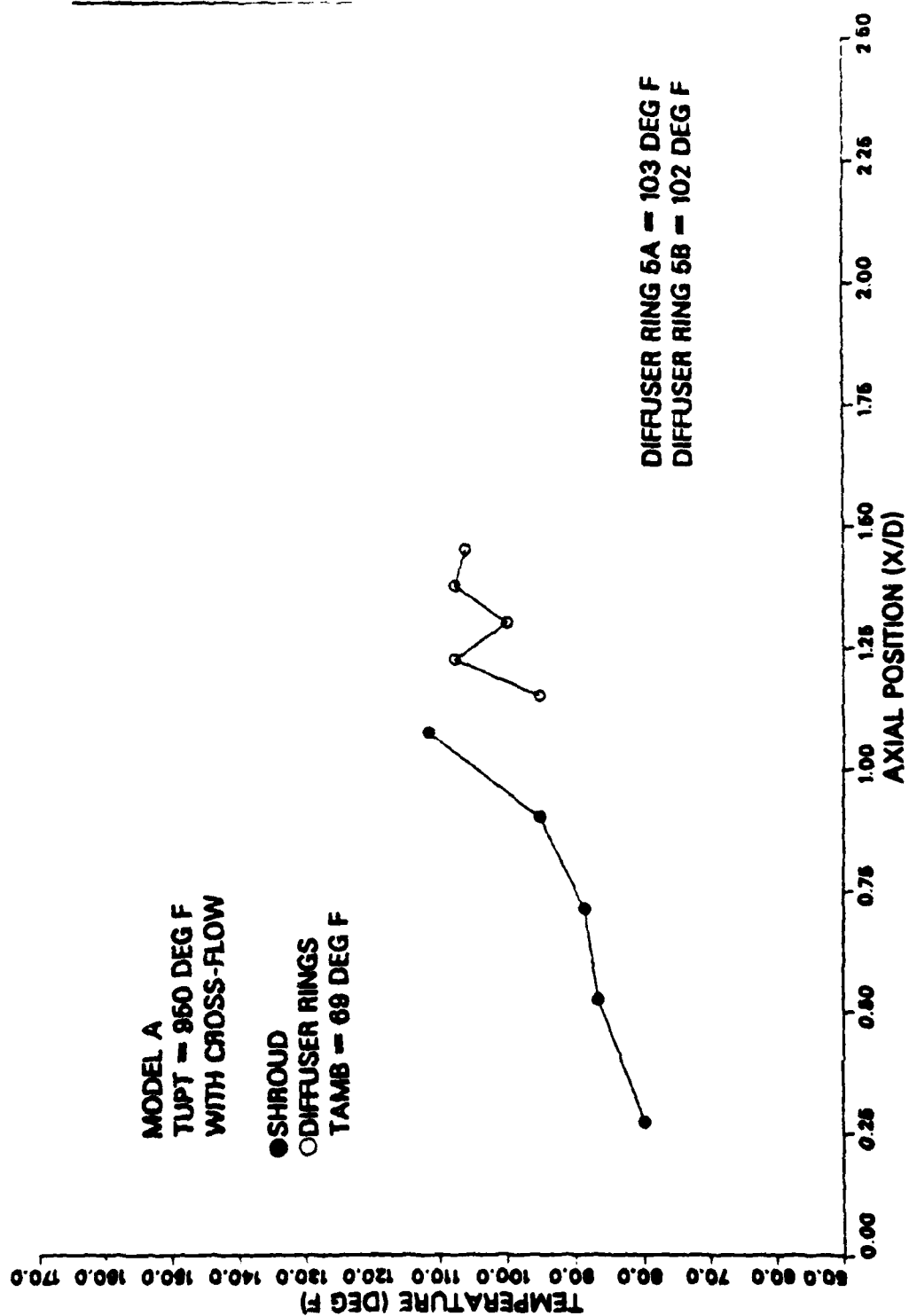
Figure 75. Type T External Temp., Model A (950 F) - Crossflow.

137
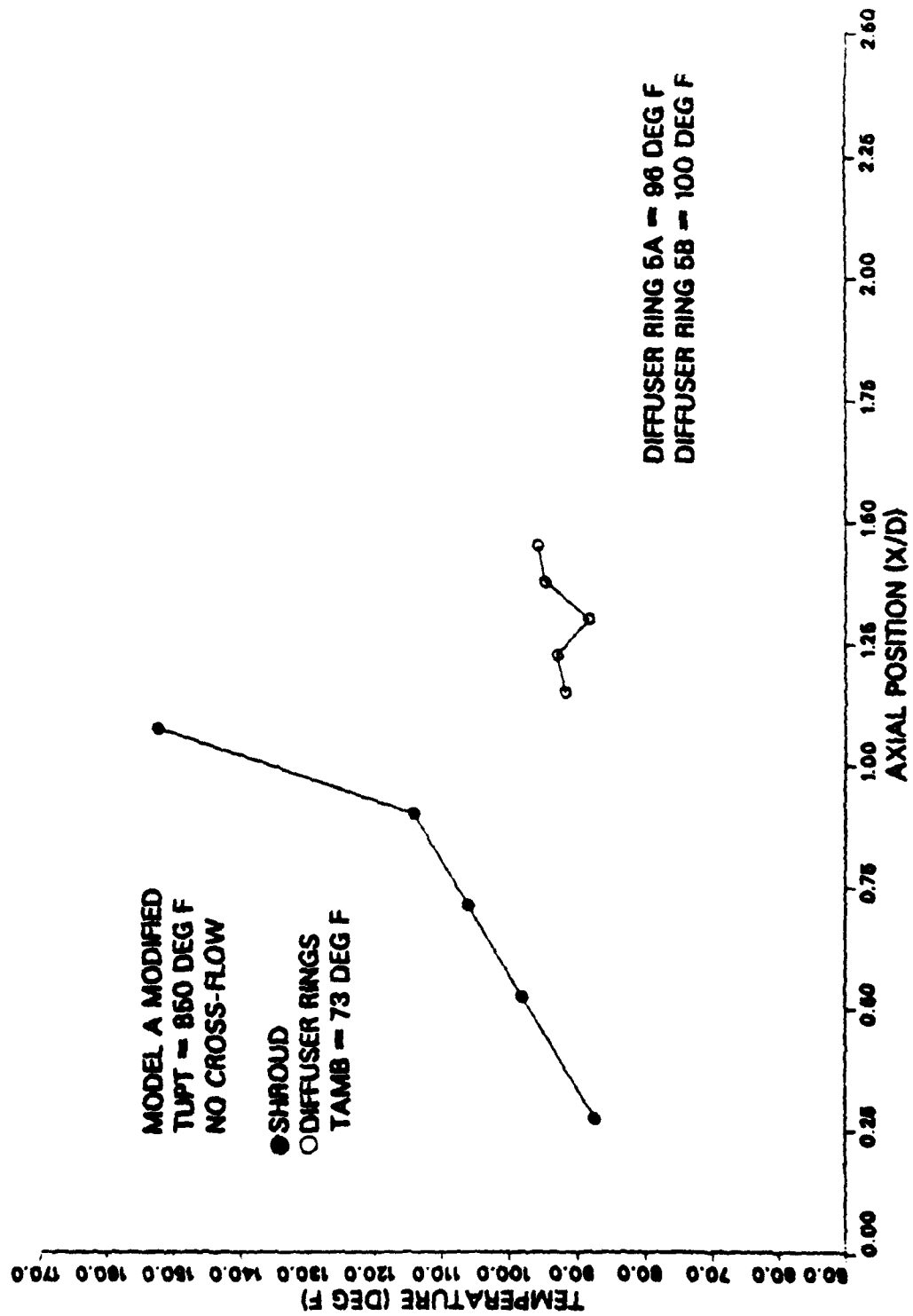
Figure 76. Type T Ext. Temp., Model A Mod (850 F) - No Crossflow.

TEMPERATURE (DEG F)

AXIAL POSITION (X/D)

MODEL A MODIFIED
TUPT = 850 DEG F
NO CROSS-FLOW

● SHROUD
○ DIFFUSER RINGS
TAMB = 73 DEG F

DIFFUSER RING 5A = 96 DEG F
DIFFUSER RING 5B = 100 DEG F

138
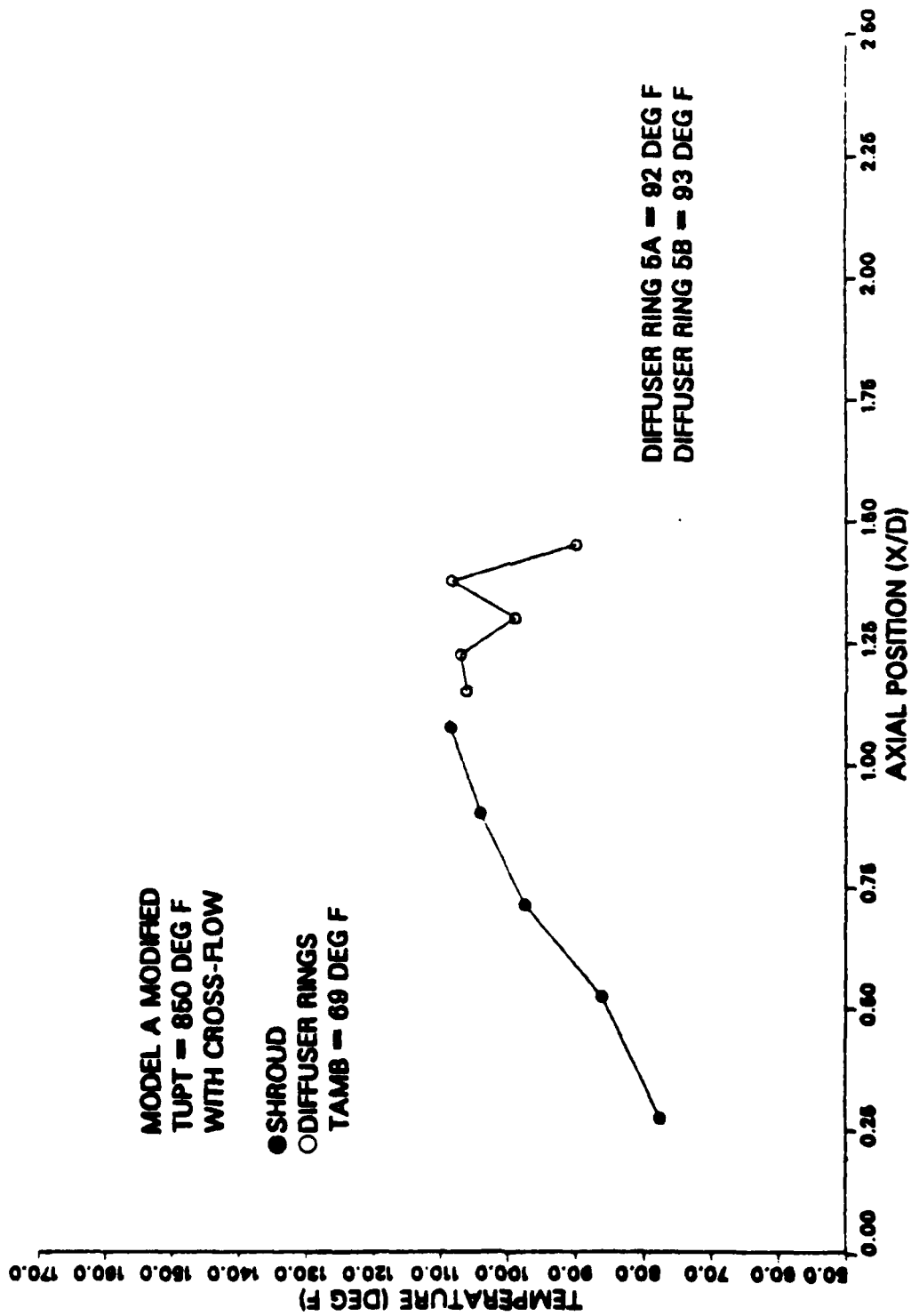
Figure 77. Type F Ext. Temp., Model A Mod (850 F) - Crossflow.
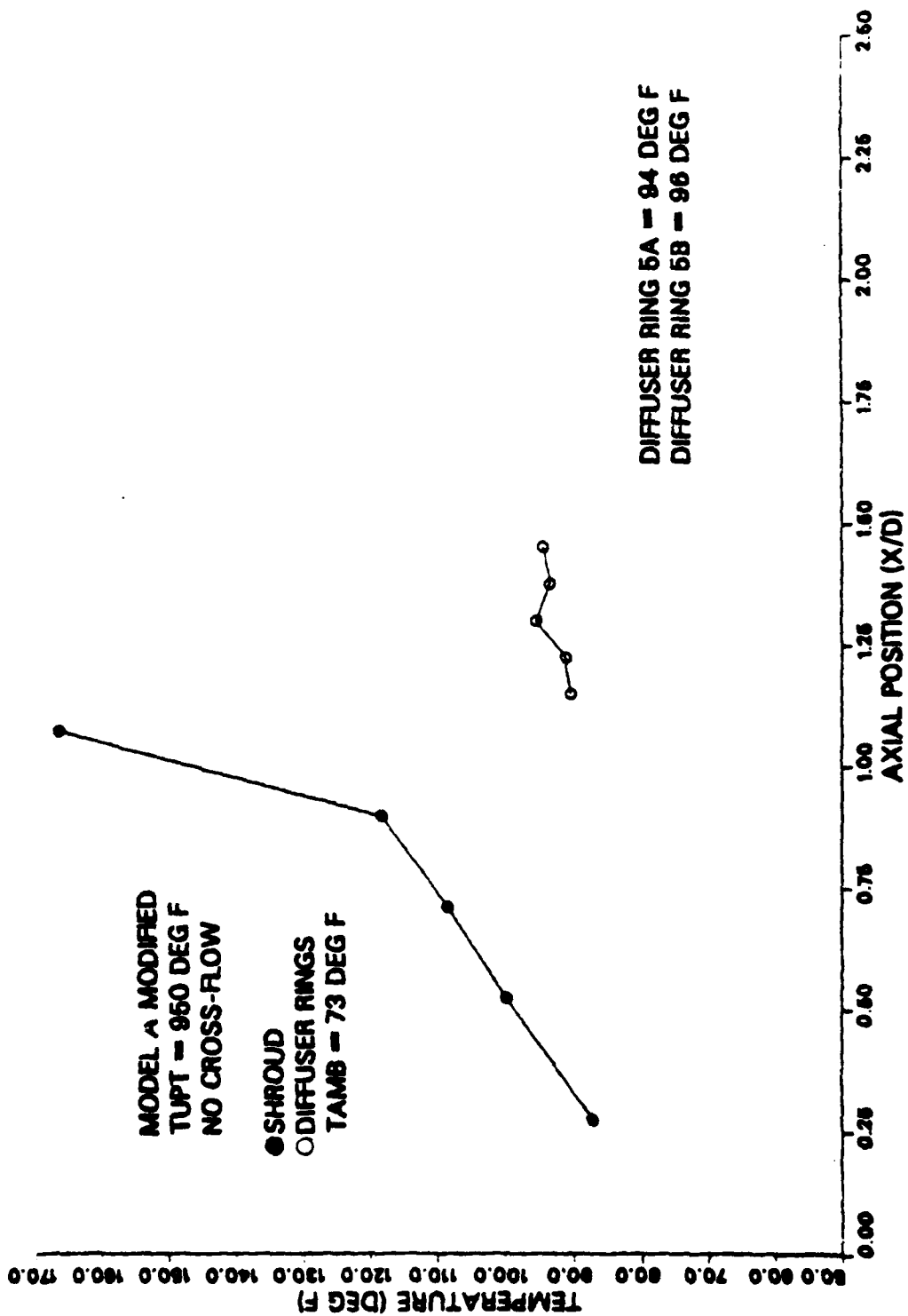
Figure 78. Type T Ext. Temp., Model A Mod (950 F) - No Crossflow.
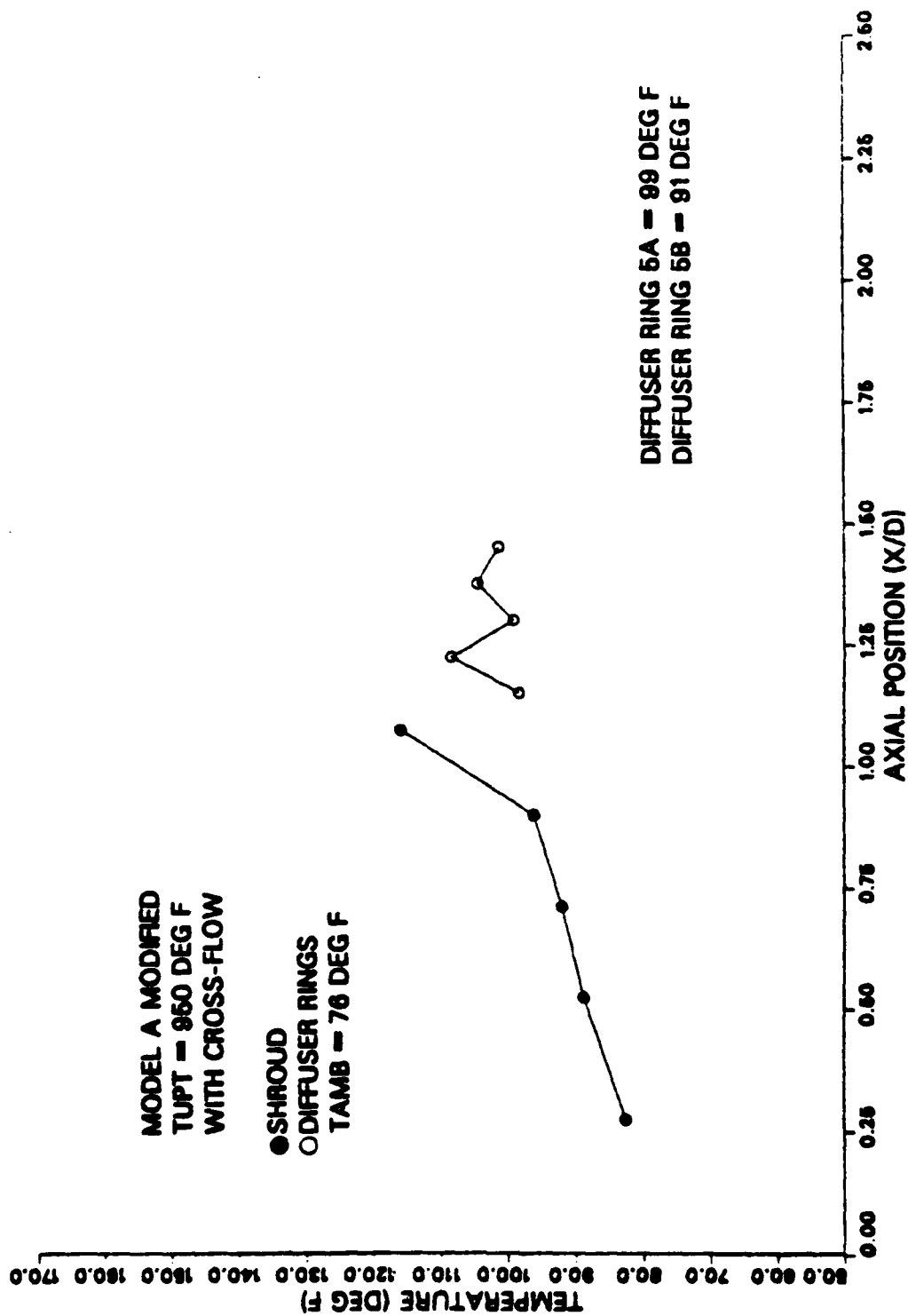
Figure 79. Type T Ext. Temp., Model A Mod (950 F) - Crossflow.
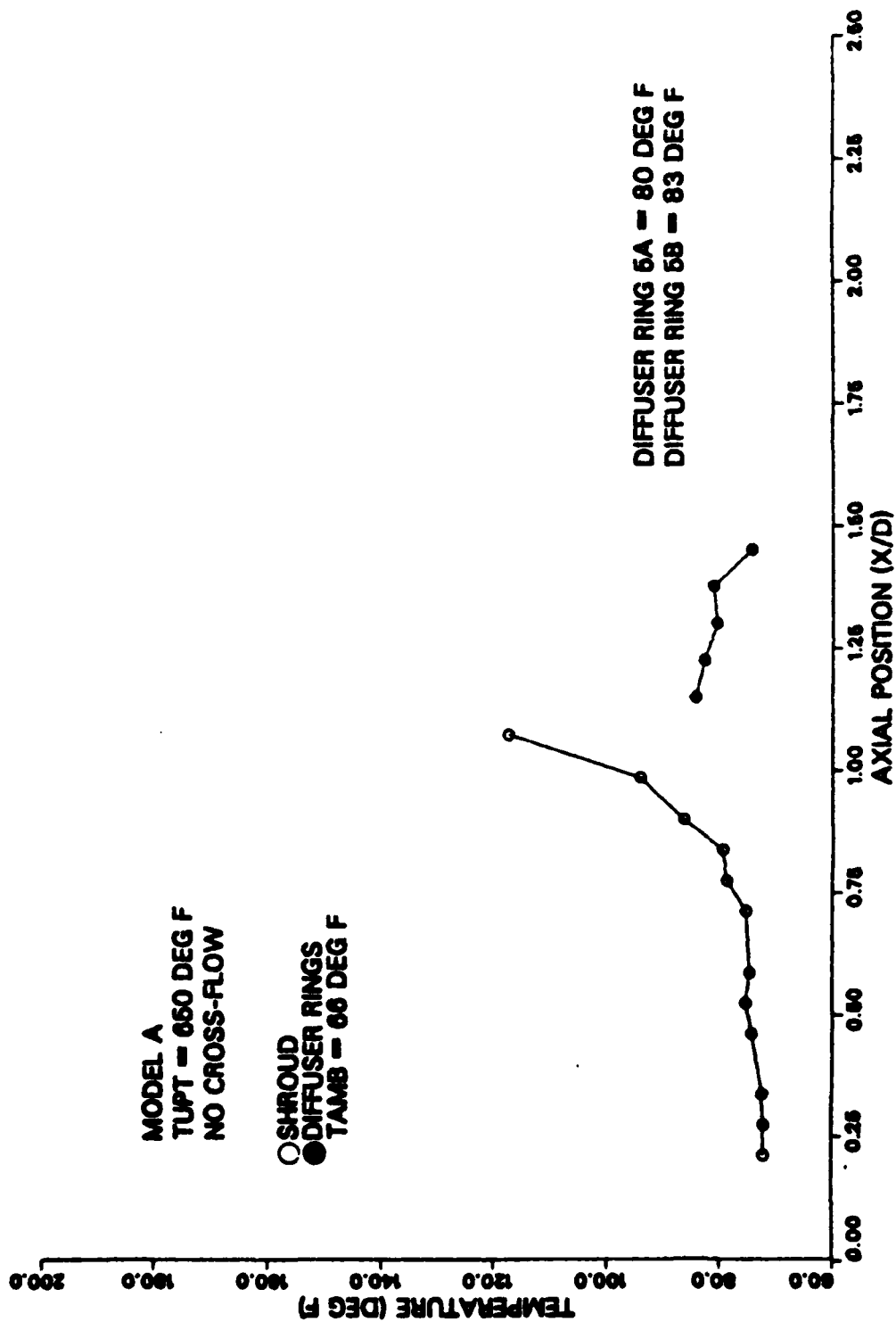
Figure 80. Omega External Temp., Model A (650 F) - No Crossflow.

142
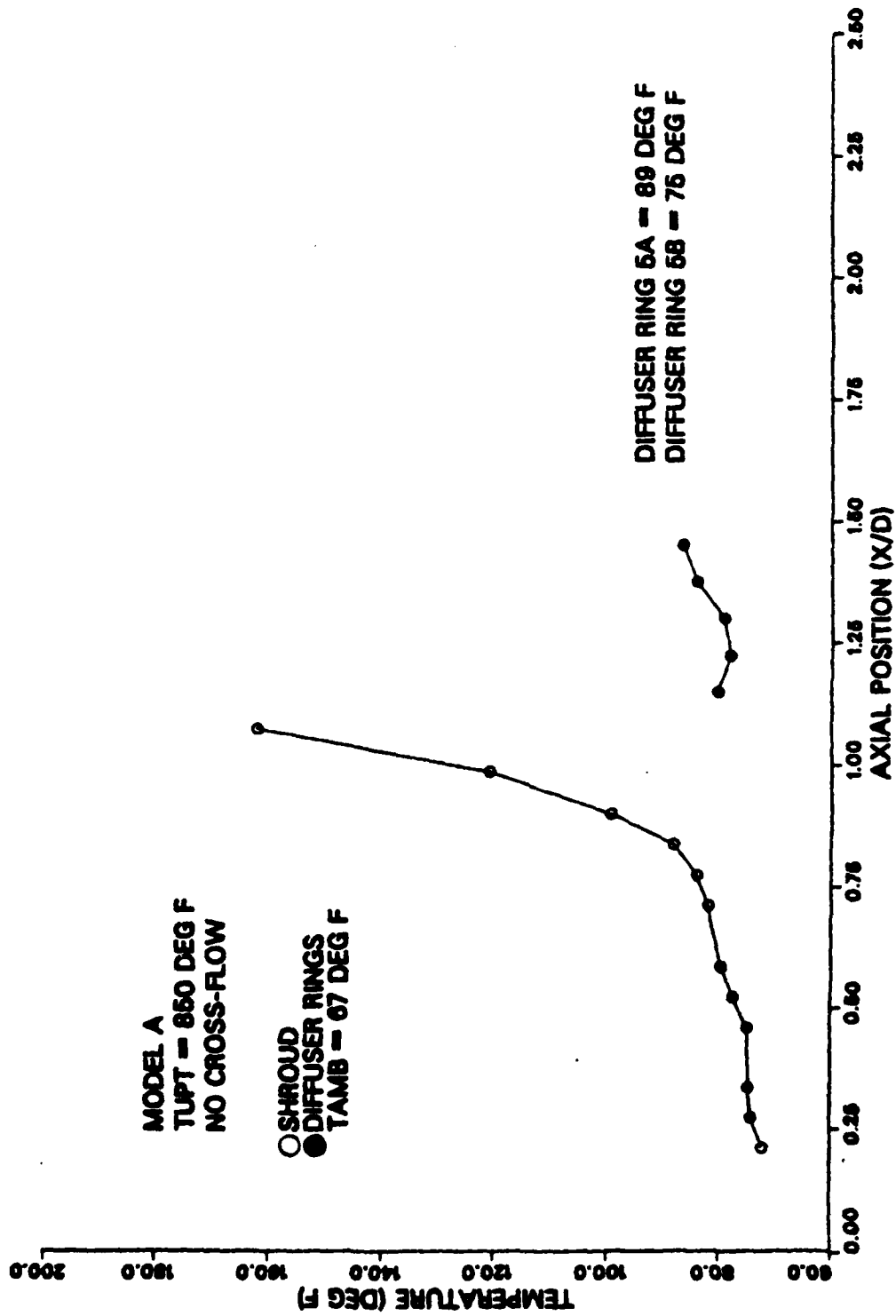
Figure 81. Omega External Temp., Model A (850 F) - No Crossflow.

143
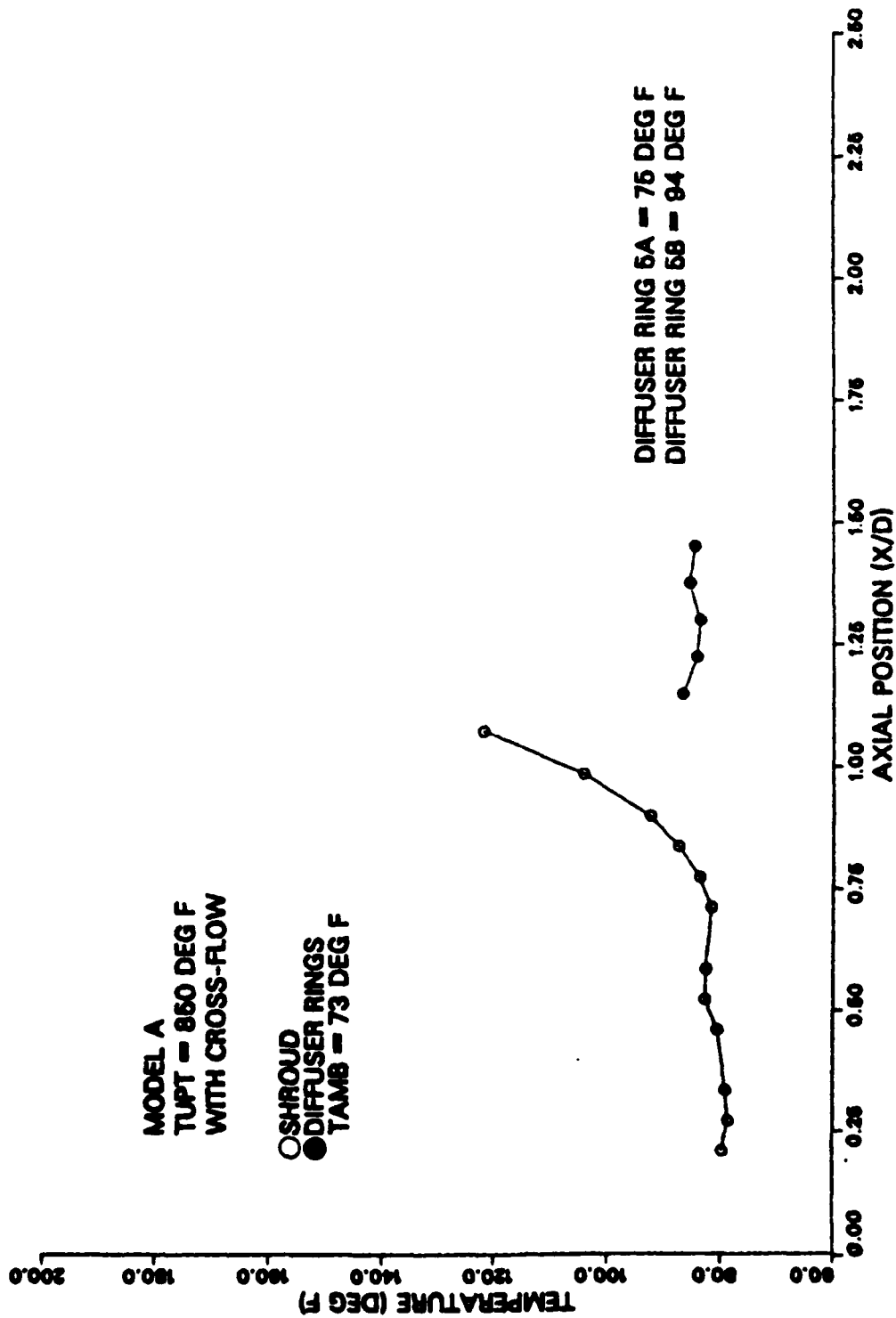
Figure 82.   Omega External Temp., Model A (850 F) - Crossflow.

144
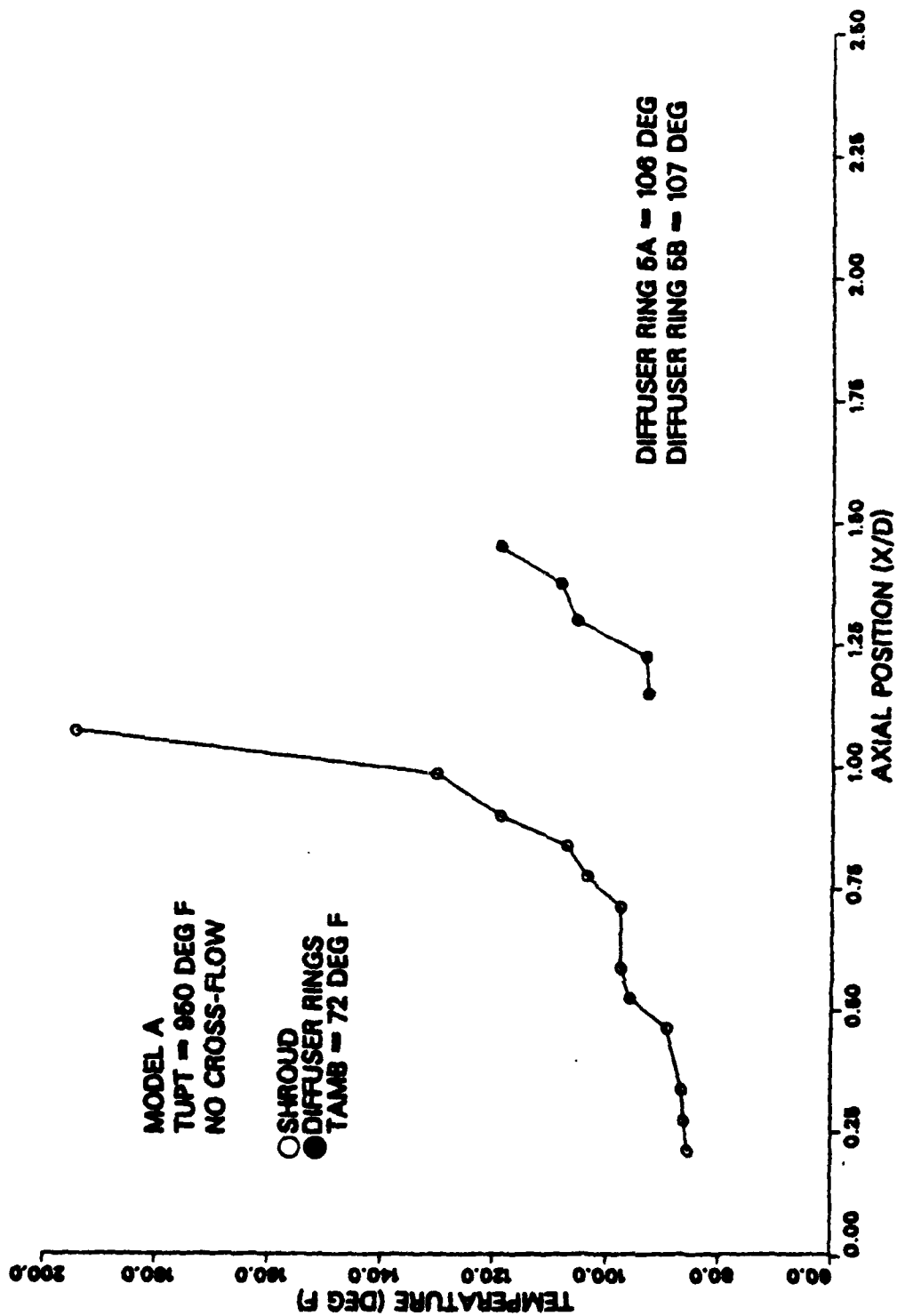
Figure 83. Omega External Temp., Model A (950 F) - No Crossflow.

145
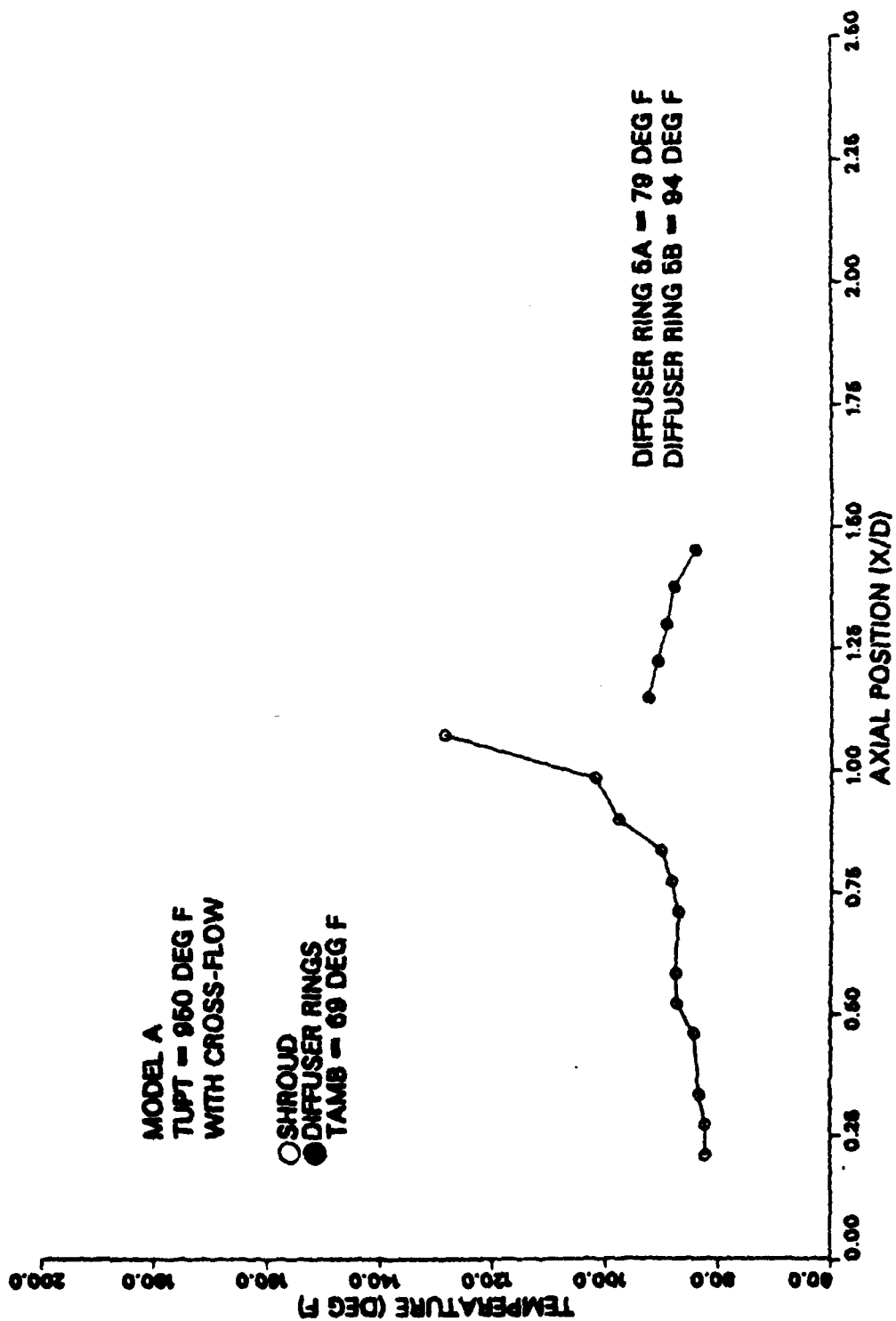
Figure 84. Omega External Temp., Model A (950 F) - Crossflow.

146
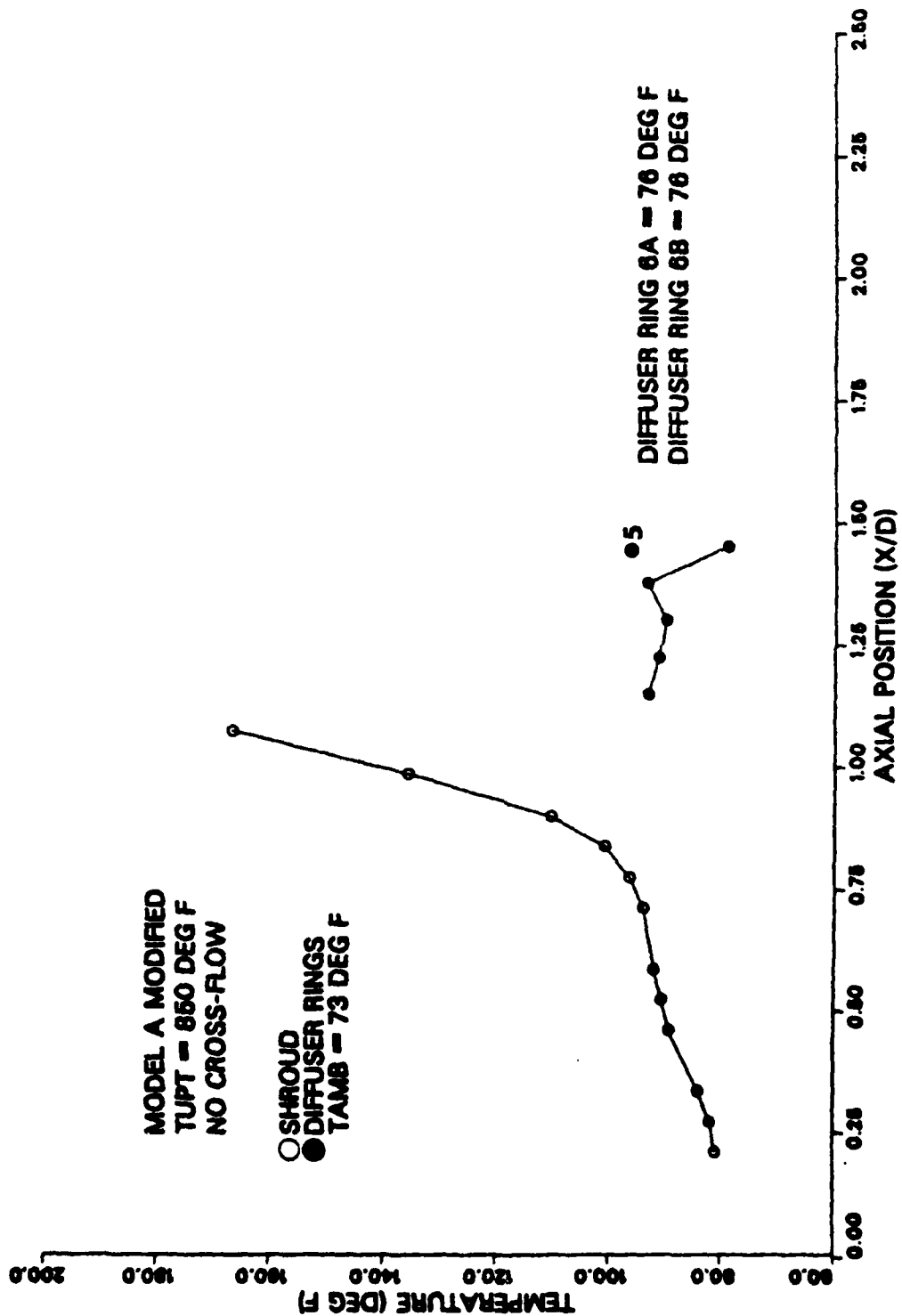
Figure 85. Omega Ext. Temp., Model A Mod (850 F) — No Crossflow.

147
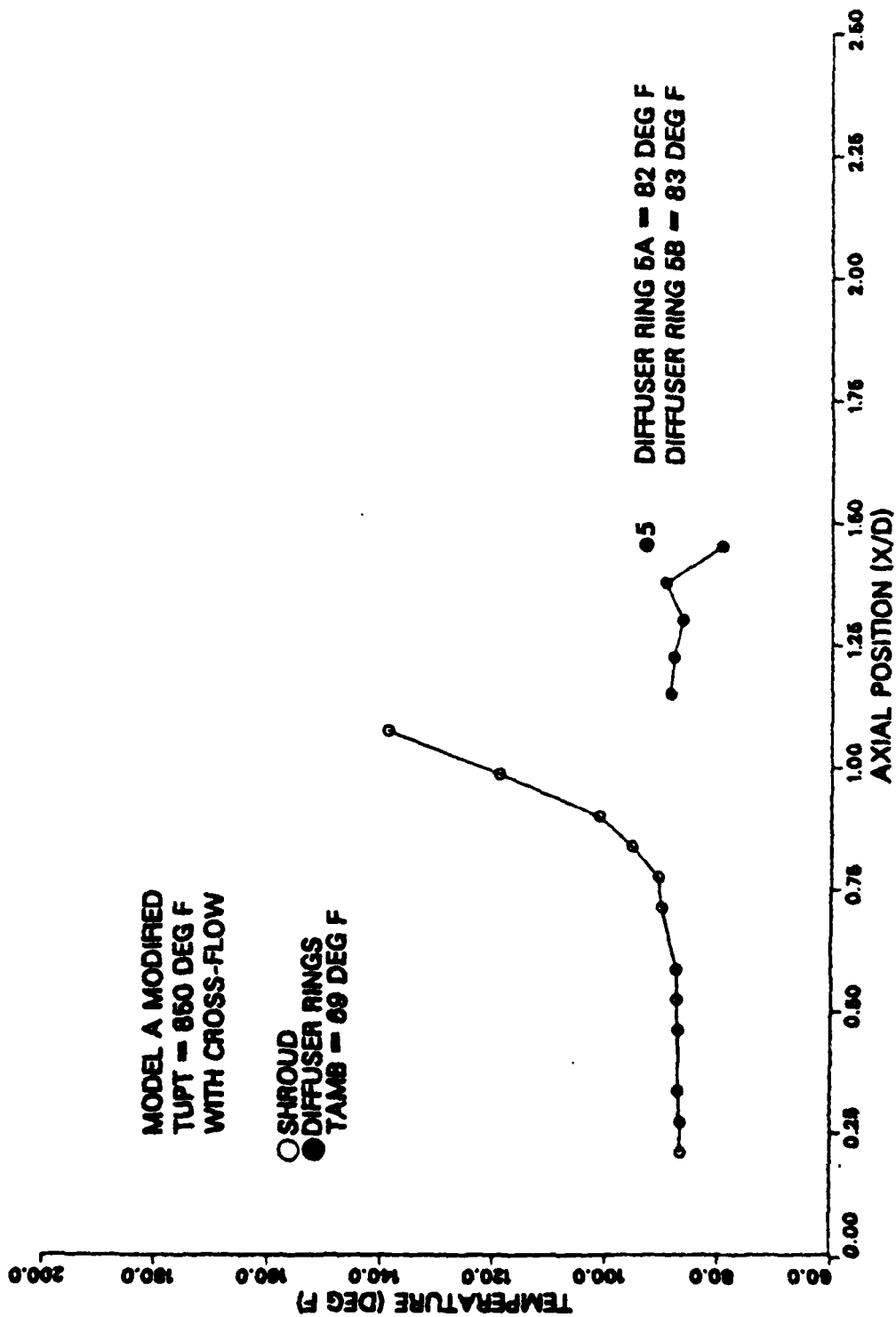
Figure 86.   Omega Ext. Temp., Model A Mod (850 F) - Crossflow.
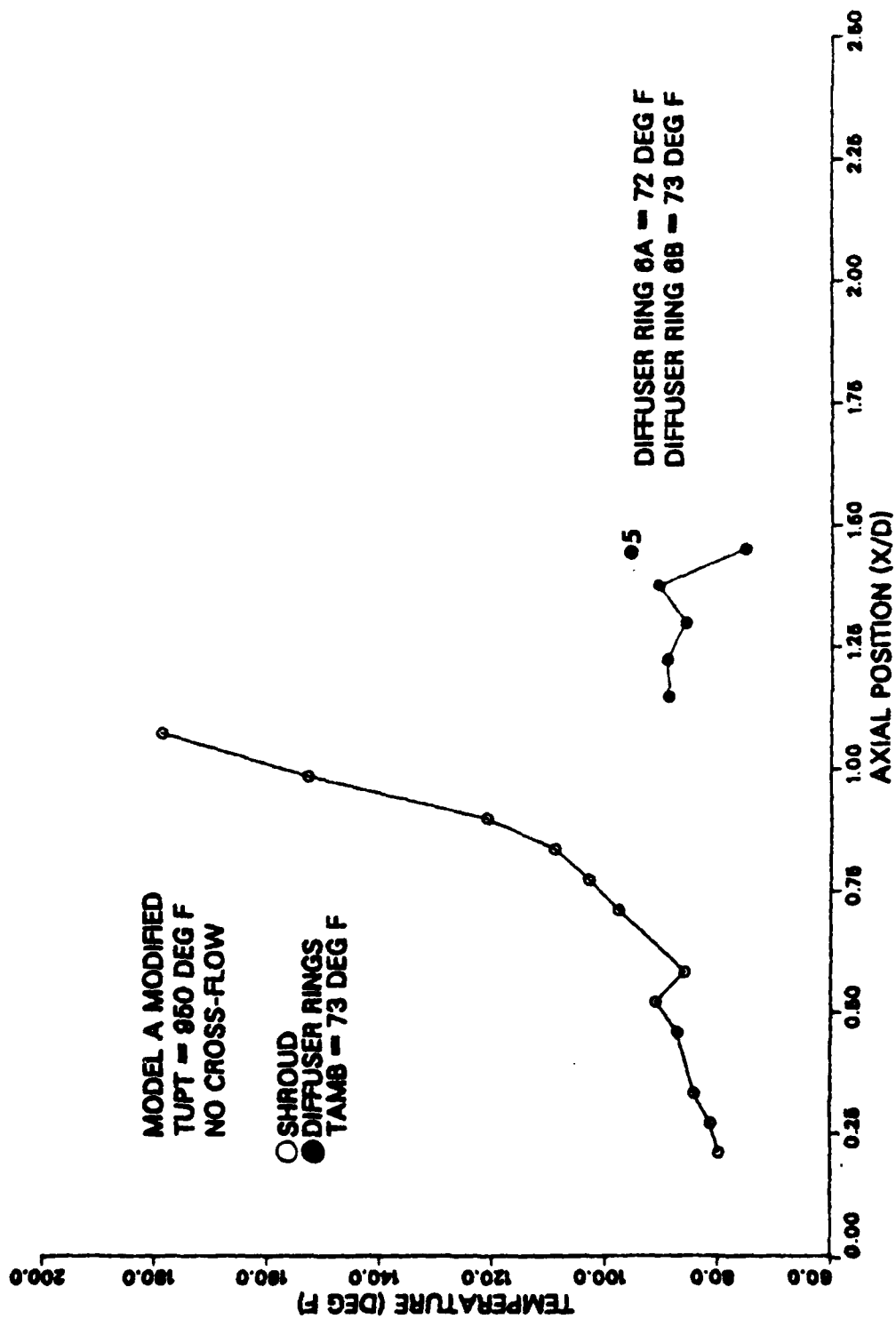
Figure 87. Omega Ext. Temp., Model A Mod (950 F) - No Crossflow.

149
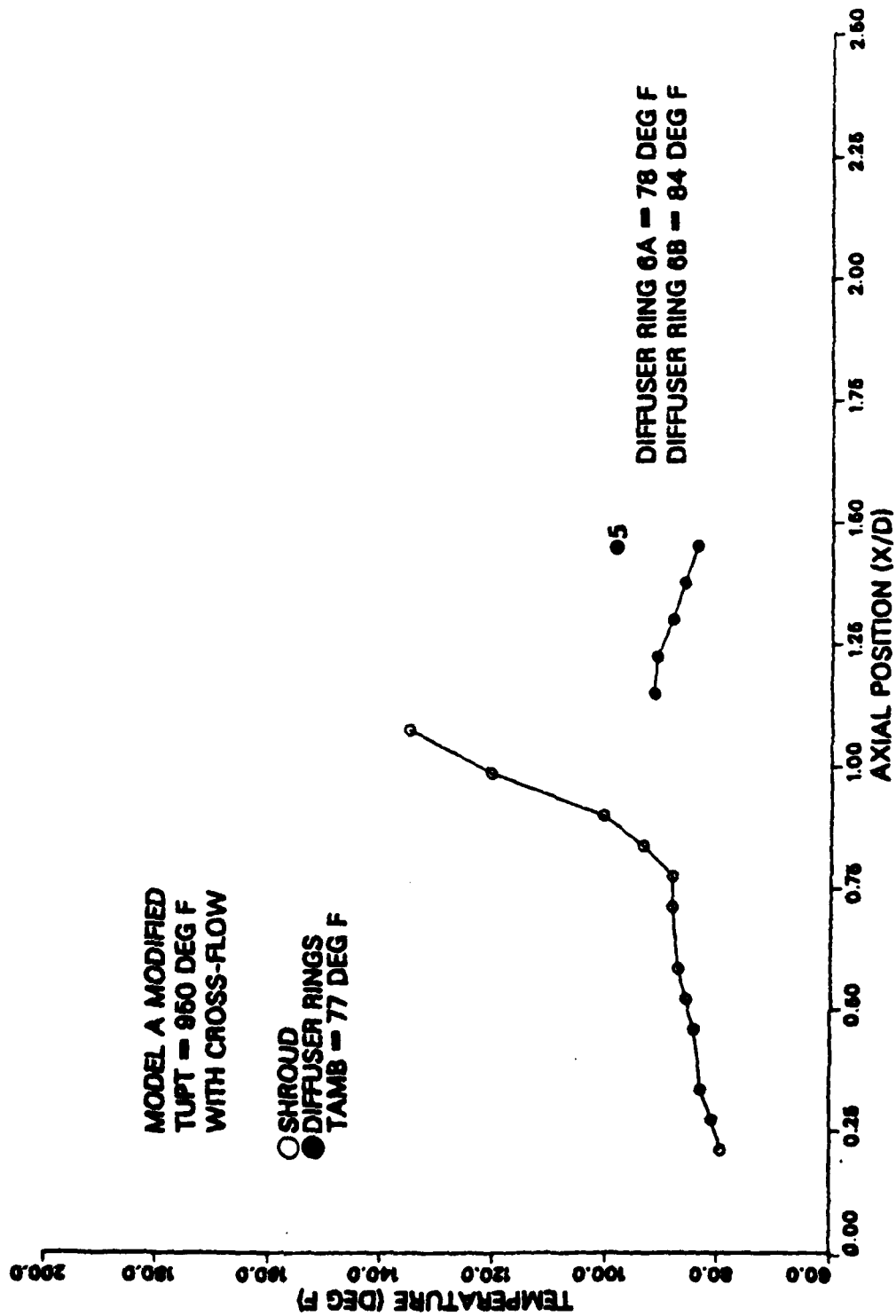
Figure 88. Omega Ext. Temp., Model A Mod (950 F) - Crossflow.
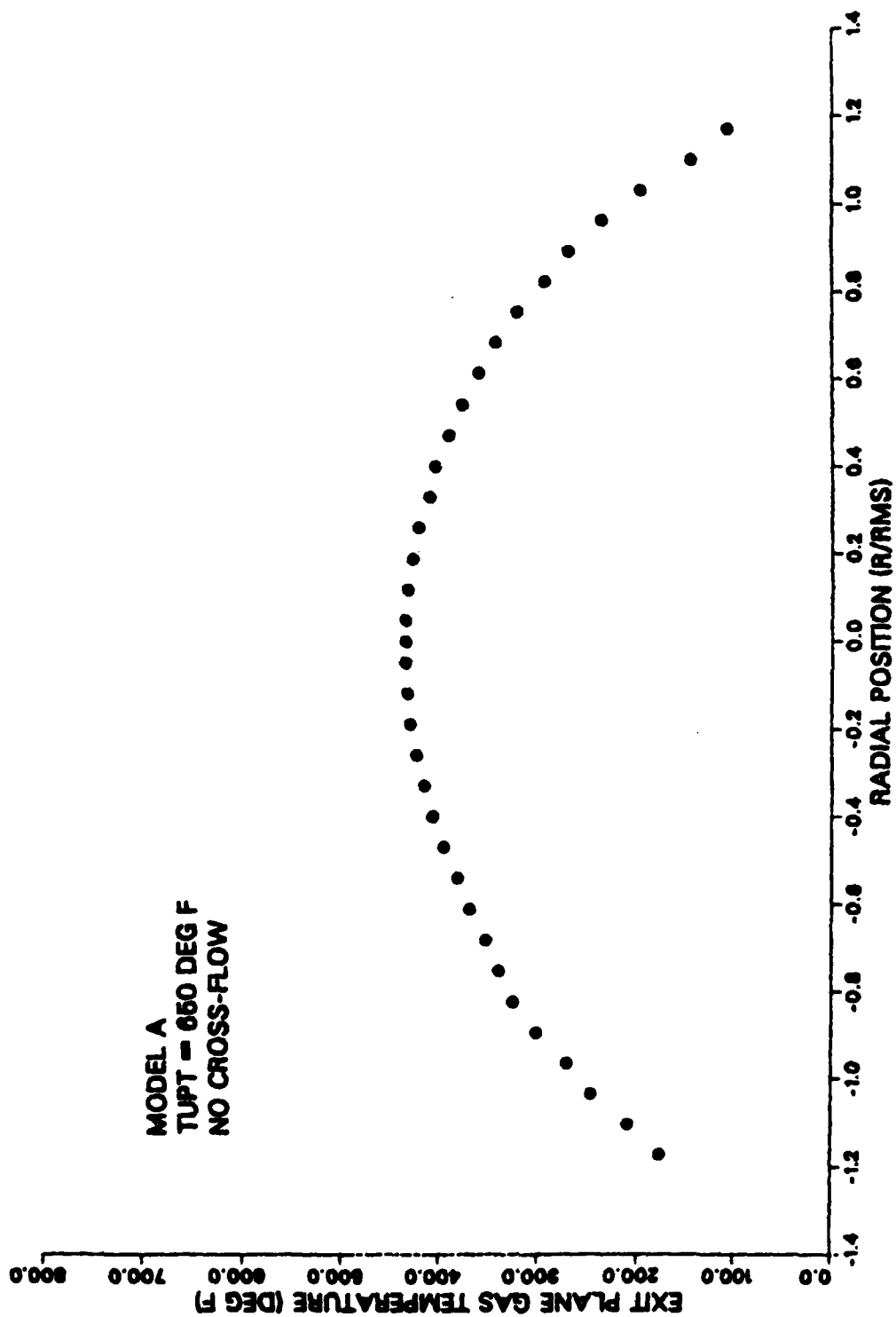
Figure 89.   Exit Plane Temp., Model A (650 F) - No Crossflow.
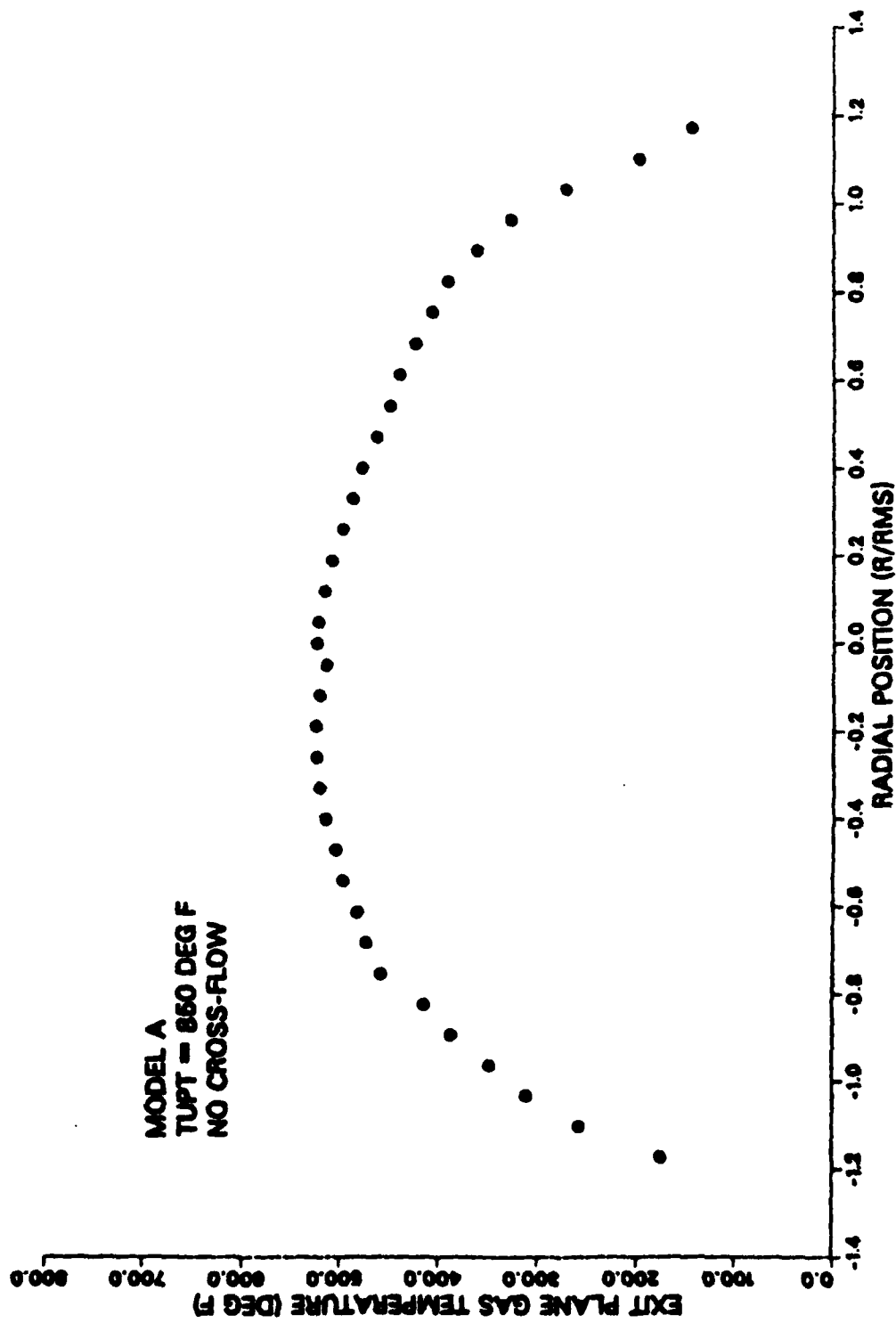
Figure 90. Exit Plane Temp., Model A (850 F) - No Crossflow.
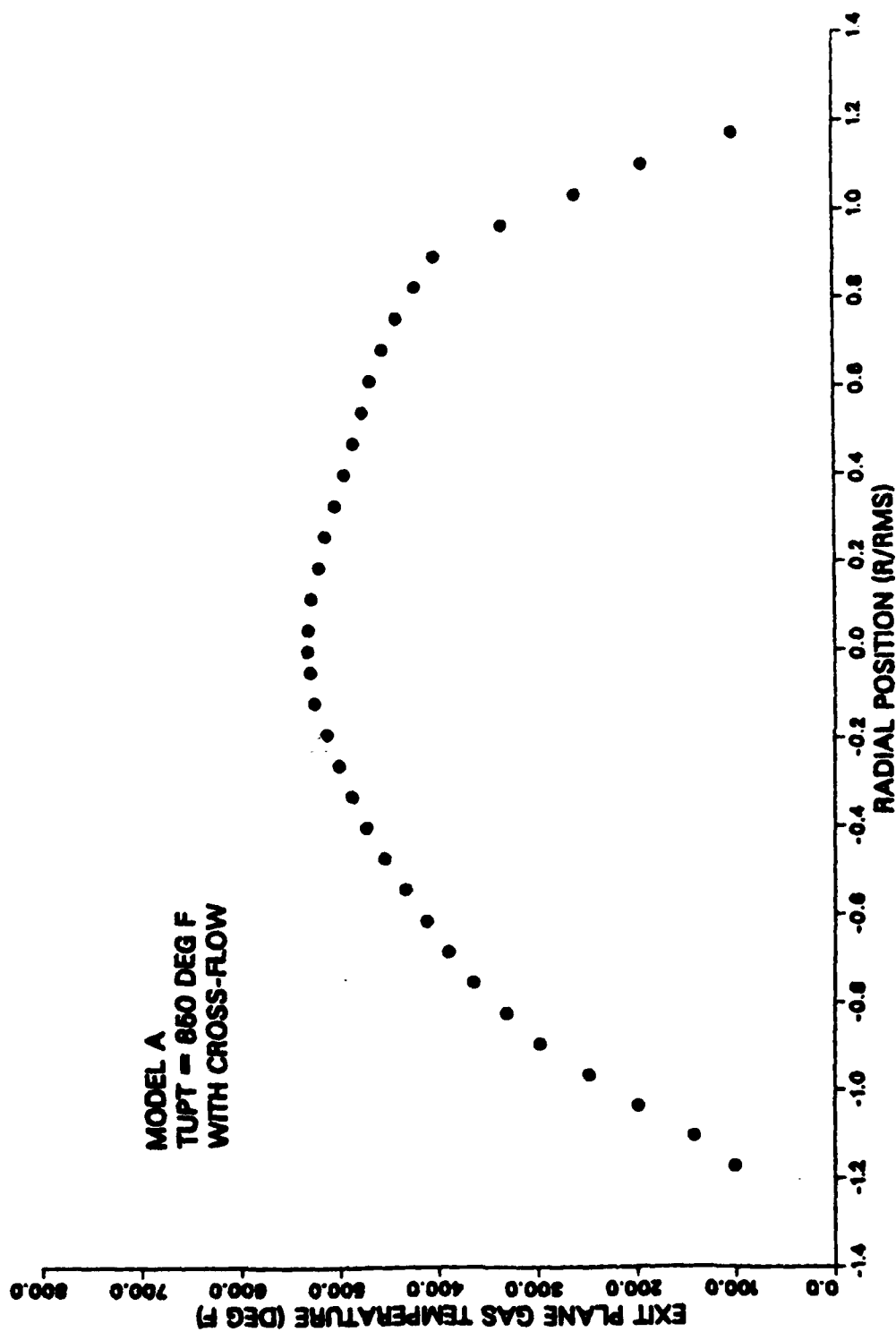
Figure 91. Exit Plane Temp., Model A (850 F) - Crossflow.
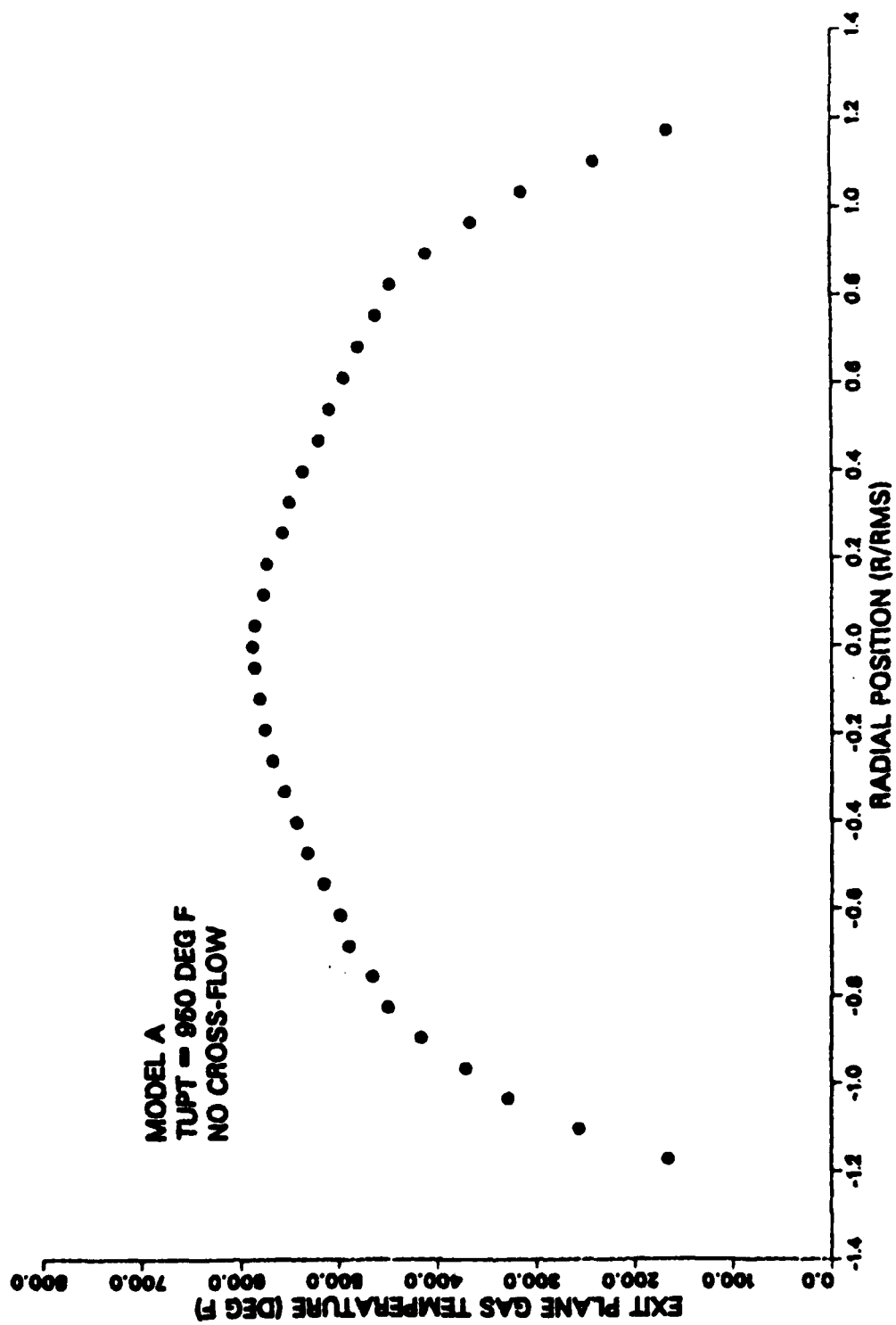
Figure 92. Exit Plane Temp., Model A (950 F) - No Crossflow.

154
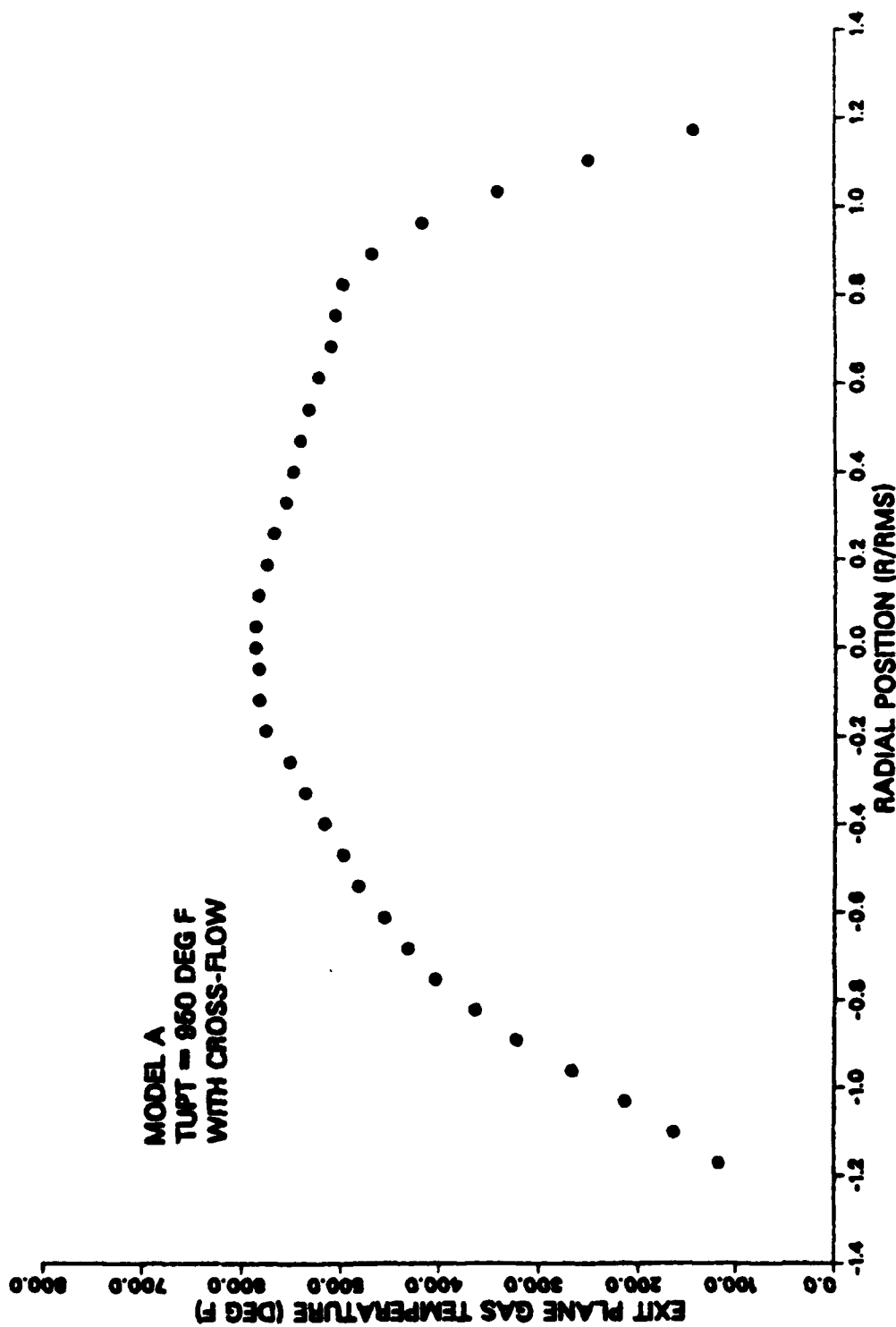
Figure 93. Exit Plane Temp., Model A (950 F) - Crossflow.

155
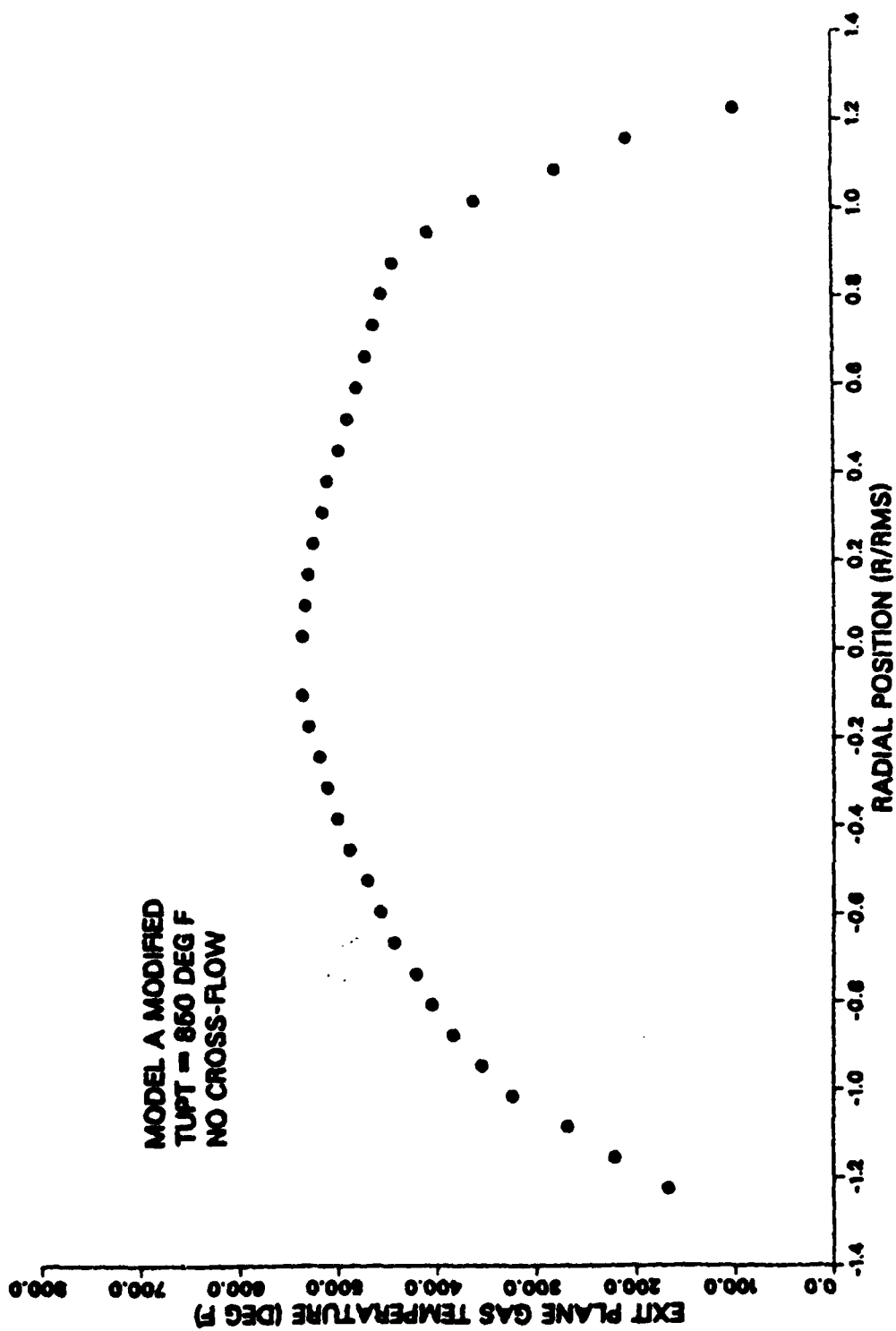
Figure 94. Exit Plane Temp., Model A Mod (850 F) - No Crossflow.
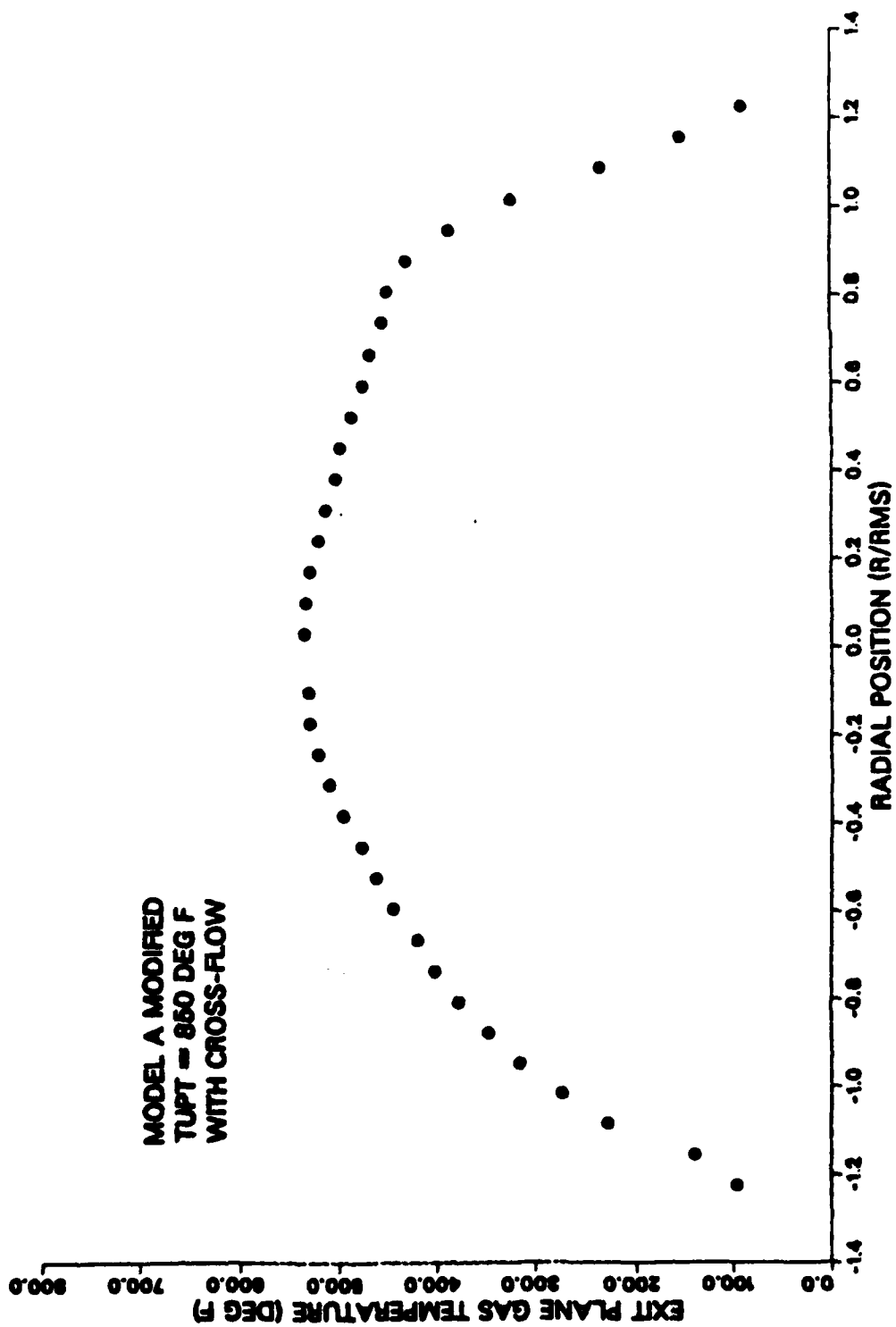
Figure 95. Exit Plane Temp., Model A Mod (850 F) - Crossflow.

157
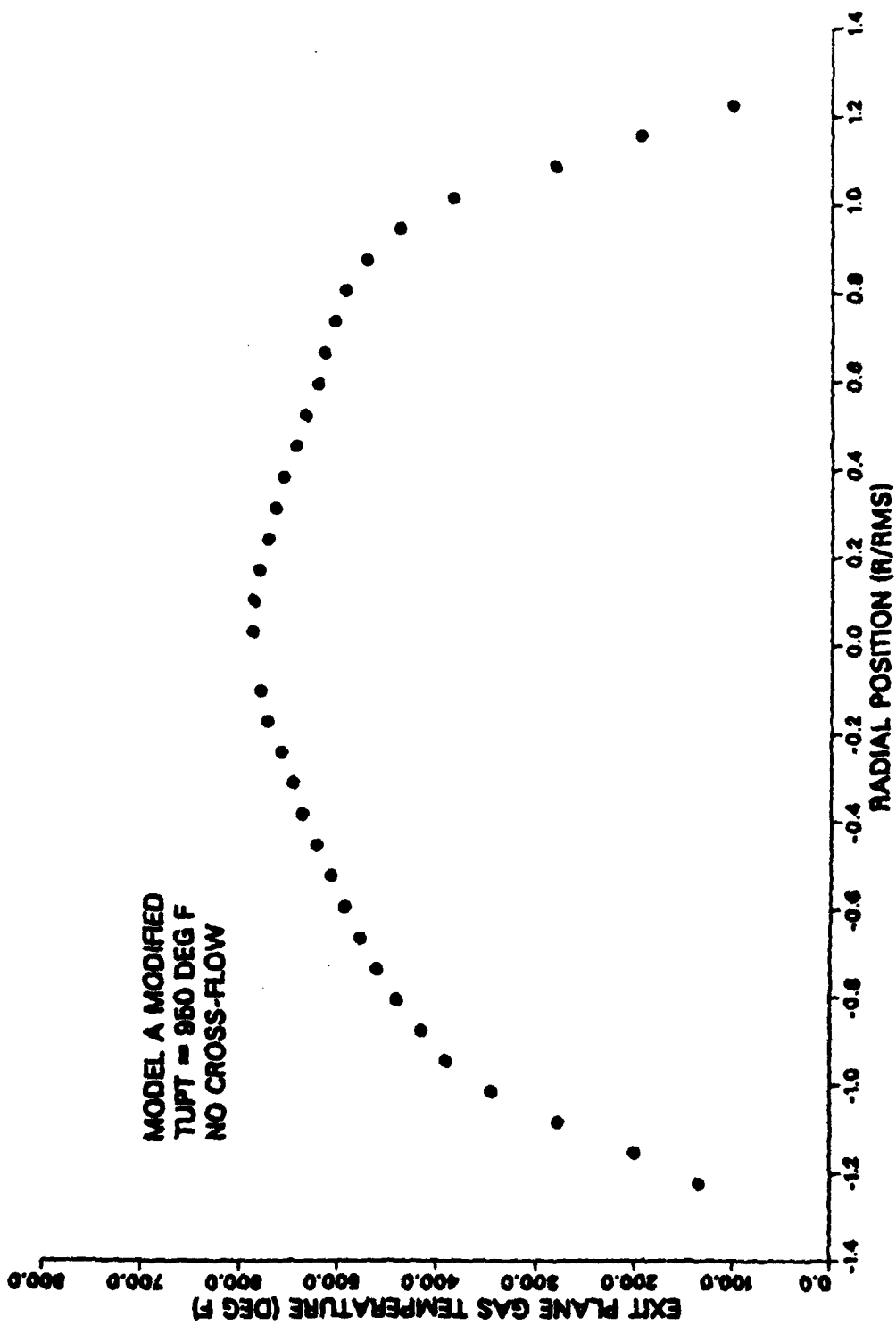
Figure 96. Exit Plane Temp., Model A Mod (950 F) - No Crossflow.

158
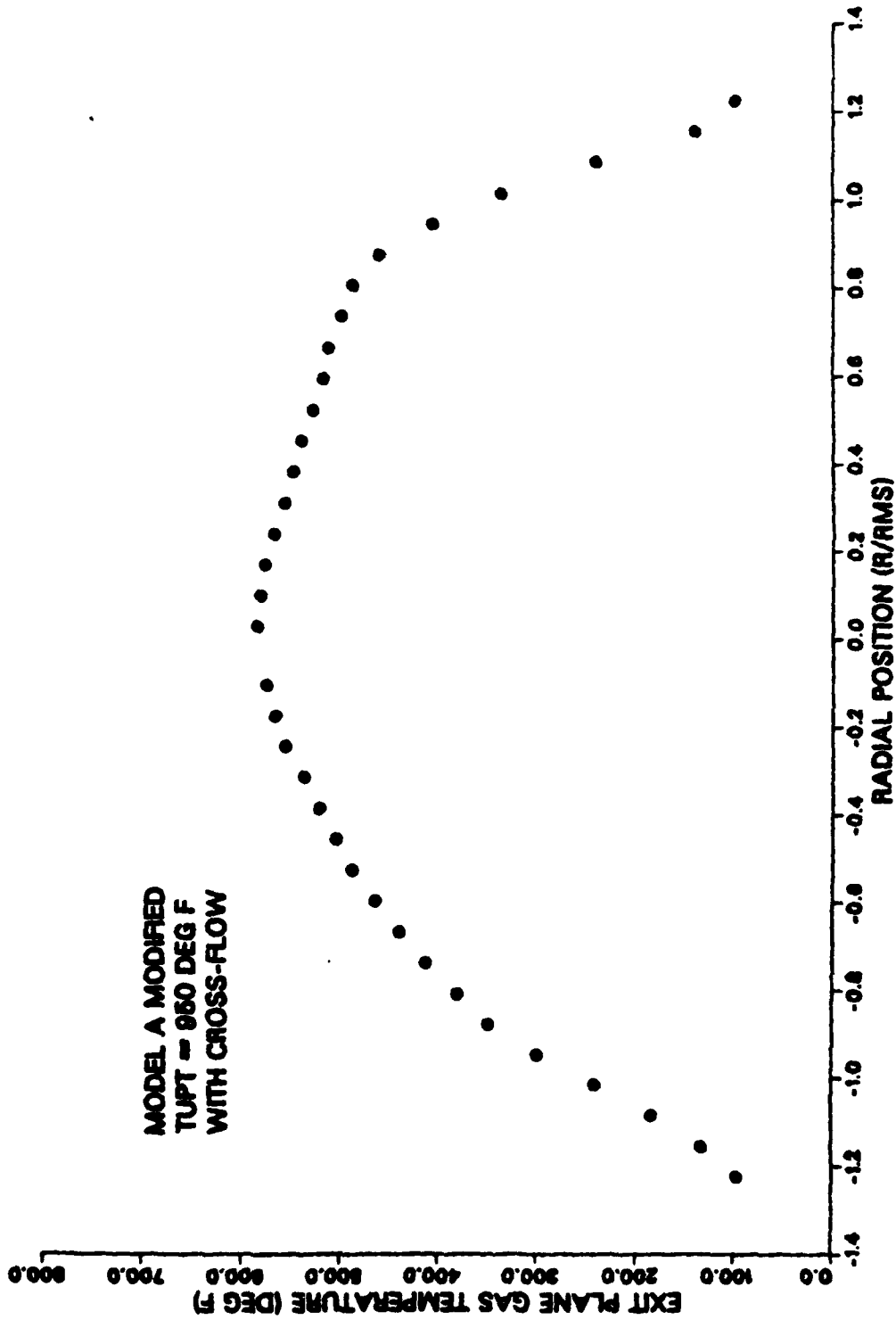
Figure 97. Exit Plane Temp., Model A Mod (950 F) - Crossflow.

159
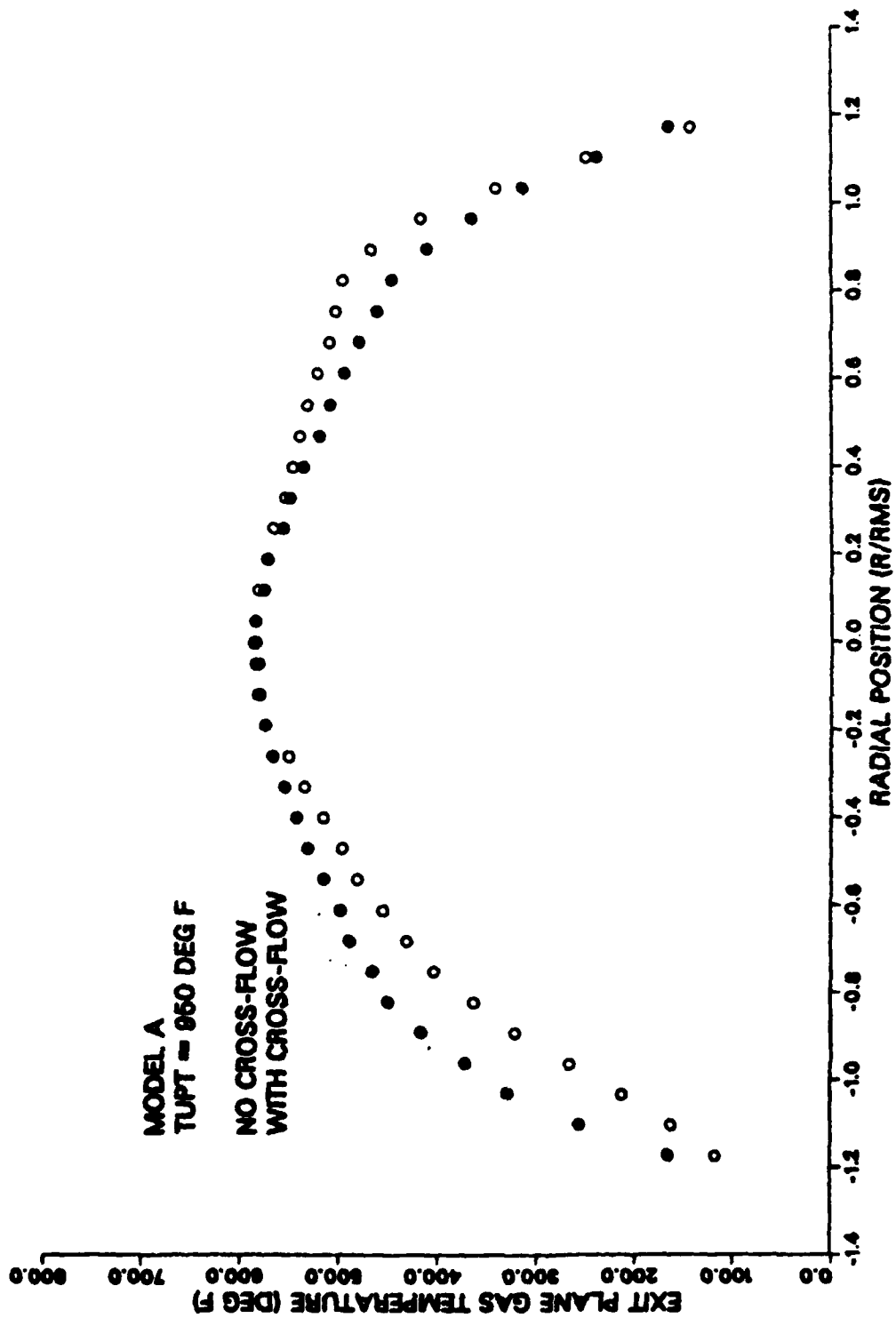
Figure 98. Exit Plane Temp. Comparison, Model A (950 F).
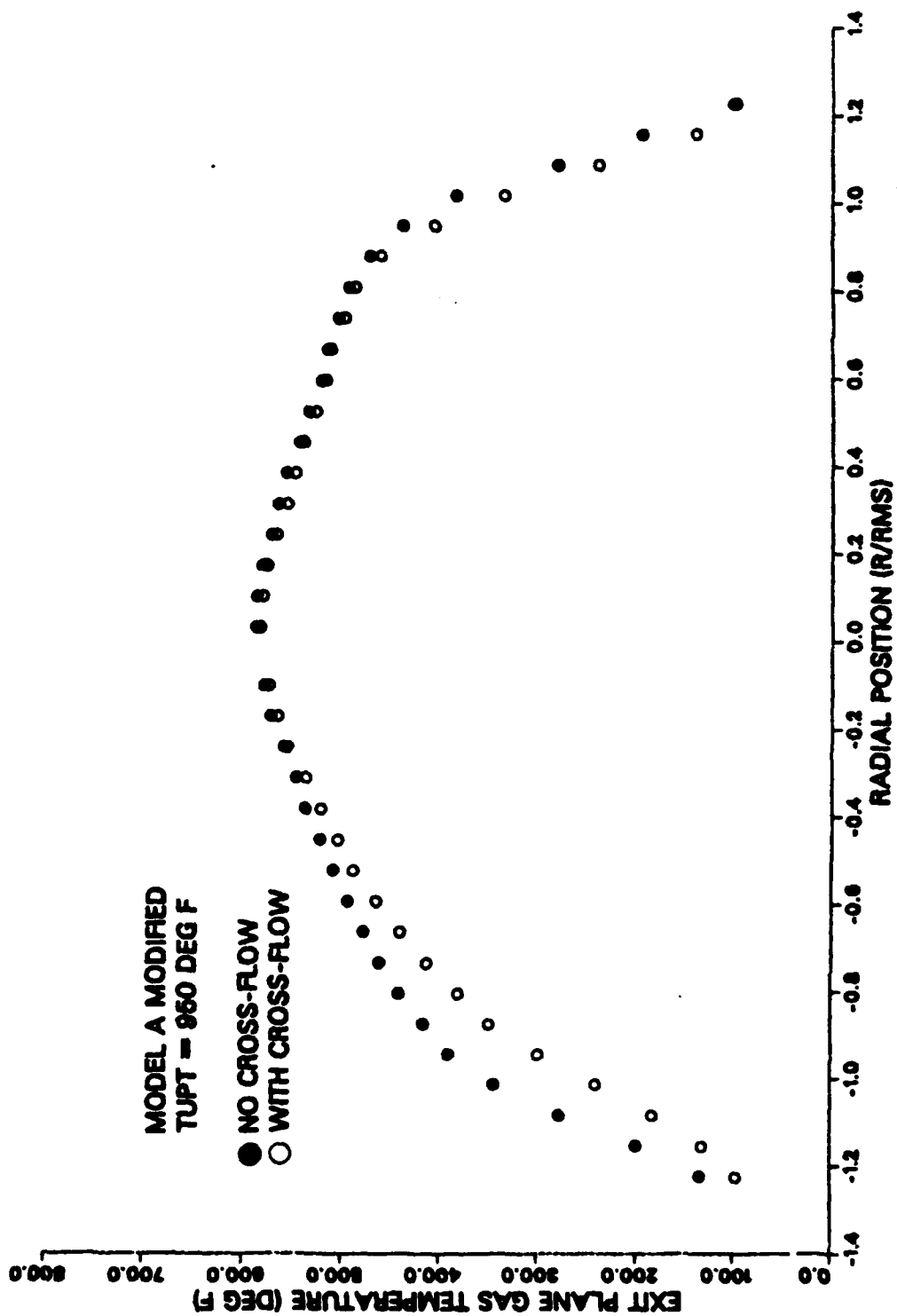
Figure 99. Exit Plane Temp. Comparison, Model A Mod (950 F).

TABLE I
Rotameter Calibration Data

Rotometer Reading	Weight Empty (gr.)	Weight Full (gr.)	Net Weight (gr.)	Time (sec.)	Mass Flow lbm/sec	Flow Rate GPH
08	67.0	29.5	37.5	120	0.689	0.345
09	84.0	30.7	53.3	120	0.979	0.490
10	103.3	31.8	71.5	120	1.314	0.657
15	173.1	31.1	142.0	120	2.609	1.306
20	256.7	31.6	225.1	120	4.136	2.070
25	381.4	31.9	349.5	120	6.421	3.214
30	520.0	31.8	488.2	120	8.696	4.489
35	342.9	32.4	310.5	60	11.41	5.710
40	397.8	32.1	365.7	60	13.44	6.725
43	423.3	32.1	391.2	60	14.37	7.194
40	757.7	32.4	725.3	120	13.33	6.669
35	651.5	31.5	620.0	120	11.39	5.701
34	629.3	32.1	597.2	120	10.97	5.491
33	603.2	32.8	570.4	120	10.48	5.245
32	582.5	32.4	550.1	120	10.11	5.058
31	558.8	32.3	526.5	120	9.613	4.841
30	530.0	32.0	498.0	120	9.149	4.579
29	500.8	32.3	468.5	120	8.607	4.308
28	475.4	32.2	443.2	120	8.142	4.075
27	450.5	31.4	419.1	120	7.700	3.854
26	426.5	32.4	394.1	120	7.240	3.624
25	395.9	31.2	364.7	120	6.700	3.353
20	267.1	32.2	234.9	120	4.316	2.160
15	169.0	31.9	137.1	120	2.519	1.261
10	104.6	31.9	72.7	120	1.336	0.669
08	72.1	31.6	40.5	120	0.744	0.372

NOTES
1) Average fuel temperature 61.7° F
2) Fuel: Number two diesel; specific gravity = 0.862

TABLE II

Thermocouple Display Channel Assignments, Type K

<u>Channel</u>	<u>Assignment</u>
1	Exit Plane (TEP)
2	Plenum Ambient Temp.
3	Uptake (TUPT)
4	Burner (TBURN)
5	Nozzle box at the position of the removed burner
6	Mixing Stack, Thermocouple (10)
7	Mixing Stack, Thermocouple (5)
8	Mixing Stack, Thermocouple (9)
9	Mixing Stack, Thermocouple (8)
10	Mixing Stack, Thermocouple (12)
11	Mixing Stack, Thermocouple (7)
12	Mixing Stack, Thermocouple (4)
13	Mixing Stack, Thermocouple (1)
14	Mixing Stack, Thermocouple (6)
15	Mixing Stack, Thermocouple (3)
16	Mixing Stack, Thermocouple (11)
17	Mixing Stack, Thermocouple (2)
18	UNUSED

TABLE III

Thermocouple Display Channel Assignments, Type T

Channel	Assignment
1	Fuel Supply
2	Ambient Air (TAMB)
3	Inlet Air Supply (TNH)
4	UNUSED
5	Model A, Diffuser Ring 2
6	Model A, Diffuser Ring 3
7	Model A Shroud, $X/D=0.625$
8	Model A, Diffuser Ring 5
9	Model A Shroud, $X/D=0.750$
10	Model A, Diffuser Ring 5A
11	Model A, Diffuser Ring 5B
12	Model A, Diffuser Ring 1
13	Model A Shroud, $X/D=1.068$
14	Model A Shroud, $X/D=0.125$
15	Model A Shroud, $X/D=0.375$
16	UNUSED
17	Model A, Diffuser Ring 4
18	UNUSED

164

TABLE IV

Model Characteristics

	Model A	Model A Modified
Mixing Stack Assembly L/D (overall)	1.5	1.5
Mixing Stack Inside Diameter (D) L/D Rows of Film Cooling Slots	7.122 1.0 4	7.122 1.0 4
Shroud Start Position (X/D)	0.15	0.15
Diffuser Number of Rings Ring Length (L/D) Half Angle	5 0.101 10	6 0.101 10
Film Cooling Clearance	0.188	0.188
Stand-off Distance (S/D)	0.5	0.5
Primary Nozzles Number Type Am/Ap	4 tilted-angled (15/20) 2.5	4 tilted-angled (15/20) 2.5

TABLE V

Pumping Coeff. Data, Model A (175 F) - No Crossflow

DATE: 10 SEP 83

NUMBER OF PRIMARY NOZZLES: 4
PRIMARY NOZZLE DIAMETER: 2.25 INCHES
UPTAKE DIAMETER: 7.510 INCHES
AREA RATIO AS/AP: 2.50
GAMMA: 1.5901

HUT RIG PERFORMANCE
5 RING DIFFUSER
TUPT: 174

DATA TAKEN BY R.E. STAPLES
MIXING STACK LENGTH: 7.42 INCHES
MIXING STACK DIAMETER: 7.122 INCHES
MIXING STACK L/D: 1.050
STANDOFF S/AP/D: 0.050
AMBIENT PRESSURE: 29.68 INCHES HG

NR	PNM IN MG	DELPR IN H2O	TNT DEG F	MOIA	TOUGN DEG F	TUPT DEG F	TAMB DEG F	PUPT IN H2O	PPLA IN H2O	SEC AREA SQ IN	UM FT/S	UU FT/S	UPACH
1	3.00	12.50	187.1	0.0	186.0	184.0	70.7	5.30	2.90	0.000	86.9	78.4	0.0630
2	3.00	12.50	187.1	0.0	181.0	185.0	71.0	5.60	2.55	1.767	93.7	78.4	0.0631
3	3.10	12.40	187.4	0.0	181.0	185.0	71.2	5.90	2.25	3.534	97.5	78.2	0.0628
4	3.10	12.40	187.4	0.0	181.0	185.0	70.8	6.20	1.95	5.301	100.9	78.1	0.0628
5	3.10	12.40	187.9	0.0	181.0	185.0	71.1	6.55	1.55	8.443	105.9	78.0	0.0627
6	3.10	12.30	188.0	0.0	181.0	186.0	70.9	6.90	1.25	11.585	109.6	77.8	0.0626
7	3.10	12.30	188.1	0.0	181.0	186.0	71.4	7.10	1.00	14.726	112.4	77.7	0.0624
8	3.10	12.30	188.0	0.0	181.0	186.0	71.3	7.50	0.50	27.293	119.8	77.6	0.0624
9	3.10	12.30	188.4	0.0	181.0	186.0	71.3	7.70	0.30	34.859	123.9	77.6	0.0623
10	3.10	12.30	188.5	0.0	181.0	186.0	71.7	7.80	0.20	52.425	126.8	77.5	0.0623
11	3.20	12.30	188.8	0.0	181.0	186.0	71.4	7.95	0.10	64.492	121.9	77.6	0.0623
12	3.20	12.30	189.4	0.0	182.0	187.0	71.4	8.00	0.00	89.000	88.1	77.7	0.0623

NR	WPA LBM/S	WF LBM/S	WS LBM/S	WP LBM/S	WM	TS	P2	PS/IS	WSTEC.04	UP FT/S	SEC AREA SQ IN	UM FT/S	UU FT/S	UPACH
1	1.689	0.000	0.000	1.689	0.000	0.824	0.266	0.323	0.000	222.8	0.000	86.9	78.4	0.0630
2	1.689	0.000	0.095	1.689	0.664	0.823	0.233	0.264	0.054	222.9	1.767	93.7	78.4	0.0631
3	1.686	0.000	0.178	1.686	0.120	0.823	0.207	0.252	0.110	222.1	3.534	97.5	78.2	0.0628
4	1.686	0.000	0.249	1.686	0.868	0.823	0.180	0.218	0.154	222.0	5.301	100.9	78.1	0.0628
5	1.686	0.000	0.354	1.686	0.238	0.823	0.143	0.174	0.219	221.7	8.443	105.9	78.0	0.0627
6	1.678	0.000	0.436	1.678	0.295	0.823	0.116	0.161	0.271	220.9	11.585	109.6	77.8	0.0626
7	1.677	0.000	0.496	1.677	0.376	0.822	0.093	0.111	0.108	220.7	14.726	112.4	77.7	0.0624
8	1.678	0.000	0.649	1.678	0.440	0.822	0.067	0.057	0.403	220.5	27.293	119.8	77.6	0.0624
9	1.677	0.000	0.735	1.677	0.497	0.822	0.024	0.034	0.456	220.3	34.859	123.9	77.6	0.0623
10	1.677	0.000	0.789	1.677	0.534	0.823	0.019	0.023	0.490	220.2	52.425	126.8	77.5	0.0623
11	1.679	0.000	0.692	1.679	0.468	0.823	0.009	0.011	0.429	220.5	64.492	121.9	77.6	0.0623
12	1.678	0.000	0.000	1.678	0.000	0.821	0.000	0.000	0.000	220.7	89.000	88.1	77.7	0.0623

166

TABLE VI

Pumping Coeff. Data, Model A (650 F) - No Crossflow

*** HOT RIG PERFORMANCE ***
5 WING DIFFUSER

TUPI: 650

DATA TAKEN BY R.E. STAPLES

MIXING STACK LENGTH: 7.22 INCHES
MIXING STACK DIAMETER: 7.122 INCHES
MIXING STACK L/D: 1.50
STANDOFF RATIO: 0.50
AMBIENT PRESSURE: 30.51 INCHES HG

DATE: 16 AUG 83
NUMBER OF PRIMARY NOZZLES: 4
PRIMARY NOZZLE DIAMETER: 2.25 INCHES
UPTAKE DIAMETER: 7.510 INCHES
AREA RATIO, AP/AP: 2.50
GAMMA: 1.3741

NR	PNH IN HG	UELPR IN H2O	TAM DEG F	HO1A	TOURN DEG F	TUPT DFL F	PUPT IN H2O	DPPR IN H2O	SEC AREA SQ IN	UM F/S	UU F/S	UPACH
1	3.00	6.20	185.9	25.0	1196.0	654.0	5.00	2.68	0.000	106.0	93.7	0.0578
2	3.00	6.70	185.7	25.0	1186.0	653.0	5.30	2.20	1.767	110.1	93.5	0.0577
3	3.10	6.20	186.0	25.0	1196.0	653.0	5.60	1.93	3.534	113.9	93.6	0.0578
4	3.10	6.20	185.9	25.0	1192.0	654.0	5.80	1.67	5.301	117.1	91.6	0.0576
5	3.10	6.20	186.3	25.0	1194.0	654.0	6.10	1.32	8.443	121.0	91.5	0.0577
6	3.10	6.20	186.4	25.0	1192.0	654.0	6.30	1.08	11.585	125.3	93.5	0.0577
7	3.10	6.20	186.2	25.0	1195.0	654.0	6.50	0.85	14.726	128.1	93.8	0.0577
8	3.10	6.20	186.5	25.0	1194.0	655.0	6.90	0.60	27.293	133.6	93.6	0.0576
9	3.20	6.20	186.2	25.0	1192.0	655.0	7.10	0.25	39.059	136.1	93.5	0.0577
10	3.20	6.20	186.6	25.0	1193.0	656.0	7.20	0.17	52.625	140.8	91.6	0.0577
11	3.20	6.20	186.3	25.0	1195.0	656.0	7.20	0.12	66.092	142.3	93.6	0.0577
12	3.20	6.20	186.9	25.0	1195.0	653.0	7.30	0.00	80.000	105.5	93.3	0.0576

NR	BHA LBM/S	DF LBM/S	WP LBM/S	MS LBM/S	WS LBM/S	PS	WS	TE	PE	WETPO.04	UP F/S
1	1.049	0.007	1.056	0.000	0.000	0.150	0.473	0.327	0.000	265.6	265.6
2	1.049	0.007	1.056	0.090	0.685	0.137	0.474	0.290	0.061	265.2	265.2
3	1.050	0.007	1.057	0.188	0.159	0.140	0.473	0.254	0.114	265.8	265.8
4	1.050	0.007	1.057	0.235	0.222	0.104	0.473	0.220	0.160	265.5	265.5
5	1.050	0.007	1.057	0.332	0.214	0.085	0.473	0.226	0.226	265.2	265.2
6	1.050	0.007	1.057	0.413	0.191	0.067	0.472	0.162	0.281	265.0	265.0
7	1.050	0.007	1.057	0.473	0.448	0.055	0.473	0.116	0.322	266.9	266.9
8	1.050	0.007	1.057	0.592	0.560	0.025	0.472	0.053	0.402	264.8	264.8
9	1.052	0.007	1.054	0.683	0.645	0.016	0.472	0.031	0.464	265.1	265.1
10	1.051	0.007	1.054	0.741	0.700	0.011	0.471	0.022	0.503	265.3	265.3
11	1.052	0.007	1.054	0.772	0.729	0.007	0.471	0.016	0.574	265.3	265.3
12	1.051	0.007	1.051	0.000	0.000	0.000	0.472	0.000	0.000	264.6	264.6

TABLE VII

Pumping Coeff. Data, Model A (850 F) - No Crossflow

*** HOT RIG PERFORMANCE ***
5 RING DIFFUSER

IUPT: 850

DATA TAKEN BY R.E. STAPLES

MIXING STACK LENGTH: 7.22 INCHES
MIXING STACK DIAMETER: 7.122 INCHES
MIXING STACK L/D: 1.030
STANDOFF RATIO: 0.530
AMBIENT PRESSURE: 30.07 INCHES HG

DATE: 31 AUG 83
NUMBER OF PRIMARY NOZZLES: 4
PRIMARY NOZZLE DIAMETER: 2.25 INCHES
UPTAKE DIAMETER: 7.510 INCHES
AREA RATIO, AR/AP: 2.50
LAMBDA: 1.3614

AR	DPM IN HG	DELPA IN H2O	IAM DEG F	HDIA	TDUAM DEG F	IUPT DEG F	MP	TAMU DEG F	TP	DUPT IN H2O	PPLN IN H2O	SEC AREA SQ IN	UP FT/S	UM FT/S	UU FT/S	UPACH
1	4.10	5.30	184.1	29.5	1156.0	847.0	0.146	68.9	0.405	6.70	2.85	0.000	243.5	117.4	103.0	0.0589
2	4.10	5.30	183.9	29.5	1151.0	846.0	0.131	68.7	0.405	7.00	2.55	1.767	243.1	121.6	102.8	0.0589
3	4.10	5.30	184.2	29.5	1156.0	846.0	0.113	68.9	0.405	7.30	2.20	3.534	292.8	125.4	102.7	0.0588
4	4.10	5.30	183.9	29.5	1156.0	847.0	0.100	68.7	0.404	7.60	1.95	5.301	242.9	124.0	102.8	0.0588
5	4.20	5.30	184.2	29.5	1156.0	847.0	0.080	68.3	0.404	7.90	1.57	8.843	293.0	146.2	102.8	0.0589
6	4.20	5.30	184.1	29.5	1142.0	846.0	0.065	68.6	0.404	8.20	1.27	11.585	243.0	138.2	102.8	0.0588
7	4.20	5.30	184.3	29.5	1152.0	847.0	0.054	68.1	0.404	8.60	1.05	14.726	292.8	141.4	102.8	0.0588
8	4.20	5.30	183.9	29.5	1152.0	849.0	0.028	68.6	0.404	8.90	0.55	27.293	242.3	149.6	102.6	0.0587
9	4.20	5.30	184.3	29.5	1145.0	849.0	0.015	68.3	0.403	9.10	0.30	34.059	242.5	152.2	102.7	0.0587
10	4.30	5.30	184.1	29.5	1142.0	849.0	0.010	67.9	0.403	9.20	0.20	52.625	242.9	144.9	102.8	0.0588
11	4.30	5.30	184.4	29.5	1156.0	849.0	0.008	67.9	0.403	9.20	0.15	66.992	292.8	157.7	102.8	0.0588
12	4.30	5.30	184.4	29.5	1156.0	851.0	0.000	67.0	0.402	9.30	0.00	909090	241.2	117.0	107.9	0.0588

NR	WPA LBM/S	WF LBM/S	WP LBM/S	WS LBM/S	WU	PO	WOTOC.AA	UP FT/S	UM FT/S	UU FT/S	UPACH
1	0.983	0.009	0.992	0.000	0.600	0.146	0.000	243.5	117.4	103.0	0.0589
2	0.983	0.009	0.992	0.046	0.697	0.124	0.065	243.1	121.6	102.8	0.0589
3	0.983	0.009	0.992	0.179	0.181	0.113	0.128	292.8	125.4	102.7	0.0588
4	0.983	0.009	0.992	0.253	0.255	0.100	0.171	242.9	124.0	102.8	0.0588
5	0.985	0.009	0.993	0.362	0.364	0.080	0.244	293.0	146.2	102.8	0.0589
6	0.985	0.009	0.994	0.446	0.449	0.065	0.301	243.0	138.2	102.8	0.0588
7	0.986	0.009	0.995	0.516	0.520	0.054	0.389	292.8	141.4	102.8	0.0588
8	0.985	0.009	0.994	0.662	0.696	0.028	0.467	242.3	149.6	102.6	0.0587
9	0.986	0.009	0.995	0.746	0.751	0.015	0.508	242.9	152.2	102.7	0.0587
10	0.986	0.009	0.995	0.802	0.606	0.010	0.540	242.9	144.9	102.8	0.0588
11	0.986	0.009	0.995	0.901	0.666	0.008	0.590	292.8	157.7	102.8	0.0588
12	0.986	0.009	0.995	0.000	0.000	0.000	0.000	241.2	117.0	107.9	0.0588

TABLE VIII

Pumping Coeff. Data, Model A (850 F) - Crossflow

*** HOT HIG PERFORMANCE ***
5 RING DIFFUSER

IUPT: 850

IN CROSS-FLOW

DATA TAKEN BY R.E. STAPLES

MIXING STACK LENGTH: 7.22 INCHES
MIXING STACK DIAMETER: 7.122 INCHES
MIXING STACK L/D: 1.50
STANDOFF RATIO: 0.50 INCHES
AMBIENT PRESSURE: 29.59 INCHES HG

DATE: 05 SEP 83

NUMBER OF PRIMARY NOZZLES: 4
PRIMARY NOZZLE DIAMETER: 2.25 INCHES
UPTAKE DIAMETER: 7.510 INCHES
AREA RATIO AP/AP: 2.50 INCHES
LAMBDA: 1.3634

NR	PINH IN HG	DELPA IN H2O	TAH DEG F	NOIA	IUUEN DEG F	IUPT DEG F	TAPU DEG F	PUPT IN H2O	PULA IN H2O	SEC AREA SQ IN	UP F/S	UM F/S	UU F/S	UPACH
1	3.00	5.30	194.4	28.0	1185.0	850.0	74.5	6.10	3.05	0.000	294.0	117.8	101.6	0.0592
2	3.00	5.30	194.5	27.5	1175.0	848.0	74.7	6.40	2.72	1.767	294.3	122.3	103.3	0.0591
3	3.05	5.30	194.9	28.0	1190.0	851.0	75.4	6.60	2.42	3.534	294.9	126.6	103.5	0.0592
4	3.00	5.30	194.7	28.0	1185.0	853.0	74.7	7.00	2.15	5.301	295.4	130.4	103.7	0.0592
5	3.00	5.30	195.0	28.0	1180.0	850.0	75.6	7.40	1.75	8.843	295.5	136.0	103.7	0.0592
6	3.00	5.30	195.1	28.0	1182.0	853.0	76.0	7.70	1.62	11.595	294.8	140.0	103.5	0.0593
7	3.00	5.30	195.3	28.0	1176.0	857.0	75.6	7.90	1.16	14.726	295.3	144.2	103.7	0.0593
8	3.00	5.30	195.2	28.0	1185.0	860.0	76.9	8.40	0.57	27.293	295.1	152.1	103.6	0.0593
9	3.00	5.30	195.1	28.0	1190.0	858.0	76.1	8.70	0.32	39.859	295.6	155.3	103.6	0.0593
10	4.00	5.30	195.0	28.0	1184.0	860.0	76.0	8.80	0.20	52.425	295.5	156.8	103.8	0.0592
11	4.00	5.30	195.3	28.0	1190.0	859.0	76.0	8.80	0.15	64.992	294.9	177.7	103.9	0.0592
12	4.00	5.30	195.3	28.0	1184.0		76.6	8.90	0.00	800000	295.5	161.0	103.8	0.0593

NR	WHA LBM/S	WF LBM/S	WM LBM/S	WS LBM/S	WS	MS	NS	TO	DO/18	WOTD/AA
1	0.957	0.008	0.966	0.030	0.600	0.161	0.408	0.408	0.395	0.000
2	0.957	0.008	0.965	0.098	0.101	0.144	0.408	0.409	0.153	0.068
3	0.958	0.008	0.966	0.184	0.191	0.128	0.408	0.408	0.314	0.128
4	0.959	0.008	0.967	0.260	0.264	0.113	0.407	0.407	0.278	0.191
5	0.958	0.008	0.967	0.374	0.387	0.092	0.407	0.407	0.226	0.260
6	0.958	0.008	0.967	0.462	0.478	0.075	0.408	0.408	0.168	0.322
7	0.958	0.008	0.966	0.531	0.549	0.061	0.407	0.407	0.150	0.370
8	0.958	0.008	0.967	0.687	0.711	0.030	0.404	0.404	0.074	0.460
9	0.958	0.008	0.967	0.756	0.782	0.017	0.404	0.404	0.041	0.525
10	0.960	0.008	0.968	0.780	0.612	0.010	0.000	0.000	0.026	0.565
11	0.960	0.008	0.968	0.856	0.872	0.008	0.000	0.000	0.019	0.585
12	0.960	0.008	0.968	0.000	0.000	0.000	0.000	0.000	0.000	0.000

TABLE XI

Pumping Coeff. Data, Model A (950 F) - No Crossflow

*** HOT WIG PERFORMANCE ***
5 RING DIFFUSER

TUMT: 950

DATE: 02 SEP 83

NUMBER OF PRIMARY NOZZLES: 2.25 INCHES
PRIMARY NOZZLE DIAMETER: 4
UPTAKE DIAMETER: 7.310 INCHES
AREA RATIO, AM/AP: 2.50
GAMMA: 1.3556

DATA TAKEN BY R.E. STAPLES

MIXING STACK LENGTH: 7.22 INCHES
MIXING STACK DIAMETER: 7.122 INCHES
MIXING STACK L/D: 1.30
STANDOFF RATIO: 0.50
AMBIENT PRESSURE: 30.58 INCHES HG

NR	PNM IN HG	UELPR IN H2O	TNM DEG F	ROTA	TUUPR DEG F	TUPT DEG F	TAMU DEG F	PUPT IN H2O	PPLN IN H2O	SEC AREA SQ IN	UM FT/S	UU FT/S	UPACH
1	6.10	5.00	184.2	31.5	1255.0	951.0	71.8	6.83	3.00	0.000	122.0	107.7	0.0595
2	6.10	5.00	184.4	31.5	1255.0	950.0	72.2	7.10	2.05	1.767	127.1	107.5	0.0594
3	6.10	5.00	184.7	31.5	1255.0	949.0	72.7	7.40	2.30	3.534	130.9	107.4	0.0591
4	6.10	5.00	184.6	31.5	1257.0	944.0	72.9	7.70	2.05	5.001	135.8	107.3	0.0593
5	6.10	5.00	184.9	31.5	1255.0	950.0	73.5	8.00	1.67	8.883	139.6	107.1	0.0592
6	6.10	5.00	184.9	31.5	1255.0	950.0	71.7	8.30	1.32	11.585	143.6	107.2	0.0592
7	6.20	5.00	184.9	31.5	1255.0	951.0	73.0	8.50	1.08	14.726	147.1	107.4	0.0591
8	6.20	5.00	184.8	31.5	1255.0	953.0	71.5	9.00	0.52	27.291	154.1	107.4	0.0592
9	6.20	5.00	185.1	31.5	1256.0	955.0	73.3	9.10	0.45	39.859	156.0	107.8	0.0592
10	6.20	5.00	185.4	31.5	1256.0	955.0	73.6	9.40	0.20	54.425	160.2	107.3	0.0592
11	6.20	5.00	185.3	31.5	1256.0	953.0	73.5	9.60	0.15	64.994	162.9	107.3	0.0592
12	6.20	5.00	186.0	31.5	1256.0	957.0	73.8	9.50	0.00	86.000	122.2	107.5	0.0592

NR	GMPA LBM/S	MP LBM/S	MS LBM/S	VS	PS	TS	MOTOR.AA	UP FT/S			
1	0.955	0.010	0.905	0.000	0.181	0.377	0.000	307.1			
2	0.955	0.010	0.904	0.098	0.125	0.377	0.066	306.5			
3	0.955	0.010	0.904	0.181	0.102	0.378	0.124	306.0			
4	0.955	0.010	0.904	0.244	0.097	0.378	0.165	305.9			
5	0.955	0.010	0.904	0.167	0.077	0.378	0.248	305.7			
6	0.956	0.010	0.904	0.354	0.062	0.377	0.307	305.5			
7	0.956	0.010	0.906	0.522	0.051	0.378	0.352	306.0			
8	0.956	0.010	0.906	0.672	0.026	0.376	0.453	306.0			
9	0.956	0.010	0.906	0.679	0.012	0.377	0.418	305.8			
10	0.956	0.010	0.905	0.749	0.009	0.377	0.539	305.6			
11	0.956	0.010	0.905	0.858	0.007	0.377	0.574	305.6			
12	0.955	0.010	0.905	0.000	0.000	0.377	0.000	306.2			

TABLE X

Pumping Coeff. Data, Model A (950 F) - Crossflow

IUPT: 950

*** HOT RIG PERFORMANCE ***
& WING DIFFUSER

IN CROSS-FLOW

DATE: 04 SEP 83

DATA TAKEN BY R.E. STAPLES

NUMBER OF PRIMARY NOZZLES: 4
PRIMARY NOZZLE DIAMETER: 2.25 INCHES
UPTAKE DIAMETER: 7.510 INCHES
AREA RATIO, AP/AP: 2.50
GAMMA: 1.3556

MIXING STACK LENGTH: 7.22 INCHES
MIXING STACK DIAMETER: 7.122 INCHES
MIXING STACK L/D: 1.50
STANDOFF RATIO: 0.50
AMBIENT PRESSURE: 29.68 INCHES HG

NR	PNH IN HG	DELPR IN H2O	TRM DEG F	NOIA	TUUPR DEG F	IUPT DEG F	TAMB DEG F	IUPT IN H2O	PHLM IN H2O	SEC AREA SG IN
1	4.50	4.90	182.5	31.5	1197.0	953.0	72.0	7.20	3.25	0.000
2	4.50	4.80	182.6	31.5	1196.0	949.0	71.7	7.50	2.95	1.767
3	4.50	4.80	182.8	31.5	1195.0	949.0	70.8	7.80	2.60	3.534
4	4.50	4.80	183.1	31.5	1201.0	950.0	72.2	8.10	2.30	4.801
5	4.50	4.80	183.1	31.5	1204.0	951.0	72.0	8.40	1.85	8.443
6	4.50	4.80	183.3	31.5	1204.0	951.0	71.7	8.80	1.50	11.585
7	4.50	4.80	183.5	31.5	1204.0	954.0	72.0	9.00	1.25	14.726
8	4.50	4.80	183.7	31.5	1211.0	956.0	72.1	9.60	0.62	27.293
9	4.60	4.80	183.2	31.5	1215.0	958.0	71.2	9.80	0.45	34.859
10	4.60	4.80	183.5	31.5	1213.0	957.0	71.5	10.00	0.22	52.425
11	4.60	4.80	183.3	31.5	1216.0	958.0	71.6	10.00	0.15	64.992
12	4.60	4.80	186.3	31.5	1216.0	961.0	71.5	10.10	0.00	99999

NR	WPA LBM/S	WF LBM/S	WL LBM/S	WS LBM/S	WE	PS	TE	PO/TS	WSTSS.44	UP F/S	UM F/S	UU F/S	UMACH
1	0.934	0.010	0.949	0.000	0.600	0.153	0.377	0.405	0.000	311.9	124.5	109.1	0.0602
2	0.924	0.010	0.935	0.102	0.104	0.142	0.377	0.377	0.071	307.4	127.8	107.6	0.0598
3	0.929	0.010	0.938	0.192	0.204	0.125	0.377	0.333	0.133	307.1	132.0	107.5	0.0598
4	0.928	0.010	0.938	0.245	0.261	0.111	0.377	0.295	0.170	307.0	134.6	107.4	0.0597
5	0.928	0.010	0.938	0.386	0.412	0.099	0.377	0.237	0.268	306.9	141.5	107.4	0.0592
6	0.928	0.010	0.938	0.477	0.509	0.073	0.377	0.193	0.331	306.8	145.9	107.3	0.0592
7	0.928	0.010	0.938	0.554	0.590	0.060	0.377	0.161	0.384	306.6	149.6	107.3	0.0592
8	0.928	0.010	0.938	0.723	0.771	0.030	0.376	0.090	0.501	306.9	158.0	107.5	0.0592
9	0.928	0.010	0.939	0.794	0.845	0.017	0.374	0.045	0.568	307.7	161.7	107.8	0.0599
10	0.930	0.010	0.939	0.827	0.881	0.011	0.375	0.028	0.572	307.3	163.2	107.6	0.0590
11	0.930	0.010	0.939	0.867	0.901	0.007	0.375	0.019	0.585	307.5	168.2	107.7	0.0590
12	0.924	0.010	0.939	0.000	0.600	0.000	0.374	0.000	0.000	307.8	127.6	107.8	0.0590

171

TABLE XI

Pumping Coeff. Data, Model A Mod (850 F) – No Crossflow

*** HOT RIG PERFORMANCE ***
6 RING DIFFUSER

DATE: 04 SEP 83

NUMBER OF PRIMARY NOZZLES: 4
PRIMARY NOZZLE DIAMETER: 2.75 INCHES
UPTAKE DIAMETER: 7.510 INCHES
AREA RATIO, AM/AP: 2.250
GAMMA: 1.3614

DATA TAKEN BY R.E. STAPLES
MIXING STACK LENGTH: 7.22 INCHES
MIXING STACK DIAMETER: 7.122 INCHES
MIXING STACK L/D: 1.50
STANDOFF RATIO, S/D: 0.50
AMBIENT PRESSURE: 29.67 INCHES HG

TUPT: 850

NR	PNM IN HG	DELPN IN H2O	TAM DEG F	NOTA	TUUAM DEG F	TUPT DEG F	TAMB DEG F	TUPT IN H2O	PPIN IN H2O	SEC AREA SQ IN
1	4.10	5.40	189.3	29.5	1202.0	851.0	72.3	6.60	3.10	0.000
2	4.10	5.40	189.5	29.5	1202.0	851.0	73.6	6.90	2.70	1.767
3	4.10	5.40	189.9	29.5	1204.0	850.0	74.2	7.20	2.35	3.534
4	4.10	5.40	190.2	29.5	1204.0	851.0	73.4	7.50	2.08	5.401
5	4.10	5.40	190.4	29.5	1213.0	852.0	73.9	7.80	1.67	8.443
6	4.10	5.40	190.4	29.5	1211.0	851.0	74.2	8.10	1.35	11.585
7	4.10	5.40	190.8	29.5	1202.0	850.0	75.0	8.30	1.10	14.726
8	4.20	5.40	190.5	29.5	1203.0	850.0	73.1	8.80	0.55	27.293
9	4.20	5.40	190.6	29.5	1213.0	850.0	75.6	9.00	0.30	34.854
10	4.20	5.30	190.8	29.5	1203.0	852.0	75.4	9.10	0.40	52.025
11	4.20	5.30	190.5	29.5	1196.0	852.0	76.1	9.20	0.15	68.992
12	4.20	5.30	190.9	29.5	1196.0	853.0	76.3	9.30	0.00	88.038

NR	WPA LBM/S	WF LBM/S	WP LBM/S	WS LBM/S	WM	PS	TS	WCTS..	UP FT/S	UM FT/S	UU FT/S	UMACH
1	0.977	0.009	0.985	0.000	0.000	0.157	0.406	0.000	300.6	120.0	105.4	0.0602
2	0.976	0.009	0.985	0.097	0.099	0.137	0.407	0.067	300.2	124.7	105.3	0.0602
3	0.976	0.009	0.985	0.182	0.185	0.120	0.408	0.124	299.6	128.6	105.1	0.0601
4	0.976	0.009	0.985	0.262	0.266	0.106	0.407	0.174	299.6	132.5	105.0	0.0600
5	0.976	0.009	0.985	0.306	0.372	0.069	0.407	0.250	299.4	137.6	105.0	0.0600
6	0.976	0.009	0.985	0.452	0.459	0.069	0.407	0.309	299.2	141.8	105.0	0.0600
7	0.976	0.009	0.984	0.518	0.526	0.056	0.407	0.354	299.4	145.1	105.0	0.0600
8	0.975	0.009	0.984	0.649	0.649	0.028	0.406	0.463	299.5	153.0	105.1	0.0600
9	0.977	0.009	0.986	0.732	0.742	0.015	0.407	0.505	299.5	155.7	105.1	0.0599
10	0.977	0.009	0.986	0.786	0.805	0.010	0.407	0.542	296.3	157.1	104.0	0.0593
11	0.967	0.009	0.976	0.845	0.665	0.008	0.407	0.582	295.9	154.7	101.8	0.0580
12	0.967	0.009	0.976	0.000	0.600	0.000	0.407	0.000	295.9	118.1	103.8	0.0593

172

TABLE XII

Pumping Coeff. Data, Model A Mod (850 F) - Crossflow

*** MUT RIG PERFORMANCE ***   TUPT: 850
6 RING DIFFUSER

IN CROSS-FLO

DATA TAKEN BY R.E. STAPLES

DATE: 05 SEP 83

NUMBER OF PRIMARY NOZZLES: 4
PRIMARY NOZZLE DIAMETER: 2.25 INCHES
UPTAKE DIAMETER: 7.510 INCHES
AREA RATIO, AM/AP: 2.050
GAMMA: 1.3616

MIXING STACK LENGTH: 7.22 INCHES
MIXING STACK DIAMETER: 7.6122 INCHES
MIXING STACK L/D: 1.50
STANDOFF RATIO: 0.50
AMBIENT PRESSURE: 29.61 INCHES HG

NR	PNM IN HG	DELPR IN H2O	TNR DEG F	HOTA	TDUEN DEG F	TUPT DEG F	TAMB DEG F	PUPT IN H2O	PMLR IN H2O	SEC AHLA SC IR
1	4.40	5.40	188.0	29.5	1197.0	847.0	73.6	6.40	2.95	0.000
2	4.40	5.40	188.0	29.5	1191.0	851.0	73.1	6.60	2.70	1.767
3	4.00	5.40	188.1	29.5	1214.0	851.0	72.6	6.90	2.40	3.534
4	4.00	5.30	188.5	29.5	1196.0	848.0	72.6	7.20	2.13	5.301
5	4.00	5.30	188.8	29.5	1204.0	849.0	73.3	7.50	1.72	8.443
6	4.00	5.30	188.8	29.5	1206.0	849.0	73.6	7.80	1.40	11.585
7	4.00	5.30	189.0	29.5	1207.0	850.0	73.7	8.00	1.15	14.726
8	4.00	5.30	188.8	29.5	1213.0	850.0	73.4	8.60	0.58	27.293
9	4.00	5.30	189.0	29.5	1213.0	852.0	74.6	8.80	0.42	39.859
10	4.00	5.30	189.1	29.5	1212.0	852.0	73.9	8.90	0.20	52.425
11	4.10	5.30	189.4	29.5	1214.0	850.0	73.7	9.00	0.15	64.992
12	4.10	5.30	189.1	29.5	1216.0	850.0	72.3	9.10	0.00	68.000

NR	WPA LBM/S	WF LBM/S	WP LBM/S	WS LBM/S	WE	PS	TE	METER.44	UP FT/S	UR FT/S	UU FT/S	UPACH
1	0.974	0.009	0.983	0.000	0.000	0.151	0.408	0.000	299.2	114.5	105.0	0.0001
2	0.972	0.009	0.983	0.097	0.099	0.137	0.406	0.067	300.0	124.6	105.3	0.0001
3	0.975	0.009	0.966	0.184	0.147	0.122	0.406	0.126	300.2	128.9	105.3	0.0002
4	0.965	0.009	0.974	0.260	0.267	0.111	0.407	0.180	296.3	131.1	104.0	0.0595
5	0.965	0.009	0.974	0.371	0.381	0.090	0.407	0.257	296.2	130.0	101.9	0.0594
6	0.965	0.009	0.974	0.460	0.472	0.073	0.407	0.318	295.0	140.9	101.9	0.0594
7	0.965	0.009	0.976	0.530	0.544	0.000	0.407	0.366	295.8	144.7	103.9	0.0594
8	0.965	0.009	0.974	0.697	0.716	0.030	0.407	0.482	295.5	152.4	101.7	0.0594
9	0.965	0.009	0.974	0.755	0.776	0.017	0.407	0.523	295.8	155.4	103.8	0.0594
10	0.965	0.009	0.974	0.786	0.807	0.010	0.406	0.543	296.3	157.1	104.0	0.0594
11	0.966	0.009	0.975	0.864	0.866	0.008	0.406	0.582	296.4	160.0	104.1	0.0594
12	0.966	0.009	0.975	0.000	0.000	0.000	0.406	0.000	296.9	118.5	104.2	0.0594

TABLE XIII

Pumping Coeff. Data, Model A Mod (950 F) - No Crossflow

*** HOT RIG PERFORMANCE ***
& RING DIFFUSER

TUPT: 950

DATE: 00 SEP 83

DATA TAKEN BY R.E. STAPLES

NUMBER OF PRIMARY NOZZLES: 4
PRIMARY NOZZLE DIAMETER: 2.25 INCHES
PRIMARY DIAMETER: 7.510 INCHES
AREA RATIO/AREA: 2.50
GAMMA: 1.3550

MIXING STACK LENGTH: 7.22 INCHES
MIXING STACK DIAMETER: 7.122 INCHES
MIXING STACK L/D: 0.50
STANDOFF RATIO: 0.50
AMBIENT PRESSURE: 29.67 INCHES HG

NR	PPM IN HG	DELPR IN H2O	TAM DEG F	HOIA	TBURN DEG F	TUPT DEG F	TAMB DEG F	DUPT IN H2O	PPLM IN H2O	SEC AREA SQ IN	UM FT/S	UU FT/S	UPRCM
1	4.40	4.80	140.0	31.5	1226.0	952.0	73.0	7.10	3.15	0.000	121.7	106.7	0.0584
2	4.40	4.80	191.9	31.5	1224.0	951.0	72.1	7.40	2.78	1.767	126.5	106.6	0.0585
3	4.40	4.80	194.4	31.5	1225.0	953.0	73.4	7.80	2.03	3.534	130.7	106.6	0.0588
4	4.50	4.80	190.2	31.5	1223.0	952.0	73.4	8.10	2.13	4.801	133.2	106.7	0.0589
5	4.50	4.80	190.5	31.5	1224.0	952.0	73.6	8.40	1.70	8.843	139.7	106.6	0.0582
6	4.50	4.80	144.4	31.5	1225.0	952.0	73.3	8.70	1.38	11.585	143.5	106.5	0.0588
7	4.50	4.80	190.6	31.5	1228.0	952.0	73.4	8.90	1.12	14.726	147.1	106.4	0.0587
8	4.50	4.80	190.2	31.5	1226.0	953.0	73.2	9.50	0.55	27.293	154.7	106.4	0.0587
9	4.50	4.80	190.5	31.5	1236.0	955.0	73.3	9.70	0.30	34.859	157.3	106.5	0.0587
10	4.50	4.80	190.2	31.5	1236.0	956.0	73.2	9.40	0.20	52.425	160.1	106.5	0.0588
11	4.60	4.80	154.5	31.5	1236.0	956.0	72.9	9.80	0.15	64.992	161.1	106.7	0.0588
12	4.70	4.80	190.1	31.5	1236.0	956.0	73.4	10.00	0.00	64.000	121.7	106.8	0.0589

NR	WPA LBM/S	WF LBM/S	WP LBM/S	WS LBM/S	WO	PS	PO	PR/PR	NOTE/.44	UP FT/S
1	0.918	0.010	0.528	0.000	0.100	0.155	0.377	0.411	0.000	304.9
2	0.919	0.010	0.528	0.099	0.107	0.137	0.377	0.361	0.069	304.5
3	0.918	0.010	0.528	0.185	0.194	0.120	0.377	0.317	0.130	304.6
4	0.420	0.010	0.930	0.235	0.253	0.105	0.378	0.278	0.165	304.7
5	0.420	0.010	0.929	0.370	0.398	0.084	0.378	0.222	0.256	304.3
6	0.420	0.010	0.930	0.457	0.492	0.068	0.378	0.180	0.120	304.0
7	0.420	0.010	0.930	0.523	0.563	0.055	0.378	0.146	0.367	303.8
8	0.420	0.010	0.930	0.680	0.731	0.027	0.377	0.072	0.476	301.7
9	0.920	0.010	0.929	0.733	0.789	0.015	0.377	0.039	0.510	303.8
10	0.920	0.010	0.930	0.787	0.847	0.010	0.376	0.026	0.551	304.0
11	0.921	0.010	0.931	0.846	0.908	0.007	0.376	0.020	0.591	304.4
12	0.923	0.010	0.933	0.000	0.000	0.000	0.376	0.000	0.000	304.8

174

TABLE XIV

Pumping Coeff. Data, Model A Mod (950 F) - Crossflow

*** HOT RIG PERFORMANCE ***   IUHT: 950

    6 RING DIFFUSER

IN CROSS-FLOW

DATE: 05 SEP 83   DATA TAKEN BY H.E. STAPLES

NUMBER OF PRIMARY NOZZLES: 6
PRIMARY NOZZLE DIAMETER: 2.25 INCHES
UPSTAKE DIAMETER: 7.510 INCHES
AREA RATIO AP/AP: 2.50
LAMDA: 1.3556

MIXING STACK LENGTH: 7.22 INCHES
MIXING STACK DIAMETER: 7.122 INCHES
MIXING STACK L/D: 1.50
STANDOFF RATIO: 0.20
AMBIENT PRESSURE: 29.61 INCHES HG

AR	PRM IN HG	DELPA IN H2O	TAM DEG F	NOIA	THUFM DEG F	IUMT DEG F	TAMB DEG F	DUPT IN H2O	PPLN IN H2O	SFC AREA SQ IN	UP FT/S	UM FT/S	UU FT/S	UPACH
1	4.50	4.90	193.6	31.5	1217.0	951.0	72.6	7.30	3.15	0.000	309.0	123.6	108.1	0.0597
2	4.50	4.90	193.6	31.5	1231.0	953.0	76.1	7.60	2.80	1.767	309.7	128.6	108.2	0.0597
3	4.60	4.90	164.0	31.5	1226.0	955.0	76.6	8.00	2.45	3.534	309.7	132.9	108.4	0.0597
4	4.60	4.90	193.8	31.5	1231.0	954.0	77.0	8.20	2.15	4.801	309.3	135.2	108.3	0.0597
5	4.60	4.90	194.2	31.5	1236.0	957.0	76.6	8.60	1.72	8.443	309.5	142.0	108.3	0.0597
6	4.60	4.80	194.3	31.5	1237.0	954.0	76.1	8.90	1.60	11.585	306.8	145.1	107.2	0.0590
7	4.60	4.80	194.5	31.5	1242.0	954.0	75.5	9.10	1.15	18.726	306.1	148.6	107.2	0.0590
8	4.60	4.80	194.5	31.5	1243.0	961.0	76.0	9.60	0.55	27.293	306.1	156.6	107.2	0.0590
9	4.70	4.80	194.9	31.5	1242.0	961.0	76.6	9.90	0.32	39.859	306.7	159.7	107.3	0.0590
10	4.70	4.80	194.9	31.0	1213.0	950.0	77.0	9.90	0.20	52.425	301.8	160.2	106.6	0.0585
11	4.70	4.80	195.4	31.0	1217.0	949.0	77.6	10.00	0.15	64.992	301.6	162.4	106.1	0.0585
12	4.70	4.80	195.6	31.0	1215.0	948.0	77.3	10.00	0.00	88888	303.0	121.0	106.2	0.0585

AR	WPA LBM/S	WF LBM/S	WP LBM/S	WS LBM/S	WE	PO	TO	PO/TO	WOTO/AA	WC
1	0.430	0.010	0.939	0.000	0.600	0.152	0.373	0.401	0.000	
2	0.430	0.010	0.939	0.049	0.105	0.155	0.374	0.356	0.069	
3	0.431	0.010	0.940	0.185	0.197	0.118	0.374	0.311	0.128	
4	0.931	0.010	0.941	0.235	0.250	0.104	0.340	0.273	0.163	
5	0.931	0.010	0.940	0.170	0.394	0.083	0.374	0.218	0.257	
6	0.931	0.010	0.930	0.459	0.403	0.069	0.378	0.181	0.321	
7	0.920	0.010	0.630	0.529	0.568	0.056	0.377	0.149	0.370	
8	0.920	0.010	0.930	0.617	0.728	0.027	0.377	0.071	0.474	
9	0.920	0.010	0.930	0.754	0.810	0.016	0.377	0.061	0.528	
10	0.921	0.010	0.931	0.784	0.842	0.010	0.384	0.026	0.551	
11	0.921	0.009	0.931	0.801	0.906	0.007	0.381	0.020	0.591	
12	0.921	0.009	0.930	0.000	0.000	0.000	0.382	0.000	0.000	

175

TABLE XV

Mixing Stack Pressure Data, Model A

Uptake Temperature	Axial Position (F)	Mixing Stack Pressure (in. water ref. to atmos.) 650	850 (NO CROSSFLOW)	950
Position A	0.00	-0.95	-1.05	-1.05
	0.25	-0.50	-0.55	-0.52
	0.50	-0.15	-0.10	-0.05
	0.75	-0.05	-0.65	-0.10
Position B	0.00	-0.90	-1.05	-1.00
	0.25	-0.25	-0.30	-0.30
	0.50	-0.55	-0.55	-0.55
	0.75	-0.40	-0.25	-0.28
		(CROSSFLOW)		
Position A			-1.10	-1.15
			-0.60	-0.60
			-0.15	-0.15
			-0.35	-0.35
Position B			-1.10	-1.15
			-0.32	-0.35
			-0.72	-0.67
			-0.55	-0.50

176

TABLE XVI

Mixing Stack Pressure Data, Model A Modified

Uptake Temperature	Axial Position (F)	Mixing Stack Pressure (in. water ref. to atmos.) 850	950
		(NO	CROSSFLOW)
Position A	0.00	-1.10	-1.10
	0.25	-0.55	-0.55
	0.50	-0.15	-0.15
	0.75	-0.25	-0.32
Position B	0.00	-1.02	-1.00
	0.25	-0.28	-0.28
	0.50	-0.55	-0.53
	0.75	-0.25	-0.24
		(CROSSFLOW)	
Position A		-1.10	-1.20
		-0.60	-0.60
		-0.15	-0.20
		-0.35	-0.40
Position B		-1.10	-1.15
		-0.32	-0.35
		-0.70	-0.70
		-0.52	-0.50

TABLE XVII

Mixing Stack Temperature Data, Model A

Thermocouple Number	Axial Position	Mixing Stack Temperature (degrees F)				
Uptake Temperature		650 NCF	850 NCF	850 CF	950 NCF	950 CF
6	0.00	101	135	110	150	123
7	0.00	106	139	115	163	129
10	0.41	67	67	79	77	75
9	0.41	195	258	231	297	263
16	0.36	158	234	189	258	231
11	0.46	74	79	87	88	100
12	0.61	198	204	290	342	324
14	0.76	241	314	308	357	343
15	0.89	226	263	283	301	301
8	0.89	230	305	301	345	336
17	0.84	73	74	103	87	91
13	0.94	258	305	314	347	340
Ambient		65	67	75	75	69

NCF - NO CROSSFLOW
CF - CROSSFLOW

178

TABLE XVIII

Mixing Stack Temperature Data, Model A Mod

Thermocouple Number	Axial Position	Mixing Stack Temperature (degrees F)			
Uptake Temperature		850 NCF	850 CF	950 NCF	950 CF
6	0.00	142	108	162	127
7	0.00	146	113	168	133
10	0.41	76	77	72	77
9	0.41	263	230	299	263
16	0.36	237	192	282	235
11	0.46	88	84	98	91
12	0.61	306	289	343	324
14	0.76	321	309	358	342
15	0.89	272	278	296	299
8	0.89	311	300	348	333
17	0.84	84	93	83	119
13	0.94	312	312	342	336
Ambient		73	69	73	76

NCF - NO CROSSFLOW
CF - CROSSFLOW

179

TABLE XIX

Shroud and Diffuser Temp. Data, Model A

	AXIAL POSITION	TEMPERATURE				(F)
UPTAKE TEMPERATURE	(X/D)	650 NCF	850 NCF	850 CF	950 NCF	950 CF
SHROUD	0.125	73.8	78.0	81.8	90.3	86.0
	0.375	81.1	88.5	86.5	101.9	86.9
	0.625	87.4	98.0	86.3	111.7	88.9
	0.750	97.2	108.8	91.5	124.5	95.3
	1.068	125.4	143.9	108.4	160.3	111.7
DIFFUSER RING	1	80.6	83.0	96.2	96.3	95.3
	2	80.7	83.5	104.1	96.5	107.8
	3	76.5	78.7	94.8	90.0	100.1
	4	82.9	85.2	101.2	97.6	107.7
	5	87.9	87.3	99.3	103.0	106.3
	5A	84.6	90.9	96.9	102.8	102.6
	5B	92.7	103.5	92.0	114.5	102.0
AMBIENT		66	67	75	75	69

NCF - NO CROSSFLOW
CF - CROSSFLOW

TABLE XX

Shroud and Diffuser Temp. Data, Model A Mod

UPTAKE TEMPERATURE	AXIAL POSITION (X/D)	TEMPERATURE			(F)
		850 NCF	850 CF	950 NCF	950 CF
SHROUD	0.125	87.5	77.7	87.4	82.7
	0.375	98.1	86.3	95.9	88.9
	0.625	106.1	97.5	109.5	92.1
	0.750	114.1	104.0	118.3	96.2
	1.068	151.9	108.4	160.2	115.7
DIFFUSER RING	1	91.8	106.0	90.6	98.3
	2	93.0	106.9	91.4	108.2
	3	88.4	99.0	95.0	99.2
	4	94.7	108.2	93.6	104.5
	5	95.8	90.1	94.5	101.4
	5A	95.5	92.2	94.1	98.5
	5B	99.7	93.2	96.2	91.2
AMBIENT		73	69	73	76

NCF - NO CROSSFLOW
CF - CROSSFLOW

TABLE XXI

Exit Plane Temperature Data, Model A

AXIAL POSITION	R/RMS	TEMPERATURE				(F)
UPTAKE TEMPERATURE		650 NCF	850 NCF	850 CF	950 NCF	950 CF
0.00	1.171	177	176	102	167	119
0.25	1.101	210	259	144	258	165
0.50	1.031	247	312	201	330	215
0.75	0.961	271	349	250	372	268
1.00	0.890	302	388	299	417	323
1.25	0.820	325	415	332	450	364
1.50	0.750	339	458	365	466	404
1.75	0.680	352	473	390	489	431
2.00	0.610	369	482	412	498	455
2.25	0.539	381	496	433	515	481
2.50	0.469	395	504	454	531	496
2.75	0.399	406	514	472	542	515
3.00	0.329	415	520	486	554	534
3.25	0.259	423	523	499	566	550
3.50	0.188	429	524	511	574	574
3.75	0.118	432	520	524	579	581
4.00	0.048	434	513	528	584	581
4.25	0.000	434	505	529	582	576
4.25	0.000	435	523	531	586	584
4.00	0.048	434	521	530	584	584
3.75	0.118	432	515	527	575	581
3.50	0.188	427	508	519	572	573
3.25	0.259	421	497	513	556	566
3.00	0.329	410	487	503	549	554
2.75	0.399	404	478	494	536	547
2.50	0.469	390	463	495	529	540
2.25	0.539	377	450	476	509	532
2.00	0.610	360	440	468	495	522
1.75	0.680	343	425	456	480	510
1.50	0.750	322	408	442	463	505
1.25	0.820	294	392	423	448	498
1.00	0.890	270	363	404	412	469
0.75	0.961	237	329	336	367	419
0.50	1.031	197	273	262	316	343
0.25	1.101	146	200	195	242	253
0.00	1.171	108	146	103	168	146

TABLE XXII

Exit Plane Temperature Data, Model A Mod

AXIAL POSITION	R/RMS	TEMPERATURE			(F)
UPTAKE TEMPERATURE		850 NCF	850 CF	950 NCF	950 CF
0.00	1.171	168	97	135	98
0.25	1.101	223	141	201	134
0.50	1.031	270	229	279	185
0.75	0.961	329	275	345	243
1.00	0.890	355	317	391	301
1.25	0.820	394	348	416	350
1.50	0.750	405	378	441	381
1.75	0.680	421	402	461	413
2.00	0.610	443	420	477	440
2.25	0.539	457	444	493	464
2.50	0.469	470	461	507	487
2.75	0.399	488	475	521	503
3.00	0.329	500	494	536	520
3.25	0.259	510	508	545	535
3.50	0.188	516	519	557	554
3.75	0.119	525	528	571	564
4.00	0.049	535	529	578	573
4.25	0.000	535	529	583	580
4.25	0.000	535	533	586	582
4.00	0.048	532	532	585	579
3.75	0.119	529	527	580	575
3.50	0.188	524	519	571	566
3.25	0.259	519	512	564	555
3.00	0.329	510	502	556	547
2.75	0.399	499	498	543	539
2.50	0.469	490	486	534	527
2.25	0.539	481	475	521	517
2.00	0.610	472	469	515	512
1.75	0.680	464	455	505	499
1.50	0.750	456	450	494	489
1.25	0.820	445	431	473	462
1.00	0.890	409	388	440	408
0.75	0.961	362	325	386	338
0.50	1.031	291	236	284	243
0.25	1.101	210	155	198	142
0.00	1.171	101	92	103	101

TABLE XXIII

Exit Plane Horiz. Pitot Traverse Data

PITOT POSITION (IN.)	DYNAMIC PRESSURE (IN. H2O)	VELOCITY (KNOTS)
0.000	0.100	12.53
0.500	0.850	36.52
1.000	0.750	34.30
1.500	0.700	33.14
2.000	0.650	31.94
2.500	0.650	31.94
3.000	0.650	31.94
3.500	0.650	31.94
4.000	0.675	32.55
4.500	0.675	32.55
5.000	0.650	32.55
5.500	0.625	31.32
6.000	0.625	31.32
6.500	0.675	32.55
7.000	0.675	32.55
7.500	0.675	32.55
8.000	0.650	31.94
8.500	0.625	31.32
9.000	0.600	30.69
9.500	0.675	32.55
10.000	0.675	32.55
10.500	0.700	33.14
11.000	0.675	32.55
11.500	0.625	31.32
11.625	0.000	00.00

184

TABLE XXIV

24 in. Standoff -Pitot Horiz. Traverse

PITOT POSITION (IN.)	DYNAMIC PRESSURE (IN. H2O)	VELOCITY (KNOTS)
0.000	0.400	25.06
0.500	0.400	25.06
1.000	0.400	25.06
1.500	0.380	24.42
2.000	0.360	23.77
2.500	0.350	23.44
3.000	0.350	23.44
3.500	0.350	23.44
4.000	0.350	23.44
4.500	0.350	23.44
5.000	0.400	25.05
5.500	0.450	26.58
6.000	0.520	28.57
6.500	0.550	29.38
7.000	0.600	30.69
7.500	0.640	31.69
8.000	0.640	31.69
8.500	0.650	31.94
9.000	0.640	31.69
9.500	0.600	30.69
10.000	0.600	30.69
10.500	0.600	30.69
11.000	0.600	30.69
11.500	0.550	29.38
11.625	0.550	29.39

TABLE XXV

24 in. Standoff - Pitot Vertical Traverse

PITOT POSITION (IN.)	DYNAMIC PRESSURE (IN. H2O)	VELOCITY (KNOTS)
0.000	0.150	15.43
0.500	0.170	16.42
1.000	0.200	17.81
1.500	0.250	19.91
2.000	0.275	20.89
2.500	0.275	20.89
3.000	0.350	23.56
3.500	0.350	23.56
4.000	0.350	23.55
4.500	0.450	26.72
5.000	0.500	28.16
5.500	0.500	28.16
6.000	0.600	30.85
6.500	0.600	30.85
7.000	0.620	31.36
7.500	0.620	31.36
8.000	0.620	31.36
8.500	0.620	31.36
9.000	0.600	30.85
9.500	0.600	30.85
10.000	0.600	30.85
10.500	0.600	30.85
11.000	0.600	30.85
11.500	0.600	30.85
12.000	0.570	30.07
12.500	0.570	30.07
13.000	0.500	28.16
13.500	0.450	26.72
14.000	0.370	24.23
14.250	0.370	24.23

TABLE XXVI

24 in. Standoff -4.5 in Pitot Vert. Traverse

PITOT POSITION (IN.)	DYNAMIC PRESSURE (IN. H2O)	VELOCITY (KNOTS)
0.000	0.300	21.70
0.250	0.300	21.70
0.500	0.230	19.00
0.750	0.325	22.59
1.000	0.480	27.45
1.250	0.550	29.38
1.500	0.600	30.69
1.750	0.610	30.94
2.000	0.610	30.94
2.250	0.610	30.94
2.500	0.610	30.94
2.750	0.590	30.43
3.000	0.580	30.17
3.250	0.560	29.65
3.500	0.550	29.38
3.750	0.530	28.84
4.000	0.510	28.29
4.250	0.500	28.01
4.500	0.470	27.16

TABLE XXVII
Pumping Coefficient Results

FIVE RING DIFFUSER		
TOPT	NO CROSSFLOW (F)	CROSSFLOW
175	0.50 *(0.54)	--
650	0.51	--
850	0.57	0.59
950	0.55	0.61

SIX RING DIFFUSER		
850	0.57	0.59
950	0.58	0.59

*PRITCHARD FROM COLD FLOW TEST

188

TABLE XXVIII

Air Mass Flow Calibration Data

$P_{NH} + B$ (IN. HG)	ΔP_N (IN. H2O)	$\left[\dfrac{(P_{NH}+B)\cdot \Delta P_N}{T_{NHR}}\right]^{0.5}$	$\dot{m}_a$ (LBM/SEC)
31.15	2.0	0.319	0.554
31.15	2.0	0.316	0.555
31.15	2.0	0.319	0.591
32.85	4.0	0.459	0.833
32.65	4.0	0.462	0.838
33.85	4.0	0.435	0.852
34.75	6.0	0.582	1.026
35.05	6.0	0.579	1.051
38.65	6.0	0.606	1.126
38.55	8.0	0.706	1.295
39.15	8.0	0.705	1.300
47.65	8.0	0.774	1.477
51.55	8.5	0.827	1.595
47.95	10.0	0.875	1.634
48.75	10.0	0.877	1.643

TABLE XXIX

Air Mass Flow vs. Pressure Product Data

$\dot{m}_a$ (LBM/SEC)	PRESSURE PRODUCT
0.554	0.319
0.555	0.316
0.591	0.319
0.833	0.459
0.838	0.462
0.852	0.435
1.026	0.582
1.051	0.579
1.126	0.606
1.295	0.706
1.300	0.705
1.477	0.774
1.595	0.827
1.634	0.875
1.643	0.877

APPENDIX A

GAS GENERATION OPERATION

I. PRIMARY AIR COMPRESSOR OPERATION   The primary air
flow for the gas generator is supplied by a Carrier Model
18P352 three stage centrifugal air compressor located in
Building 230. The compressor is driven through a Western
Gear Model 95HSA speed increasing gearbox by a 300 horse-
power General Electric induction motor. The compressor
serves various other experiments both in building 230 and
249. Figure (14) is a schematic of the compressor system
layout. The cooling water system serves both the Carrier
compressor and the Sullivan compressor for the supersonic
wind tunnel in building 230.

Lube oil for the compressor and speed increaser bearings
is supplied from an external sump by either an attached pump
or an electrically driven auxiliary pump. The lube oil is
cooled in a closed loop oil to fresh water heater exchanger.
Cooling water circulates within its own loop and is cooled
in an evaporative cooling tower which stands between build-
ings 230 and 249. Makup is automatically provided to the
fresh water loop by a float operated valve in the cooling
tower.

It is recommended that the lube oil system for the
compressor be started approximately one hour prior to

191
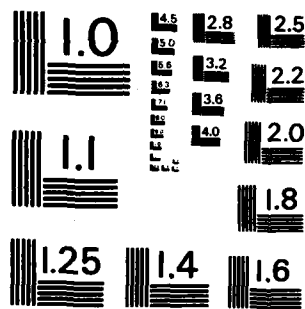
MICROCOPY RESOLUTION TEST CHART

NATIONAL BUREAU OF STANDARDS-1963-A

compressor lightoff. This ensures adequate pre-lubrication and warms the oil to some degree, decreasing starting loads. This is critical, as the compressor operates at near the capacity of the breaker in the supplying substation. Should this breaker trip out during the starting sequence it will be necessary to call the trouble desk and have base electricians reset it.

During periods when operations are being conducted daily or when it is desired to operate early in the morning, it is permissable to leave the auxiliary oil pump running overnight with the cooling water system secured. This will maintain the lube oil at a temperature suitable for lightoff and eliminate this delay.

When fully warmed up the compressor supplies air to the gas generator at 170-190°F. It normally takes the compressor about one hour to reach stable operation at this temperature. Although it is possible to obtain a gas generator lightoff with a lower air supply temperature, stable operation enhances data taking and reduces the number of control adjustments required during data runs. It is, therefore, desirable to allow the system to fully stabilize prior to lighting off the gas generator or collecting data. The following lightoff sequence is recommended:

A) Check the oil level in the compressor's external sump. Oil should be within four inches of the top of the sight glass.

B) Start the auxiliary oil pump by positioning the "hand-off automatic" switch (Figure 15) in the "hand" position. The electric pump will start and oil pressure should register approximately 30 PSIG. Inspect the system for leaks and note the level in the external sump.

C) Wait 45 minutes to one hour. During this period the compressor bearing temperatures should rise to approximately 70°F.

D) Line up the combustion gas generator for operation.

   1) Open the two manometer isolation valves at the pressure taps on either side of the inlet reducing section (Figure 5). Reconnect manometer tubing at the manometers if it has previously been disconnected.

   2) Ensure the main air supply butterfly valve is fully closed (Figure 6).

   3) Open the air supply bypass globe valve two and one quarter turns (Figure 6).

   4) Open the manually operated 4 inch butterfly isolation valve (Figure 5).

193

5) Energize the main power panel (Figure 9) and open the electrically operated burner air supply and cooling air bypass valves fully.

6) Ensure the gas generator exhaust area is clear.

E) Start the air compressor fresh water cooling system:

1) Check the water level in the cooling tower it should be at the level of the inlet line.

2) Vent the cooling water pump casing. Open the petcock on the suction side of the pump casing until all air in the suction line is expelled.

3) Ensure valve "A" to the Sullivan compressor is closed.

4) Open valve "B" to the Carrier compressor.

5) Start the cooling water pump and cooling tower fan (Figure 17). The fan is interlocked with the pump and will not start unless the pump is running.

6) Inspect the cooling tower drip lattice to ensure water is circulating.

F) Open the drain on the air compressor air cooling bank (Figure 19).

G)   Ensure the compressor air suction valve is fully
     closed (indicator vertical) (Figure 20).

WARNING   When in operation the compressor produces
hazardous noise.   Ensure all personnel in the
vicinity are wearing adequate hearing protection
prior to starting the compressor.

H)   Start the air compressor motor (Figure 13), the
     controller uses an automatic two stage start
     circuit.

I)   When the compressor is fully up to speed, switch
     the auxiliary lube oil pump to the "automatic"
     position. Lube oil pressure should remain about
     24-30 PSIG. Oil is now being supplied by the
     attached pump driven by the speed increasing gear-
     box. If the oil pressure should fall to 12 PSIG,
     the auxiliary pump will start automatically.

J)   When compressor operation has stabilized, slowly
     open the suction valve until the indicator is in

the full open (horizontal) position. Air is now
being supplied to the gas generator. Bypass air
from the supply to other experiments will also
be discharged outside the rear of building 230.
Normally it is not necessary to secure this
bypass flow, but in unusual circumstances it
may be stopped by closing the isolation valve
on the cooling bank (Figure 19).

K) Operation of the air compressor should be monitored
periodically.

1) Normal oil pressure from the attached pump
is 24 PSIG. Specified bearing pressure are
20-25 PSIG.

2) Normal oil pressure from the auxiliary
electric pump is 30 PSIG.

3) Normal oil temperature at the outlet of the
lube oil cooler is 100-105°F (135°F maximum).

4) Normal Bearing temperatures for the compressor
are 140-160°F. Speed increaser oil tempera-
ture is normally 120-130°F.

5) Do not allow any bearing temperature to exceed
200°F. In the event bearing temperatures rise
above 180°F during normal operation, the oil
cooler should be inspected for proper water
temperature and flow rate.

II. <u>GAS GENERATOR LIGHT OFF</u>   Allow the air compressor to operate for approximately one hour in order for air inlet temperature to the gas generator to stabilize.

A) Approximately 15 minutes prior to gas generator light off, line up the fuel system and place it in operation.

1) Open the fuel tank suction valve (Figure 22) and bulkhead isolation valve (Figure 21).

2) Ensure the solenoid operated emergency fuel cutoff valve is closed and close the HP pump manual discharge valve.

3) Open the nozzle box drain valve.

4) If this is the first time the system is being placed in operation, open both the fuel control valve (Figure 8) and the needle trimmer valve (Figure 24) fully. If the trimmer valve is known to be properly set, it need not be adjusted as described in this and following steps.

5) Start the fuel supply pump. Fuel supply pressure will be 14-16 PSIG.

6) Start the HP pump. With both trimmer and fuel control valves fully open the discharge pressure

197

will be 25-30 PSIG. With the trimmer valve properly set and the fuel control valve fully open, the HP pump discharge pressure will be 80 PSIG.

7) If the trimmer valve is to be adjusted, close the fuel control valve with the trimmer valve fully open. Observing the HP pump discharge pressure, slowly close the trimmer valve until the HP pump pressure reaches 350 PSIG. The trimmer valve is now set and the fuel control valve should provide smooth control over a range of 80-350 PSIG HP pump discharge pressure. All subsequent fuel control adjustments will be made using the fuel control valve.

8) Using the fuel control valve, set the HP pump discharge pressure at 200 PSIG and allow the system to recirculate for 10-15 minutes to warm the fuel. This facilitates combustion and ensures a clean lightoff.

B) When the inlet air temperature reaches $170-180^{\circ}F$, the gas generator may be lighted off.

1) Adjust inlet air bypass valve to obtain a pressure of approximately 4.0 in Hg at the upstream side of the inlet reducing section (PNH).

198

2) Ensure the burner air valve is fully open.
Adjust the bypass cooling air valve to obtain
a pressure drop across the U-tube of 1.60
inches H_2O. In some cases it may be necessary
to leave the cooling air bypass valve fully
open and reduce the inlet air pressure (PNH)
slightly to obtain this setting. The pressure
drop across the inlet reducing section (DELPN)
will be about 15 inches H_2O. This provides
the recommended lightoff air fuel ratio of 20.

3) Open the HP pump manual discharge valve fully.

4) Set the high temperature (Type K) readout to
monitor burner temperature (TBURN). Set the
low temperature (Type T) readout to monitor
air inlet temperature (TNH).

5) Ensure the gas generator exhaust area is clear.

6) Adjust the HP pump discharge pressure to 150
PSIG.

7) Depress and hold down the spring loaded ignitor
switch for 10 seconds.

8) While continuing to hold the ignitor switch
depressed, open the solenoid operated emergency
fuel cutoff valve. Ignition should be observed
in 6-12 seconds. If the gas generator fails to
light, close the emergency fuel cutoff valve

199

and release the ignitor switch. Allow the system to purge for 5 minutes or until no raw fuel is being expelled from the primary nozzle. If the gas generator fails to light, raw fuel will be expelled from the primary nozzles and will collect in the base of the secondary plenum. This should be wiped up prior to continuing.

9) When ignition is observed, release the ignitor switch.

10) Observe the burner temperature. When the burner temperature reaches 1000°F begin reducing fuel pressure toward minimum (70-75 PSIG at the burner nozzle, (PNOZ)) to stabilize burner temperature between 1000 and 1300°F.

```
┌─────────────────────────────────────────────────┐
│                                                 │
│  WARNING  Do not allow burner temperature to    │
│  exceed 1500°F.                                 │
│                                                 │
└─────────────────────────────────────────────────┘
```

It will be necessary to close the cooling air bypass valve to about 50 percent open to achieve stable operation at the desired burner temperature.

CAUTION   Do not allow burner temperature to
fall below 1000°F.   The gas generator will
begin to emit white smoke when the burner
temperature falls to about 950°F and combus-
tion will cease at a burner temperature of
about 800°F.   If combustion ceases there will
be a noticable change in sound intensity
accompanied by quantities of white smoke and
rapidly falling burner temperature; immedi-
ately close the emergency fuel cutoff valve.
Readjust fuel and air controls to lightoff
settings and reinitiate the lightoff sequence.

The prescribed lightoff sequence usually leads to
stable operation with an uptake temperature of
400-500°F and an uptake Mach number of about 0.07.

```
|-----------------------------------------------------------|
| |                                                       | |
| | WARNING Do not allow uptake temperature to            | |
| | exceed 1200°F at any time.                            | |
| |                                                       | |
|-----------------------------------------------------------|
```

11) When stable operation has been established,
close the nozzle box drain valve prior to
attempting to adjust the uptake Mach number.

III.   TEMPERATURE/MACH NUMBER CONTROL

The control process consists of a iterative sequence of
adjustments in the uptake temperature (TUPT), inlet air
pressure (PNH), and bypass cooling air mass flow. Some
practice is necessary to achieve reasonable accuracy in
the adjustment process. It must be kept in mind that
effect of the bypass cooling air valve varies depending on
the valve's initial position. When the bypass valve is
more than 50 percent open, opening the valve reduces air
flow through the burner, increasing burner temperature
(TBURN), however, the increase in the proportion of cool
bypass air mixing with the combustion gas results in a
lower uptake temperature. When a majority of the air flow
is already passing through the combustion chamber, that
is, when the bypass valve is less than 50 percent open,

202

and particularly when it is less than 25 percent open, the increase in burner temperature resulting from opening the bypass valve more than offsets the increased proportion of cooling air and the uptake temperature will raise when the bypass valve is opened. With these cautions in mind, the following adjustment procedure is recommended:

A) Adjust the fuel control valve to obtain the desired uptake temperature. Do not allow burner temperature to fall below $1000^{\circ}F$ or to exceed $1300^{\circ}F$ during this process.

B) As burner temperature approaches one of the limits, change air flow through the burner either by adjusting the bypass valve or the inlet globe valve. Choice of control device depends on the prior operating state. If the system has been stabilized at the desired Mach number it is usually best to control burner temperature during transitions by using the inlet globe valve. The key operating parameters are uptake temperature (TUPT) and uptake pressure (PUPT). Burner temperature is monitored to ensure safe combustion is maintained. For operation with uptake an Mach number of approximately 0.065, the values in Table XXII are recommended:

Recommended Initial Control Settings

TUPT ($^\circ$F)	PUPT (inches H O)
950	13.3
850	11.1
750	10.5
650	9.6
550	9.0
175	8.8

C) Compute the uptake Mach number (UMACH) using

the formula:

$$UMACH = 1.037 \times 10^{-1} (TUPTR/\gamma)^{0.5} \times ((((PNH - B) \times DELPN$$
$$/ TNHR)^{0.5} - (2.318 \times 10^{-4} \times ROTA) - 2.085 \times 10^{-1})$$
$$/ (B + (PUPT / 13.5717)))$$

(eqn A.1)

where:

UMACH = Uptake Mach number

TUPTR = Absolute uptake temperature (R)

γ = Ratio of specific heats for air

Values of the Ratio of Specific Heats for Air

TUPT (^{O}F)	γ
175	1.3991
550	1.3805
650	1.3741
750	1.3677
850	1.3614
950	1.3556

PNH = Air pressure before the inlet reducing section (inches Hg)

B = Corrected atmospheric pressure (inches Hg)

DELPN = Pressure drop across the inlet reducing section (inches H_2O)

TNHR = Absolute air temperature before the inlet reducing section (R)

ROTA = Fuel mass flow rotameter reading

PUPT = Gas pressure in the uptake section (inches H_2O)

D) Adjust the uptake temperature and pressure as neces-
sary using a combination of inlet globe valve,
cooling air bypass valve, and fuel control valve
changes until the desired test Mach number is
obtained.

E) If inlet air temperature has been allowed to
stabilize prior to gas generator operation, it will
be found that, once the desired uptake temperature
and Mach number have been set, no adjustments to
the system will be required during data runs.
Uptake temperature will be maintained within plus
or minus four degrees and uptake Mach number will
vary less than 0.001 under most circumstances. The
largest variations in uptake Mach number observed
have been during pumping coefficient runs when
changes in secondary flow induce large changes in
uptake pressure. If the gas generator is at the
operating point prior to closing the plenum, it
will be unnecessary to make adjustments for the
slight increase (0.0005 to 0.0010) in Mach number
which occurs when secondary flow is shut off.

IV. SECURING THE SYSTEM

A) When data runs are complete, shut down the gas
   generator by reducing the fuel pressure to minimum
   and immediately closing the solenoid operated emer-
   gency fuel cutoff valve.

   1) Shut off the high pressure fuel pump.

   2) Shut off the fuel supply pump.

   3) Open the cooling air bypass valve fully.

   4) Open the inner bypass glove valve until an
      inlet pressure (PNH) of 4.0-5.0 inches Hg is
      obtained.

   5) Allow the gas generator to run in this manner
      until the uptake temperature drops to approxi-
      mately the inlet air temperature.

   6) Close the fuel system bulkhead and tank isola-
      tion valves. It is good practice to refill the
      fuel service tank at the end of each operating
      period. Keeping the tank full of fuel reduces
      moisture buildup from condensation. Any water
      or sediment which might enter the tank during
      filling will have time to settle out and can
      be removed through the stripping connection
      prior to the next lightoff.

B) When the gas generator has cooled sufficiently, the
    air compressor may be shut down.

    1) Close the compressor suction butterfly valve.

    2) Stop the electric motor.

    3) When the compressor oil pressur falls below 20
        PSIG, switch the auxiliary oil pump control from
        the "automatic" to the "hand" position.

    4) Allow the lube oil system to run for one hour or
        until the compressor bearing temperatures are
        less than 80°F.

    5) Stop the auxiliary lube oil pump.

    6) Stop the cooling tower fan and cooling water
        pump.

C) Close the 4 inch butterfly manual isolation valve.

D) Close the inlet bypass globe valve.

E) Open the nozzle box drain valve.

F) Close the manometer isolation valves. It is also
    good practice to disconnect the inlet air pressure
    (PNH) and reducing section pressure drop (DELPN)
    manometers at the manometer. Other users of the
    compressor operate at pressures sufficient to over-
    pressurize these instruments. Over-pressurization

of the mercury manometer which measures the inlet
pressure could result in a hazardous mercury spill.

G) De-energize the main power panel and shut off the
thermocouple readouts.

APPENDIX B

CALIBRATION

The use of pressure drop data across nonstandard metering devices requires that the flow restrictor be calibrated to a known or well defined measuring standard. In the case of the experimental apparatus used in the conduct of this experimental work, calibration of the entrance nozzle was essential in effective determination of the air mass flow rate.

The entrance nozzle calibration arrangements utilized was that of Ross [Ref. 6]. An ASME standard Hershel-type Venturi was used as the primary flow measuring device. Data was recorded over a range of inlet pressure drop values from 2.0 in. water to a maximum nominal pressure drop of 10.0 in. water. This data is shown in Table XXVIII.

For the Hershel-type Venturi the mass flow rate is given by equation II-III-15C of [Ref. 15]

$$\dot{m}_a = 0.099702 \ C_d Y_d^2 F \ (1-\beta^4)^{-0.5} \ (\rho h_w)^{0.5} \quad \text{(lbm/sec)} \quad \text{(eqn B.1)}$$

where "C_d" is the discharge coefficient of the venturi, "Y" is the expansion factor, "d" is the throat diameter (in.), F is the area thermal expansion factor, "β" is the ratio of throat diameter to entrance diameter, "ρ" is the density of the fluid and "h_w" is the differential pressure (in. water).

210

After analyzing the data recorded in Table XXIX, it was decided that a linear curve fit in the range of mass flow rates most commonly encountered in previous experimental work would provide the best predictor of the actual mass flow conditions. The range of mass flow rates selected was approximately 0.875-1.740 lbm/sec of air which is considered to effectively bracket the range of experimentally encountered mass flows.

The entrance nozzle calibration is shown in Figure 42 with the data utilized being contained in Table XXIX.

The entrance nozzle was modeled as a venturi using the functional relationship

$$\dot{m}_{air} = f \ (P \cdot \Delta P/T)^{0.5}$$

which is given by equation II-III-15C of [Ref. 15]. Detailed entrance nozzle mass flow calibration calculations are contained in [Ref. 6], Appendix A.

APPENDIX C

UNCERTAINTY ANALYSIS

The determination of the uncertainties in the experimentally determined pressure coefficients and pumping coefficients was made using the methods described by previous researchers. The basic uncertainty analysis for the cold flow eductor model test facility was conducted by Ellin [Ref. 2] and Hill [Ref. 9] follows this development in analysis of the hot flow facility. Hill's analysis has been corrected for changes in the measured uncertainties resulting from the installation of new fuel flow measuring equipment. The uncertainties obtained using the second order equation were applicable to the experimental work conducted during the present research and are listed here.

UNCERTAINTY IN MEASURED VALUES

Parameter	Value	Uncertainty
TAMB	537 R	± 1
TUPT	1415 R	± 1
B	29.83 in Hg	± 0.005
DELPN	6.20 in H_2O	± 0.05
PUPT	13.6 in H_2O	± 0.05
ROTA	28.0	± 0.2
PNH	5.9 in Hg	± 0.05
TNH	649 R	± 0.2
PPLN	5.18 in H_2O	± 0.01

UNCERTAINTY IN CALCULATED VALUES

P^*/T^*	1.7%
$W^*T^{*0.44}$	1.4%

LIST OF REFERENCES

1. Charwat, Andrew, "DD-963 Exhaust Stack Studied,"
   University of California at Los Angeles, July 10, 1971.

2. Ellin, C. R., Model Test of Multiple Nozzle Exhaust
   Gas Eductor Systems for Gas Turbine Powered Ships,
   Engineer's Thesis, Naval Postgraduate School, June 1977.

3. Pucci, P. F., Simple Eductor Design Parameters, Ph.D.
   Thesis, Stanford University, September 1954.

4. Moss, C. M., Effects of Several Geometric Parameters
   on the Performance of Multiple Nozzle Eductor System,
   Master's Thesis, Naval Postgraduate School, September
   1977.

5. Harrell, J. P., Jr., Experimentally Determined Effects
   of Eductor Geometry on the Performance of Exhaust Gas
   Eductors for Gas Turbine Powered Ships, Engineer's
   Thesis, Naval Postgraduate School, September 1981.

6. Ross, P. D., Combustion Gas Generator for Gas Turbine
   Exhaust Systems Modelling, Master's Thesis, Naval
   Postgraduate School, December 1977.

7. Welch, D. R., Hot Flow Testing of Multiple Nozzle
   Exhaust Eductor Systems, Engineer's Thesis, Naval
   Postgraduate School, September 1978.

8. Lemke, R. J. and Staehli, C. P., Performance of Multiple
   Nozzle Eductor Systems, Master's Thesis, Naval Postgraduate
   School, September 1977.

9. Hill, J. A., Hot Flow Testing of Multiple Nozzle Exhaust
   Eductor Systems, Master's Thesis, Naval Postgraduate
   School, September 1979.

10. Eick, I. J., Testing of a Shrouded, Short Mixing Stack
    Gas Eductor Model Using High Temperature Primary Flow,
    Master's Thesis, Naval Postgraduate School, October 1982.

11. Kavalis, A. E., Effect of Shroud Geometry on the Effec-
    tiveness of a Short Mixing Stack Gas Eductor Model,
    Master's Thesis, Naval Postgraduate School, June 1983.

214

12. Pritchard, N. D., Jr., <u>Characteristics of a Four Nozzle, Slotting Mixing Stack with Slanted Shroud, Gas Eductor System</u>, Master's Thesis, Naval Postgraduate School, June 1983.

13. Drucker, C. J., <u>Characteristics of a Four-Nozzle, Slotted Short Mixing Stack with Shroud, Gas Eductor System</u>, Master's Thesis, Naval Postgraduate School, March 1982.

14. Holman, J. P., <u>Experimental Methods for Engineers</u>, Third Edition, pp. 253-258, McGraw-Hill, 1978.

15. American Society of Mechanical Engineers Interim Supplement 19.5 of Instrumentation and Apparatus, <u>Fluid Meters</u>, Sixth Edition, 1971.

INITIAL DISTRIBUTION LIST

No. Copies

1. Defense Technical Information Center   2
    Cameron Station
    Alexandria, Virginia 22314

2. Library, Code 0142   2
    Naval Postgraduate School
    Monterey, California 93943

3. Department Chairman, Code 69   2
    Department of Mechanical Engineering
    Naval Postgraduate School
    Monterey, California 93943

4. Professor Paul F. Pucci, Code 69Pc   2
    Department of Mechanical Engineering
    Naval Postgraduate School
    Monterey, California 93943

5. Dean of Research, Code 012   1
    Naval Postgraduate School
    Monterey, California 93943

6. Commander   1
    ATTN: NAVSEA, Code 0331
    Naval Sea Systems Command
    Washington, DC 20362

7. Mr. Olin M. Pearcy   1
    NSRDC, Code 2833
    Naval Ship Research and Development Center
    Annapolis, Maryland 21402

8. Mr. Mark Goldberg   1
    NSRDC, 2033
    Naval Ship Research and Development Center
    Annapolis, Maryland 21402

9. Mr. Eugene P. Wienert   1
    Head, Combined Power and Gas Turbine Branch
    Naval Surface Ship Engineering Station
    Philadelphia, Pennsylvania 19112

10. Mr. Donald N. McCallum   1
    NAVSEC Code 6136
    Naval Ship Engineering Center
    Washington, DC 21362

11.   LCDR Ira J. Eick, USN   1
      P.O. Box 248
      Lebanon, New Jersey 08833

12.   LT Carl J. Drucker, USN   1
      1032 Marlborough Street
      Philadelphia, Pennsylvania 19125

13.   LCDR C. M. Moss, USN   1
      625 Midway Road
      Powder Springs, Georgia 30073

14.   LCDR J. P. Harrell, Jr., USNR   1
      1600 Stanley
      Ardmore, Oklahoma 73401

15.   LCDR J. A. Hill, USN   1
      RFD 2, Box 116B
      Elizabeth Lane
      York, Maine 03909

16.   CDR R. J. Lemke, USN   1
      2902 No. Cheyenne
      Tacoma, Washington 98407

17.   LCDR C. P. Staehli, USN   1
      2808 39th St., N.W.
      Gig Harbor, Washington 98335

18.   LT R. S. Shaw, USN   1
      147 Wampee Curve
      Summerville, South Carolina 29843

19.   LCDR D. L. Ryan, USN   1
      6393 Caminito Luisito
      San Diego, California 92111

20.   LCDR C. C. Davis, USN   1
      1608 Linden Drive
      Florence, South Carolina 29501

21.   LCDR D. Welch, USN   1
      1036 Brestwick Commons
      Virginia Beach, Virginia 23464

22.   Department Chairman   1
      Department of Marine Engineering
      Maine Maritime Academy
      Castine, Maine 04421

No. Copies

1

23. LCDR R. E. Staples, Jr., USN
     2440 Broomsedge Trail
     Virginia Beach, Virginia 23456

DATE

ILMED

8